POLITECNICO
MILANO 1863

SCUOLA DI INGEGNERIA INDUSTRIALE
E DELL'INFORMAZIONE

Multidisciplinary evaluation of 3D models in hepatobiliary surgery.

TESI DI LAUREA MAGISTRALE IN
BIOMEDICAL ENGINEERING
INGEGNERIA CLINICA

Author: **Serena Bassetto**

Student ID: 970527
Advisor: Prof. ssa Veronica Cimolin
Co-advisor: Ing. Daniela Motta
Dott. Christian Cotsoglou
Academic Year: 2021-2022

Abstract

The safety and effectiveness of hepatobiliary surgery is based on a preoperative plan that fits the anatomy of the patient. The liver is a particularly vascularized organ that contains, inside the parenchyma, a complex vascular structure, which can be subject to anatomical variations. For this reason, it is difficult for even the most experienced surgeons to determine by two-dimensional images, typically computed tomography or magnetic resonance, the correct relationship between the tumour and the nearby vascular structures. In addition, any variations from the planned surgical strategy are associated with an increased risk of adverse clinical events in the intra- and post-operative phases.

Developments in medical imaging have provided new technologies to support surgeons in performing advanced clinical procedures in order to improve patient benefits and safety.

3D reconstruction allows individualized visualization of the lesion and its spatial relationship with the surrounding vascular structures. It empowered a more accurate and personalized preoperative simulation and intraoperative navigation for a customised guided surgical procedure. The aim of this thesis is to evaluate in a multidisciplinary and multidimensional way the effects of the adoption of 3D reconstruction technology in hepatobiliary surgery.

Liver cancer is an increasingly widespread problem in the world with a low survival rate, especially if it involves the bile ducts. For this reason, the use of three-dimensional reconstructions in the pre-operative image acquisition process for surgical planning is increasingly being introduced. These 3D models derive from a post-processing of two-dimensional images, with the aim of creating a reconstruction that respects quality standards, being as close as possible to reality. The advantages in terms of understanding the patient's anatomy were verified through an ad hoc questionnaire administered to several experienced surgeons. They answered to precise anatomical questions first by looking only at the two-dimensional images and then visualizing the corresponding 3D model. The power of 3D in understanding the anatomy of vascular infiltration have been analysed as some surgeons have changed their response by looking at 3D reconstructions and, in most cases, this response is the same as the actual surgical finding.

In addition, the benefits to patients were assessed by analysing an intervention (3D) and a control (2D) group of patients. Intra- and post-operative outcomes are improved with the use of 3D reconstruction. Among the advantages, a decrease of bleeding during the operation, a decrease of the duration of hospitalization and a less recurrence of the tumour have been evidenced. This leads to an improvement in the quality of life of patients during the follow up and a lower expenditure of resources by the hospital, caused by long hospital stays with complications and comorbidities. Thus, it can be concluded that, despite the limited number of patients involved, 3D has many advantages from different points of view. It represents the surgical and dynamic perception of the anatomy of a specific patient, a tool that does not replace traditional two-dimensional images, but it makes preoperative planning more immediate and 'surgical like'.

Key-words: 3D reconstructions, 3D models, rendering, hepatobiliary surgery, surgical planning, intraoperative navigation.

Abstract in italiano

La sicurezza e l'efficacia della chirurgia epatobiliare si basa su una pianificazione chirurgica adeguata all'anatomia del paziente. Il fegato è un organo particolarmente vascolarizzato che racchiude dentro il parenchima una complessa struttura vascolare, che può essere soggetta a varianti anatomiche. Per questo motivo, risulta difficile anche ai chirurghi più esperti determinare tramite immagini bidimensionali, tipicamente tomografie computerizzate o risonanze magnetiche, la corretta relazione tra il tumore e le strutture vascolari vicine. Inoltre, eventuali variazioni dalla strategia chirurgica pianificata, sono associate ad un aumento del rischio di eventi clinici avversi in fase intra- e post-operatoria. Gli sviluppi nel campo dell'*imaging* medico hanno fornito nuove tecnologie per supportare i chirurghi nell'esecuzione di procedure cliniche avanzate, al fine di migliorare i benefici e la sicurezza dei pazienti. La ricostruzione 3D permette la visualizzazione individualizzata del sito della lesione e della sua relazione spaziale con le strutture vascolari circostanti. Attraverso una più accurata simulazione preoperatoria e navigazione intraoperatoria, il 3D permette una procedura chirurgica personalizzata a guidata. L'obiettivo di questa tesi è quello di valutare in modo multidisciplinare e multidimensionale gli effetti dell'adozione della tecnologia di ricostruzione 3D in chirurgia epatobiliare. Il tumore al fegato è un problema sempre più diffuso nel mondo e con un basso tasso di sopravvivenza, soprattutto se si tratta di tumore alle vie biliari. Per questo motivo, si sta inserendo sempre di più l'utilizzo delle ricostruzioni tridimensionali nel processo di acquisizione delle immagini preoperatorie per la pianificazione chirurgica. Tali modelli 3D derivano da una successiva elaborazione dell'immagine bidimensionale, al fine di ottenere una ricostruzione che rispetti gli standard di qualità e che sia il più vicino possibile alla realtà. I vantaggi in termini di comprensione dell'anatomia del paziente sono stati verificati attraverso un questionario somministrato a diversi chirurghi esperti, i quali hanno risposto a precisi quesiti anatomici prima guardando solo le immagini bidimensionali e poi visualizzando anche il corrispondente modello tridimensionale. Sono stati così analizzati i vantaggi del 3D nella comprensione dell'anatomia dell'infiltrazione vascolare poiché alcuni chirurghi hanno cambiato la loro risposta guardando le ricostruzioni 3D e, nella maggior parte dei casi, tale risposta è uguale all'effettivo riscontro operatorio. Inoltre, sono stati valutati i benefici nei confronti dei pazienti, analizzando un gruppo di intervento (3D) e di controllo (2D). Gli *outcomes* intra- e post-operativi risultano migliorare con l'utilizzo della ricostruzione 3D. Tra i vantaggi, sono stati evidenziati soprattutto una diminuzione delle perdite ematiche durante l'intervento, una diminuzione della lunghezza del ricovero ed una minore recidività del tumore. Questo comporta un miglioramento della qualità della vita del paziente dopo il decorso operatorio ed un minore dispendio di risorse da parte dell'ospedale, causato da lunghe degenze con complicanze e comorbidità. Quindi, si può concludere che, nonostante il limitato numero di pazienti coinvolti, il 3D risulta avere numerosi vantaggi sotto diversi punti di vista. Rappresenta la percezione chirurgica e dinamica dell'anatomia di uno specifico paziente, uno strumento che non sostituisce le tradizionali immagini bidimensionali, ma che rende la pianificazione preoperatoria più chiara ed immediata. **Parole chiave:** ricostruzioni 3D, modelli 3D, rendering, chirurgia epatobiliare, pianificazione chirurgica, navigazione intraoperatoria.

Contents

1 Introduction

1.1 State of the art

One of the biggest challenges of modern medicine is to apply technology to deliver the best care service to patients. Developments in medical imaging and their integration have provided new opportunities to support surgeons in performing advanced procedures and to enhance patient benefits and safety. Thanks to the use of three-dimensional reconstruction, it became possible to make more and more similar to reality the complex anatomy of a specific body district of a cancer patient, who will have to undergo a delicate and complex surgery (Figure 1).

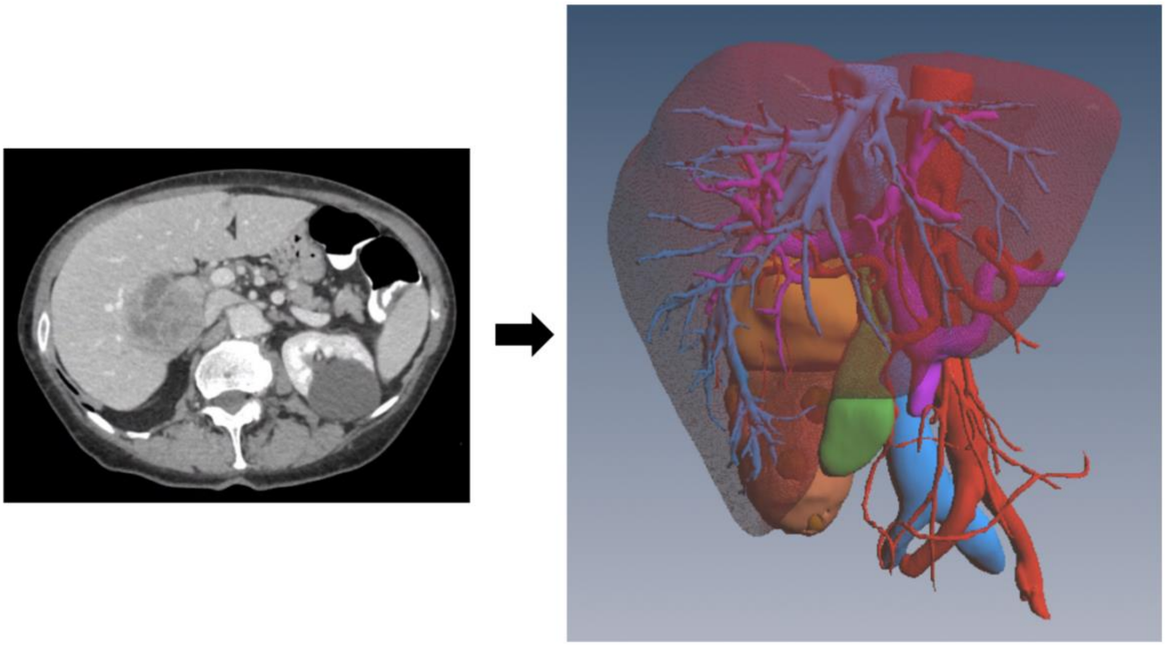

Figure 1 From bidimensional to three-dimensional images.

In the history of 3D rendering, the target organs were especially those parenchymatous, as the liver, kidney, and pancreas. The parenchyma is a specific tissue, which gives the organ its structural and functional characteristics surrounding and covering inside a multitude of vascular-biliary structures. For this reason, attention was focused specifically on hepato-bilio-pancreatic surgery (HBP), offering great advantages especially in high complexity liver surgery that involves vascular reconstruction [1] [2].
The practical applications of 3D technology can be divided into 3 macro areas: preoperative surgical planning, guided intraoperative navigation system and educational-informative purpose.
Nowadays, it is a very well-known concept, that while maintaining solid and stable anatomical principles, each patient keeps its subjective uniqueness and individuality, both in

relation to some personal anatomical variants and regarding the position of that specific tumor with respect to the frames of references of that particular organ. In this regard, an important aspect in preoperative planning are anatomical variants that can be misunderstood or underestimated during the study of CT (computerized tomography) or MRI (magnetic resonance imaging).
3D reconstruction allows to identify the presence of subjective anatomical variants: when they are known at the beginning, they can be addressed in total control in the intraoperative phase. Figure 2 shows some examples of anatomical variations of vascular structure inside the liver.

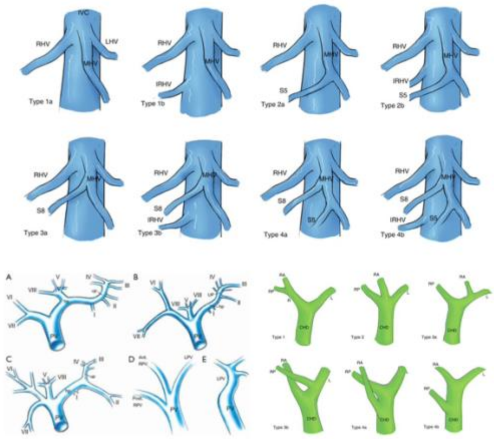

Figure 2 Anatomical variants.

Three-dimensional reconstruction not only helps to refine the surgical technique according to the anatomy of the patient, but in some cases it allows a drastic change in the therapeutic strategy [3]. In the case shown in Figure 3, the left surgery (that consists into removing the dark gray part of the liver) allows to have a remaining volume of 72%, while the second strategy on the right is characterized by a remaining volume of 27.8%. From this analysis, the first strategy would seem to be the best way forward the patient's health, in order to avoid post-intervention liver failure.

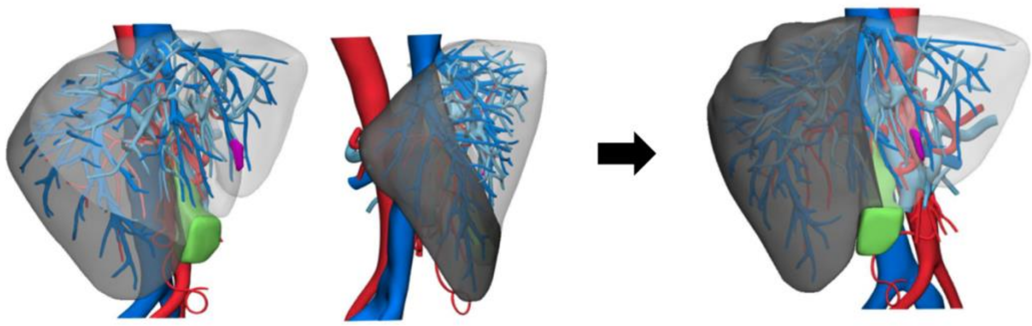

Figure 3 Different operative plans.

However, thanks to a three-dimensional and interactive vision it was seen that, if the therapeutic strategy of the left had been adopted, the tumor would not have been completely removed due to a thrombus present in the portal vein, indicated with the arrow in Figure 4.
This is an emblematic example in which 3D reconstruction permits to identify the most appropriate surgical strategy for each clinical case.

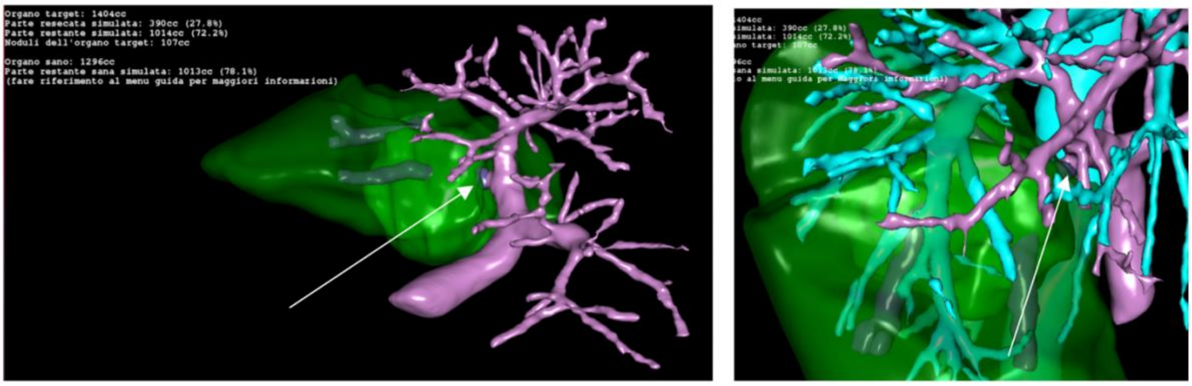

Figure 4 Presence of thrombus near the tumor.

During intraoperative navigation, the great advantage that this method brings can be seen in the removal of the so-called vanishing lesions, also named "small invisible tumors". These lesions are no longer viewable during intraoperative hepatic ultrasound, because of an impressive response to chemotherapy. In the cases in Figure 5, the use of 3D reconstruction is fundamental, since otherwise the surgeon would not remove the tumor completely.

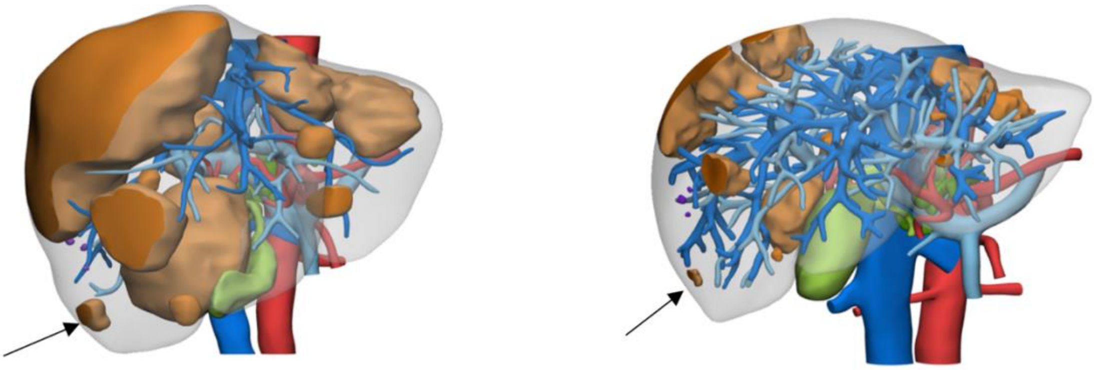

Figure 5 Example of vanishing lesion before (left) and after (right) chemotherapy.

Finally, the 3D model is the most intuitive and simple method to explain to the patient and his family the risks associated with a certain complex surgical procedure. In addition, this technology has a key role in the academic-educational field for training surgeons, reducing learning time and allowing them to have a more direct and practice view of the complexity of surgery [4].

Until now, the only way to plan preoperatively the intervention was the close interpretative collaboration of two professional figures such as the radiologist and the surgeon, based on CT scans and MRI. Furthermore, multidisciplinary is important also in 3D in order to achieve a high final detail in tridimensional reconstructions, since it’s fundamental the collaboration of different professional figures such as radiologists, surgeons, biomedical and software engineers and technicians. This allows to avoid deviations from reality that could increase risk of adverse clinical events. Indeed, the engineer is able to translate into technical and numerical terms the radiologist and surgeon’s perception and interpretation of the anatomical structures [5]. Therefore, the three-dimensional technology represents the surgical perception and the anatomy of that specific individual: a tool that certainly cannot replace the radiologist’s information, but it makes more immediate and surgical-like the pre-operative planning.

Among the advantages of this innovative technology, there are the benefits against patients operated using 3D compared to the traditional procedure. In recent studies, it emerged that the use of 3D reconstruction allows a substantial decrease in operating time, thanks to a better vision of the anatomical structures, a decrease in blood loss intraoperative and a decrease in the volume of blood transfused, favoring the prognosis of the patient.
Moreover, an important aspect in liver surgery is the calculation of the residual volume, which should not be under 25% otherwise the patient risks liver failure. In this regard, a smaller difference was found between the volume of liver removed, calculated by 3D rendering, and the volume of liver actually resected, compared to the preoperative evaluations based on the 2D image. This definitely decreases the risk of liver failure and improves the safety of surgery.
Finally, it has been seen how the use of 3D reconstruction can reduce damage to the vascular and biliary system, facilitating the recovery of liver functions during postoperative hospitalization [6].
Even though this technology facilitates to increase the effectiveness and safety of complex surgery, evidence of its effects remains limited.

1.2 Thesis structure

This thesis work aims to validate, using the health technology assessment (HTA) framework, if 3D reconstructions help, during pre-operatory planning, the determination of the most suitable therapeutic strategy according to the anatomy of the patient in liver surgery.
HTA is a multidisciplinary and multidimensional approach, that analyzes the impact of the introduction of a new technology in the healthcare system.
HTA was born in 1967 by Battista as a form of policy research that examines short- and long-consequences considering any improvement of health or wellbeing of a new technology compared with its comparators. It supports decision makers into the evaluation of how to allocate resources form the health care system, from the patient/caregiver (e.g., time, transport, mental care, out of pocket resources) and from other sectors (e.g., rehabilitation, industrial economic system, non-profit organization, social enterprises).

As shown in Figure 6, there are two different loci: decision-making locus and research locus. The HTA must be able to provide evidence that can help decision makers to decide how to allocate the budget and which are the better technologies for the healthcare system. It must be able to provide evidence: information should be useful, rigorous, and feasible.
Anyway, it’s important to underline that assessing is not deciding. On one hand, decision making is responsibility of decision makers and policy makers who must decide. On the other hand, researchers have the responsibility to assess different characteristics [7].

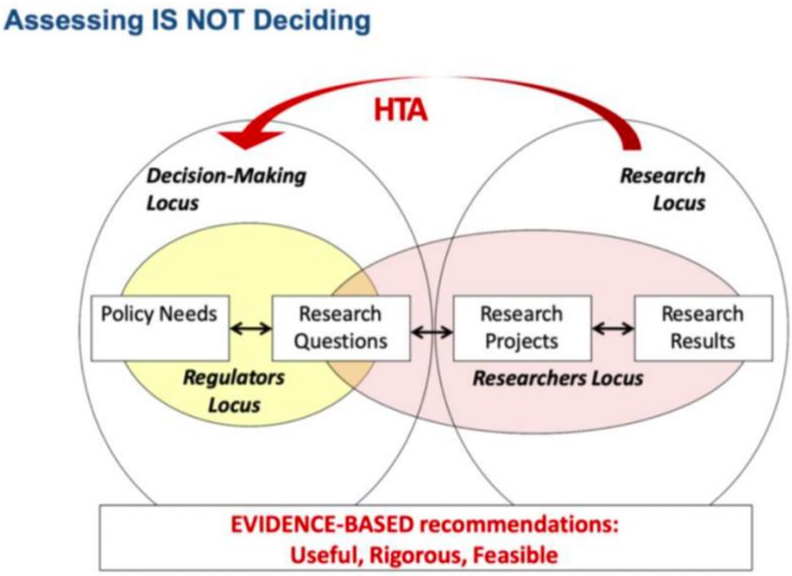

Figure 6 HTA connects 'research locus' with 'decision making locus' [7].

In 2005, with the Health Program of the European Commission, EUnetHTA was established, a network for HTA across Europe that help to produce reliable, timely, transparent and transferable information about health care technologies, through efficient resource use, knowledge sharing and good practice in HTA methods [7].

Based on EUnetHTA core model, shown in Figure 7, a comprehensive assessment consists of a technical description of the technology and its current use, an analysis of the clinical effectiveness, safety, economic and organizational impact, as well as the implications that the technology could have on patients and society, from a social, ethical and legal point of view [8].

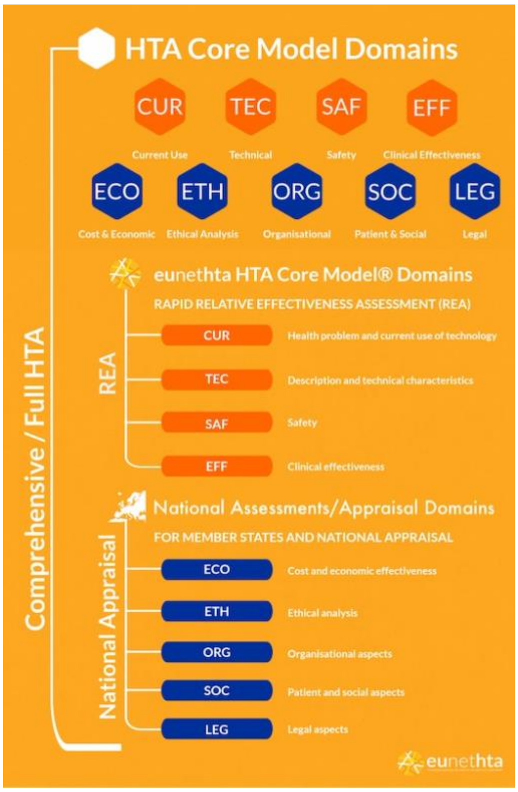

Figure 7 EUnetHTA Core Model [8].

In Italy the HTA is a tool to support the National Health System (NHS) in the application of the principles expressed in article 1 of D.Lgs. 502/92 concerning equity in access to care, the quality of care and suitability for specific needs, as well as the cost-effectiveness analysis of the use of resources, enabling scientific evidence to support decisions on the adoption or not of new healthcare technologies.
AGENAS (*Agenzia Nazionale per i Servizi Regionali*) plays a key role in the coordination of evaluation activities. For this reason, since 2005 the agency has been participating in the EUnetHTA network.
The model used in this thesis work is the one designed by AGENAS called 'full HTA', with the aim of producing a comprehensive analysis based on the available resources.
The domains typically dealt with in a full HTA report by AGENAS are:

- health problem and clinical context: this domain describes the target conditions, including the underlying mechanism (pathophysiology), natural history (i.e., course of disease), available screening and diagnostic methods, prognosis, and epidemiology (incidence, prevalence);
- description of the technology and its comparators: identification of the technical details related to the technology in question and the alternatives available on the Italian market. Description of operating principles, components, setting, clinical use and regulatory requirements, certifications, and approvals;
- current use of the technology in the national health system: this report estimates the use and dissemination of the technology;
- analysis of clinical effectiveness: the focus is to determine the magnitude of health benefits or of the net benefit (benefit minus harms) that are caused by the technology. At this point, it's important to underline the difference between efficacy and effectiveness. The former means that the technology does better than harm under ideal circumstances, the latter is related to usual circumstances of health care practice. The research question within this domain is focused on effectiveness;
- safety analysis: all complications, pre-, intra- and post-procedural, reported in the analyzed clinical studies are taken into account and synthesized to describe a safety profile;
- analysis of the patient's point of view: in this context, issues relevant to patients, individuals and caregivers are presented to assess the acceptability and impact of technology on everyday life, the compliance of the patient and his expectations. The term 'individual' is sometimes used synonymously with 'patient', but it can also refer to a healthy individual (for example, a person taking part of a screening program);
- analysis of organizational aspects: this domain analyzes the organizational modalities related to the use of technology and the necessary different kind of resources, such as material, human skills and knowledge, money, attitude, and work culture;
- analysis of economic aspects: value-for-money judgments about health technologies, with information about costs, health related outcomes and economic efficiency [8][9].

This is the schema of the 'full HTA'. However, AGENAS also proposes other types of documents that can be used to evaluate a technology in the healthcare, based on the objective, production time and degree of complexity. These different types are shown in Table 1 Summary of the highlights of HTA products by AGENAS [9].
If the goal is to save resources and to include the results in the decision-making process more quickly, the model called 'rapid HTA' can be used. This document does not provide for the direct collection of data (relatively time-consuming phase), and it contains less information than full HTA, but it is useful for responding to specific questions in a timely manner.

Another type of proposed document is called ‘horizon Scanning’ (HS). It contains information on the potential impact that innovative and emerging health technologies can have in healthcare systems. The innovativeness is not only related to the operating principles or to the recent technological details, but it is also linked to the level of diffusion and use of the technology and the recent CE approval within the European market. HS reports investigate all domains but evaluating the potential impact that a technology could have in the reference context if it will be introduced or, if already in limited use, the effects it generates when compared to a standard technology.
The last model proposed by AGENAS is called 'adapted HTA report' and it consists in using, as a basis of evidence, an already published HTA report and "adapt" it to the national or reference context. The purpose of the adapted HTA report is to provide policy makers, in a resource-saving and time-saving way, with evaluations already produced in other countries but adapted to the Italian context. This activity has the advantage of making more information available to national and regional decision-makers, with equal resources available and avoiding duplication of information.
The choice of the type of assessment to be carried out regards, mainly the domains to consider for the chosen technology. It is dictated by the answer to the questions known as policy and research questions and by the human and time resources available for its implementation.

Product	Production time	Degree of complexity	Language
Full HTA Report	12 months	High	English (with summary in Italian)
Rapid HTA Report	6 months	Medium	English (with summary in Italian)
Adapted HTA report	6-8 months	Medium	Italian
Horizon Scanning Report	2-3 months	Low	English and Italian

Table 1 Summary of the highlights of HTA products by AGENAS [9].

The production of an HTA document (full, rapid, adapted) or HS begins with the preparation of a research protocol that aims to clarify the assessment strategy prior to the research and analysis of evidence. It defines the policy question and translates it into research questions for each of the domains. In particular, the methods that will be used for the search of the evidence, the comparator against which the technology will be evaluated, the types of primary and secondary outcomes, the research strategy, inclusion/exclusion criteria of studies (PICO-population, intervention, comparator, outcome) will be primarily defined.
The production of each type of evaluation report requires a systematic and exhaustive research of the available tests and studies, published or not, related to the specific health technology being evaluated. This approach ensures that the greatest number of studies relevant to the subject of the assessment are identified and considered for the analysis.
Also, context data may be collected through ad hoc investigations that are usually conducted when the available information is not present or is not sufficiently detailed for the purposes of the assessment. For this reason, both qualitative research methods such as interviews and quantitative ones as structured questionnaires can be used or data can be collected through context information sources [9].

1.3 Contextualization

All the data used in the thesis were collected at Vimercate hospital.
The "village of the market" (from which then Vimercate) was already known in the Middle Ages as a reference centre for travellers and traders, thanks to its strategic location in one of the main streets that connected the Alps to Milan. For this reason, the hospital has a thousand-year tradition: it was born as a shelter for pilgrims in 833 A.D.
At the end of the eighteenth century, the hospital was renovated and later expanded, adding more and more specialized pavilions in the following years to cope with population growth. In these years the hospital remained known not only for the care of the sick but also for the educational purpose (it was the first municipal school) and for the supply of medicines to poor people [10].
From the early 2000s the project for the construction of a new hospital on an area of almost 100,000 square meters for a total of 500 beds was born. Built in just 3 years and designed by architect Mario Botta, the hospital came into operation in 2010. Its architecture (Figure 8), technology and organization are all aimed at placing the patient at the centre of the logistical and diagnostic-therapeutic paths, with his pathologies, family, and social experience.

Figure 8 Architecture of Vimercate Hospital [11].

The assistance is organized according to the model of intensity of care. The pattern is configured as an orthogonal lattice order, accessible by external and internal patients without overlapping or crossing of flows. On the sides, are located the vertical circulation cores and hospital shafts, which facilitate maintenance operations and allow the insertion of new technologies with minimally invasive interventions compared to the continuity of hospital activities.

The areas for the ordinary hospitalization are distributed within 4 volumes, called "petals" for their semi-curved shape, which open to the park located west of the hospital [12].
Primary objective of the installed technologies is to offer in a more complete and efficient way digital services for medical, nursing, technical and administrative, in order to optimize and facilitate different processes.
The innovative technological field includes electronical health records, digitization of diagnostic tests, integration of surgical rooms, clinical monitoring, and the possibility of telecommunication outside for the execution of consultations and other remote activities.
The complete computerization of all the clinical-health processes of the Hospital of Vimercate, from diagnostics to reception, from the clinical record to the supply chain of the drug, allows to no longer request the printed press of the documentation, thus achieving the goal of paperless hospital.
In 2014, the structure reached level 6 in the ranking of digitalization certified by HIMSS Europe, an European division of the global non-profit organization that aims to improve the health of the population through the usage of information and communication technologies (ICT).
The evaluation model used is called EMRAM. It allows to analyse the level of diffusion of information technologies in hospitals, focusing mainly on the widespread dissemination in all departments of the Electronic Health Record (EHR) and the complete digitization of clinical and instrumental images. It is focused also on the complete digitization of the drug therapy process, the widespread use of business intelligence systems for the multidimensional analysis of structured data of the electronic health record and the double data centre to ensure the highest level of service to users and maximum accessibility to patient data [13].

2 Health problem and clinical context

2.1 Anatomy of the liver

The liver, weighing about 2 kg, is the largest gland of the human body, attached to the digestive system. It is therefore part of the endocrine system, which oversees the production of hormones. In particular, the liver produces bile, which is essential for the digestion of fats. In the organ there is also the most important glycogen deposit, which represents about 6-7% of the total weight of the organ [14].

The liver is in the right part of the abdomen, below the diaphragm, protected by the lowest part of the rib cage. It is also surrounded by the Glisson capsule, which does not contribute to its wedge shape, defined by its relationships with adjacent organs and muscles. Indeed, through the Glisson capsule, the liver is in contact with the diaphragm and it has anatomical relationships with the right kidney, gallbladder, colon, stomach, duodenum, pancreas, and large blood vessels [15][16].

Elements characterizing the anatomy of the liver are ligaments, hepatic hilum, and vascular structures.

As shown in Figure 9, the liver has different ligaments that connect it to other organs, the anterior abdominal wall and the diaphragm: falciform ligament, coronary ligament, round ligament, left triangular ligament, right triangular ligament, venous ligament [17].

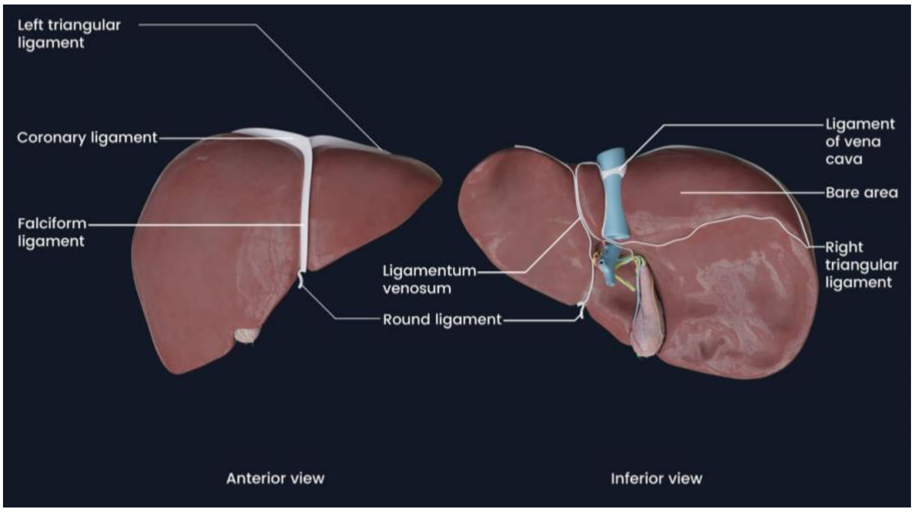

Figure 9 Hepatic ligaments [18].

The vascular system (Figure 10) of the liver is particularly complex; the blood supply of about 1.5 liters per minute is guaranteed by a dual system that includes hepatic artery and portal vein.

The hepatic artery is the main arterial vessel that supplies the liver. At the origin it is called common hepatic artery, later curved above and behind in front of the portal vein, branching into left hepatic artery and right hepatic artery.

The liver has two venous systems: the portal and the hepatic veins. The portal vein is responsible for channeling blood from intestinal digestion and spleen to the liver.
Furthermore, the three hepatic veins (left, middle and right) originate from the inferior vena cava and constitute the second venous system of the liver. Their course in the hepatic parenchyma allows to divide the liver into sectors, their peduncles allow to divide each sector into additional segments [17].

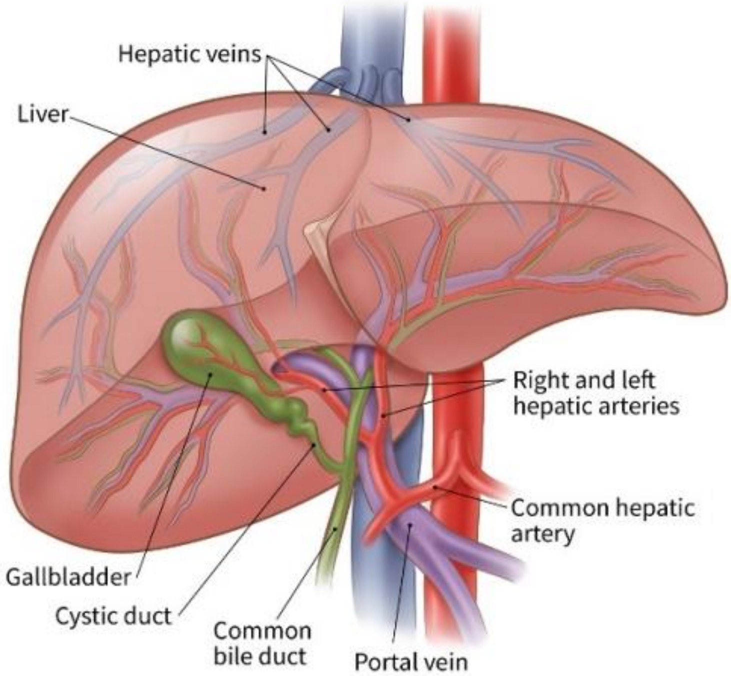

Figure 10 Hepatic vascular structures [19].

The depression placed on the lower surface of the liver constitutes the hepatic hilum. Through it, the hepatic artery and the portal vein enter inside the liver to provide the vascularization of the organ.
From the hepatic hilum comes out the main biliary duct that conveys the bile produced by the liver inside the first portion of the small intestine, the duodenum, where it favors the absorption of food. The main bile duct is connected to the gallbladder via a small duct called the cystic duct.

The liver consists of 4 types of cells, and it is classically divided into 4 lobes (right, left, quadrate and caudate) and 9 segments.

The most numerous cells in the liver are hepatocytes. They represent 80% of the volume and they have a polyhedral shape. They turn out to be one of the cellular types in which the organelles are more developed, because of the high metabolic needs and the great variety of tasks they must perform. Two adjacent hepatocytes form bile ducts with their plasma membranes, where numerous bile-containing vesicles accumulate. Another type of cells are stellate cells, that have an irregular shape. They are essential in the regeneration of the liver after an injury or surgery. In case of injury, they can replace the damaged hepatocytes and by secretion of collagen form scar tissue. The last two types of hepatic cells are: sinusoidal endothelial cells and Kupffer cells. The former constitutes the endothelium of the capillaries. The latter removes the debris in the blood and, at the same time, stimulate the immune system [17].

The liver is divided into 4 different lobes (Figure 11). The right lobe is the most voluminous and has a vaguely copular shape. The left lobe has a volume equal to about half of the right with a triangular shape. Both the quadrate lobe and the caudate lobe are represented as protrusions of the posterior surface of the liver. In the first case, the lobe is bounded on the right by the gallbladder, on the upper by the hepatic hilum, laterally by the round ligament. The caudate lobe is bounded below by the hepatic hilum, laterally by the venous ligament, above the hepatic veins and medially by the inferior vena cava [17].

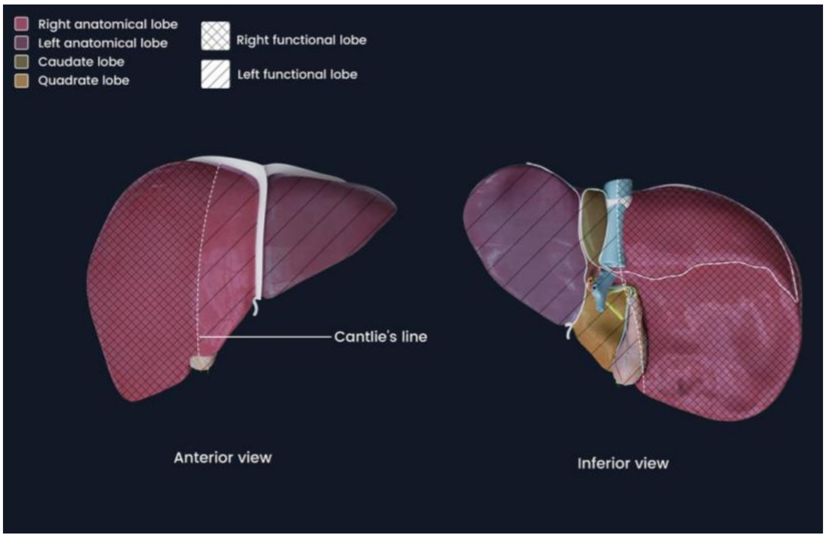

Figure 11 Functional and anatomical lobes of liver [18].

Because of its peculiar vascularization, the liver is anatomically separated into 9 portions called segments, numbered from 1 to 8 (the fourth is in turn divided into 4a and 4b). The liver segments, shown in Figure 12, are functional units independent of each other and, for this reason, they can be treated separately without compromising the functioning of the residual liver [20].

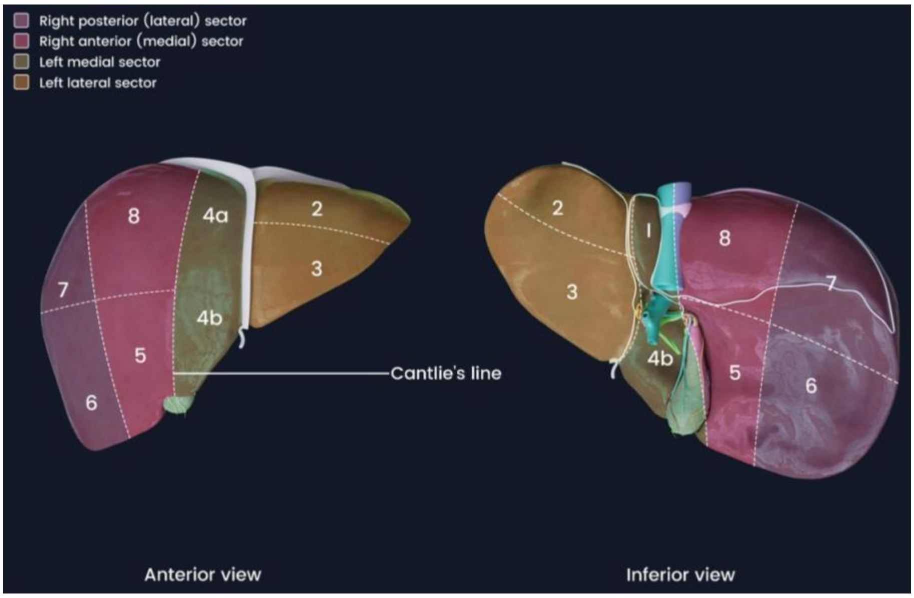

Figure 12 Liver segments [18].

2.2 Liver physiology

The main functions of the liver are: synthesis, accumulation, catabolism, excretion.
The liver produces bile that allows the digestion of fat and fat-soluble vitamins. Bile does not pass all directly into the duodenum, but a part is stored in the gallbladder until the fats arrive from the stomach to the intestine.
At the hepatic level, also coagulation factors are synthesized that permit to the blood to remain fluid and avoid the formation of aggregations that hinder the circulation.
The liver is the organ in which glycogen, triglycerides, fatty acids, proteins, vitamins, iron, and copper are accumulated. Hepatocytes are fundamental not only for the disposal of fats, but also cholesterol and triglycerides.
It has an important role in the management of the body's metabolic balances, as it is able to transform the accumulated glycogen into glucose, when the body requires it. The liver can modulate the level of sugar by breaking down insulin and other transformations of proteins for energy purposes.
It has fundamental catabolic functions: its cells have useful characteristics to neutralize toxic substances and drug residues. It's able to dispose of damaged red blood cells and recognize pathogens, thanks to Kupffer cells [14].

2.3 Liver and biliary tract diseases

Pathologies of the liver can be roughly divided into 3 large classes: acute hepatocellular damage, chronic liver disease, biliary tract obstruction.
In addition to the clinical evaluation by anamnesis and objective examination, laboratory tests for liver function, such as transaminases, prothrombin time, bilirubin (total, direct and indirect) help in the study of the liver. Instrumental examinations such as ultrasound, CT, MRI are also conducted.
A warning sign of liver and biliary disease is jaundice, a yellowish discoloration of the skin caused by an increase in blood concentration of bilirubin.
It is pre-hepatic jaundice when there is an increase in indirect bilirubin, probably linked to hemolysis (destruction of red blood cells). When direct bilirubin increases, it is called post-hepatic jaundice, due to biliary tract obstruction. When both types of bilirubin increase due to lesions of the hepatic parenchyma it is called hepatocellular jaundice [15].

2.3.1 Hepatitis

Hepatitis is an inflammation of liver cells caused by a virus. It can be symptomatic or asymptomatic and the evolution of this pathology can be self-limiting or chronic. Hepatitis A, B and C viruses are the main causes of acute and chronic hepatitis. However, the spread of viral infections has changed considerably over the last decade thanks to the general improvement in sanitary conditions and the compulsory vaccination for A virus and B virus. Together with the vaccine, it is important to adopt an active lifestyle, a healthy diet and a reduced or zero consumption of alcoholic beverages.
The A virus infection is an acute disease that does not become chronic. The clinical framework is flu-like with jaundice that heals without any problems in most patients. Infection occurs through infected feces that contaminate food. The disease is lethal by 0.02% of cases.

Symptoms of B virus infection are similar, but in 5% of cases the infection becomes chronic. The B virus can then lead to cirrhosis, liver cancer and liver failure (explained later). Infection occurs through contact with infected material, and it is lethal in 0.5% of cases.
Hepatitis C virus infection chromicize in 60-85% of cases. Acute disease is very often asymptomatic, but it can cause cirrhosis, hepatocarcinoma and liver failure. The causes of infection are the same of B virus, but it is less infectious. Acute hepatitis C can be fatal in 0.1% of cases.
In the case of hepatitis A, specific treatments are not necessary, as it spontaneously recedes in a couple of months. In the case of hepatitis B, treatment typically involves antivirals, which are not able to eliminate the virus, so they must be taken for life. Anyway, there are available antiviral drugs that completely eliminate the hepatitis C virus [21].

2.3.2 Cirrhosis

Cirrhosis of the liver is the formation of fibrous tissue within the liver to replace dead hepatocytes. Liver cell death can be caused by viral hepatitis, alcoholism, or intoxication by other toxic substances.
Cirrhosis restricts liver function and, if untreated, it can be fatal. The formation of fibrous scars reduces blood flow in the organ and it makes the body weaker against infections, due to the inability to properly process nutrients. Cirrhosis also increases the risk of liver cancer, and if the organ is no longer able to remove bilirubin from the blood, it can manifest as jaundice.
Tests that can be conducted to confirm the diagnosis include blood tests to verify the level of bilirubin, liver enzymes, albumin, platelets, and prothrombin time. Also, instrumental examinations can be performed such as ultrasound, elastography, CT, MRI, and liver tissue biopsies.
The most suitable treatment varies depending on the cause of cirrhosis. The ultimate goal is always to slow the progression of scarring while preventing the appearance of any complications or reducing their symptoms [22].

2.3.3 Hepatic failure

Liver failure occurs when an extended part of the liver is impaired. It can be caused by many types of hepatopathy, including viral hepatitis, cirrhosis and liver damage from alcohol or drugs.
The liver is no longer able to properly metabolize bilirubin and to remove it from the body. Bilirubin tends to accumulate in the blood and deposited in the skin. This causes jaundice.
In case of hepatic failure, the liver can no longer synthesize enough proteins to promote clotting and it can cause both ascites and encephalopathy because the liver cannot remove toxic substances as it normally does, and these accumulate in the blood.
Subjects may also have metabolic abnormalities and immune system malfunction that increases the risk of infection.
Treatment involves acting on the causes with dietary restrictions (limiting the consumption of sodium and alcohol). In case of acute liver failure, the patient should be immediately treated in intensive care units.
In extreme cases, liver transplantation can be used to restore liver function [23].

2.3.4 Hepatic steatosis

Hepatic steatosis involves the accumulation of lipids in the liver.
People with hepatic steatosis feel fatigued or have a slight abdominal discomfort but have no other symptoms, even though advanced hepatic steatosis sometimes causes more serious liver diseases such as cirrhosis.
To confirm the diagnosis and ascertain the extent of the damage, a liver biopsy may be required. The doctor will focus on controlling or eliminating the cause of liver steatosis, such as metabolic syndrome or the consumption of large amounts of alcohol.
Hepatic steatosis (with or without fibrosis) due to any condition, except the consumption of large amounts of alcohol, is called non-alcoholic hepatic steatosis (NAFLD). NAFLD develops more often in subjects with overweight, elevated blood lipid levels and insulin resistance [24].

2.3.5 Ascites

Ascites is the accumulation of protein-containing fluid (ascites) in the abdominal cavity.
Many disorders can be a cause of ascites, but the most common is hypertension in veins that carry blood to the liver (portal hypertension), usually due to cirrhosis.
If large amounts of fluid accumulate, the abdomen dilates enormously causing the subject lack of appetite, shortness of breath, and a sense of discomfort.
Ascites can be diagnosed by a medical examination, diagnostic imaging or by taking an ascitic fluid sample.
Usually, a low-salt diet and diuretics can help eliminate excess fluid [25].

2.3.6 Encephalopathy

Hepatic encephalopathy consists in the deterioration of brain functions due to the accumulation in the blood of toxic substances, normally removed by the liver, that reach the brain.
Hepatic encephalopathy appears in subjects with long-term (chronic) hepatopathy.
It can be triggered by bleeding of the digestive tract, an infection, failure to take drugs as prescribed or by another stress.
People are confused, disoriented, and sleepy, with changes in personality, behaviour, and mood.
The doctor bases his diagnosis on the symptoms, the results of the objective examination and the response to treatment. If the patient eliminates the trigger and takes lactulose (a laxative) and rifaximin (an antibiotic), he contributes to the disappearance of symptoms [26].

2.3.7 Benign Tumours

Benign liver tumours are relatively common and, in most cases, are asymptomatic.
Diagnosis is usually possible with imaging techniques, but biopsy may be necessary for diagnostic confirmation. Treatment is needed only in a few specific circumstances.
Hepatocellular adenoma is the most important benign liver neoplasm. It develops mainly in women of childbearing age, especially in those taking oral contraceptives, with estrogenic effect. Most adenomas are asymptomatic, although larger ones can cause pain. In rare cases, it can turn into a malignant neoplasm.

Another type of benign tumour is focal nodular hyperplasia, which purges histologically to cirrhosis. In this case, therapy is rarely necessary.
Finally, haemangiomas represent another type of benign tumour, they are usually small in size and asymptomatic. Symptoms, most likely > 4 cm in size, include discomfort, fullness, and, less often, anorexia, nausea, early satiety, and pain secondary to bleeding or thrombosis. These tumours often have a characteristic highly vascular appearance. Usually, no precise treatment is indicated. Resection can be considered if symptoms are bothersome or if a haemangioma increases in size rapidly [27].

2.3.8 Cancer

Liver cancer may be primary as hepatocellular carcinoma or cholangiocarcinoma, or it may present as metastases of cancer in other areas of the digestive tract.

2.3.8.1 Hepatocellular carcinoma (HCC)

Hepatocellular carcinoma or hepatocarcinoma (CEC or HCC) is the most common form of liver cancer. It develops mainly in cirrhotic livers of people around fifty and seventy years old. Indeed, it has been found to be often caused by pre-existing liver disease, such as cirrhosis or infection caused by viral hepatitis. Although in the more industrialized countries it is diagnosed in the early stages in the absence of symptoms (25% of cases), thanks to the screening of cirrhotic patients, who usually show abdominal pain, weight loss, ascites, dyspepsia, abdominal swelling, anorexia, and asthenia.
The most common staging classification is TNM: "Primary cancer, lymph nodes and distant metastases" (Table 2). This classification is adopted by the AJCC (American Joint Committee on Cancer) and the UICC (International Union Against Cancer) [28].

Cancer Stage	Description
Tx	Primary tumour not definable
T0	No evidence of primary tumour
Tis	Tumour in situ
T1	Histologically bound tumour to bile duct wall
T2	Tumour extended beyond the bile duct wall
T3	Tumour that invades the liver, gallbladder, pancreas and/or a single branch of the portal vein
T4	Tumour that invades one of the following structures: main portal trunk or its branches bilaterally, common hepatic artery or other adjacent organs such as colon, stomach, duodenum, or abdominal wall
Nx	Regional lymph nodes not definable
N0	Absence of metastases in regional lymph nodes
N1	Presence of metastases in regional lymph nodes
Mx	Distant metastases not definable
M0	Absence of distant metastases
M1	Presence of distant metastases

Table 2 Cancer classification.

2.3.8.2 Cholangiocarcinoma (CCA)

Cholangiocarcinoma is a malignant neoplasm of the biliary ducts and it is the second most common primary liver cancer. The most widespread classification of CCA is based on its anatomical location. CCA are commonly staged into intrahepatic (IH- CCA) and extrahepatic (EH-CCA) tumors. EH-CCA can further be subdivided into perihilar CCA, which are also called Klatskin, and distal tumors.
Major signs and symptoms of cholangiocarcinoma include impaired liver function tests, abdominal pain, jaundice, weight loss and sometimes generalized itching, fever, abnormalities in stool or urine color. The disease is diagnosed through a combination of blood tests, imaging techniques, endoscopy, and surgical exploration. It often manifests itself at an advanced stage and this may limit treatment options.
Blood tests of liver function in patients with cholangiocarcinoma often reveal high levels of bilirubin, of transaminase and CA 19-9 (explained later).
An important part of diagnostic evaluation is staging, which determines the structures and organs affected by cancer. Assessing the stage helps to define the prognosis and to select therapies. The most common system is the four-stage TNM system, as seen before.
However, cholangiocarcinoma is considered an incurable and rapidly fatal disease. There is no potentially curative treatment, except surgery, but most patients present an advanced and inoperable disease at the time of diagnosis. Patients with cholangiocarcinoma are generally managed, even if not treated, with chemotherapy or radiotherapy, as well as palliative care. These methods are also used as post-surgical adjuvant therapy in cases where resection has been successfully performed [29].

2.4 Liver surgery: hepatectomy

2.4.1 What it is

Liver resection is a surgical procedure that involves the removal of a portion of the liver. Hepatectomy or resection is always indicated by the presence of a neoplasm that can be benign or malignant.
Among the pathologies, for which liver resection is a frequent indication, there are:

- benign pathologies
- cystic pathologies
- hepatocarcinoma
- intrahepatic cholangiocarcinoma
- extrahepatic bile duct neoplasms (Klatskin’s cancer)
- neoplasm of the gallbladder
- liver metastases from colorectal neoplasm or other sites.

In most cases it is possible to make a diagnosis of the nature of the injury before surgery, through the patient’s clinical history, the level of particular onco-markers in the blood and pre-operative imaging (typically computed tomography or magnetic resonance with a dye), or in doubtful cases by percutaneous biopsy puncture of the lesion and subsequent histological examination of the sample taken. In some cases, however, the pre-operative examinations listed above are not straight and the diagnosis can only be made intraoperatively with the help of an extemporaneous histological examination or sometimes only after surgery thanks to the final histological examination of the removed piece.

In addition to the malignant or benign nature of the lesion to be removed, other parameters considered by the surgical team during the planning of the intervention are represented by the size and location of the neoplasm and the functionality of the patient’s liver, especially when greater hepatectomy is necessary for oncological radicalism.
In these cases, the postoperative functionality of the liver is evaluated through the calculation of the residual liver volume after surgery on the basis of the performed pre-operative imaging (volumetrics) and through the execution of the indocyanine green test, little invasive and easily achievable in surgery, which analyzes the rate of metabolization of this substance by the liver: the greater the functionality of the liver the greater the volume of removable liver without incurring in post-surgical liver failure.
In relation to the number of segments to be removed, partial hepatectomy interventions are divided into:

- minor hepatectomy (consisting in the removal of up to 2 adjacent hepatic segments):
  - atypical liver resection or "wedge resection"
  - segmentectomy (a single segment)
  - bisegmentectomy (two segments)
  - septicaectomy (two sectors)
  - left lobectomy (or left lateral septicemia or bisegmentectomy II - III)

- major hepatectomy (consists in the removal of at least 3 adjacent hepatic segments):
  - trisegmentectomy
  - mesohepatectomy
  - right hepatectomy
  - right hepatectomy enlarged to segments 4a and 4b
  - left hepatectomy
  - left hepatectomy enlarged to segments 5 and 8

Some types of hepatectomy are shown in Figure 13.

Figure 13 Different types of hepatectomy [30].

In some cases, together with hepatectomy, for anatomical reasons, it is also necessary to remove the gallbladder, or proceed to partial or radical resection of the biliary ducts with a consequent need to rebuild the bilio-digestive continuity through a bile anastomosis (i.e., seams) between the remaining bile ducts and the intestine, to restore the bile outflow in the digestive tract.

In addition, in the perspective of oncological radicality or diagnostic deepening, the removal of regional lymph nodes, that drain the lymphatic fluid, can be performed.

In particular situations it is considered appropriate to proceed to a surgical treatment in two stages: the first surgery is aimed at the removal of the localized disease in one of the two emi-livers; the second operation is interspersed with a time interval varying between a few days and a few weeks, in order to allow adequate residual liver growth to support vital functions and allow the completion of the removal of the disease without compromising the postoperative functionality of the organ.

Whether it is one-time or two-time resections, there are radiological and endoscopic procedures to optimize liver function before surgery and to minimize possible postoperative complications (for example, placement of bile drainage/endoprostheses, placement of nutritional probes).

2.4.2 Surgical procedure

Prior to surgery, the patient must undergo tests to assess the suitability of the general state of health.

The surgery requires a general anaesthesia, which allows the loss of consciousness, the relaxation of all muscles to make the surgery possible and an adequate pain therapy. For this purpose, in addition to routine preoperative examinations (blood tests, electrocardiogram and chest X-ray), there will be an anaesthesiologic specialist visit during which the suitability for general anaesthesia will be evaluated, including the request for further investigations (for example, cardiological, pneumological, haematological investigations).

Access to the abdominal cavity for surgery can be performed by laparotomy or by minimally invasive laparoscopic technique.

The laparotomy technique consists of a single incision under the right rib arch, also known as a J incision. This mode of access allows the surgeon to operate any type of liver resection.

The operation with laparoscopic technique is, instead, realized through small cutaneous incisions that allow the introduction of surgical instruments through the abdominal wall without extended incisions. Under the guidance of the images taken by an optical fibre camera inserted through one of the entrances, the surgeon is able to perform the planned surgery.

The conversion of laparoscopic surgery to the traditional open abdomen technique remains possible at any time and it is considered by the surgeon in the face of intraoperative situations that make it appropriate (anatomical reasons, techniques, anaesthesiology). The probability of conversion varies 10-20% depending on the type of yield and the characteristics of the disease.

During surgery it may be necessary to perform an extemporaneous histological examination of the lesion and based on the results or due to intra-operative findings not highlighted in pre-operative investigations, the procedure could be extended beyond the set limits. For the same reasons, it may be necessary to remove other abdominal organs (or parts of them) that may be involved in the disease, and which cannot be kept for radical reasons.

2.4.3 Post-operative hospitalization

After the surgery, the patient returns to the ordinary inpatient ward, where he will be followed by highly specialized medical and nursing staff throughout the hospitalization. At the end of the surgery, the patient will be carrying a bladder catheter (which will allow monitoring of diuresis) and one or more venous accesses (which will allow the administration of fluids and drugs intravenously).

For a quick and effective recovery, it will be important to follow the instructions of the medical and nursing staff, in particular times and methods of mobilization. The patient will be stimulated to sit in an armchair for a few hours from the day after the surgery and to walk for short stretches from the second day, using an elastic girdle suitable to prevent the onset of post-surgical hernias (incisional hernias).

It will also indicate the most suitable times and methods for an effective recovery of food, according to the specific type of intervention. Generally, the patient resumes drinking the day after the surgery (after the removal of the nasogastric tube), and he starts to take an oral diet during the second day after the surgery and then switch to a free diet if well tolerated.

Upon exit from the operating room the patient may be provided with all or only some of the following devices:

- central venous catheter (CVC): a small-caliber catheter inserted into a vein in the neck that is needed to infuse high volumes of fluid, to allow monitoring of certain parameters and the administration of drugs, particularly useful in the presence of severe heart disease. As a rule, CVC is not positioned, unless the patient needs prolonged infusions in the postoperative period, parenteral nutrition, or to administer specific drugs. Also, in case of difficulties in finding peripheral veins, the placement of the CVC is indispensable. It is removed when the patient no longer needs to receive infusions and drugs from this route.
- nose-gastric tube (NGT): this is a catheter that enters from the nose and it ends in the stomach. It aims to aspirate the secretions produced by the stomach. Generally, the SNG is removed the day after surgery. In cases where a bilious digestive anastomosis or intestinal resection were performed, the SNG will remain in place for several days.
- abdominal drainage: these are soft tubes that allow to drain the material produced by the body as a result of surgery; it generally has serous characteristics with blood traces. In the case of biliary fistula (see below), it allows to drain the bile outside. In case of liver failure with the formation of ascites (explained later), the drains allow to quantify the amount of ascitic fluid produced and to drain it outside avoiding stagnation at the level of the surgical site. In both cases, this decreases the risk of the formation of infected collections that would require additional medical and possibly interventional therapies. The drains are removed as soon as possible, with a simple manoeuvre, directly into the hospital bed.
- fasting catheter for supplementary nutrition: catheter that enters one of the first loops of the intestine and it is used for the administration of additional nutritional mixtures to normal oral nutrition. Its positioning will be considered in case of unsatisfactory nutritional status or at the end of extensive liver resections. This device will be removed about two months after the surgery if not more necessary or, if not, also used at home to continue the nutritional supplementation started in hospital.
- percutaneous transhepatic biliary drainage (PTBD): in some patients there is finally a biliary drainage. It is a thin tube that enters the bile duct through the hepatic parenchyma and ends in the intestine. The drainage is then closed and placed under dressing, and then removed after about 4-6 weeks from its placement.

In the post-operative period, the patient can be subjected to blood tests, abdominal ultrasound, chest x-ray and other instrumental investigations to better evaluate the course of surgery and functional recovery of the liver.
In the absence of complications, the patient can be discharged at home after 5-7 days from surgery.
The convalescence usually provides for a period of four/five weeks during which limitations of movements are manifested in a variable and subjective way, related to pain at the surgical site. This affects a temporary total or partial work disability, depending on the type of work performed and also in relation to the type of surgical approach used ("open" or laparoscopic).
Within five/six weeks of surgery, it is possible to fully resume working and sports activities.

2.4.4 Benefits

The purpose of hepatic resection is the lifelong removal of the pathology under-diagnosed, for the purpose of symptoms improvement and prevention of possible complications. This type of treatment is in many cases the only therapeutic option that can offer healing to the patient, and therefore to prolong their life expectancy and maintain a good quality.
For cancer patients, liver resection is a treatment of the multimodal therapeutic path: it follows or precedes complementary treatments (chemotherapy, radiotherapy, biological therapies, interventional radiological procedures), with the aim to optimize long-term results.
For patients with benign diseases, the purpose of liver resection is to preserve the quality of life and prevent possible complications of the disease; moreover, symptomatic benign diseases find in liver resection their definitive and optimal treatment.

2.4.5 Potential risks and complications

Like all invasive procedures, even hepatectomies present perioperative risk and may require a very variable post-operative stay, related especially to the possible onset of complications. They have an important impact on the total hospitalization: the state of the liver, the general condition of the patient and his age, the amount of liver removed, the presence of concomitant diseases (heart disease, renal and respiratory diseases, diabetes, etc.).
Major hepatectomies, unlike the minor ones, have a greater risk of post-operative liver failure, especially in cases of particularly extensive resections.

Complications after liver surgery have a very variable incidence with a range between 4.8% and 46%:

- moderate/intense abdominal pain at the end of the effect of anaesthesia. This is managed through administration of peridural, intravenous and/or oral painkillers;
- bowel closed to the faeces for 2-3 post-operative days, especially after "open" surgery. usually, this situation is resolved spontaneously, in case of constipation, it is resolved with laxatives for one month;
- inappetence, also resolved spontaneously after a few days;
- skin wounds can repair abnormally, and the scar can become thicker and redder (scars hypertrophic and keloid);
- pleural effusion: consists of the accumulation of fluid between the chest wall and the lung. It is caused by irritation of the diaphragm muscle which, for anatomical reasons, can be repeatedly manipulated during liver resection. It is usually reactive in nature and it is absorbed spontaneously, however in some cases it is necessary to proceed to

thoracentesis (evacuation of pleural fluid through aspiration) or to placement of a chest tube removed as soon as possible, and always before discharge;

- bleeding: the liver is a very vascularized organ. About 20-30% of patients need blood transfusions during or after the surgery. In the case of bleeding that occurs during the postoperative period, there is a possibility that a further surgery is necessary to stop the bleeding and remove the clots;
- biliary fistulas: consists of the escape of bile from the section surface of the liver. When the liver is dissected, bile ducts are broken and sutured. In most cases, the bile is drained from outside by drains placed during surgery. Other times the healing of the fistula is facilitated by the insertion of a percutaneous or endoscopic hepatic drainage. In the case of high-flow fistulas, surgical re-intervention may be necessary;
- liver failure: after a major hepatic resection, liver function may be insufficient and cause various problems (alteration of both synthesis and metabolization of substances resulting in the development of ascites, hepatic encephalopathy, coma). Usually, the liver regenerates with appropriate medical therapies and often it is possible to overcome this critical phase after a variable period of time. In cases where this is not possible and where there is the presence of criteria for inclusion in the list, irreversible liver failure may require urgent liver transplantation;
- infections: both in the liver and abdomen (abscesses) and in the skin wound (subcutaneous collections). Abscesses are usually emptied under CT or ultrasound guidance and the patient undergoes antibiotic therapy. Only rarely it is necessary a re-intervention;
- incisional hernias: abdominal hernias that can form at the surgical wound and may require a reconstructive surgery of the wall;
- lesions of nearby organs (stomach, intestines, etc.): if recognized during surgery, they can easily be repaired. If they are evident in the postoperative period, a re-intervention may be necessary;
- adhesions: can be formed between the abdominal organs and between them and the abdominal wall. This is more likely after "open" interventions, especially in those involving extensive resections and concurrent resections of organs other than the liver. They can appear at any time in life, resulting in an intestinal occlusion that may require surgical re-intervention;
- postural injuries: possible for positioning the patient on the operating bed and influenced by the duration of the surgery. They are usually nervous or muscular in nature and they resolve within a variable time ranging from a few days to a few weeks;
- in most cases, the mortality rate in patients with healthy liver, without concomitant pathologies and in which a proportion of liver tissue less than 60-70% of the total is removed is less than 1%. The mortality rate can reach 10% in the case of extended liver resections in patients with liver impaired by liver cirrhosis, prolonged chemotherapy, or significant jaundice (as is often the case for patients with Klatskin’s cancer). Mortality is more frequently due to postoperative liver failure and infections (usually abdominal or pulmonary).

  In order to reduce the risk of mortality linked to postoperative liver failure, the adequacy of the remaining liver portion in anticipation of extended hepatic resection will be evaluated from the volumetric (through CT or MRI volume) and/or functional (by sequential hepatobiliary scintigraphy) point of view. In the case of suboptimal preoperative values, a preventive procedure may be proposed to stimulate the increase of liver volume and its functionality [20] [31].

2.5 Epidemiology

Before analysing the spread of malignant liver tumours, it is necessary to report the epidemiology of the main liver pathologies that can cause cancer, namely hepatitis and cirrhosis.

2.5.1 Hepatitis

According to the World Health Organisation (WHO), viral hepatitis is still a major public health problem worldwide. According to WHO data, in 2020 325 million people in the world live with a chronic infection of hepatitis B or C and 1300 thousand people die every year due to liver complications caused by infections.
More precisely, in 2016 the hepatitis A virus caused 7134 thousand deaths worldwide. Anti-HAV vaccination, together with good sanitary conditions and increased attention to food safety, are the most effective preventive measures.
Based on the prevalence of HAV, three geographical areas can be distinguished:

- high endemic areas (low and medium-income countries) with poor sanitary conditions. In these areas, infection usually does not occur in epidemic form, as most of the infected are children under 10 years of age, while adolescents and adults are immune;
- intermediate endemic areas, which include middle-income countries with variable sanitary conditions. In these areas, infection occurs especially in adults and important epidemics can also occur;
- low endemic areas, which include industrialized countries with good sanitary conditions. In these countries, the infection affects adolescents and adults the most. The main risk factors are travel to endemic areas and consumption of contaminated food or water.

Regarding the hepatitis B virus (HBV), there are about 257 million chronic carriers, of which it is estimated that only 10% are aware of their carrier status. Without proper management, approximately 20% will die early of liver failure or hepatocellular carcinoma. Indeed, in 2015 the WHO estimates that about 887 thousand people died because of the consequences of hepatitis B. The vaccine is the most effective preventive measure. HBV burden and mortality are high but are expected to decline because of universal childhood vaccines programs that have scaled up since 2010 but it will take 15 to 20 years to see the full effect.
According to the WHO, around 71 million people worldwide are chronic carriers of the hepatitis C virus (HCV). WHO estimates that 399,000 people died in 2016 from liver disease related to this virus. Hepatitis C is a blood-borne virus and currently there's no vaccine that can prevent infection.

In Italy, the improvement of hygienic and socio-economic conditions and a greater knowledge and awareness of the risk have been associated with a great change in the epidemiology of viral hepatitis. In the last 30 years there has been a progressive decrease in the incidence of hepatitis A and, even more, of hepatitis B and C.
In recent years, the Integrated Epidemiological System of Acute Viral Hepatitis (SEIEVA) in Italy has recorded 0.5 to 0.2 new cases of acute infection per 100,000 inhabitants, with a mortality rate linked to the pathology of about 8-10 thousand people/year (Figure 14) [32].

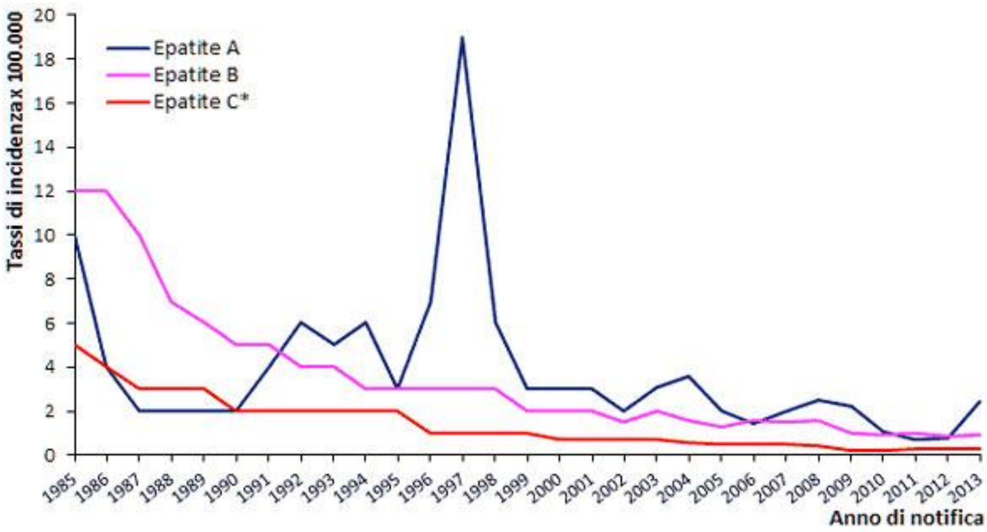

Figure 14 Incidence rates per 100 000 inhabitants of acute viral hepatitis, per year, in Italy [32].

2.5.2 Cirrhosis

Cirrhosis is one of the main causes of death and morbidity in the world. In 2016 it was registered as the eleventh cause of death (2.2%) and the fifteenth cause of morbidity (1.5% of disability adjusted life years) in the world.
The prevalence of cirrhosis has been estimated at around 0.15% in the United States, with data substantially similar in Europe and with numbers even higher in most African and Asian countries (where chronic viral hepatitis B or C are common).
Currently the total number of people with liver's cirrhosis worldwide is estimated to be 1.5 billion. As shown in Figure 15, the main causes are NAFLD (59%), followed by HBV (29%), HCV (9%) and alcoholic liver disease (ALD) (2%) [33].

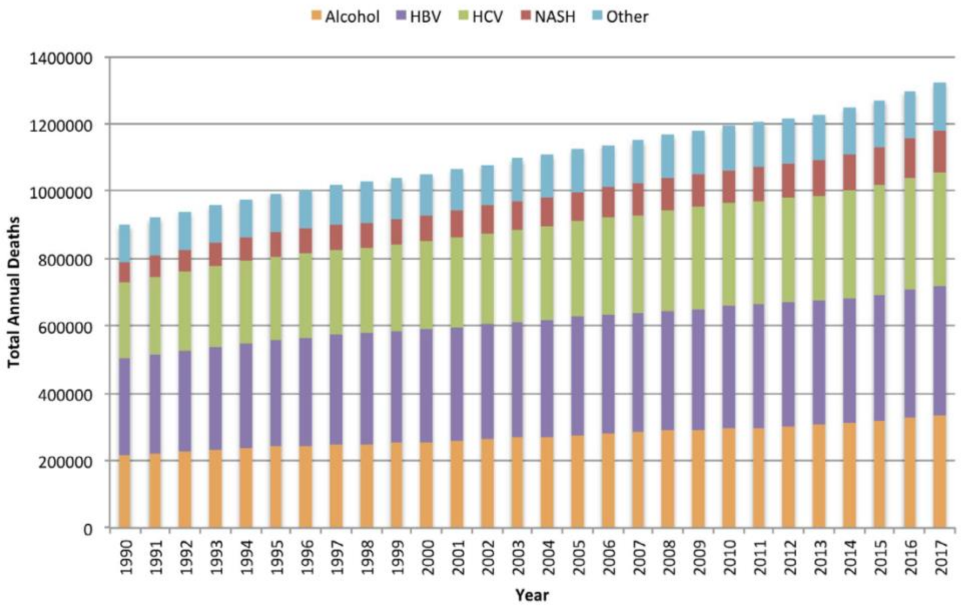

Figure 15 Total global deaths from cirrhosis per year [33].

In the future, on one hand, NAFLD and ALD are expected to increase given that most of the world is experiencing increasing obesity rates and many areas are experiencing increasing alcohol consumption. On the other hand, HBV's burden will most likely decline with greater vaccination coverage [33].
The mortality rate for cirrhosis in Italy increased sharply between 1960 and the second half of the 1970s and then showed a downward trend; this trend led to an annual mortality rate of 14.8 per 100,000/inhabitants in 1961, in the late 1970s, the rate was around 40, and in 1998 it was below 20.
Mortality has therefore halved over the last 30 years, in particular as a result of the reduction in the number of new infections with HBV and HCV over time (the peak of new infections occurred about 40-60 years ago, through the use of sanitary equipment not adequately sterilized or with blood transfusions of contaminated blood) [34].

2.5.3 Primary Liver Cancer

Primary liver cancer is the fifth most common type of cancer worldwide and is the second most common cause of death in cancer patients, with Africa and Asia leading by the highest rate of incidence.
In 75% of cases, it is hepatocellular carcinoma (HCC). In the years between 1978 and 2012, the incidence of HCC spread decreased in some areas such as Asia and even Italy, but it increased in other countries such as India, America, Oceania, and most European states. In 2018, the estimated global incidence rate of liver cancer for 100,000 person-years was 9.3 while the corresponding mortality rate was 8.5 (Figure 16). This happens in all regions of the world because the prognosis is not excellent, so incidence and mortality have similar values.
In most populations, people with HCC have an average age of 75 years, even though the average age of diagnosis is a little lower. For example, in the United States, the average age is between 60 and 64, whereas for women it is between 65 and 69. Moreover, in most countries, incidence rates among men are two to four-fold higher than rates among women.
Variations in geographical area, gender and age vary mainly due to the prevalence of risk factors. The main exposures to risk are determined by HBV and HBC, whose epidemiology has been explained above. These factors could be replaced by NAFLD and ALD in the future [35].

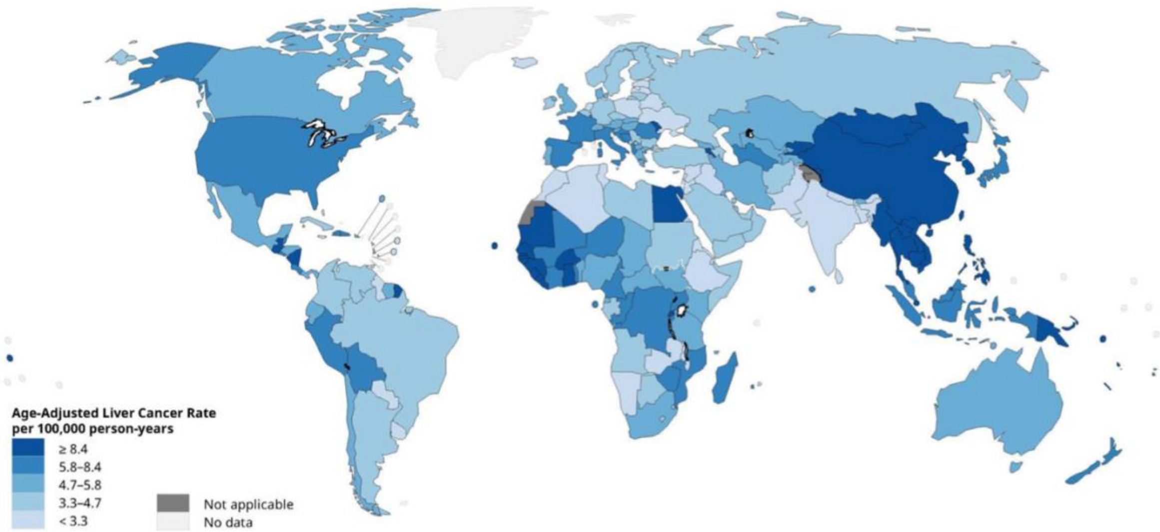

Figure 16 Global age-adjusted incidence rates of liver cancer, estimated for 2018 [35].

In Italy in 2018, the diagnosis is about 12 800 new cases of HCC, about 3% of all new cases of cancer. Southern Italy is characterized by higher incidence and mortality. This incidence decreases in northern Italy, probably due to the different incidence of hepatic virus infections and in particular hepatitis C virus. Although HBV is a pathogenic factor of HCC, its incidence in Italy is mitigated by the availability of an effective vaccine administered to all subjects born from 1978 onwards.
The report AIRTUM 2018 (Italian Association of Cancer Registry) shows that in Italy live 33 thousand people with previous diagnosis of hepatocellular carcinoma. The proportion of people aged 75 years old with cancer is 25% higher than those aged 64-74.
In Italy, HCC is among the first 5 causes of death from cancer in males of any age, but it ranks third in the 50-69 age group. This mortality is higher in the South (22.5 deceases x 100 000 inhabitants/year in males, 8.8 in females) than in the center and north. However, since the early 1990s, mortality has declined: in males 1.6% per year and in females 1.3% [36].

The incidence of cholangiocarcinoma differs according to the geographical areas (Figure 17), demonstrating a different exposure to multiple risk factors and a different genetic heritage. Nowadays, the world incidence is highest in Asian countries with rates ranging from 3.5 to 14.7/100,000 in Japan, Korea and Thailand. Also, in Europe the trend is increasing, especially in England (2.17/100.000), Austria (2.67/100.000) and Germany (3/100.000).

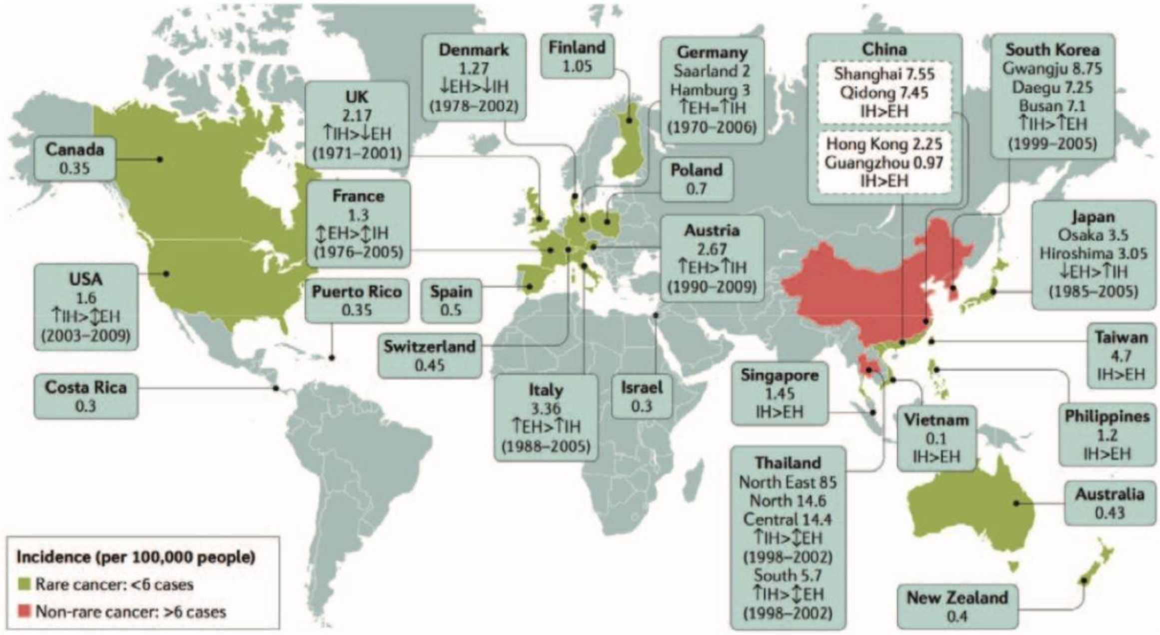

Fig. 1. Global incidence rates of CCA [71].

Figure 17 Global incidence rates of CCA [37].

The WHO database shows an increase in IH-CCA (increased by 128% in the United States between 1973 and 2012), while the incidence of EH-CCA remains stable.
In the same years, a drastic decrease in the incidence of non-primary liver cancer occurs. Probably because with the improvement of diagnostic techniques, many tumors wrongly considered not primitive have been traced back to IH-CCA.
Indeed, among malignant liver diseases, IH-CCA emerges as mortality more than tripled in both women and men between 1998 and 2008. In the same period, the mortality of HCC and EH-CCA remained stable.
The number of subjects with IH-CCA also increased in the same years.
Most patients are diagnosed with CCA after 75 years and more in men than in women [37].

For what concern Italy, the incidence is about 5000 cases expected per year (or 1% of all new cases of cancer). However, these incidence rates are continuously increasing of about 4.5% per year. It is estimated that, by 2035, worldwide more or less 50% of the causes of death from primary liver cancers will be attributed to this neoplasm [38].

3 Description of the technology and its comparators

3.1 Imaging workflow in CAS

Computer aided surgery (CAS) system is a set of devices mastered by computers aiming at increasing the dexterity (manual ability). It provides visual and haptic feedback, augmenting information for the surgeon at the time of intervention. Three-dimensional reconstruction is an example of CAS systems, that optimize and help the activity of the surgeon.
The typical workflow, shown in Figure 18, starts from bidimensional images to a patient specific model.
The first step is image acquisition (CT, MRI) in order to provide bidimensional images that will be preprocessed through data conversion, interpolation and filtering. For complicated liver diseases, 3D reconstruction can be performed based on fusion imaging of MRI and CT.
The goal of imaging workflow in CAS is to generate a 3D rendering: a visualization (with different level of elaboration) of anatomopathological models (surfaces/volumes) obtained from bioimages. Therefore, segmentation is a fundamental preliminary step to obtain a 3D rendering. It means the manual, semi-automatic or automatic extraction of specific features on 2D images.
The final output can be surface-based rendering or voxel-based rendering.
To make the first one, it's fundamental to come back to 2D and define contours, that will be connected between slices to make a surface representation. However, tissue density information could be useful for surgical planning. In this case, a voxel-based rendering is obtained, providing more realistic information [39].

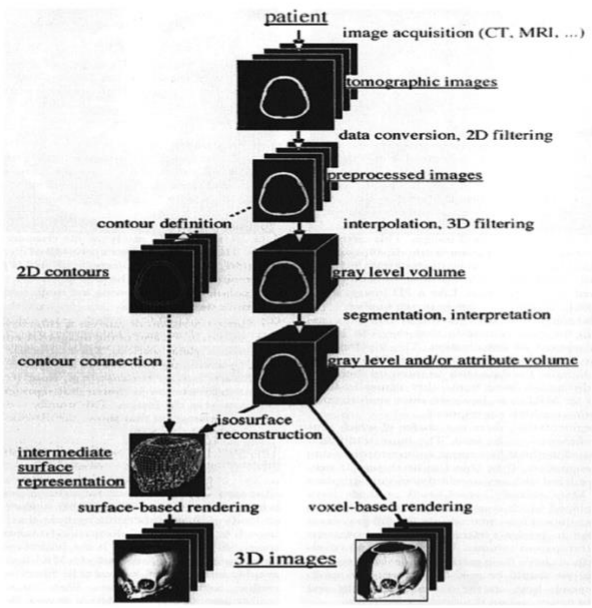

Figure 18 Imaging workflow in CAS system [39].

3.1.1 Tomographic images

Three dimensional renderings are usually done from CT images.
Computerized tomographs are among the most used technology in diagnostic imaging.
In traditional systems, image acquisition was slice per slice: tube starts from still, it rotates while accelerating and it decelerates after complete rotation. Couch is still during acquisition, and it advances for the following slice. This mechanism is characterized by long scanning time for coach and tube inertia and many artifacts generating by the starting and stopping of the technology.
Nowadays, helical CT is the dominant technology. Tube rotates continuously with no acceleration or deceleration while couch advances continuously. This new technology is characterized by shorter scanning time and artifacts reduction, even if they are still present.
A further innovation is multislice CT, composed of between 4 to 64 detector arrays that allow determining longitudinal spatial resolution (slice thickness) as function of beam collimation.

A schematic of fixed-array detector geometry for a multislice spiral scanner is represented in the left part of Figure 19. As it can be seen in the right side, four configurations connecting the data acquisition channels to single or multiple elements of the arrayed detectors produce four different slice thicknesses. For a thickness of 5 mm, the collimated beam shown on the left covers all 16 detectors. The degree of collimation can be decreased progressively to cover only the central 12 detectors (3,75 mm of thickness), the central 8 detectors (2,5 mm slices of thickness) or the central 4 detectors (1,25 mm thickness of thickness).

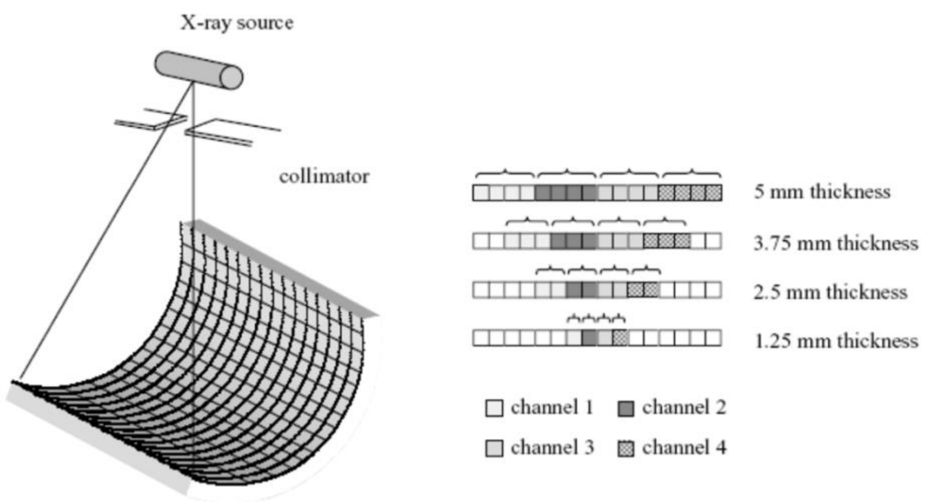

Figure 19 Longitudinal spatial resolution and beam collimation [39].

Each CT slice is the 2D representation of the densities of 3D elements (voxel). Typical voxel dimensions are 0,98x0,98x3 mm. These sizes are relevant in terms of defining resolution. The first two dimensions are given by the field of view divided by the number of pixels. Only slice thickness (third dimension) is selected by the operator: to have a more accurate image is necessary to stablish the minimum slice thickness.
Moreover, another characterizing parameter is the pitch: TF (table feed in mm per 360° rotation)/(N (number of detector rows) x SC (slice collimation in mm)).

CT images are acquired in DICOM format, standard method for storage and communication of bioimages. It is based on object-oriented architecture: information from the real world (patient, images) are modeled as informative objects named Information Object. Specific operations, named as Service Class, are allowed on each object (storage, print, query, retrieve) [39].

Image file consists of header, which contains relevant tags such us patient data, examination data and other administrative information and if consist of image data with the number of rows, columns, and grey levels.

3.1.2 Image acquisition recommendation for three-dimensional visualization

The workflow to build the three-dimensional rendering from CT images is shown in Figure 20.

A routine normal CT scan should be performed with the patient supine, scanning from the upper diaphragm to the lower level of both kidneys to ensure coverage of the entire liver and portal vein.

Typically, a contrast medium is administered. For bolus injection, the usual dose is 1.0 to 2.0 ml/kg (1.5 ml/kg for obese patients) at an injection rate of 4.7 to 5.0 ml/s. Scanning begins immediately after administration. The arterial phase is acquired with a delay of 20-30 s. Portal, venous and delayed scans begin, instead, with a delay of 60-70 s and 2 min from the start of contrast agent administration.

The scan interval should be adjusted according to the clinical status of each patient and the scan parameters should be set according to the specific CT scanner.

Acquisition characteristics also depend on pathology. For patients with hepatocellular carcinoma, more attention should be given to the quality of the image in the arterial, portal, and venous phase, and for those with cholangiocarcinoma, particular attention should be paid to the image quality of the delayed phase.

Multiphase images (arterial phase, portal venous phase and delayed phase) should be obtained from a 64 or superior slice helical CT scanner with a cross-section thickness of 0.625-1 mm. Data must be stored in the DICOM database and exported via storage devices. Recommended CT parameters are: tube voltage of 100-140 kV, or set the optimal voltage according to the size and weight of the patient, pitch 0.891-0.915, wide scanning range, standard reconstruction algorithm and thin layer reconstruction if necessary [5] [40].

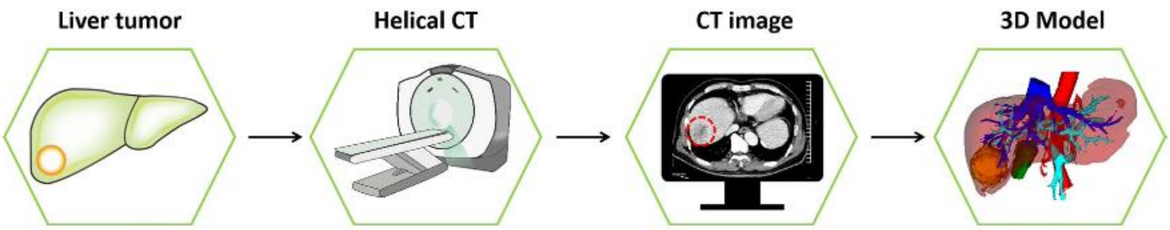

Figure 20 Flowchart depicting the workflow from image acquisition to 3D model visualization [5].

3.1.3 Image pre-processing

Easing the manual or semi-automatic segmentation is the aim of pre-processing. It means to apply geometric transformation, select region of interest (ROI), resampling (enhance spatial resolution through interpolation increasing the ability to differentiate multiple levels of grey) and filtering. The last one technique means to reduce noise and enhance contrast of valuable structures. There are different filtering techniques: smoothing, average, median filtering and filter based on image statistics.
Smoothing means to reassign to every pixel v_0 a value which is obtained from weighted average of surrounding pixels. Typically, the cluster taken in consideration is made by 8 pixels, but difference choices are available depending on the level of smoothness.

The rule (3.1) is the general rule of smoothing:

$$g_0(v_0) = \frac{\sum_{j=0}^{n} w_j g_i(v_j)}{\sum_{j=0}^{n} w_j} \tag{3.1}$$

With:

- $g_0(v_0)$: v_0 intensity for filtering procedure
- $g_i(v_j)$: pixel intensity (v_j) before filtering
- w_j: weights assigned to pixels.

Trough smoothing, gaussian errors can be cancel out but regions with different grey levels are also smoothed. For this reason, it’s important to define a tradeoff between errors elimination and smoothness [39].

3.1.4 Segmentation

Segmentation process means to delineate anatomical structures, through the classification of pixel/voxel, regions, and contours. It’s not an easy task: it varies a lot as function of specific structure with transient gradient not really sharp.
Many manual, automatic and semi-automatic methods are available.

3.1.4.1 Region-based method

The first one is called region-based: pixels are classified for homogeneity as belonging or not to a structure. Two different techniques are thresholding and region growing.
In the former (Figure 21), a gray level is selected as threshold and pixels are classified as under/over threshold (binarization), as shown mathematically by the formula (3.2):

$$\begin{aligned} g(i,j) &= 1 \qquad if \qquad f(i,j) \geq T \\ g(i,j) &= 0 \qquad if \qquad f(i,j) \leq T \end{aligned} \tag{3.2}$$

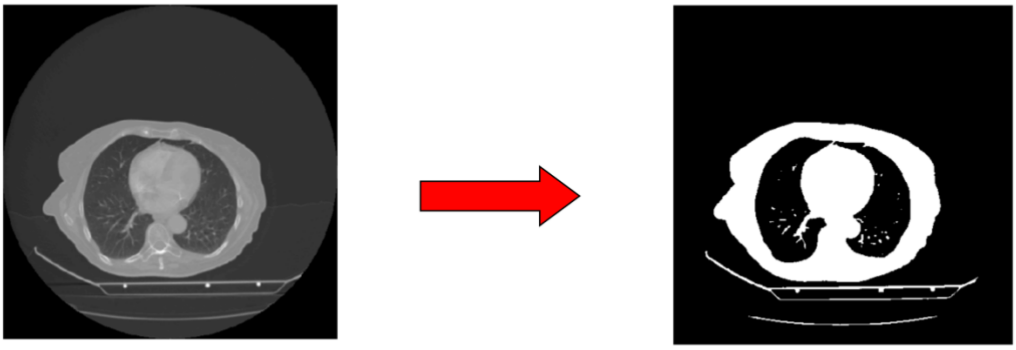

Figure 21 Example of application of thresholding method[39].

Threshold selection is crucial. It can be selected through a trial-and-error technique or looking at histogram of grey levels of the image or of specific image portion, in a unimodal, bimodal, or multimodal way. Bi-level thresholding can be defined as in the equation 3.3:

$$g(i,j) = 1 \quad if \quad f(i,j) \in D, \quad with\ D\ specific\ gray\ level\ interval \tag{3.3}$$

Region growing is another technique based on homogeneity, where pixels with similar features are clustered, starting from one or more initial pixel (seed), which is manually defined. If homogeneity criteria are met, pixels are included in the growing region. These inclusion criteria can be the single pixel, the average or variance of pixels intensity belonging to a specific interval [39].

3.1.4.2 Edge-based method

Edge-based method is a segmentation technique that searches for intensity discontinuity. The edge groups the pixels which separate 2 different regions. Ideally the intensity changes abruptly in correspondence of the edge, as shown below Figure 22.

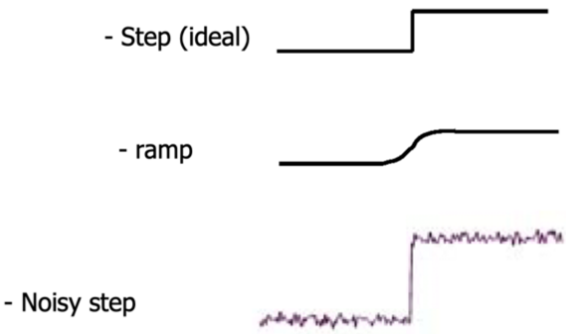

Figure 22 Edge typology.

In order to identify rapid variations, derivative operators can be used, searching for the maxima of the first derivative or the zeros of the second derivatives of the image function. The derivative operation equals the convolution between the image and a kernel, being this latter defined to be sensitive to intensity variations.

$$O(i,j) = \begin{bmatrix} I_{11} & I_{12} & I_{13} & I_{14} & I_{15} & I_{16} & I_{17} & I_{18} & I_{19} \\ I_{21} & I_{22} & I_{23} & I_{24} & I_{25} & I_{26} & I_{27} & I_{28} & I_{29} \\ I_{31} & I_{32} & I_{33} & I_{33} & I_{34} & I_{35} & I_{36} & I_{37} & I_{38} \\ I_{41} & I_{42} & I_{43} & I_{44} & I_{45} & I_{46} & I_{47} & I_{48} & I_{49} \\ I_{51} & I_{52} & I_{53} & I_{54} & I_{55} & I_{56} & I_{57} & I_{58} & I_{59} \\ I_{61} & I_{62} & I_{63} & I_{64} & I_{65} & I_{66} & I_{67} & I_{68} & I_{69} \\ I_{71} & I_{72} & I_{73} & I_{74} & I_{75} & I_{76} & I_{77} & I_{78} & I_{79} \\ I_{81} & I_{82} & I_{83} & I_{84} & I_{85} & I_{86} & I_{87} & I_{88} & I_{89} \\ I_{91} & I_{92} & I_{93} & I_{94} & I_{95} & I_{96} & I_{97} & I_{98} & I_{99} \end{bmatrix} \times \begin{bmatrix} K_{11} & K_{12} & K_{13} \\ K_{21} & K_{22} & K_{23} \end{bmatrix}$$

$$= \sum_{k=1}^{m} \sum_{l=1}^{n} I(i+k-1, j+l-1) \times K(k,l)$$

$$with\ i = 1 \dots M - m + 1\ and\ j = 1 \dots N - n + 1 \tag{3.4}$$

For instance, a result can be:

$$O_{57} = I_{57}K_{11} + I_{58}K_{12} + I_{59}K_{13} + I_{67}K_{21} + I_{68}K_{22} + I_{69}K_{23}$$

Finally, there are different types of kernels and some of them combine a smoothing procedure.

3.1.5 Deep learning

Feature extractions can be performed also by machine learning algorithms, able to learn patterns from existing data and applies it to a new data.
Deep learning is a subset of machine learning in which artificial neural networks adapt and learn from a great amount of data. It is composed by computational model based on the interconnection of basic processing units (artificial neurons). Neurons are trained to filter and detect specific features or patterns by receiving weighted input, transforming it with the activation function and passing it to the outgoing connections.
An example of artificial neural network is convolutional neural network (Figure 23).
It presents multiple layers of transformations (convolution), which are applied on top of each other to extract a progressively more sophisticated representation of the input. The learning method is based on the generation of an error signal that measures the difference between the predictions of the network and the desired values and then the usage of this error signal to change the weights in order to make predictions more accurate. Finally, the output layer combines those features to make predictions.

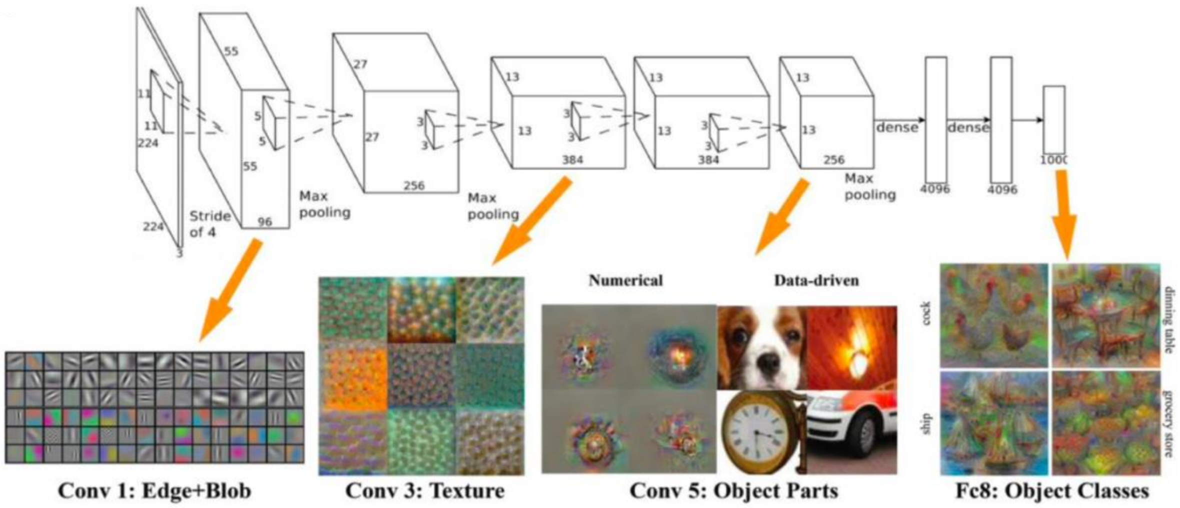

Figure 23 Convolutional neural network [39].

3.1.6 3D model generation

3.1.6.1 Surface based rendering

Surface based rendering drops volumetric information coming from CT volume reducing computational costs. There are two different main methods: contours connection and Delaunay triangulation.

3.1.6.2 Contours connection (tiling)

Tiling method considers points sequence P and Q on two contiguous slices (Figure 24). Between the two slices, polygons are formed following these rules:

1. all vertices must lie on P and Q;
2. if $Q_j - P_i$ is a side of a triangle, then $Q_jP_iP_{i+1}$ or $Q_jP_iQ_{j+1}$ is the adjacent triangle in the tiling process;
3. each triangular element has at least one vertex on P and one on Q.

The above listed constraints are satisfied for each path from upper left corner to the lower right corner on the plane P-Q (right image). For this reason, there is the need of an additional heuristic optimization criteria for example an initial condition, a triangular area minimization or a maximization of volume.

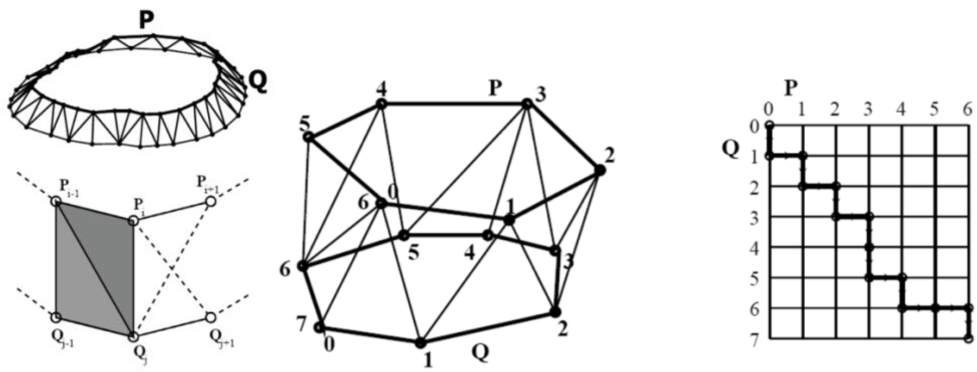

Figure 24 Contours connection [39].

3.1.6.3 Delaunay triangularization

Delaunay triangularization is a general method of generating surface from points in space (it works also for points scattered out or regular distribution of points available after methodical segmentation). It is based on the 2 following rules:

1. given a set of n points (2D), Voronoi diagram produces a partition of the plane in n cells such that for each point q belonging to the i-th cell associated to point p_i, it holds: $dist(q, p_i) < dist(q, p_j)$ for each p_j con $j \neq i$.
2. the triangle which connects 3 generator points of the Voronoi cells with a side in common is the unit element of the Delaunay triangulation.

The triangulation is performed on 3D points projected on a plane perpendicular to a specific direction, as shown in Figure 25. Triangle vertices are raised to recover the initial elevation position and create the 3D surfaces. The disadvantage of this method is that concave scattered points distributions lead to non-singularity, requiring specific preprocessing.

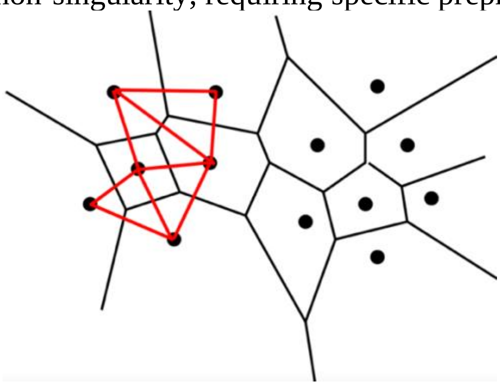

Figure 25 Voronoi diagram and Delaunay triangulation [39]

3.1.6.4 Volume based rendering

A volume-based rendering is called 'Ray-casting' (Figure 26). It is capable of transforming a limited form of data into a three-dimensional projection with the help of tracing rays from the viewpoint into the viewing volume. The ray will pass through the voxels, and it come across different sampling stations. For each sampling stations, color and opacity information are saved. From these information a volume-based rendering is built.
The more sampling stations are present, more computationally heavy, and accurate will be the result. However, there are methods for computational optimization like early ray termination: as soon as the ray found a sampling station with opacity equal to one, the algorithm stops.

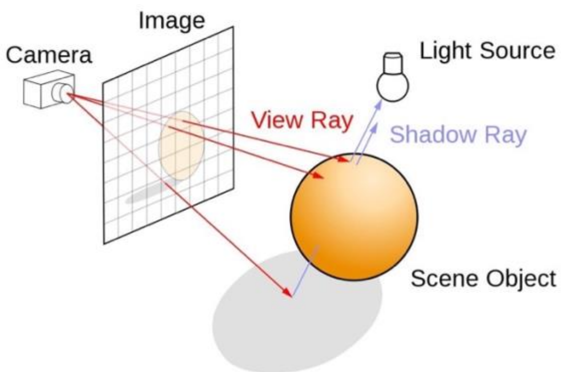

Figure 26 Ray casting method [39].

3.2 Software available in the market

In the last years, different 3D reconstruction software for surgical planning and intraoperative navigation have become widespread.
Among these, there are HepaVision (Mevis, Germany) [41][42], Liver Analyzer (Mevis, Germany) [43], MI-3DVS (Southern Medical University, China) [44], 3D VSP and VR-Anat (IRCAD, France) [45], Scout Liver and Explorer Liver (Pathfinder Technologies, USA) [46], SYNAPSE VINCENT (Fujifilm Medical, Japan) [47][4], Virtual Place (AZE, Japan) [48], Hitachi Image Processing System (Hitachi Medical, Japan) [49] and so on.

However, in this thesis work will be deepened 3D software with which the complex operating unit of general surgery in Vimercate hospital collaborates, namely Hyper Accuracy 3D (Medics3D, Italy), Visible Patient (Johnson&Johnson, France) and Virtual Clone (AIMS Academy, Italy) [50][51].

3.2.1 Medics 3D Tools for Medicine

Medics was founded in 2016 as a startup within the Innovative Enterprises Incubator of the Polytechnic of Turin. It is now a leading company in the field of 3D anatomical modeling applied to pre-operative planning and intra-operative support of complex surgeries.
Hyper Accuracy 3D (HA3D) allows to obtain a three-dimensional and patient-specific anatomical reconstruction extremely precise and faithful, which is used by the doctor and his team for the elaboration of an optimal surgical planning. The surgeon can manage the 3D models of his patients using a private section on the website, after registration. He uploads bidimensional images with some notes about the surgical interventions he proposes to make, and the rendering will be ready within 72 hours in a PDF3D format.
To obtain 3D models, segmentation takes place both manually and automatically, through proprietary algorithms identified by software such as MATLAB and guaranteed by medical certification. However, the tools of automatic recovery are not enough to ensure a high level of precision and accuracy of patient's anatomy. For this reason, a manual segmentation is also made by technicians specialized in different surgical fields. The post-processing, to ensure a high quality of 3D reconstructions in short term, is made by biomedical engineers who, after a close collaboration with radiologists for the determination of different levels of gray, are able to recognize the different anatomical structures.
It is important to underline that the 3D model is a more immediate and complete support, ready-to-use and interactive but it does not want to replace CT images, on which the radiologist makes the medical record.

Currently the segmentation is not performed through algorithms based on neural networks or artificial intelligence, but a project was launched, that plans to decrease the timing, completely optimizing the process.

In addition, using ICON3D, hardware accessory that can be brought into the surgical room, the surgeon can retrace the steps of planning during the intra-operative phase. Referring to the three-dimensional reconstruction, the surgeon has the possibility to verify the maneuvers carried out and to identify the different anatomical landmarks more easily. This facilitates the identification and resection of planned and simulated vascular branches, even in presence of complex anatomical variants. Hence, it promotes the reduction of unforeseen and

complications intra- or post-operative and it guarantees every patient a tailor-made surgical treatment.
ICON3D has hand-tracking sensor that allows the surgeon to manipulate the HA3D models through coded manual gestures in a touchless mode.
At the same time, the other members of the surgical team have the possibility to insert commands through standard mouse and keyboard, thus strengthening the team's cooperation in all conditions (sterile and not sterile) [52].

3.2.2 Visible Patient

Visible Patient was created in 2013 by IRCAD (Research Institute against Digestive Cancer, Strasburg) with the aim of develop a computer assisted surgery. In 2020 it has signed an agreement cooperation with an international pharmaceutical company, Johnson & Johnson.

The process is similar to that of Medics but, in this case, to view the model the surgeon needs to download a specific software, available for all operating systems.
Through this software, the surgeon can visualize Visible Patient Data (.vpz), read DICOM images and simulate virtual resection. Indeed, selecting a particular vascular structure, the surgeon can simulate the surgical procedure and read the corresponding resected volume [53][54].

3.2.3 Virtual Clone

Inspired by IRCAD, AIMS Academy was born in Milan in 2010. It's a multidisciplinary training center dedicated to the learning and development of minimally invasive surgery within the Niguarda Hospital.
Virtual Clone (VIC) is a virtual platform, accessible online, for the planning of HBP surgical interventions under development.
To use the service, the user accesses VIC from the Web, by typing the portal address (https://app.vic-virtualclone.com) or by using a search engine. The portal supports access from any browser. All users before registering and using the services, are invited to carefully read and accept the Terms and Conditions of the website use.
After registration and login, the user can upload the file that is accepted in two formats that, from the point of view of privacy, differ respectively for the presence or not in the file of identifying or sensitive data:

- DICOM
- NRRD

When uploading a DICOM file, the VIC service de-identifies the file and converts it to the NRRD format. Therefore, only the transformation of the DICOM file into NRRD ensures that the personal data of patients and doctor associated with the diagnostic image are permanently removed and the files are not re-identifiable.
Once the file is acquired in NRRD format, the image is processed and transformed into a three-dimensional version by the Virtual Clone software application, using advanced techniques of machine learning, already explained in paragraph 3.1.5. The image is then quickly processed and returned to the doctor.

In 2018 the first prototype for pancreatic surgery was completed and it was subjected to a usability test involving a small panel of experts, from which excellent results were obtained. Nowadays, the academy is working on the algorithm to make it able to recognize other organs such as the liver, spleen, kidneys, and nearby vascular structures. However, it's necessary to have a large CT images dataset already segmented to train the neural network [55].

3.3 Regulation requirements

Both Visible Patient and Hyper Accuracy 3D ® are certified as medical device for use in Europe with CE marking. Visible Patient is also certified with FDA clearance in the United States.

Since 1998, in Italy, all medical devices were subject to Directive 93/42, to ensure a high level of protection and performance provided by the manufacturer.

This legislation defines as a medical device any instrument, apparatus, plant, substance, or other product, including computer software, used alone or in combination intended by the manufacturer to be used in humans for the purpose of:

- diagnosis, prevention, control of disease therapy or attenuation;
- diagnosis, control, therapy, mitigation or compensation of an injury or disability;
- study, replacement, or modification of anatomy or of a physiological process;
- intervention on conception

whose main action desired in or on the human body is not achieved by pharmacological or immunological means, but whose function can be assisted by these means.

The term manufacturer refers to the physical or legal person responsible for the design, manufacture, packaging and labelling of a device that it will be placed on the market, whether these operations are carried out by that same person or by a third party on his behalf.
The obligations of the directive, which are imposed on the manufacturer, are also applied to the natural or legal person who composes, provides for the packaging, processes and re-processes, labels one or more prefabricated products and/or assigns them the intended use for placing on the market on his own behalf.
The intended use is very important because it indicates the end use provided by the manufacturer. It does not only mean what the device is for but also it defines exactly for what pathologies it should be used for.

The devices that can enter the market are the only ones that:

- meet the essential requirements of the design, manufacture, and materials directive;
- have followed a product and/or farm approval process by a notified body;
- carry the CE marking followed by the identification number of the Notified Body that followed the controls of the production phase [56].

In 2007 the European Parliament and Council amended the previous version of its directive on medical devices. In this version, it's declared that software in its own right, when specifically intended by the manufacturer to be used for one or more purposes set out in the definition of a medical device, is a medical device. Moreover, software which is intended to process, analyze, create, or modify medical information can be qualified as medical device if the creation or modification of that information is governed by a medical intended purpose.

In 2021 the Directive 93/42 was replaced by Regulation 745, that must be applied in its entirely across Europe.

After these changes and the conformity assessment procedure, Visible Patient and Hyper Accuracy 3D can be considered medical device, obtaining the CE mark, mandatory conformity marked for certain products sold in the European Economic Area (EEA) [57].

3.4 Certification

Both Visible Patient and Hyper Accuracy 3D are in compliant with the regulation ISO 13485:2016.
This is an internationally recognized standard for quality management systems in medical devices. The main objective is to promote the harmonization of regulatory requirements for medical devices and quality management systems. It is therefore a basic voluntary standard that applies to the different systems and regulations on the quality of production and marketing of medical devices, from simple gauze to the most sophisticated diagnostic imaging devices or minimally invasive surgical instruments.
This regulation is applied when an organization needs to demonstrate its ability to regularly provide medical devices and related services which comply with customer and with regulatory requirements applicable to medical devices and related services.
ISO 13485 makes mandatory 23 documented procedures, 37 registrations and 9 documented requirements.
Procedures define

- what needs to be done,
- by whom,
- when, where, how,
- with which materials, equipment, documents,
- with which controls, measurements, records.

Instead, registrations relate to the design, production, distribution, and operations of the management system. Other requirements include that appropriate clinical evaluation, that must be completed before delivery or usage.

Through this certification companies declare a quality policy focused on the care of the safety and health of patients, dedication to customer satisfaction and aspiration towards continuous improvement through innovative and high-quality products. Companies therefore undertake to certify the quality of their products and services, according to international standards, by engaging in study and experimentation, offering added value through assistance, training and counselling to healthcare professionals, ensuring that patients have access to modern and high-quality surgical planning [56][58].

3.5 GDPR compliance

All previously mentioned 3D software are compliant with the EU Data Protection Regulation (GDPR).
GDPR is effective since 2018. It was designed to harmonize data privacy laws across Europe to protect and empower all EU citizens data privacy and to reshape the way organizations approach data privacy. It’s applied to all companies processing the personal data of data

subjects residing in the Europe, regardless of the company location. For GDPR, any information related to a natural person or 'data subject' that can be, directly or indirectly, identified is a personal data [59].

Access to Hyper Accuracy and Visible Patient websites implies the user's full acceptance of the General Terms of use and the Cookies Policy, as already explained in paragraph 3.2.3 about Virtual Clone.
First, last name, email address and additional personal data from the user are collected. These personal data are used in order to respond to user's requests and inquiries, and they are provided as long as they have a direct contact with the user. Personal data are contained behind secured networks and they are only accessible by a limited number of persons who have special access rights to such systems and are required to keep the information confidential.
According to the GDPR, each user has the following rights:

- access: the right to obtain confirmation that personal data are being processed and all necessary information to make the process transparent;
- rectification: the right to require rectification of inaccurate data;
- restrict processing: the right to restrict processing of data under certain specified circumstances;
- data portability: the right to request user's personal data for the receipt or the transfer to another organization, in a machine-readable form;
- object to processing: the right to object, on grounds relating to a particular situation, at any time to the processing of personal data;
- withdraw consent: when the user has given his explicit consent for the processing of personal data, he can withdraw it at any time without justification.

Moreover, all DICOM images will be previously anonymized through the elimination of all metadata contained in the header of DICOM standard, as previously explained (see paragraph 3.1.1) [60].
Anonymization means a processing operation on personal data that aims to generate data for which the identification of the individual or individuals referred to is impossible or highly unlikely. It consists in the removal of the standard Data Elements that are divided into 9 categories:

1. Patient
2. Visit
3. Study
4. Step procedure
5. Series
6. Image
7. Results
8. Interpretation
9. Equipment

In particular, the patient data (ID, name, surname, gender, date of birth, age) and the doctor (first and last name) are removed.

The identification process shall not include:

- the technical data needed to display the image;
- identification of study and series;

- the description of the study;
- the date of acquisition.

This means that EU Regulation 2016/679 (GDPR) is not applied to such images, because they do not contain personal data.

To define the requirements that the anonymization's process must have, it is important firstly to define the concept of re-identification. It consists in the search of those identifying elements that have been eliminated during the anonymization phase and their subsequent reconnection to the anonymized data and, consequently, to the subjects they originally referred to [61].
It is defined as a solid process of anonymization, the method that makes impossible the re-identification. To determine the feasibility of re-identification, all the methods, which the controller or a third party can reasonably use to identify that physical person directly or indirectly, are evaluated.
Factors to consider include:

- the context, the rarity of the phenomenon object of the data, the density;
- the nature of the data, the volume of data;
- existing technologies and technical abilities;
- the potential third "intruder";
- costs and resources;
- the time needed;
- the competences;
- the information available;
- personal knowledge;
- the value of the data: interest and effort/benefit ratio [62].

The risk assessment of re-identification should be carried out considering the security measures that have been put in place to prevent the anonymized data being successfully re-identified. It is the responsibility of the data controller and, in general, of all those involved in the de-identification process and who process the anonymized data, to mitigate the risk of re-identification with the most appropriate security measures, so that a hypothetical re-identification process cannot succeed.
According to the Information Commissioner's Officer (ICO), it is possible to carry out the so-called "motivated intruder test". This means assessing whether the real risk of re-identification appears reasonable considering the de-identification operations carried out, the technical measures and the organizational measures put in place, thus assessing if a subject, by accident or intentional action, would be able, from the anonymized data, to re-identify such data.
Intruder shall mean a person who has no prior knowledge, reasonably competent, who is able to identify different data sources (such as the internet, libraries, public databases), who has access to such resources, and he knows how to manage its contents. He uses basic investigative techniques without special expertise and does not resort to crime [63].

In terms of technical measures taken to ensure patient confidentiality, the 3D reconstruction software described above uses data cleanup software that automatically removes metadata from uploaded files. In this way, companies do not have access, even accidentally, to any personal data.

Hence, the actions that should be put in place in order to re-identify consist of:

- the violation of the IT systems or the archives, paper or electronic, of the health facility or the doctor, so as to have access to the diagnostic images complete with the patient's data and be able to compare the image processed with the original one;
- the violation of the computer where the diagnostic images are processed, having access to the diagnostic images complete with the patient's data and be able to compare the processed image with the original one;
- the corruption of a health care provider or doctor who has access to the original diagnostic images and credentials of the user's profile to receive information on the identity of a patient.

Each of these actions described above falls within the scope of crime, so it can be concluded that the data of patients can be considered anonymized. Indeed, the risk of re-identification of such data is low and ultimately acceptable [63].

4 Current use of the technology in the National Health System

For what regard the diffusion of 3D technology in Italian hospitals, Medics in 2020 had already reached over 40 hospitals in Italy, with more than 400 cases made (Figure 27).
As shown in the Figure 27, almost 100%, of the Italian territory is covered, reaching the major centers such as Rome, Naples, Turin, Verona and Milan [64].

Figure 27 Italian Medics Network.

However, the potential reference market to which Medics could address is much larger: 1135 hospital facilities in Italy and 26085 throughout Europe [64].

Indeed, it is estimated that the world of 3D printed medical devices is growing. After expanding to a 15.9% CAGR between 2017 and 2021, Future Market Insights predicts that the medical device 3D printing market will likely slow to a 12.5% CAGR between 2022 and 2032 [65].

In a strategic perspective, Medics business model foresees the management of 3D printers directly at health facilities, offering its tools even in emergency situations.
Many realities, such as *Bambino Gesù* Hospital in Rome, *San Matteo* Polyclinic in Pavia and the University Hospital of Pisa, have designed or are about to design 3D Laboratories inside the hospital, called 3D Lab.

A 3D laboratory inside a hospital is a center to produce anatomical information directly connected with radiology, from which bidimensional images are obtained. They are processed within the 3D LAB to return to the clinician 3D anatomical models detailed and complex. It is very important to highlight the role of a 3D LAB in establishing multidisciplinary links between the surgical team and the paramedic staff who often find themselves within this structure to discuss and collectively deal with complex clinical cases. The 3D Lab is in fact a point of reciprocal and continuous exchange between doctors, biomedical engineers, and technicians in a strongly interdisciplinary perspective. All aimed at increasing the understanding of complex pathologies and pre-operative planning of major surgeries.

Technically a 3D laboratory in a healthcare context must respond to architectural and infrastructural features that can support the activities that will take place within it. The necessary equipment includes two or more powerful computer capable of working with 3D models. Generally, this type of computer is called "3D workstations" because they are assembled in compliance with the minimum hardware and software requirements able to guarantee fluidity during the post-processing of radiological images. Typically, these workstations are equipped with 3D software specific and certified for use in the biomedical sector. It is also necessary to use a medium-large graphic tablet that, thanks to the use of a pen directly on the screen, allows to perform 3D reconstructions of anatomical parts with much more ease and precision.
Finally, if the 3D model needs to be printed, printers able to produce a physical object from a virtual 3D model are necessary. Finally, there are virtual reality technologies such as headsets or haptic systems for virtual control of anatomical models in an immersive mode.

A 3D hospital laboratory is a production center of "biomedical information" that houses specific professional figures able to interface with the doctors of the structure. These are figures prepared with specific competence in everything that revolves around the world of 3D technology applied to medicine.
In particular, the figures that, more than others, are consistent with this role are:

- radiologist: is the crucial clinical figure, indispensable within a 3D LAB hospital. He’s the one who, indeed, oversees all the 3D reconstructions done by non-medical personnel. It is the professional who interfaces primarily with the rest of the physicians from whom he understands specific clinical needs and demands;
- biomedical engineer: professional figure able to manage and use the most innovative 3D technologies with specific skills acquired in the biomedical and medical-surgical field. It deals specifically with the reconstruction of 3D anatomical models from radiological images such as CT or magnetic resonance. He is able to manage and govern the technological instrumentation such as 3D printers with skills also in maintenance operations and possible customization of such tools;
- technical personnel: these are very important professional figures (e.g. Medical radiology technician) able to follow practically the printing processes and deal with the technical production phase of the models [66].

5 Analysis of clinical effectiveness

Clinical effectiveness was analyzed through an ad hoc survey to assess whether 3D reconstruction improves the comprehension of tumor localization and through the analysis of the difference between intra-operative and post-operative outcomes of patients whose surgical planning was done on 3D (intervention group) and on 2D (control group).

5.1 Survey

The primary aim of the study is to determine whether 3D reconstruction improves the understanding of the relationship of the tumor with neighboring vascular structures with respect to the standard 2D CT scan imaging.
The accuracy of the 2D and 3D evaluations of the vascular structures invaded by tumors will be compared to the actual invasion observed during surgery.

5.1.1 Pilot study

First of all, a small preliminary study was conducted in order to verify the feasibility and the potential for a future full-scale project. It helped to identify design issue, practicality, resources, time, and cost before the large-scale research.
Even if pilot study should not be used to test hypothesis since the appropriate power and sample size was not calculated, it provides preliminary data that insight into the potential results of the proposed experiment.
In the pilot study only one clinical case was evaluated by nine surgeons.
The rendering use in this preliminary analysis is reported in the Figure 28.

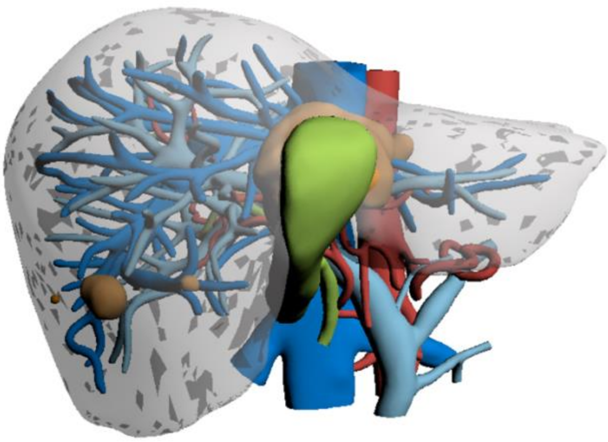

Figure 28 3D rendering of the clinical case evaluated in the pilot study.

The raters answer to six different questions choosing between four possible answers for each question. These inquiries were all about invasion of the principle vascular structures such as the medium hepatic vein, the cava vein, left portal vein, right anterior portal vein, right anterior biliary tract, and right hepatic artery. The selection of these vessels was made based on the critical anatomical relationship of them with the tumor.
Moreover, multiple choices were standardized. The possible answers were no infiltration, tangential infiltration, circumferential infiltration and not valuable. Tangential infiltration means that the tumor touches tangentially the vessel without crushing it, while circumferential means that the tumor surrounds for more than 180 degrees the vessel. However, it is also possible to insert 'non valuable' as answer in case the vascular structure is not clearly visible in CT and 3D. This is especially the case of the bile ducts.

The results of this pilot study are shown below.

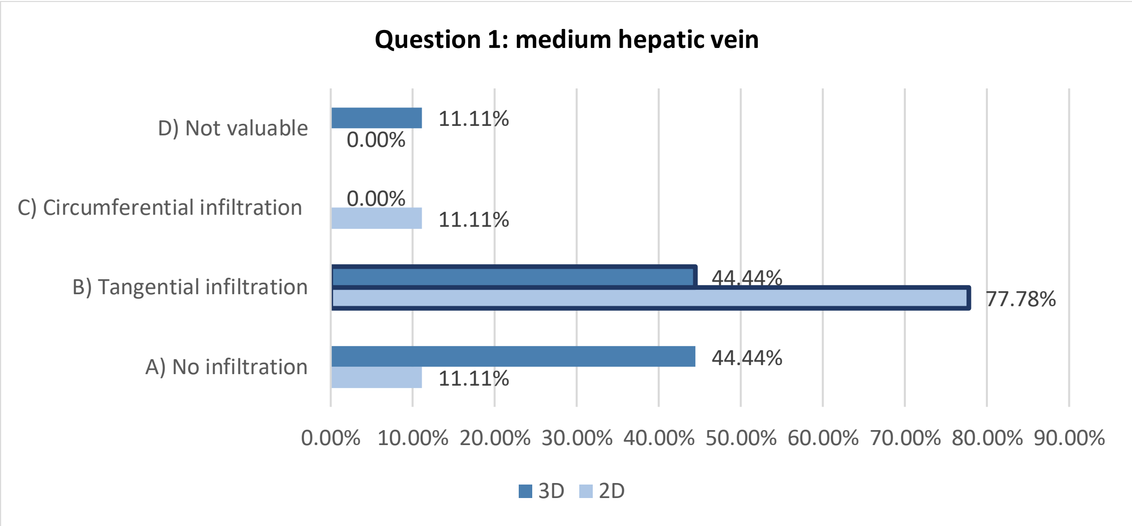

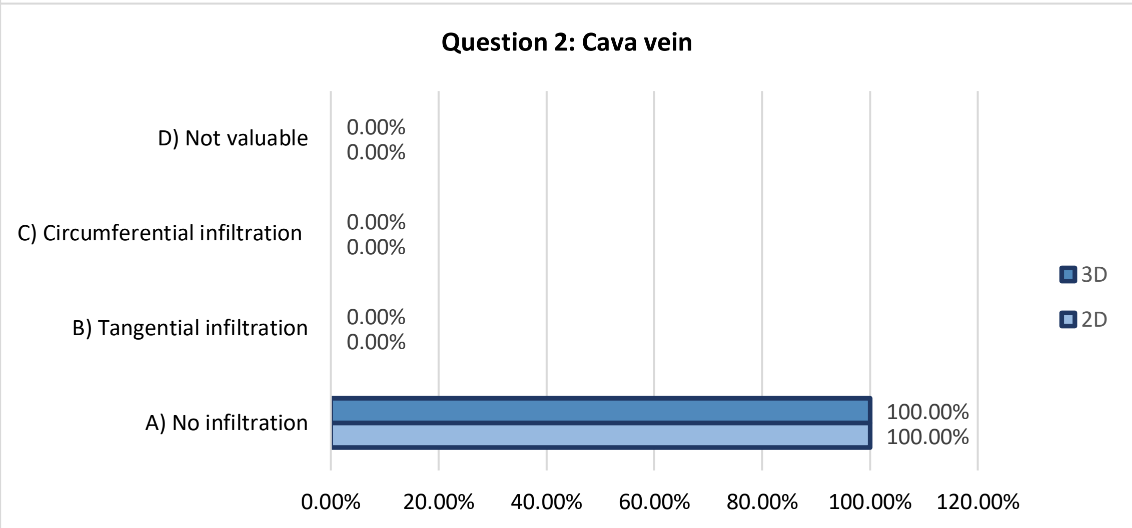

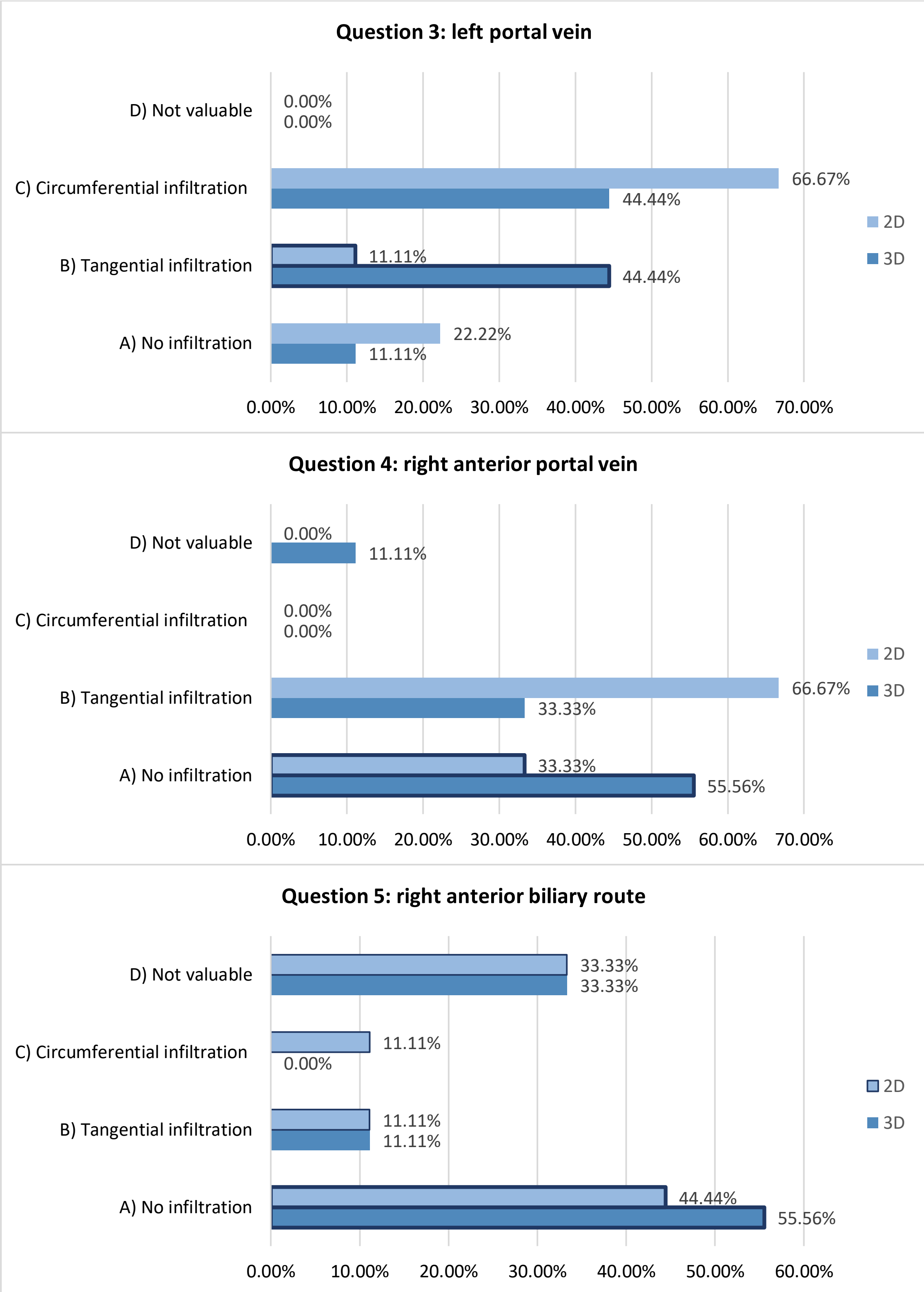
Question 3: left portal vein
D) Not valuable
C) Circumferential infiltration
B) Tangential infiltration
A) No infiltration
0.00%
0.00%
66.67%
44.44%
11.11%
44.44%
22.22%
11.11%
0.00% 10.00% 20.00% 30.00% 40.00% 50.00% 60.00% 70.00%
2D
3D
Question 4: right anterior portal vein
D) Not valuable
C) Circumferential infiltration
B) Tangential infiltration
A) No infiltration
0.00%
11.11%
0.00%
0.00%
66.67%
33.33%
33.33%
55.56%
0.00% 10.00% 20.00% 30.00% 40.00% 50.00% 60.00% 70.00%
2D
3D
Question 5: right anterior biliary route
D) Not valuable
C) Circumferential infiltration
B) Tangential infiltration
A) No infiltration
33.33%
33.33%
11.11%
0.00%
11.11%
11.11%
44.44%
55.56%
0.00% 10.00% 20.00% 30.00% 40.00% 50.00% 60.00%
2D
3D

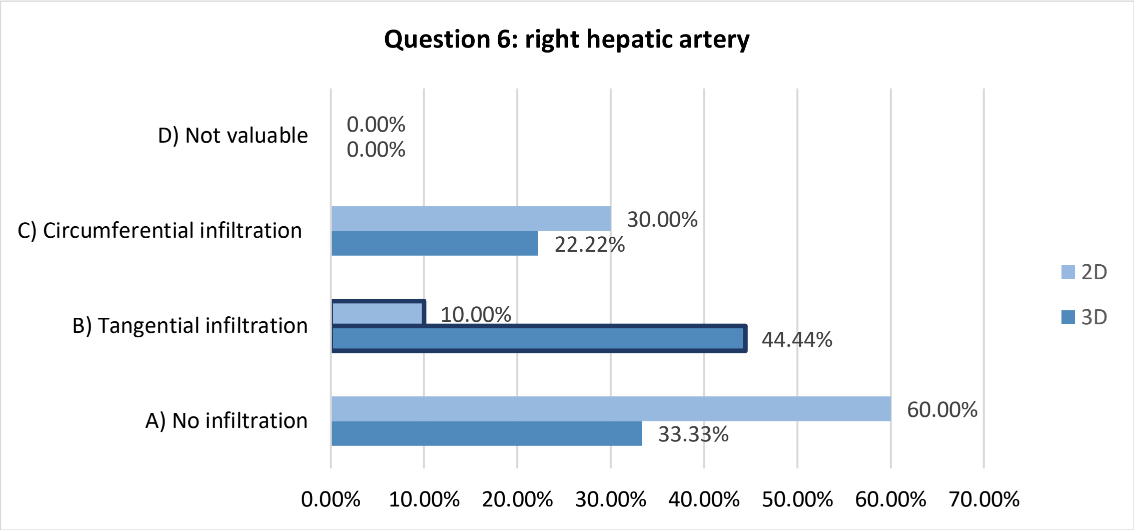

The answers to the first question do not reflect the desired result, because with the 3D reconstruction many raters changed their minds and got the answer wrong. It would seem that 3D confuses ideas instead of clarifying them. This uncertainty is probably caused by the fact that by rotating the 3D model, the vision of the position of the tumor relative to the medium hepatic vein is limited by the presence of left and right hepatic veins, as seen in Figure 29. Probably some raters, in doubt have preferred to answer that there is no vascular infiltration.

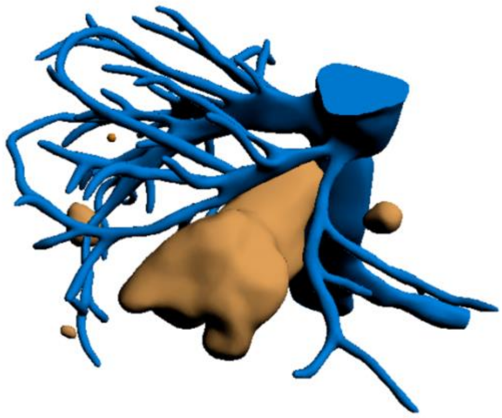

Figure 29 Tumor localization with respect to the hepatic veins in the clinical case used for the pilot study.

In the second question there is no difference between the answers given based on 2D and 3D. It was probably already clear in the two-dimensional images that there is no vascular infiltration of the vena cava. All the other questions instead show that 3D helps the correct interpretation of the spatial relationship between the tumor and the nearby vascular structures, because the percentage of correct answers (highlighted in black in the graphs above) increases when raters visualize 3D rendering.
Given these results of the pilot study, it was decided to continue with the survey enlarging the population analyzed both in terms of patients involved and in terms of surgeons.

5.1.2 Full scale survey

5.1.2.1 Methods

To validate the results of the pilot study, a survey with eleven clinical cases was conducted. However, in Vimercate Hospital, eight 3D reconstructions were already made by Hyper Accuracy and Visible Patient. But three of them were excluded from the study because one rendering was made for a patient suffering pancreatic tumors, another one for a patient who was not surgically operated, and another was used in pilot study.

For this reason, other 6 patients with a particularly complex liver anatomy (with the tumor very close to the main vascular structures) were retrospectively selected. Their contrast-enhanced CT scan images were downloaded anonymously from Vimercate Hospital PACS system. These CT DICOM images were elaborated to obtain a full virtual 3D model.

5.1.2.1.1 3D model generation

First of all, the six bidimensional CT images were uploaded in Virtual Clone Platform through the following link: https://app.vic-virtualclone.com/ .

The first stage of segmentation was performed automatically: neural networks determine the principle anatomical structures. However, as previously mentioned in paragraph 3.3.3, AIMS' software is a work in progress, and it is not able to produce an accurate and ready to use 3D model. Hence, different labels were post processed using 3D Slicer.

As shown in Figure 30, the segmentation needs to be manually post-processed with 3D Slicer, because Virtual Clone is not able to determine all anatomical structures such as the tumor and the bile ducts. Moreover, because of the complex vascular structure, Virtual Clone is not able to differentiate between hepatic and portal veins.

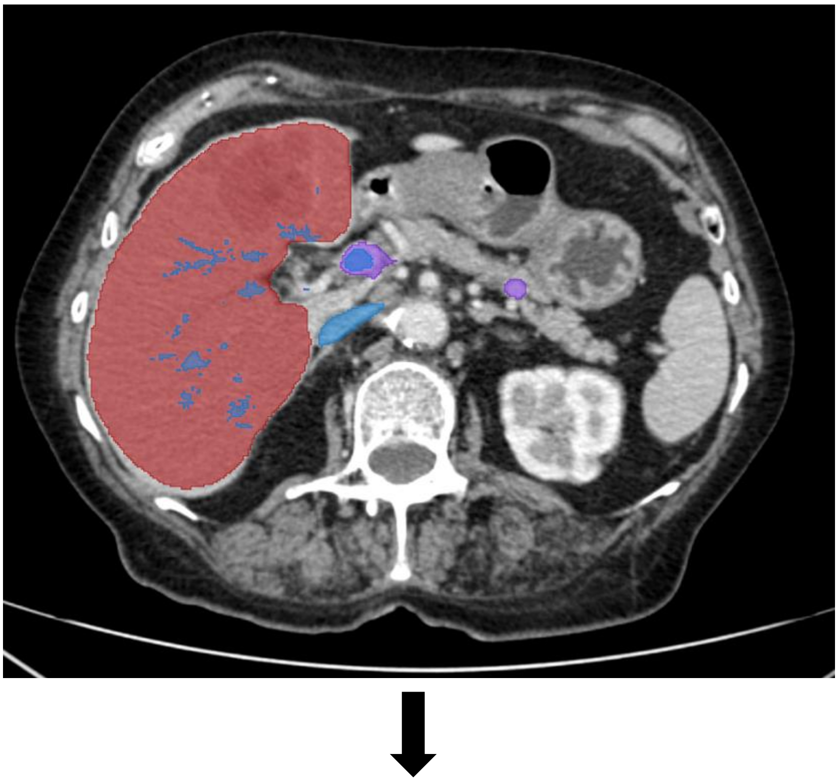

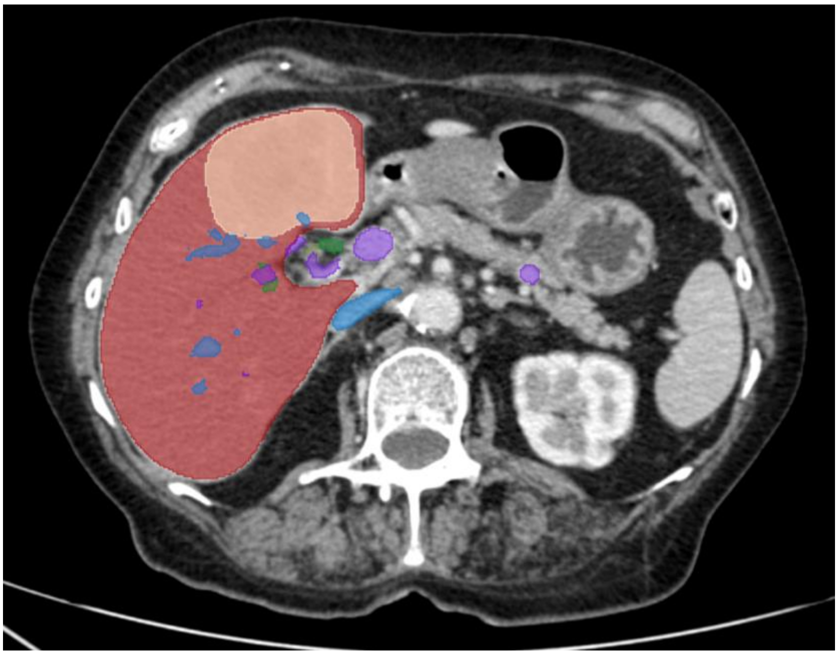

Figure 30 Same slice of a CT image segmented with Virtual Clone (above) and post-processed with 3D Slicer (below). Arteries are not represented because a CT in venous phase is shown.

The number of operations made through 3D Slicer in the post-processing phase depends on the complexity of the clinical case. If the tumor is very large and it deforms neighboring vascular structures as in Figure 31, Virtual Clone makes much effort to correctly determine even the main anatomical structures. Hence, a fussy and accurate work is needed to get a reliable 3D model.

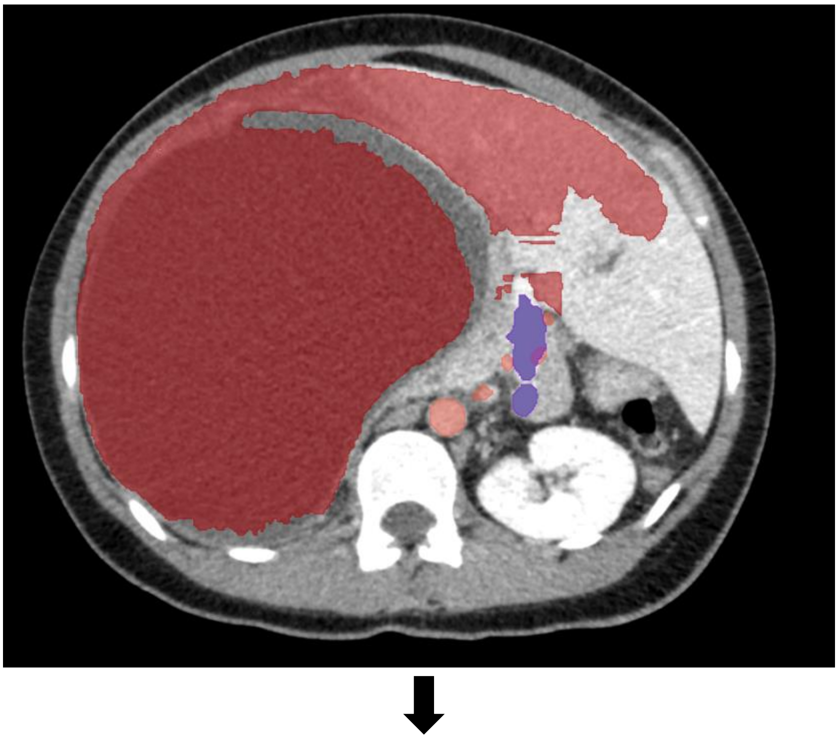

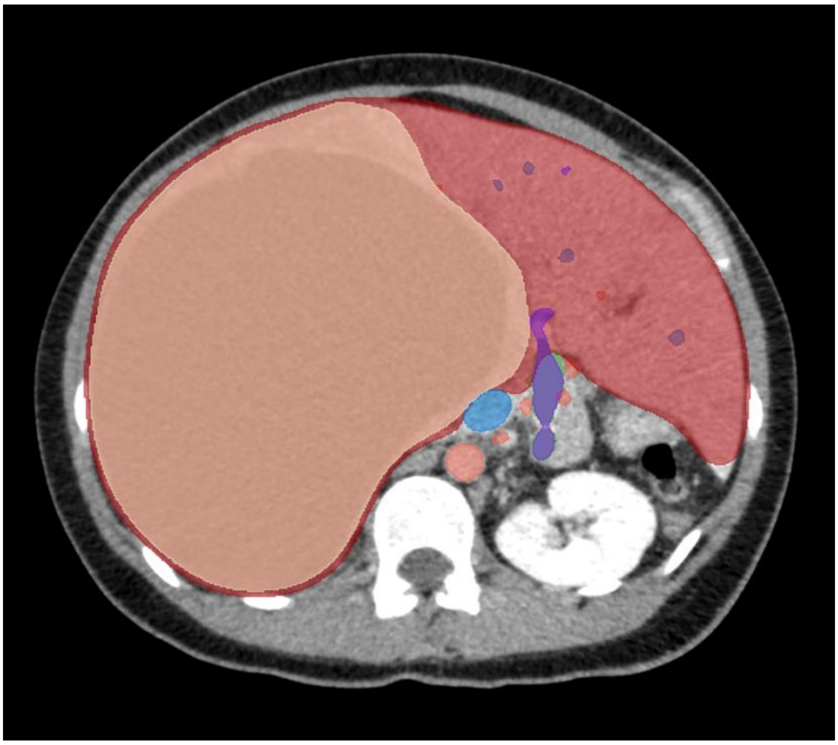

Figure 31 Same slice of a CT image segmented with Virtual Clone (above) and post-processed with 3D Slicer (below). Arteries are not represented because a CT in venous phase is shown.

5.1.2.1.2 3D Slicer

3D Slicer is a free, open-source software available on multiple operating systems like Linux, macOS and Windows. It supports multi-modality imaging including MRI, CT, US, nuclear medicine and microscopy and it is highly extensible (users can add more libraries by installing additional modules from the 'extensions manager'). This software is applicable for visualization and analysis of medical images.
3D Slicer is built on a modular architecture. Most important modules are the so called DICOM that permits to import and export DICOM images, Volumes, used for changing the appearance of various volume types in order to see better contrast enhanced structures, Segmentations, that displays properties and import/export segmentations and Segment Editor [67].

When all labels from Virtual Clone are uploaded in 3D Slicer, the post-processing is performed via Segment Editor Module to obtain a more realistic and accurate 3D model. To extract features from the CT image, different effects within this module were used:

- paint: pick the radius of the brush to apply, left click and drag to fill a region. There's the sphere mode that applies the modifications to slices above and below the current slice;
- erase: same as paint effect, but the highlighted regions are removed from the selected segment instead of added;
- level tracing: moving the mouse defines an outline where all the pixels have the same background value. Clicking the left mouse button, the outline is applied to the label map;
- grow from seeds: draw segment inside each anatomical structure. As described in the paragraph 3.1.4, this method starts from 'seeds' and grow them to achieve a complete segmentation;

- fill between slices: create complete segmentation on selected slices. A few slices between segmented ones can be skipped and this method will fill them by interpolation;
- margin: grows or shrinks the selected segment by the specified margin;
- smoothing: as already described in paragraph 3.1.3, this effect permits to fill in holes and/or remove extrusions. Furthermore, in this module there are different available methods:
  - median smoothing: it removes small extrusions and fills small gaps while keeps small contours mostly unchanged;
  - opening: it removes extrusions smaller than the specified kernel size;
  - closing: it fills sharp corners and holes smaller than the specified kernel size;
  - gaussian: it's the strongest smoothing method but it tends to shrink the segments;
  - joint smoothing: smoothing of multiple segments at once, preserving watertight interface between them;
- scissors: clip segments to the specified region or fill regions of a segment.
- island: this tool is used to connect regions that are defined as groups of non-empty voxels which touch each other but they are surrounded by empty voxels.
- logical operators: it applies basic copy, clear, fill and boolean operations to the selected segments [68].

The segmentation is then exported from 3D Slicer in .gITF format and the 3D models are visualized in an online platform (*https://3dviewer.net*), interactive and easily shared.

5.1.2.2 Design

For each included patient *i*, the surgeon *j* will answer to a standardized questionnaire (see Appendix A) outlining 16 different vascular structures (items) potentially invaded by the patient's tumor.

In comparison with the pilot study, the number of questions has increased in such a way that the same vascular structures are always involved, and not only those characterizing each specific clinical case. This also allows to standardize and better compare results. The number of responses and typology remained similar to the ones in the feasibility study. The possible answers were 5: no vascular invasion, tangential, circumferential, vascular deformation and not valuable. As already described in the pilot study, if the vascular structure is completely surrounded by the tumor or the tumor wraps around the vessel for more than 180 degrees, then it is circumferential infiltration. If the tumor touches the vessel for less than 180 degrees or deforms it, these cases correspond respectively to tangential infiltration and vascular deformation.

The survey is managed using the platform *sondaggio-online.com*.
Each participant, before answering each patient's questions, finds a link to download their two-dimensional CT images in DICOM format.
By viewing the CT images, it will be possible to answer the questions, where only one is the correct response. It is mandatory to answer all the questions and raters cannot go back to edit the answers given based on 2D once they have viewed the 3D model.

The 3D model in the online viewer appears as in Figure 32.
By clicking and moving the cursor, the participant can rotate and zoom the rendering.
In addition, on the left, in the section called 'Meshes', he can turn on/off the display of certain parts, by clicking on the eye.

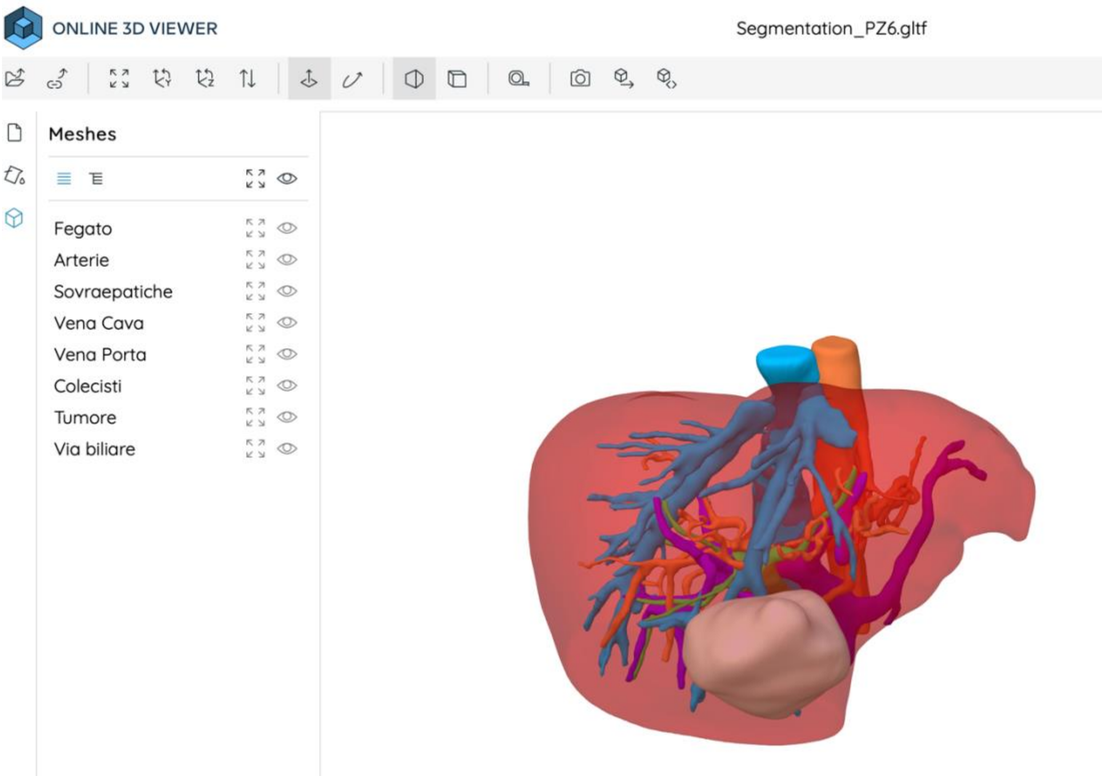

Figure 32 Online three-dimensional reconstruction representation through online 3D viewer.

By viewing the 3D model, it will then be possible to answer the related questions (equal to those already filled out in the first part, which will no longer be editable).
This procedure is repeated for all patients involved.

5.1.2.3 Statistical consideration

For the sample size and statistical power calculations, it is assumed as the alternative hypothesis a clinically significant improvement of 3D reconstruction over 2D imaging.
The inter-surgeon agreement is assumed to be good enough, while the trial is expected to involve a total of minimum 10 surgeons.
Under this assumption, 11 independent patients are required to achieve at least 80% power to reject the null hypothesis.

For each included patient *i (i=1…11)*, the surgeon *j* (j=1…M) will answer to a standardized questionnaire about the vascular invasion of 16 different vascular structures (see Appendix A). Each surgeon will answer to these questions looking to bidimensional images. Once he has finished the first part, he can answer to the same 16 questions looking to the correspondent three-dimensional images.

The total of the combinations will be: Mx11x16x2.

For each combination, the level of vascular infiltration evaluated with 2D and 3D, and the level of vascular infiltration observed during surgery will be reported.
In case of agreement between the 2D/3D method and the observation during surgery, it will be given a score equal to 1, in case of disagreement score 0.

For each combination surgeon j and patient i, the number of correct assessments made with the 2D method ($\Sigma 2Dji$) and the 3D method ($\Sigma 3Dji$) will be added together, and the difference $\delta ji = \Sigma 3Dji - \Sigma 2Dji$ will be calculated.

This difference will be considered the main measure of interest in assessing the difference in accuracy of the two methods.

For each surgeon j the mean value δj calculated on the 11 patients will then be calculated.
Finally, the average difference Δ will be computed on all surgeons as the arithmetic mean of M δj.

The main assumption is that 3D accuracy is greater than 2D.
This is equivalent to saying that $\Delta>0$.
Hence, the null hypothesis H0 is that the accuracy is the same with the two methods: $\Delta=0$.

The result will be considered statistically significant if p-value will be less than 0.05.

5.1.2.4 Results

Answers came from experienced HBP surgeons who perform at least 150 complex liver resections annually in the following hospitals:

- *Polo Ospedaliero Interaziendale Trapianti San Camillo-Forlanini e l'IRCCS L. Spallanzani* (Roma);
- *Azienda ospedaliera universitaria integrata* (Verona)
- *Grande Ospedale Metropolitano Niguarda* (Milano)
- *Ospedale Generale Regionale F. Miulli* (Bari)
- *Istituto Nazionale Tumori G. Pascale* (Napoli)
- *Ospedale San Gerardo* (Monza)

In the analysis of the results were included surgeons who answered more than half of the questions. Seventeen surgeons completed the questionnaire entirely while only one surgeon completed the 72,80% of questions, answering to 8 out of 11 patients. However, the requested sample size was reached, as more than 10 surgeons completed the questionnaire in full.
A graphical analysis of the results is shown in Appendix C.
Instead, the mean of the score difference obtained by each rater in the 2D and 3D part of each patient is inserted in Table 3. The score of each question has been calculated equal to 1 if the answer is equal to the operative response, while it has been calculated equal to 0 if the operative response is different from the given answer. Furthermore, the sum of the scores $\Sigma 2Dji$ and $\Sigma 3Dji$ and their difference was computed for each patient analyzed by each surgeon.
Finally, the mean of the difference for each surgeon was retrieved. A mean difference greater than zero means that 3D helps the comprehension of vascular invasion.

Surgeon j	Mean difference δj
1	1,875
2	1,09090909
3	3,18181818
4	0,90909091
5	2,36363636
6	2,36363636
7	0,81818182
8	1,18181818
9	2,27272727
10	0,27272727
11	0,90909091
12	2
13	1,81818182
14	2
15	4,90909091
16	1,36363636
17	0,72727273
18	1,09090909

Table 3 Mean of the difference between the scores obtained using 3D and 2D for each rater.

The overall mean Δ computed as mean of the values in the second column is 1,72.
Since the $\Delta > 0$, it has been demonstrated that using 3D renderings the accuracy in the comprehension of the relationship between the tumor and the closer vascular structures is higher than the accuracy achieved using bidimensional images.
Furthermore, the p-value has been computed trough a two sides t-test of the different scores Σ2Dji and Σ3Dji of each patient i, evaluated by each surgeon j.
The results are summarized in Table 4.
Since p-value is less than 0,001, the study is extremely statistically significant.

	2D	**3D**
Mean	10,2	12,44102564
Variance	10,3051546	56,56738039
Number of observations	195	195
Degrees of freedom	262	
Stat t	-3,8268394	
P(T<=t) one tail	8,1187E-05	
T critic one tail	1,65069028	
P(T<=t) two tails	**0,00016237**	
T critic two tails	1,96905972	

Table 4 T-test of Σ3Dji and Σ2Dji.

5.2 Comparative analysis of intra-operative and post-operative outcomes

In this thesis work, clinical effectiveness is also evaluated comparing retrospectively intraoperative and post-operative outcomes of operations planned with 3D reconstructions (intervention group) against surgery with 2D images (control group).
Also, preoperative clinical data were analyzed in order to identify if the two groups shared similarities, because if only people with a clinical status already compromised were considered, intraoperative and postoperative outcomes will be affected.

5.2.1 Analysis of published literature

In literature, studies considered the difference between the intervention group and the control group statistically significant when the p-value is less than 0.05.

5.2.1.1 Preparative data

Concerning the baseline characteristics, clinical effectiveness is measured between groups with no significant difference in age, sex, BMI, previous abdominal surgery, cirrhosis, and viral hepatitis. Furthermore, the two groups did not significantly differ according to preoperative liver function, defined through laboratory measurements. Also outcomes based on preoperative imaging were compared: the two groups have similar tumor size, number of tumors, vascular invasion and tumor differentiation but there was a significant difference in the measures of tumor diameter, probably because patients selected for the new technology were in a more critical situation [44] [69].

5.2.1.2 Intraoperative outcomes

Similarity between intervention and control group is also confirmed in terms of operative method. Concerning intraoperative characteristics, all studies analyzed underline a statistically significant reduction in terms of operative time, because the surgeon through the 3D model has been able to plan more accurately the operation and to share it with the team in the surgical room [44][70][71][72][73][74][75][76][6][77].
The majority of papers also agree that the use of 3D reconstructions allow to have a lower intraoperative blood transfusion and intraoperative blood loss because the position of the tumor and its related vascular invasion are preliminary known with more precision [71][6][73][77][75][70]. For this reason, some papers underline also shorter time of blockage of hepatic blood flow [44][73].

5.2.1.3 Postoperative outcomes

For what regard short-time and long-time post operative outcomes, no particular differences have been noted between the two groups in terms of hospitalization time: papers that analyze this data show that the difference is not statistically significant [70][71].
Furthermore, data regarding the number of complications after surgery are different. Zhang et al. points out a statistically significant decrease in comorbidity [76], while other papers argue that there is no difference or little [44][75][76]. The complications typically taken in consideration are: bile leakage, intra-abdominal abscess, ascites, pleural effusion and biliary fistula [44][44][73]. Also laboratory results after surgery were compared: the intervention group results having lower bilirubin, higher hemoglobulin and albumin [44][66][67][72].
Moreover, the use of three-dimensional models allows the surgeon to have a more realistic idea of the position and size of the tumor. For this reason, tumor recurrence and tumor related death are lower [66][73][74].

An outcome, that most of papers underline is a statically significance difference between 3D and 2D about the calculation of resected volume and future liver remnant volume (FLRV). It’s important to leave at least 30% of liver after major hepatectomy [44][68][74][75]. Indeed, Zhu et al. report that the number of patients with hepatic failure is lower in the intervention group rather than in the control group [76].

5.2.2 Analysis of patients from Vimercate Hospital

In order to verify whether these results are confirmed even within Vimercate Hospital, two different groups of patients were considered. Patients whose preoperative planning was based on the corresponding 3D reconstruction were included in the intervention group. As already mentioned, eight 3D models were available. However, in this analysis, the intervention group includes only six patients because one patient was not operated, and another was suffering from pancreatic cancer. In the control group there are clinical cases that have undergone major hepatectomy before the introduction of 3D technology. All these patients had a tumor close to the main vascular structures with a particularly complex anatomy. Some of these are the same patients who were selected to do 3D rendering with Virtual Clone and Slicer with the aim of having more reconstructions for the survey. However, some of them were excluded in order to consider patients with similar baseline characteristics with respect to those in the intervention group. Hence, other patients were selected with complex anatomical relationship between tumor and nearby vascular structures.

Thanks to the full integration and interoperability of different software in Vimercate Hospital, several outcomes were retrieved. The choice of which outcomes are interesting in the evaluation of preoperative planning technology was made based on what was already highlighted in literature and which outcomes are actually reported in the electronic health record.
First of all, a query (see Appendix B) was used within the hospital’s database to retrieve these data of patients who undergo major hepatectomy:

- identification data (name, surname, ID patient, date of birth, sex and fiscal code);
- ID hospitalization;
- date and time acceptance;
- date and time dismission;

- date and time of death;
- ID diagnosis;
- diagnosis description;
- ID surgical operation;
- date and time surgical operation;
- procedure description.

Once patient and hospitalization were found, outcomes collection starts from the EHR.

In particular, data were retrieved mainly from:
- the hospital discharge letter;
- operating report;
- report of the outpatient visit;
- histopathological examination report;
- laboratory exams;
- letter of transfer to the intensive care unit;
- past medical history;
- physical examination.

5.2.2.1 Preoperative Data

The selected baseline characteristics for each patient are the age at the time of the surgery, sex, height, and weight. From the last two, using the formula 5.1 the BMI was computed:

$$BMI = \frac{weight}{(height)^2} \tag{5.1}$$

This information is important because obesity is closely related to NAFL and NASH, as already mentioned in the paragraph 2.3.4. Non-alcoholic steatohepatitis (NAFLD) occurs when the excess of fat in the liver turns into inflammation (enlarged liver) and fibrosis (scar tissue) of the liver, causing serious liver diseases.

There are also indications regarding patient’s abdominal surgical history and alcohol consumption, that can be:
- very frequently
- frequently
- occasionally
- rarely
- very rarely
- do not use.

Excessive alcohol consumption can lead to hepatopathy, a degenerative process characterized by three diseases of the liver: steatosis, alcoholic hepatitis, and cirrhosis of the liver. The cause is a transformation of alcohol into toxic substances that damage the liver irreversibly and chronically, with a high risk of liver failure and cancer.

In addition to BMI and alcohol consumption, it is important to also record information about viral hepatitis and cirrhosis, since chronic infections (such as hepatitis B and C) are, together with cirrhosis, the most important risk factor for the development of liver cancer.

Furthermore, in the electronic medical record, nurses shall periodically complete scales indicating the patient's state of health. Data collection allows a correct planning of nursing care with a timely detection of care needs. To avoid that the data collected are influenced by subjective elements related to the experience and competence of each nurse, it is good to resort to the use of scientifically validated scales and care indexes. Assessment scales and care indexes support:

- an objective and comparable reading of welfare phenomena;
- a uniform quantitative assessment of assistance;
- communication or exchange of information between the different disciplines.

BRASS, BARTHEN and BRADEN are examples of scales used inside the hospital.

5.2.2.1.1 BRASS index

BRASS index is a tool used to identify patients at risk of prolonged hospitalization or difficult discharge. Data is collected by filling out the scale, interviewing relatives or assisting the patient. It is very useful when the patient is admitted to hospital, investigating 10 dimensions:

- age;
- life situation;
- social support;
- functional status;
- cognitive state;
- behavioral model;
- sensory deficits;
- previous admissions/access to first aid;
- active clinical problems;
- number of drugs taken.

Each answer given, in each dimension, is associated with a score. This identifies 3 risk classes (0-10) low, (11-19) medium, (20-40) high [80].

5.2.2.1.2 BARTHEL index

The aim of the Barthel index is to determine the degree of independence of the patient. It's made up of 10 items that involve the common daily activities (ADL Activities of Daily Living):

- feeding;
- dressing/undressing;
- personal hygiene;
- take a bath or shower;
- intestinal sphincter control;
- bladder sphincter control;
- displacements between chair and bed;
- toilet use;

- mobility walking on flat ground;
- going upstairs or downstairs.

Each item is assigned a score, the sum (maximum 100), indicates the degree of autonomy of the patient in the performance of daily life activities [81].

5.2.2.1.3 BRADEN index

Braden's scale is a risk assessment scale for the occurrence of pressure lesions, i.e., areas of skin and underlying tissue that have been damaged by the combination of pressure and other factors. When soft tissues undergo prolonged compression between the bony prominence and a solid surface, the risk of lesions and cellular necrosis is very high. This assessment must be carried out with all those patients who are not able to move in total autonomy.
This scale is based on six different factors:

- sensory perception (ability to respond to discomfort dictated by compression);
- skin moisture (sweating, moisture linked to urinary and/or fecal incontinence);
- motor activity (level of physical activity);
- mobility (ability to control/change body position);
- nutrition (adequate intake of calories, proteins, vitamins and minerals is essential to counteract the occurrence of new lesions);
- friction and slipping (the friction force created with the solid surface can accelerate the onset of pressure lesion).

If the sum of the scores for each factor is up to 6, the risk is high, up to 16, the risk is medium, up to 23 the risk is low [82].

5.2.2.1.4 ASA score

Another datum reported for each patient, is the ASA score.
In 1941, The American Society of Anesthesiologists (ASA) studied a system for the collection and tabulation of statistical data in anesthesia to allow anesthesiologists to record the overall health status of a patient prior to surgery. The aim was to determine predictors for operative risks but it's really difficult to forecast. For this reason, in 1963 ASA proposed a classification to assess the physical status of preoperative patients [83].
The ASA score defines patient's overall health status based on five classes (Table 5).

ASA classification	Definition	Examples including, but no limited to:
ASA I	A normal healthy patient.	Healthy, non-smoking, no or minimal alcohol use.
ASA II	A patient with mild systematic disease.	Mild diseases only without substantive functional limitation, e.g., current smoker, social alcohol drinker, pregnancy, obesity (BMI>30).
ASA III	A patient with severe systematic disease.	Substantive functional limitations: one or more moderate to severe diseases. For example: poorly controlled diabetes mellitus (DB) or hypertension (HTN), chronic obstructive pulmonary disease (COPD), morbid obesity (BMI>40), active hepatitis, alcohol dependance or abuse, implanted pacemaker, moderate reduction of ejection fraction, end stage renal disease (ESRD) undergoing

		regular scheduled dialysis, premature infant, history (>3 months) of MI (myocardial infraction), CVA (cerebrovascular accident), TIA (transient ischemic attack) or CAD (coronary artery disease).
ASA IV	A patient with severe systematic disease that is constantly threated during the entire life.	Examples include (but not limited to): recent (<3 months) MI, CVA, TIA or CAD/stents, ongoing cardiac ischemia or severe valve dysfunction, severe reduction of ejection fraction, sepsis and ESRD not undergoing regularly scheduled dialysis.
ASA V	A moribund patient who is not expected to survive without the operation.	Examples include (but not limited to): ruptured abdominal/thoracic aneurysm, massive trauma, intracranial bleed with mass effect, ischemic bowel and significant cardiac pathology.

Table 5 Classification of ASA score [83].

5.2.2.1.5 Laboratory results

Preoperative outcomes are also considered as laboratory tests such as blood and urine tests before surgery. All these measurements indicate the functionality of the liver.

Table 6 summarizes the main indicators, their meaning, and the normal range:

Laboratory result	Measurement	Meaning	Range
Hemoglobulin (HGB)	g/dL	Hemoglobin is the protein that transports oxygen from the lungs to all tissues. The correlation between hemoglobin and the liver is iron, which is mostly deposited in the liver, and it makes possible to construct hemoglobin. Without iron, the patient develops anemia.	13-18
Platelets	[x10^9/L]	Platelets are circulating cellular fragments that intervene in the hemostatic system. An indicator of liver function is the presence of thrombopoietin that helps to control the number of circulating platelets.	150-450
Prothrombin time	s INR	Prothrombin is a glycoprotein that participates in the process of blood clotting and it is synthesized by the liver. The time of prothrombin indicates the time necessary for the blood to clot. The value can be measured either in seconds or using the international normalized ratio (INR), which eliminates the variability of the results obtained in different laboratories. A high prothrombin time could be a clue to liver problems.	24-38 s 0.8-1.2 INR
Bilirubin	mg/dL	Bilirubin is a substance produced by the body during the degradation of hemoglobin, contained in damaged red blood cells. Bilirubin is processed by the liver in the final stage, to allow its elimination from the body. If bilirubin is high, it means that liver function is impaired.	0-1.2
Indirect Bilirubin	mg/dL	It’s the bilirubin that has not yet been	0-0.90

		processed by the liver. An increase in indirect bilirubin in the blood may be the result of excess production (as in the case of hemolytic diseases) or a defect in liver activity (e.g., cirrhosis).	
Direct Bilirubin	mg/dL	It is the bilirubin that has been brought to the liver and processed. An increase in direct bilirubin may be caused by biliary stasis due to hepatitis, cirrhosis, or obstruction of the bile ducts.	0-0.30
Albumin	g/dL %	Albumin is the protein in plasma. It is produced by the liver and has the functions of transporting and eliminating waste substances, balancing oncotic pressure, and constituting a reserve of amino acids for the body. A decrease in blood albumin can be caused by cirrhosis of the liver, acute and chronic hepatitis or even liver failure.	3.7-5.3 55-66
Aspartate tranferase AST	U/L	AST is an enzyme that is found mostly in the cells of the heart and liver. Like all transaminases it is fundamental for the metabolic processes of energy transformation within the cell itself. In healthy subjects, AST values in the blood are low. When the liver is damaged, this transaminase is released into the blood. This makes AST a useful marker of liver damage.	5-43
Alanine transferase ALT	U/L	See AST	3-45
Antigen Carbohydrate 19-9 (CA 19-9)	U/mL	CA 19-9 is a protein that is produced in excess by the cells of many forms of gastrointestinal tumors. An increase in CA 19-9 may indicate the presence of neoplastic processes in the pancreas, biliary duct, stomach and colon.	0-37
Carcinoembryonic antigen (CEA)	ng/mL	CEA is a protein that can be produced in large quantities by cells of many cancer forms, including the tumor of the liver.	0-5
Alfa fetoprotein (AFP)	U/mL	AFP is a glycoprotein with functions similar to albumin, mainly synthesized by the liver. Alfa fetoprotein is a tumor "marker", that is, one of those substances that can be found in increased quantities - in the blood, urine or other body fluids - in the presence of some neoplastic processes. Indeed, this protein is produced by certain types of liver cancer. The parameter is also useful for monitoring the course of chronic liver diseases, such as cirrhosis, hepatitis B and hepatitis C.	0-5.80

Table 6 Laboratory measurements for defining hepatic functions.

5.2.2.1.6 Child-Pug Classification

For each patient also the Child-Pugh score is computed.
This scoring system was designed in 1964 to predict mortality in cirrhosis patients. It divides patients into three categories:

- A: good hepatic function
- B: moderately impaired hepatic function
- C: advanced hepatic dysfunction.

After some modifications, nowadays the scoring system used five clinical and laboratory measurements to categorize patients: serum bilirubin, serum albumin, ascites, neurological disorder, and prothrombin time. A score indicating the severity is associated with each measurement, as shown in Table 7 [84].

Clinical and lab criteria	**Points**		
	1	**2**	**3**
Encephalopathy	None	Mild to moderate	Severe
Ascites	None	Mild to moderate	Severe
Bilirubin (mg/dL)	<2	2-3	>3
Albumin (g/dL)	>3.5	2.8-3.5	<2.8
Prothrombin time (INR)	<1.7	1.7-2.3	>2.3
Child-Pug classification: - Class A = 5 to 6 points - Class B = 7 to 9 points - Class C = 10 to 15 points			

Table 7 Child-Pugh classification [84].

5.2.2.1.7 Tumor classification

Preoperative characteristics include information about the disease that are usually obtained through histopathological exams. Data are summarized in Table 8.

Datum	**Description**
Tumor types	The different types of liver tumor reported are: - primary malignant tumors of the liver - secondary malignant liver tumors, specified as metastatic - biliary malignant tumor - malignant tumor of extrahepatic bile ducts Full explanation was already done in paragraph 2.7.8.
Number of tumors	It indicates if only one tumor or multiple node metastasis are present in different liver segments.
Tumor size [cm]	This is often a determining factor in the definition of the T-stage (see paragraph 2.3.8.1), but in many cancers it allows a more precise detail of extension, important for the evaluation of diagnostic sensitivity.
Tumor localization	Localization is defined through the liver division in segments (see segmentations in paragraph 3.1.4).
Vascular invasion	It concerns tumor invasion of the principle vascular structures, such as:

	▪ cava vein ▪ hepatic vein ▪ portal vein
Peritumor lymph vascular invasion	It correlates with regional lymph node metastasis, suggesting that lymphatic vessel invasion implies a high probability of lymph node metastases [85].
Tumor differentiation	The degree of differentiation describes how the neoplasm deviates, in its histological aspect, from the normal tissue from which it originated: ▪ g1: well-differentiated (low grade) ▪ g2: moderately differentiated (intermediate grade) ▪ g3: poorly differentiated (high grade) ▪ g4: undifferentiated (high grade) [86].

Table 8 Preoperative characteristics: tumor classification.

5.2.2.2 Intraoperative data

The first two intraoperative data are the surgical procedure (right/left hepatectomy, extended right/left hepatectomy) and the surgical technique (laparotomy or laparoscopy). All patients considered both in the intervention group and control group must share similarity because if a surgery is less invasive, the recovery will be easier and faster.
Among the intraoperative outcomes, there are also reported blood losses and the duration of the operation, which in the literature are highlighted as the main advantages of using 3D reconstructions in the preoperative planning.

5.2.2.3 Postoperative data

Continuing with the results highlighted in literature as the most relevant, the duration of hospitalization, 90 days mortality, morbidity and recurrence rate of liver cancer have been reported as post-operative outcomes.
Moreover, the same laboratory results of the preoperative data are reported, but, in this case 5 days and 10 days after surgery.

5.2.2.3.1 Surgical margins

The recurrence rate is strictly related to the surgical margins. The desired effect is to see fewer cancer-free margins when surgery is planned with a 3D reconstruction. Surgical margins classification, shown in Table 9, is based on the absence or presence of residual tumor tissue after surgery [87].

Symbol	Description
RX	The presence of the remaining tumor cannot be established.
R0	Surgical margins free of neoplasm.
R1	Surgical margins at focally limit with neoplasm.
R2	The tumor arrives on the resection shear.

Table 9 R classification of surgical margins [87].

5.2.2.3.2 Clavin-Dindo classification

Between postoperative data, there are mostly complications after surgery, such us pleural effusion, bleeding, wound infection, bile leakage, biliary fistula, incisional hernia, intra-abdominal abscess, hemorrhage, ascites, hepatorenal syndrome, lesions of near organs, and adhesions (for full description see paragraph 2.4.5).

However, the classification of post-operative complications mostly used in literature is the Clavien-Dindo classification. It is very useful to compare the different surgical methods and to measure the different levels of severity of surgical complications. Table 10 shows the Clavien-Dindo classification which differentiates all complications in 5 degrees. The first two grades are those least at risk for the patient and they require no procedures but only additional specific pharmacological therapeutic supports, blood transfusions or total parenteral nutrition. The last two include radiology procedures or interventional endoscopy or surgical re-interventions until the need for hospitalization in intensive care units with dysfunction of one or more organs [88].

Grade	**Description**
Grade I	It defines complication any change in the normal postoperative course that does not determine the use of pharmacological, surgical, endoscopic or radiological treatment; while therapies with antiemetics, antipyretics, analgesics, diuretics, electrolytes and physiotherapy are allowed. It is included in this degree the treatment of surgical site infections by opening the wound at the sick person's bed.
Grade II	Need for drug treatment other than that allowed in the previous degree; blood transfusions and parenteral nutrition are included in this degree.
Grade IIIa	Surgical, endoscopic, or radiological need not under general anesthesia.
Grade IIIb **Grade IV**	Surgical, endoscopic, or radiological need under general anesthesia.
Grade IVa	If it turns out life-threatening with need of hospitalization in intensive care unit with single organ dysfunction (including dialysis).
Grade IVb	If it turns out life-threatening with need of hospitalization in intensive care unit with multiple organ dysfunction.
Grade V	Patient's death.

Table 10 Clavien-Dindo classification [88].

5.2.2.3.3 Hepatic failure at postoperative day 5

As already explained, major hepatectomy has the risk of liver failure because FLRV is not enough to bear the regrowth of the liver. For this reason, laboratory results at post operative day 5 are collected in order to verify liver functionalities.
The International Study Group of Liver Surgery (ISGLS) gives a definition and grading to post hepatectomy liver failure. They define it as "*impaired ability of the liver to maintain its synthetic, excretory, and detoxifying functions, which are characterized by an increased international normalized ratio and concomitant hyperbilirubinemia (according to the normal limits of the local laboratory) on or after postoperative day 5*" [89].
The severity of liver failure is graded as shown in Table 11:

Grade	**Description**
Grade A	Postoperative deterioration of liver function that does not require a change in patient's clinical management. This grade is diagnosed based on deterioration from preoperative laboratory tests indicating a postoperative impairment of liver function. These patients have no clinical symptoms deviating from a normal, expected postoperative course, not requiring additional diagnostic evaluation. They are managed in the regular ward.

Grade B	Deviation from regular postoperative clinical pathway that can be managed without invasive treatment, such as administration of albumin, daily diuretics, and noninvasive ventilation. These patients commonly need additional diagnostic evaluation, like abdominal ultrasonography or CT, to exclude biliary obstruction and the presence of intra-abdominal fluid collection, respectively, chest radiography and culture of sputum, blood, and urine if there are signs of infection. Furthermore, patients with grade B may present a clinically relevant ascites, more weight, mild respiratory insufficiency, and mild symptoms of encephalopathy.
Grade C	Patients who need invasive procedure such as hemodialysis, intubation and mechanical ventilation, extracorporeal liver support, circulatory support, rescue hepatectomy, and transplantation. Patients with grade C are in a critical clinical condition and they should be monitored in an intensive care unit.

Table 11 Grading to assess the hepatic failure by ISGLS [89].

5.2.3 Pre-operative, intra operative and post operative data

In Tables 12-16, data of patients from Vimercate hospital divided in 3D group and 2D group are listed.
Continuous data are presented as mean ± standard deviation, while categorical variables are presented as n (%).

5.2.3.1 Pre-operative

Datum	3D	2D
Age [y]	61 ± 8,24	72 ± 3,16
Sex - **M** - **F**	 3 (50%) 3 (50%)	 2 (33,33%) 4 (66,66%)
Height [m]	1,68 ± 0,059	1,67 ± 0,084
Weight [kg]	59 ± 12	65 ± 8,24
BMI	23,11 ± 3,29	23,78 ± 3,49
BRASS scale	3,5 ± 2	3 ± 0
BARTHEL INDEX	100 ± 0	94 ± 14
BRADEN INDEX	22 ± 2	22,66 ± 0,81
ASA score - **ASA I** - **ASA II** - **ASA III**	 3 (50%) 1 (16,6%) 2 (33,33%)	 3 (50%) 0 3 (50%)
Child Pug score - **A** - **B** - **C**	 6 (100%) 0 0	 6 (100%) 0 0
Previous abdominal surgery - **YES** - **NO**	 3 (50%) 3 (50%)	 4 (66,66%) 2 (33,33%)
Chornic hepatitis - **B** - **C** - **NEGATIVE**	 0 0 6 (100%)	 0 0 6 (100%)
Chirrosis - **YES**	 0	 0

- NO	6 (100%)	6 (100%)
Alchol intake - VERY FREQUENTLY - FREQUENTLY - OCCASIONALLY - RARELY - VERY RARELY - DO NOT USE	 0 0 2 (33,33%) 2 (33,33%) 0 2 (33,33%)	 0 0 2 (33,33%) 3 (50%) 0 1 (16.6%)
TBIL [mg/dL]	1,29 ± 1,002	0,99 ± 0,873
ALT [U/L]	28 ± 20,4	27,3 ± 15
AST [U/L]	25 ± 11,44	32 ± 16,40
ALB [%]	59 ± 4,37	60 ± 2,53
Platelets [x10^9/L]	249 ± 114	242 ± 90
Prothrombin time [INR]	1,12 ± 0,141	1,08 ± 0,0796
Partial prothrombin time [s]	29 ± 2,315	31 ± 5,64
Partial prothrombin time[ratio]	0,95 ± 0,044	1,05 ± 0,203
HGB [g/dL]	12,46 ± 2,04	12,98 ± 1,02
Indirect bilirubin [mg/dL]	0,78 ± 1,09	0,06 ± 0
Direct bilirubin [mg/dL]	1,27 ± 0,66	2,7 ± 0
CA19-9 [U/mL]	49 ± 63,09	73 ± 54,73
CEA [ng/mL]	15 ± 24	19 ± 27,36
AFP [IU/mL]	143 ± 324	139 ± 326
Number of tumors - SINGLE - MULTIPLE	 4 (66,66%) 2 (33,33%)	 6 (100%) 0
Tumor size [cm]	6,13 ± 4,65	5,9 ± 4,03
Vascular invasion - YES - NO	 6 (100%) 0	 6 (100%) 0
Tumor differentiation - G1 - G2 - G3	 2 (33,33%) 1 (16,66%) 3 (50%)	 1 (16,66%) 1 (16,66%) 4 (66,66%)
Invasion of the cava vein - YES - NO	 3 (50%) 3 (50%)	 0 6 (100%)
Invasion of the hepatic vein - YES - NO	 5 (83,33%) 1 (16,6%)	 4 (66,66%) 2 (33,33%)
Invasion of the portal vein - YES - NO	 2 (33,33%) 4 (66,66%)	 4 (66,66%) 2 (33,33)
Peritumor lymph vascular invasion - YES - NO	 1 (16,66%) 5 (83,33%)	 4 (66,66%) 2 (33,33%)

Table 12 Preoperative results.

5.2.3.2 Intraoperative

Datum	3D	2D	p-value
Surgical procedure			
- right hepatectomy	1 (16,6%)	1 (16,66%)	
- right extended hepatectomy	1 (16,6%)	1 (16,66%)	
- left hepatectomy	0	2 (50%)	
- left extended hepatectomy	3 (50%)	2 (50%)	
- left lateral lobectomy	1 (16,66)	0	
Surgical technique			
- laparotomy	6 (100%)	6 (100%)	
- laparoscopy	0 (0%)	0 (0%)	
Intraoperative blood loss [mL]	320 ± 383	1100 ± 1000	0,19
Operative time [min]	399,16 ± 136	339,16 ± 119	0,21

Table 13 Intraoperative results.

5.2.3.3 Postoperative

Datum	3D	2D	p-value
Length of hospital stay [days]	36 ± 29,42	53 ± 37,62	0,19
Recurrence rate of liver cancer	1 (16,6%)	3 (50%)	0,24
90 days mortality	1 (16,6%)	1 (16,6%)	1
Margin R0	0.90 ± 0,141	0.66 ± 0,509	0,16
Margin R1	0.05 ± 0,134	0.00 ± 0	0,18
Margin R2	0.04 ± 0,101	0.33 ± 0,56	0,11
Clavien Dindo score			0,63
- **Grade I**	0	0	
- **Grade II**	3 (50%)	1 (16,6%)	
- **Grade IIIa**	0	2 (50%)	
- **Gradee IIIb**	1 (16,6%)	0	
- **Grade IVa**	1 (16,6%)	2 (50%)	
- **Grade IVb**	0	0	
- **Grade V**	1 (16,6%)	1 (16,6%)	
Pleural effusion	4 (66,66%)	4 (66,66%)	1
Bleeding	1 (16,6%)	1 (16,6%)	1
Wound infection	1 (16,66%)	0	1
Bile leakage	2 (33,33%)	3 (50%)	1
Biliary fistula	4 (66,66%)	2 (33,33%)	0,56
Laparocele	0	0	1
Intra-abdominal abscess	1 (16,66%)	0	1
Hemorrhage	0	0	1
Ascites	1 (16,66%)	0	1
Hepatorenal sindrome	0	1 (16,66%)	1
Lesions of near organs	2 (33,33%)	1 (16,66%)	1
Adhesions	2 (33,33%)	1 (16,66%)	1
Posture injury	1 (16,66%)	0	1

Table 14 Postoperative results.

Laboratory test at day 5			
Total BIL [mg/dL]	2,50 ± 0,589	1,90 ± 0,64	0,14
Indirect bilirubin [mg/dL]	0,75 ± 0,589	0,40 ± 0,848	0,18
Direct bilirubin [mg/dL]	1,75 ± 0,515	1,50 ± 0,698	0,24
ALT [U/L]	150 ± 131,14	107.5 ± 134,81	0,25
AST [U/L]	55,66 ± 29,25	65,83 ± 33,04	0,29
ALB [g/dL]	2,404 ± 1,27	2,9 ± 0,56	0,27
Platelets [x10^9/L]	198 ± 82,10	197 ± 52,16	0,48
Prothrombin time [INR]	1.46 ± 0,223	1.27 ± 0,2	0,08
Prothrombin time partial [s]	28.83 ± 5,6	30.6 ± 6,8	0,32
Prothrombin time partial [ratio]	0,95 ± 0,141	1,008 ± 0,244	0,33
HGB [g/L]	10,66 ± 1,64	10,63 ± 0,99	0,48
Hepatic Failure at postoperative day 5			0,02
- **Grade A**	0	0	
- **Grade B**	2 (33,33%)	1 (16,66%)	
- **Grade C**	4 (66,66%)	5 (83,13%)	

Table 15 Lab results five days after surgery.

Laboratory test at day 10			
Total BIL [mg/dL]	2,35 ± 1,29	1,55 ± 0,509	0,1
Indirect bilirubin [mg/dL]	0,99 ± 0,717	0,398 ± 0,1646	0,07
Direct bilirubin [mg/dL]	1,63 ± 0,7	1,298 ± 0,435	0,19
ALT [U/L]	39.83 ± 20,85	53.83 ± 43,04	0,24
AST [U/L]	30.16 ± 12,08	167.33 ± 324,75	0,17
ALB [g/dL]	-	-	-
Platelets [x10^9/L]	246 ± 0,4	277 ± 0,1128	0,369
Prothrombin time [INR]	1,56 ± 0,4105	1,24 ± 0,105	0,06
Prothrombin time partial [s]	30 ± 3,16	44,66 ± 40,53	0,316
Prothrombin time partial [ratio]	0,985 ± 0,097	1,55 ± 1,5104	0,16
HGB [g/L]	9,2 ± 0,9186	9,83 ± 1,424	0,19

Table 16 Lab results 10 days after surgery.

5.2.4 Statistical Analysis

Statistical analysis was performed using Microsoft Excel 16.66. Continuous data are presented as mean ± standard deviation, while categorical variables are presented as count and percentage for each possible answer.
In this case, the null hypothesis to reject is that a preoperative planning with two-dimensional images is better than that with 3D rendering, based on intraoperative and postoperative outcomes.
Due to a sample size too small, a p-value less than 0.05 would never have been reached.
For this reason, in all cases, statistical significance was defined as $p < 0.20$.
This means to assume the 20% of probability of returning a significant result (and thus reject the null hypothesis) when in reality the null hypothesis is true.
Assuming the confidence level of 80%, in this percentage, the alternative hypothesis (3D better than 2D) will be correct.

Since a two-sample t-test is defined as statistical hypothesis testing technique in which two independent samples are compared to determine if the means of two populations are statistically different, continuous variables were compared with the Student’s t-test.
This choice was made under the assumption that data are independent, normally distributed and patients’ measurements represent a simple random sample from the population. Moreover, one tail t-test was used because the priory hypothesis of 3D outcomes better than 2D outcomes was made.

For statistical analysis, categorical variables were compared using the chi-square test or Fisher’s exact test. They permit to verify whether the differences between the two data may be due to the randomness. The Fisher’s exact test is used when two dichotomous nominal variables and small samples are present. The objective of the test is to verify whether the dichotomous data of two samples, usually summarized in a contingency table 2x2, are compatible with the null hypothesis and therefore any differences observed through the data are due to a pure and simple case.
If the number of categories taken into account for a specific outcome was higher, the chi-square test was used.

5.2.5 Comparison between 3D and 2D

First of all, the analysis of preoperative data shows a high similarity between the intervention and control group especially in those parameters that classify the general state of the patient as: BMI, results of the scales compiled by nurses, previous surgical history and ASA score. This similarity is confirmed by specific indicators of liver disease such as child-pug score, hepatitis, cirrhosis, oncological markers, and alcohol use. On the other hand, there is much variability about the laboratory tests performed during the pre-hospitalization, especially as regards bilirubin. The biggest difference is found in direct and indirect bilirubin: this is because these data are not reported for all patients, so it is difficult to calculate an average within the group.
Regarding the parameters inherent the lesion, in both groups, patients have a tumor of about 6 cm in size that invades the vascular structures. The similarity between the two groups is confirmed in the case of invasion of the hepatic vein. However, in the intervention group, there were more clinical cases with invasion of the cava vein, while in the control group the number of patients in which the lesion also involves the portal vein and lymph nodes is greater.
It's important to underline that the two patients in the intervention group present multiple tumors, while in the control group all patients have a single lesion.

In the intervention group, blood loss was found to be lower although the procedure and surgical technique do not differ particularly between the two groups. However, operations performed with pre-operative planning have a slightly shorter duration. This is because in the intervention group there are two patients with localized cancer in different parts of the liver. Such pathology definitely requires more time in the surgical room. Despite this, the difference in terms of blood loss is statistically significant: if the surgery is planned with the use of a 3D reconstruction, the surgical technique will be more precise.

The advantages of the postoperative course are evident especially in terms of duration of hospitalization and surgical margins. In these cases, the difference is statistically significant. Indeed, if the surgery has been planned with the use of 3D, the surgeon has a more precise

idea of the location of the tumor, and he manages to remove it completely. Hence, a surgery planned precisely according to the anatomy of the patient leads to a shorter and more regular course of surgery.
Although the difference is not statistically significant, in Table 12, it can be noted that cases with a higher Clavien-Dindo degree are found mainly in the control group. There is not much difference between the two groups about the variability of the type of post-operative complications: pleural effusion is the most common complication in both groups.

The results of post-operative laboratory tests differ considerably between the two groups. However, in the control group the number of patients with Grade C liver failure studied according to ISGLS is higher. For this outcome, the difference between the two groups is statistically significant with a p-value even lower than 0.05 (typically used value).

It can be concluded that the use of 3D rendering in preoperative planning results in less blood loss during surgery, less hospitalization time, and more precise surgical margins.

6 Safety analysis

Safety depends on the quality of 3D: if the rendering is not accurate enough, the surgical planning will not be adequate to the needs of the patient due to a distortion of reality.
The quality of a surface rendering depends on how two-dimensional images were captured and how they were interpreted. For 3D models, both the CT scan and the MRI scan can be used, both acquired with contrast medium and in an adequate way to have the maximum of the spatial resolution. Nevertheless, the best method is the fusion of images, but it still little adopted due to the difficulty of integration in the software development phase.
In addition, there must be a good interpretation of the image, also determined by the accuracy of the clinical question: for example, if the surgeon wants to do a right hepatectomy, the left part can be approximated.
Anyway, the most important part in building a 3D rendering is segmentation, closely related to the interpretation of the image. The 3D model represents what and how the two-dimensional image was interpreted by the operator who performed the reconstruction.
If distortions are present, they could be caused by an abundant use of smoothness techniques as they rely on interpolation, creating lines where there is no specific data in the 2D image.

Fang et al. in a consensus recommendation define the optimal CT parameters that should be used during data acquisition for 3D rendering (see paragraph 3.1.2) [5].
To assess the accuracy level of a three-dimensional reconstruction, they define a 3D visualization quality score (3DVQS). This quality control system refers to preoperative surgical simulation, intraoperative 3D surgical navigation and postoperative 3D reconstruction. It consists in numerous recommendations (Table 18) with the related classification of quality of evidence and grade of strength (Table 17) and 16 different criteria (Table 19) used to compute the score [5].

Grade	Classification	Content
Quality of evidence		
High	A	The true effect lies close to the estimated effect.
Moderate	B	The true effect is likely to be close to the estimated effect, but there is a possibility that it is substantially different.
Low	C	The true effect may be substantially different from the estimated effect.
Strength of recommendation		
Strong	1	The desirable effects outweigh the undesirable effects.
Weak	2	The desirable effects possibly outweigh the undesirable effects.

Table 17 Quality of evidence and strength of recommendation [5].

Recommendation Number	Description	Quality of evidence	Strength of recommendation
Recommendation 1 (operator)	Sufficient anatomical basis and solid knowledge of liver surgery are required, along with at least 30 cases of standardized operation made for training.	B	Strong
Recommendation 2 (examinee)	The patients should fast for at least 4 h prior to CT exam, rest for 10–20 min, and hold their breath during scanning.	A	Strong
Recommendation 3 (homogenous 3D model)	It is suggested to select 64-slice or above helical scanner with a slice thickness of 0.625–1.0 mm for 3D reconstruction.	A	Strong
Recommendation 4	It is suggested that the original 3D model will be repeatedly discussed, verified and modified by at least 2 abdominal imaging attendings and at least 2 attending physicians.	A	Strong
Recommendation 5	It is suggested that analysis of hepatic veins, hepatic arteries, portal veins, and bile ducts should be performed by at least 1 abdominal imaging attending and 1 attending physician for vascular system classification.	A	Strong
Recommendation 6	It is suggested to perform virtual simulation surgery using 3D model before operation, to select the optimal surgical approach and surgical resection plane and calculate the residual functional liver volume on an individual basis.	A	Strong
Recommendation 7	It is suggested to determine the final surgical planning by combining the results of multidisciplinary discussion based on 3D visualization, as well as the wishes of patients and their family.	A	Strong
Recommendation 8	It is recommended to measure the volume of liver specimen and compare it with that of virtual resection to obtain the discrepancy between surgical planning and actual operation.	A	Strong
Recommendation 9	For patients with liver diseases diagnosed and treated by 3D visualization, it is recommended to follow the quality control steps of 3DVT and conduct quality scoring, which is conducive to standardize the effect of clinical evaluation.	A	Strong
Recommendation 10	It is necessary to follow the quality control steps and conduct quality scoring, no matter what 3D visualization software is used.	A	Strong

Table 18 Recommendations of the quality control system [5].

The criteria in Table 19 are used for quality scoring. A score no more than 15 is recognized as undesirable, while a score more than 15 points is recognized as desirable.

Number	Criteria	Points
1	Diagnosis of liver diseases by preoperative imaging (ultrasound, CT or MRI).	+1
2	Patients fast for at least 4 h prior to CT scan, orally take 0.5L–1.0L of clear liquid 20 to 30 min prior to the exam and take another 500 ml prior to the exam.	+1
3	Train the patients to hold their breath in full inspiration before scanning and instruct them to do so during each scan phase to achieve maximum management of artifacts due to respiratory motion.	+1
4	Select 64-slice or above spiral CT scanning with slice thickness of 0.625–1.0 mm.	+1
5	CT scanning ranges from the top of the diaphragm to the lower level of both kidneys, and, furthermore, perform dynamic abdominal scan after intravenous contrast medium administration; perform CT celiac arteriography. The arterial phase, portal venous phase, and delayed phase scans start at a delay of 20–25 s, 50–55 s, and 2 min, respectively.	+1
6	3D reconstruction should be performed by attending physicians or professionals who are engaged in the diagnosis and treatment of liver diseases.	+1
7	Evaluate the integrity of the course, shape, and continuity of hepatic artery reconstructed by 3D visualization to determine whether manual revision is required (manual revision is unnecessary when the tertiary branches of artery can be reconstructed).	+1 (no manual revision); − 1 (manual revision required)
8	Evaluate the integrity of the course, morphology, and continuity of hepatic vein reconstructed by 3D visualization to determine whether manual revision is required (manual revision is unnecessary if the tertiary branches of hepatic vein can be reconstructed).	+1 (no manual revision); − 1 (manual revision) required)
9	Evaluate the integrity of the course, morphology, and continuity of portal vein reconstructed by 3D visualization to determine whether manual revision is required. The branches of the portal vein system with the diameter ≥ 5 mm should be reconstructed (it is unnecessary if the tertiary branches of portal vein can be reconstructed).	+1 (no manual revision); − 1 (manual revision required)
10	Evaluate its course, morphology, continuity, and integrity of the 3D reconstructed biliary duct (manual revision is unnecessary if the tertiary branches of biliary tree can be reconstructed).	+ 1 (biliary system reconstructed); − 1 (no biliary system reconstructed)
11	Evaluate the morphology, size, and distribution of lesions in the 3D reconstructed model and whether they are consistent with CT images.	+ 3 (basically consistent, no manual revision required); + 2 (mostly consistent, manual revision required); -1(inconsistent, manual revision required)

12	The overall 3D model should be validated by at least 2 abdominal imaging attendings and at least 2 attending hepatologists in comparison with the original CT images, and finally confirmed by a senior physician.	+1
13	Perform simulation surgery based on 3D model. The simulation of various schemas should be carried out and the optimal surgical approach and surgical resection plane should be selected by two attending physicians, and finally confirmed by a senior physician.	+2
14	A multi-disciplinary team (MDT) should be formed based on the individualized 3D model and the results of clinical examinations.	+2
15	The consistency between preoperative 3D models and intraoperative conditions (lesions, vascular variance, and range of hepatectomy) should be assessed.	+ 3 (completely consistent); + 2 (basically consistent); − 1 (inconsistent)
16	The volume of the virtual resected liver with that of the actual resected liver (reference standard is intraoperative dewatering method) should be compared. The volume error (< 5%) is completely consistent, the volume error (< 10%) is basically consistent, and the volume error (> 10%) is inconsistent.	+ 3 (completely consistent); + 2 (basically consistent); − 1 (inconsistent)

Table 19 Process measures [5].

The quality management system operated by Medics 3D and Visible Patient follows the standard ISO 13485:2016.

As already explained in paragraph 3.4, The UNI EN ISO 13485 standard concerns:

- manufacturers of devices subject to CE marking;
- suppliers of particular processes associated with the realization of the devices (e.g. sterilization, storage, transport);
- companies that distribute and market medical devices;
- companies providing device related services (installation, maintenance, and repair/service).

The UNI EN ISO 13485 standard:

1. provides a focus on activities associated with the effective use to ensure that the safety and performance requirements of devices are met throughout their life cycle;
2. stresses the need to assess the "usability" of medical devices;
3. pays particular attention to the role and responsibilities of the different parties that play a decisive role in the life cycle of devices: suppliers, logistics service providers, distributors, importers, etc.
4. recognizes service providers, processes and semi-finished products as important players in the implementation cycle of medical devices;
5. introduces the design transfer requirement;
6. provides for the monitoring of products after marketing to be subjected to new requirements;
7. provides for the validation of the design transfer requirement;
8. provides for the validation of the software used for the quality management system and for the software involved in the production and service delivery processes;
9. places great emphasis on the risk-based approach to process management.

Concerning point 2, Sternini et al. evaluate the usability of a new medical device intended to assist the intraoperative planning with the visualization of 3D patient-specific organ models. The visualization is aided by a touchless user interface that tracks and identify the hands of the user, without the need for additional sensors. The surgeon can position, zoom and orientate specific part of the model, previously selected [90].

As suggested by the International Electrotechnical Commission, the methodology for the usability assessment was performed firstly with a formative evaluation and then with a summative evaluation.
The former evaluation is iterated until a satisfactory quality level is reached and it began during the early stage of the development of the device. While the summative evaluation is the last phase of the usability assessment, and it is intended to confirm the usability of the medical device. Therefore, the device involved in the study shall be consistent with the final version of the medical device and it shall present all the features of the medical device. In this phase, the moderatos asked the user to complete some complex actions while observing the device use and annotating the performance of the user for each task. The moderators classified each task completed by the user in 4 classes, based on the errors made. The users completed correctly 60% of the tasks, while 20% of the tasks were classified as use errors. The remaining 18,59% of tasks were not performed by the users and technical errors occurred in 1,41% of the tasks.
After the completion of the simulated tasks, all users were asked to compile some questionnaires about the risks of the device, elements that violate the usability, aspect of user interface and visualization mode.
No users report to become nervous during the device use: it is considered very good, despite the users pointed out that they had difficulties during the management of the model and the use of gestures. Good results are collected also during the summative evaluation: the safety of the device was confirmed, and additional information for further improvements are collected, both in terms of evaluation of user interface and about the training provided to users.
This is an example of usability evaluation of 3D model visualization, very important especially during the intraoperative phase [90].

7 Analysis of the patient's point of view

Another advantage of using 3D models is the most immediate communication with the patient. 3D rendering, especially when printed, allows to give clearer and understandable explanations to the patient and his family, who do not have particular clinical skills. In this way, the patient also has a clearer and broader idea of the risks associated with a certain complex surgical procedure.

7.1 Patient perception

Porpiglia et al. show 3D printed models to their respective patients. A specific ten-points rating scale questionnaire about the utility of the model was administered. Questions were focused on the overall satisfaction about the conversation and the case discussion of the surgeon with the patient in order to highlight the usefulness of the model in better understanding the disease and the surgical procedure planned [91].
The questionnaire was created according to the Face and Content validity concepts. Content validity, measured trough objective questions, means that the set of items comprehensively cover the different components of health to be measured. While, face validity defines where the items of each domain are sensible, appropriate and relevant and it is measured through subjective questions [92].

The questions were:

- Q1: "how do you evaluate the conversation with the physician before surgery?"
- Q2: "how do you evaluate the usefulness of 3D printed model during the clinical case discussion?"
- Q3: "do you think that 3D printed model can offer additional information for the comprehension of the surgical procedure?"
- Q4: "do you think the 3D printed model can simplify the clinical case discussion with the surgeon?"

Eighteen patients' questionnaire were collected and analyzed. Results were expressed as medians and interquartile range (IQR).
The patients were satisfied with the conversation with the respective surgeon (QP1: 9/10–IQR 7–9) and they appreciated the use of 3D printed model during the clinical case discussion (QP2: 10/10–IQR 9–10). They expressed a better comprehension of the disease (QP 4 10/10–IQR 9–10) and the intervention (QP4: 10/10–IQR 9–10), as shown in Figure 33:

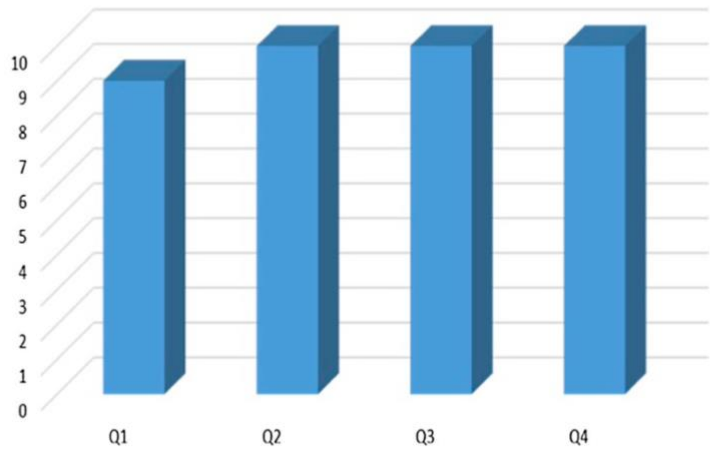

Figure 33 Results from the filled questionnaire by the patient [91].

These results confirm the report by Bernhard et al. who analyze patient education using personalized 3D printed models of kidney and tumor anatomy.
Two different questionnaires were created to prospectively evaluate the level of patients' preoperative knowledge and understanding.
The first evaluation was based on the previously delivered information and CT scan images. The day before surgery scan images were used as a teaching aid to deliver information on the organ itself, the disease, and the surgery. After this phase, the first questionnaire was compiled: it consisted of 22 questions to evaluate four components of patient knowledge:

- basic kidney physiology;
- basic kidney anatomy;
- tumor characteristics;
- planned surgical procedure.

The second questionnaire was administered using the 3D printed model to assess the improvement following model presentation. In addition to the 22 questions, patient satisfaction was investigated.

The results of this study underline that patients show an overall improvement in understanding with 3D printed model of 37.6%. Patient's understanding was significantly improved on basic kidney physiology ($p = 0.018$), basic kidney anatomy ($p = 0.026$) and planned surgical procedure ($p = 0.026$).
Moreover, the overall mean satisfaction score among the group was 9.4/10, and five patients over 7 rated their experience with their own model at the maximum level [93].

These results highlight that also patients can benefit from the introduction of personalized physical 3D models because they facilitate mutual understanding between patient and physician.

7.2 Quality of life

Patients’ perception using 3D model was properly tested in literature, while their quality of life after surgical intervention was not determined. This analysis has the aim to make a comparison of patients’ health status after surgery planned trough bidimensional images against three-dimensional ones.

7.2.1 Definition and measurement methods

Quality of life (QoL) is defined by the World Health Organization as "*an individuals’ perception of their position in life in the context of the culture and value systems in which they live and in relation to their goals, expectations, standards and concerns*". It can be measured against some dimensions such us mobility, self-care, usual activities, pain and discomfort, anxiety, and depression. But it can also include other factors like employment, environment, physical and mental health, education, recreation and leisure time, social belonging, religious beliefs, safety, security and freedom.

There are two types of approaches for QoL measurement:

- measurement of the individual preferences: the assumption is that QoL is a personal reflection. Even if the dimensions taken in consideration are similar, the QoL can be different because every patient has a different perception of the concept of QoL.
- measurement of the state of health: the main assumption is that the QoL is explained by the state of health. If two state of health are similar, also the QoL would be similar [7].

Moreover, it is used to define utility in terms of QALY: quality adjusted life years.

7.2.1.1 Measurement of individual preferences

7.2.1.1.1 Rating Scale

Rating Scale is typically used in the 80/90% of cases. Patients are asked to attribute a value between 0 and 1 (or 100) to their health state (0 = worst imaginable health scenario, 1 = best imaginable health scenario). It is a comprehensive free evaluation of patient’s QoL but it cannot be used in case of neurological pathologies [7].

7.2.1.1.2 Time trade-off

Time trade-off is a sophisticated and expensive method.
Let assume that the patient lives in the state D for almost 10 years (state D means unable to perform some tasks at home and/or at work, unable to perform all self-care activities or able but with some difficulties, unable to participate in many types of leisure activity).
The investigator gives opportunity to change patient’s situation. Patient is asked to choose between two alternatives:

- live longer with lower QoL: less than perfect health for a period (T);
- live shorter with perfect QoL: perfect health for (x = length of life after treatment) year, with $x < T$.

Time x must be varied until the patient is impartial between the two alternatives. When the patient cannot decide between the two alternatives, this means that the utility of the two alternatives is equal and quality of life of the state D, that can be measured as x/T [7].

7.2.1.1.3 Standard gamble

This method is similar to the previous one but in this case the investigator asks to the patient to simulate the participation in a gamble (magic or innovative treatment). The patient has to choose between two alternatives:

- imperfect health: the patient rejects the innovative treatment and decide to stay as he or she is;
- participate to a gamble with a probability x of perfect health and a probability 1-x of death.

The investigator asks to the patient what his/her current health status is. So, the physician tells the patient that there is a new treatment where probability of perfect health is 50%. The patient doesn't accept. To persuade the patient, the physician increases the probability of perfect health to 70%. At this point, the patient accepts. After that the physician decrease the probability of perfect health to 60%. The patient tells the physician that he or she can't decide, he or she is indifferent. The patient is not able to decide because the utility that the patient can have from the two alternatives is the same. The quality of life is exactly the probability x, the probability of success. Since the patient stopped the exercise when the probability is 0.7, that means that the QoL is 70%, accepting a probability to die of 30%. The limitations of this method are that the patient is not engaging so much (he knows that it is a fake exercise and answers cannot be honest) and different physicians might bias the patient's answer, persuading the patient, also with body language.

7.2.1.2 Measurement of the state of health

7.2.1.2.1 Health related quality of life (EQ-5D-3L)

This method assumes that once the health status is known, also the quality of life of that patient is known. The health status is described by 5 dimensions:

1. mobility
2. self-care
3. usual activities
4. pain, discomfort
5. anxiety, depression.

One of these three levels of severity are associated to each dimension:

1. no problem: everything is perfect;
2. some problems: some limitations respect to some dimensions;
3. extreme problems: all dimensions are fully compromised.

The patient gives a value from 1 to 3 (the level) to each dimension (for example 11111 means perfect health), this is important for the researcher in order to profile patient's health status.
If the investigator is able to have a profile of the patient, he can define the quality of life.
To compute the QoL from the level, the researcher uses an algorithm that is based on an empirical analysis assessed to be much as possible near the reality. In the study researchers try to find the coefficients of the regression analysis that translate the 5 dimensions into the QoL.

At the end the QoL is equal to 1 minus the coefficients, shown in Table 20. There are also 2 constants to subtract: 0.081, if there is at least a level different to 1, and N3, if there is at least a level equal to 3.

Dimension		**Coefficient**
Constant		0.081
Mobility	Level 2	0.069
	Level 3	0.314
Self-care	Level 2	0.104
	Level 3	0.214
Usual activities	Level 2	0.036
	Level 3	0.094
Pain, discomfort	Level 2	0.123
	Level 3	0.386
Anxiety, depression	Level 2	0.071
	Level 3	0.236
N3		0.269
QoL=1-coefficients		

Table 20 Quality of life trough EQ-5d-3l [7].

7.2.2 Findings

To determine if there are differences in quality of life after a planned operation with 2D against 3D images, the last described method, EQ-5D-3L, was used.
Mobility, self-care, usual activities, pain and discomfort, anxiety and depression of patients previously selected for clinical effectiveness measurements (paragraph 5.2) were analyzed 4 months after surgery. This allowed to analyze in a standard way each dimension, which has been given a score from 1 to 3 and evaluate any difference between the intervention group (patients whose planned surgery was made using 3D images) and the control group (surgery planned traditionally through 2D images).
Once the scores were awarded, the quality of life for each patient was calculated using the coefficients listed in Table 20.
The average quality of life after 4 months from the planned surgery with 3D rendering is 0.70, while the average QoL of patients in the control group is 0.33. This difference is mainly caused by the fact that many patients in the control group, 4 months after surgery, still carried out drainage and chemotherapy due to the recurrence of the tumor or they were hospitalized again.
This finding shows that adequate and personalized surgical planning leads to better results in the long term, as demonstrated in the chapter on clinical effectiveness.
The results are summarized in Table 21 and Table 22.

	Mobility	**Self-care**	**Usual Activities**	**Pain and discomfort**	**Anxiety and depression**	**QoL**
Patient 1	2	1	2	1	1	0,81
Patient 2	1	1	1	1	1	1
Patient 3	2	1	2	1	1	0,81
Patient 4	1	1	1	1	1	1
Patient 5	3	3	3	3	1	0,59
Patient 6	Death					0

Table 21 QoL of patients from intervention group.

	Mobility	**Self-care**	**Usual Activities**	**Pain and discomfort**	**Anxiety and depression**	**QoL**
Patient 1	2	2	2	2	2	1,00
Patient 2	3	3	3	1	1	1,00
Patient 3	Death					0,00
Patient 4	3	2	2	2	1	0,07
Patient 5	1	2	2	2	1	0,66
Patient 6	1	1	1	1	1	1,00

Table 22 QoL of patients from control group.

8 Analysis of organizational and economical aspects

8.1 Organizational aspects

The organizational procedure of Medics and Visible Patient is very similar.
The surgeon must subscribe on to the portal cloud based. In his/her private section, the doctor can open a new case, upload the relevant DICOM images (CT, angiography and RMI), enter the details of the case and his own specific requests.
The company can accept or reject the case through specific segmentation protocols that must be executed to allow 3D reconstruction. Images must be made according to uniquely defined standards, as seen in paragraph 3.1.2.
Within 72 hours of the opening of the case, the anatomical reconstruction elaborated by engineers starting from the DICOM images and the requirements of the surgeon, is ready. It becomes viewable in the specific section on the web portal of the surgeon. Once the model is displayed, the surgeon can decide whether to opt for the surgery simulation. Multiple simulations of the surgery can be done and if a simulation is atypical, the surgeon must indicate which vessels are involved.

Medics 3D create rendering in PDF3D format that can be easily download and visualized using Adobe Acrobat. A 3D model is initially displayed as a two-dimensional preview image. By clicking on the 3D model, it is activated, the 3D toolbar is opened, and the animations are played. It is possible to use the 3D toolbar to zoom in, shrink, rotate, view the details of the object, and hide or isolate parts of the rendering, making them transparent. The 3D model can be rotated both in all directions and only vertically or horizontally. The zoom allows the surgeon to move closer or further away from the objects in the scene when he is dragging vertically. In the toolbar he can also use the 3D measurement tool, which allows the surgeon to measure the dimensions and distances of the parts in the model. In addition, the surgeon can choose different lighting effects, to better display the object, the background color to bring out some parts and turn on or off the cross-section.
With the 3D model, the surgeon can display a case description with information about the quality of bidimensional images, the anatomy of the principle vascular structure, the size of the tumor, its relationship with near vascular ducts and the volume computation based on the different alternatives of surgery operation proposed by the surgeon. In this way, 3D models help the determination of resection margins and in the planning of surgery with parenchyma savings, ensuring an adequate future liver remnant that constitutes a concrete resource within a multidisciplinary management of complex oncological pathology.

With Visible Patient, the 3D model visualization is a little bit different: it is necessary to install a specific software for full interaction with the model. The surgeon can click on a specific vein and a corresponding hepatic resection is simulated following that vessel as a resection plan. In addition, it is possible to instantly visualize the calculation of the remaining volume and remove it to allow adequate preoperative planning without risk of liver failure.

Even in the Virtual Clone portal it is necessary for the surgeon to register to have a private section where to upload different clinical cases, but the goal in this case is to provide a tool that will be completely integrated in the workflow of imaging acquisition, able to provide the patient with an immediate 3D reconstruction.

8.2 Economic analysis

Decision making in healthcare must be informed by identification, measurement and valuation of the elements that characterize different alternatives. Between these elements there are not only consequences (any improvement of health and well-being due to the adoption of a healthcare technology) but also costs, such us resources from:

- the healthcare system (hospital, nursing homes, local health agencies);
- patient, caregiver, family (patient's time, family time and travel costs);
- other sectors (social care, non-profit association).

The final choice will be a tradeoff between consequences and costs.
Moreover, there are different economic analysis that can be performed for supporting decision making in healthcare:

- cost-of-illness analysis: a determination of the economic impact of an illness or condition (typically on a given population, region, or country) e.g., of smoking, arthritis, or diabetes, including associated treatment cost;
- cost minimization analysis (CMA): specific methodology that is used when technology A and technology B have the same consequences, so the decision makers prefer the alternative that is more efficient (same benefit, less costs);
- cost-effectiveness analysis (CEA): a comparison of costs in monetary units with outcomes in quantitative non-monetary units:
  - cost-utility analysis (CUA) is a form of cost-effectiveness that compare costs in monetary units with outcomes in terms of their utility e.g., QALYs;
  - cost-consequences analysis: a form of cost-effectiveness analysis that presents costs and outcomes in discrete categories, without aggregating or weighting them;
- cost-benefit analysis (CBA): compares costs and benefits, both of which are quantified in common monetary units;
- budget-impact analysis (BIA): determines the impact of implementing or adopting a particular technology or technology-related policy on a designated budget, e.g., of a drug formulary or health plan [94].

In Table 23 there is a summarization of the different types of economic analysis:

Analysis type	**Valuation of costs**		**Valuation of outcomes**
Costs of illness	$	vs	None
Costs minimization	$	vs	Assume same
Cost effectiveness	$	÷	Natural units
• **Cost consequences**	$	vs	Natural units
• **Cost utility**	$	÷	QALYs
Cost Benefit	$	÷	$

Budget impact	$	vs	None

Table 23 Different types of economic analysis for HTA [94].

The flowchart below helps to decide which economic analysis is the most appropriate.

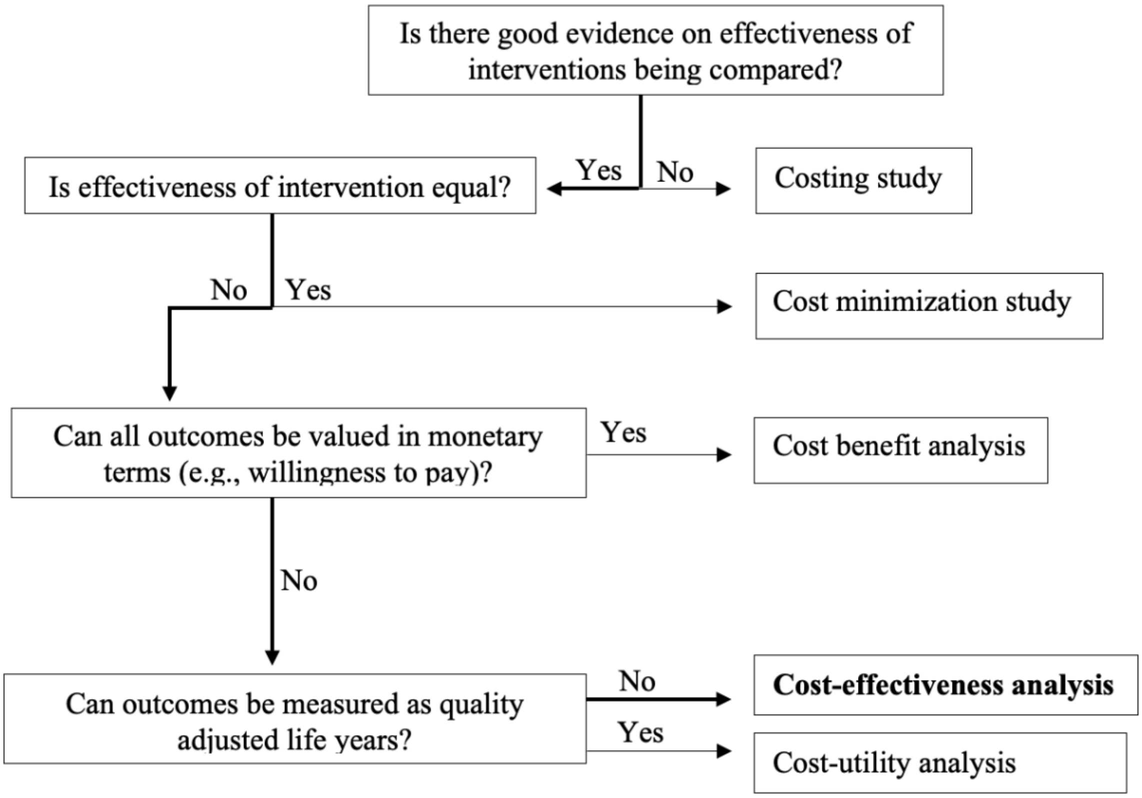

The bold path in the flowchart leads to the choice of the correct economic analysis for the evaluation of 3D technology compared to 2D.
Cost-effectiveness analysis attempts to identify where more health benefit can be produced at the same cost or where the same health benefit can be achieved for a lower cost (considering health care budget and lost productivity).
Outcomes within CEA, measured in natural units, can be:
- life years saved
- cancers detected
- reduction in blood pressure
- heart attacks avoided.

A CEA that reports the cost per life year saved will not capture potentially important impacts on patients' quality of life.
Hence, in this case it's difficult to quantify the life years gained but in Chapter 7 a computation of quality of life for each patient was done, based on the follow up visit 4 months after surgery.
This analysis underlined that the QoL of patients operated after a 3D planning was greater than the QoL of patients operated using the traditional 2D images. The difference between the intervention group and the control group was 0.37. This means that using 3D rendering there's an improvement in QoL.

About costs, 3D technology does not require additional resources from patient, family, caregiver, or other sectors because the patient must only come to the hospital for bidimensional images acquisition, which must however be done in the best possible way even if only 2D images will be used. In addition, the patient can go to the nearest hospital and send the 2D images with the report to the surgeon later. As for the resources spent by the hospital, each 3D rendering with simulation of the operation costs about 1000 euros.

Then given these data, it’s possible to compute the cost-effectiveness ratio (CER) with the formula below:

$$CER = \frac{COST_{3D}(€) - COST_{2D}(€)}{EFFECT_{3D}(\text{QoL}) - EFFECT_{2D}(\text{QoL})} = 27\ euros\ for\ quality\ of\ life\ gained \tag{8.1}$$

Thus, it can be estimated that the cost of 3D technology is mitigated by the increased benefits to patients in terms of quality of life.

8.3 Economic impact

The difference in outcomes analyzed in Chapter 5 can be used to verify the economic impact of adopting 3D for complex hepatobiliary surgery cases. The effectiveness analysis showed that there was a statistically significant difference in the length of hospitalization.
The DRG (diagnosis related group) system is used to quantify the economic value attributed to each treatment.
A certified software, called grouper and supplied to all healthcare facilities, analyzes the activity carried out on a patient during admission, which can be deduced from the hospital discharge letter (SDO).
Therefore, to every hospitalization concluded, one and only one of the 492 DRGs is associated, each of which has a different economic weight. The 492 categories, to which the universe of the possible clinical cases refers, are homogeneous within them in terms of consumption of care resources (workloads, drugs, direct costs, indirect costs, ...).
The diagnoses and interventions, which can be deduced from the SDO and used as grouper input, are automatically encoded in international standard codes. The group initially operates only on the main diagnosis (in the presence of more diagnosis, is the one that, in the subjective opinion of the doctor, is judged to characterize the hospitalization), leading the hospitalization to one of the 25 main diagnostic categories (MDC, major diagnostic category, Figure 34) [95].

MDC	Diseases and disorders of the nervous system
MDC2	Diseases and disorders of the eye
MDC3	Diseases and disorders of the ear, nose, mouth and throat
MDC4	Diseases and disorders of the respiratory system
MDC5	Diseases and disorders of the circulatory system
MDC6	Diseases and disorders of the digestive system
MDC7	Diseases and disorders of the hepatobiliary system and pancreas
MDC8	Diseases and disorders of the musculoskeletal system and the connective tissue
MDC9	Diseases and disorders of the skin, subcutaneous tissue and breast
MDC10	Endocrine, nutritional and metabolic diseases and disorders
MDC11	Diseases and disorders of the kidney and urinary tract
MDC12	Diseases and disorders of the male reproductive system
MDC13	Diseases and disorders of the female reproductive system
MDC14	Pregnancy and the childbirth
MDC15	Newborns and other neonates with conditions originating in the perinatal period
MDC16	Diseases and disorders of the blood and blood forming organs and immunological disorders
MDC17	Myeloproliferative diseases and disorders, and poorly differentiated neoplasms
MDC18	Infectious and parasitic diseases
MDC19	Excluded from Tw-DRG
MDC20	Excluded from Tw-DRG
MDC21	Injuries, poisonings and toxic effects of drugs
MDC22	Burns
MDC23	Factors influencing health status and other contracts with health
MDC24	Multiple significant trauma

Figure 34 Major diagnostic category [95].

A DRG therefore covers a set of possible clinical cases, concerning similar pathologies, whose course requires on average the same intensity of resources for treatment.

The economic weight of each DRG is determined by the Ministry of Health at national level and it is calculated based on the average resources absorbed considering both direct costs (e.g., care during hospitalization) and general costs (e.g., related to the administrative management of the shelter).

The economic weight associated with each DRG therefore does not directly express the severity of the pathology, but only the amount of resources to be used to treat the pathology in the standard case of the standard patient.

In practice, for non-standard cases, reimbursement allows for correction mechanisms, e.g., due to abnormal length of hospitalization.

Treatment of patients with particular clinical conditions leading to exceptionally long inpatient stays (outliers) may result in a significant deviation in resource consumption compared to the average of their category. Therefore, for each DRG a threshold value has been identified beyond which, for the sake of fair distribution, an additional remuneration is paid. For abnormal duration of hospitalization, the standard rate is reimbursed, increased by a value given by the product between the number of days in hospital over the "threshold value" and a specific daily rate of the DRG to which the hospitalization belong. However, the threshold value does not constitute a maximum period of admission.

As for hepatobiliary surgery, the corresponding DRGs are summarized in the Table 24 (CC=comorbidities and complications).

DRG	DRG description	MDC	MDC description	Rate ordinary hospitalization (€)	Threshold (days)	Rate per day of hospitalization above threshold (€)
191	Surgery on pancreas, liver and shunt with CC	7	Diseases and disorders of the pancreas	18833	27	345
192	Surgery on pancreas, liver and shunt without CC	7	Diseases and disorders of the pancreas	7549	48	147
193	Biliary interventions except isolated cholecystectomy with or without exploration of the common bile duct with CC	7	Diseases and disorders of the pancreas	13064	30	254
194	Biliary interventions except isolated cholecystectomy with or without exploration of the common bile duct without CC	7	Diseases and disorders of the pancreas	6118	51	146

Table 24 DRG of hepatobiliary surgery.

In Table 25 and Table 26, the DRGs were calculated for each patient in both the intervention (3D) and the control (2D) group.
The formula used for the calculation is as follows:

$$Hospedalization\ Costs = \ rate\ ordinary\ hospitalization + days\ above\ threshold \times \ Rate\ per\ day\ of\ hospitalization\ above\ threshold \quad (8.2)$$

Patient	DRG	Length of hospitalization (days)	Cost of hospitalization (€)
Patient 1	192	22	7549
Patient 2	192	14	7549
Patient 3	193	45	16874
Patient 4	191	24	18833
Patient 5	193	92	28812
Patient 6	194	19	13064

Table 25 DRG of patients in the intervention group (3D).

Patient	DRG	Length of hospitalization	Cost of hospitalization
Patient 1	192	19	7549
Patient 2	193	112	33892
Patient 3	192	12	7549
Patient 4	191	79	36773
Patient 5	191	44	24698
Patient 6	191	56	28838

Table 26 DRG of patients in the control group (2D).

From these tables it immediately emerges that the average cost of inpatient stays operated using 2D is higher than the cost of inpatient stays whose preoperative planning was based on 3D, despite the additional cost of rendering. This is because, as previously demonstrated, the use of the 3D causes a decrease in the duration of hospitalization and therefore a lesser use of resources.

In addition, the rate of the extra days is lower than the average cost of the single day of stay in an ordinary hospital. This increases the costs that the hospital faces if the length of stay increases, as the total use of resources is not fully reimbursed. Therefore, if the use of 3D models decreases the duration of hospitalization, consequently it decreases the costs that the hospital must face.

9 Conclusion and future developments

Safety and effectiveness of hepatobiliary surgery is based on detailed and personalized knowledge of the anatomy of each individual patient. Pre-operative planning is crucial because the structures of the organs involved are complex and vascularization is subjected to change. It remains difficult even for more experienced surgeons and radiologists to determine by CT or magnetic resonance imaging, the correct relationship between the tumor and the nearby anatomical structures. In addition, any variations from the surgical treatment planned are associated with an increased risk of adverse clinical events.
Developments in the field of medical imaging and their integration have provided new opportunities to support surgeons in performing advanced surgical procedures to improve the benefits and safety of patients. 3D reconstruction allows individualized visualization of the spatial relationship of the tumor for a more accurate and personalized pre-operative planning and intraoperative navigation, that brings such simulation into the surgical room to guide surgeons during tumor resection. This technology facilitates and increases the effectiveness of surgery, but evidence of its effects on operating results remains limited in literature.

The aim of this thesis is to perform a multidisciplinary HTA-style evaluation of three-dimensional reconstructions in the preoperative and intraoperative phase, to determine a more appropriate customized therapeutic strategy in hepatobiliary surgery.
From a clinical point of view, the liver is a particularly vascularized organ because it performs vital functions for human body. It consists of two venous systems, an arterial system and bile ducts. Moreover, there are several common pathologies that can affect the liver. These include hepatitis, cirrhosis, steatosis, ascites, encephalopathy, and benign tumors such as cysts.
Furthermore, there are different types of liver cancer depending on its origin and location. However, the surgical treatment is always the same: the hepatectomy. Such operation involves a variable number of liver segments, and it can cause complications in the postoperative course. For this reason, it is necessary a three-dimensional reconstruction, which allows to have a detailed view of the vascular anatomy of the liver and a preliminary calculation of the residual liver’s volume remaining after surgery to prevent the patient from risking liver failure.
In addition, the development of medical technologies is important to keep up with the epidemiological needs. Primary liver cancer is the fifth most common cancer worldwide and it is the second most common cause of death in cancer patients. Diagnosis is typically made through two-dimensional images (CT or MRI). These 2D images are post-processed after acquisition to obtain 3D models. To produce renderings as close to reality as possible, it is important that 2D images are captured with high quality. For example, the smaller the thickness of the CT slices, the greater will be the level of detail in the rendering.
The image after being acquired is segmented to identify the main anatomical structures. This step can be done either manually or automatically. In the latter case, segmentation can be performed using deep learning algorithms, such as neural networks.

Then the 3D rendering is performed: in most cases it is surface based because density and what is inside the anatomical structures are not considered.
Currently there are several companies that produce 3D anatomical renderings for clinical use. However, in this thesis, the software used in Vimercate hospital (ASST Brianza, Italy) were taken into consideration.
The workflow is similar. The surgeon has a private area in a web portal where he can open a new case and request 3D rendering after loading the two-dimensional images in DICOM format. The reconstruction time can vary according to the detail required: a ready-to-use and particularly detailed reconstruction certainly requires more time than a rendering that needs a subsequent manual reworking.
In addition, the surgeon can make a simulation of different hepatectomies that he thinks to do. In this way he knows the future liver remnant volume, and he can make the most appropriate decision to the individual patient.

DICOM images are uploaded to the web portal in a totally anonymous form. This makes impossible the re-identification of the patient and the process does not require GDPR regulation. Different is the matter for the treatment of the personal data of the single surgeon, who subscribes the portal and requires each 3D reconstruction. In this case, the identification data are covered by the GDPR regulation.
Moreover, commercially available 3D reconstruction software are medical devices intended by the manufacturer to be used in humans for diagnosis, prevention, control, and therapy, without pharmacological and immunological means. Furthermore, the quality of 3D rendering is also regulated by ISO 13485, which defines the regulations ensuring that the quality management system complies with the requirements of medical device standards.

Anyway, the most substantial part of this thesis concerns the clinical effectiveness, in terms of patients' benefits. This evaluation has been carried out in two ways.
First, several experienced surgeons answered to a questionnaire where 11 different clinical cases were proposed. Each rater answered 16 specific questions regarding vascular infiltration of the tumor, first looking at two-dimensional images and then looking at the corresponding 3D reconstruction. The goal of this study was to assess whether the three-dimensional model helps the understanding of the anatomical relationship between the tumor and nearby vascular structures. This objective was demonstrated by a statistically significant result: some answers to the same question about the same patient changed after seeing the 3D model and they were then equal to what was found in the operating room.
After testing that the use of 3D reconstructions helps the understanding of the patient’s anatomy, any differences in patient benefits were analyzed. For this part, 12 patients from Vimercate hospital were considered: on one hand the surgical treatment of 6 of these patients was planned with the 3D model, on the other hand the intervention of the remaining 6 patients was traditionally planned with 2D images. For the analysis both preoperative characteristics were considered in order to verify that there were no substantial differences between the two groups. Then both intraoperative and post-operative outcomes were analyzed. It turned out that the use of 3D reconstructions allows less blood loss during surgery, a shorter hospitalization, and less cancer recurrence. This is because the knowledge of the liver’s internal anatomy can lead to a faster recovery and a completely resection of the tumor, while maintaining a residual volume that allows the liver to reconstitute.

Finally, the patient’s point of view and the organizational economic aspect were also analyzed. In the literature, the use of 3D has highlighted a greater awareness of the patient and

his family of the type of disease and the proposed surgery since the visualization of the 3D model allows a more immediate and intuitive understanding even to those who have no particular medical knowledge.
In addition, the quality of life of the patients was evaluated 4 months after surgery. Patients in the intervention group after four months found greater autonomy in mobility, self-care and usual activities without any pain and depression problems. This is related to tumor recurrence: if the tumor has not been completely removed during surgery, after 4 months the patient will be treated again.

As last dimension, the economic and organizational aspect was analyzed. It is closely related to the quality of life and the length of the hospitalization. The high cost of each 3D model is compensated by an increase in quality of life of patients measured 4 months after surgery. Moreover, in Italy the cost of a hospitalization is calculated in a standard way through the DRG system. Hepatectomies are usually complex interventions that most likely will cause complications and comorbidities. But using 3D, hospitalization will be shorter, and the hospital should spend less resources to treat the patient, facing lower costs.

It can be concluded that 3D seems to have advantages over standard practice from different points of view. However, this study is limited by the number of participants involved. This limit has been exceeded in the administration of the questionnaire as 3D renderings have been made even of patients operated using 2D, so that the results have a greater statistical power.
A future development of this analysis can be an evaluation, based on HTA framework, about different 3D techniques applied to a larger number of patients in hepatobiliary surgery. However, even though the limited number of participants, this thesis still provides a preliminary analysis of each dimension that is clearly favorable towards the use of 3D.

9.1 3D printed models, augmented, mixed and virtual reality

In the future, more and more advanced technologies will spread in hepatobiliary surgery in which visualization of the 3D model is only one part of a complex and innovative system.

For an adequate and custom-made preoperative planning, 3D models are important to understand the precise knowledge of vascular anatomy due to its high variability. However, sometimes the visualization is not enough, and the 3D model will be printed, to obtain a concrete manipulation.
Current literature on 3D printing in liver surgery usually is focused on preoperative planning as well as education and training.
Huber et al. from December 2017 and December 2019, performed the challenging operation planning of 10 cases using a full-size 3D print. The 3D model was built using the same methods described for 3D rendering visualization, but in addition each structure was exported to mesh-type file (stereolithography). The geometric model was printed with a combination of material injectors with 3D printing machines.
Anyway, to have a 3D printing model, more time is needed: the online virtual model was available within 4 days, however printed models were delivered within 10 days after data transfer. It also has higher costs: for each case, 3D printing costs between 1500 € and 2000 €, while 3D PDF costs 900-1000 € and it does not require additional hardware.

The 3D printed models were used in 1.8% of all liver resections and vascular reconstruction was performed in the 70% of printed cases. This demonstrate how useful it is the 3D model for understanding the complex vascular anatomy that has high variability.
Furthermore, the surgical team reveals as major benefit the visualization of critical areas of vascular reconstruction, the identification of the type of vascular infiltration and the position of multifocal tumors. This reduces the risk of devascularization and complications, facilitating intraoperative detection of small and deeply locate tumors [4].
Indeed, Igami et al. used a 3D printed model of a liver to perform an hepatectomy on two patients with synchronous multiple liver metastases, because due to preoperative chemotherapy, one of the tumors become smaller and invisible to ultrasound. The small tumor, invisible by both preoperative and intraoperative ultrasonography, was also not palpable upon laparotomy. This type of tumor is called 'vanishing lesion'.
The only way to determine the appropriate resection line, is by referring to the 3D printed model. Finally, they confirm that the planned resections were successful, with histological negative surgical margins [96].

Aside from 3D print, augmented and mixed reality applications provide the preoperative data in the operating room during liver surgery. The virtual environment allows the transparency of the structure to be altered and scaling and to be enlarged or minimized according to the users' preferences, in order to make the preoperative planning more flexible.

Augmented reality (AR) shows great potential to enhance both laparoscopic and laparotomy surgery.
Prevost et al. analyze retrospectively all patients on which laparoscopic liver resection with AR surgery system was conducted, from January 2018 to March 2018.
Firstly, a 3D reconstruction of vascular territories and relevant structures like portal vein, hepatic arteries, hepatic vein, and tumors based on preoperative CT and MRI was obtained.
The intraoperative set up (shown in Figure 35) comprises a tower with a 32″ screen with pure (none augmented) 3D image, positioned to the right of the patient's head and the augmented image on a 26″ screen was centered at the patient's head together with the infrared tracking camera.
A touch screen for the controlling of the navigation system was draped by a transparent, plastic sheet and it was used by the assistant standing [97].

Figure 35 AR set up in the operating room [97].

Tracking instruments were accomplished by attaching a retro-reflective spheres onto the laparoscopic probe, which were tracked by a passive optical tracking system.
Calibration is very important in image guided systems.
Camera calibration was conducted utilizing a planar pattern observed by the camera at four different distances, while the laparoscope and laparoscopic probes were calibrated using a geometrical guide on the calibration tool (Figure 36). Furthermore, a rigid surface-based method was used for patient to image registration. Four points were chosen on the preoperative 3D model and matched to the actual liver by defining the same points using the optically tracked and calibrated laparoscopic probe (Figure 37).

Figure 36 Tracked laparoscope and gasper [97].

Figure 37 Landmark definition on virtual model [97].

Two navigation modes were available. The first one is the overview mode that permits to augment the 3D laparoscopic image with the complete preoperative reconstructed information. As shown in Figure 38, the different types of vessels, as well as liver segments and tumors can be selected for display.

Figure 38 Augmented reality overlay on live-laparoscopic image (left), virtual liver model with anatomical structures of interest (right) [97].

The second modality is that of resection where the 3D image is displayed in a circular area, the center of which is located by the surgical instrument and the radius can be selected by the operator. Resection modality is shown in Figure 39.

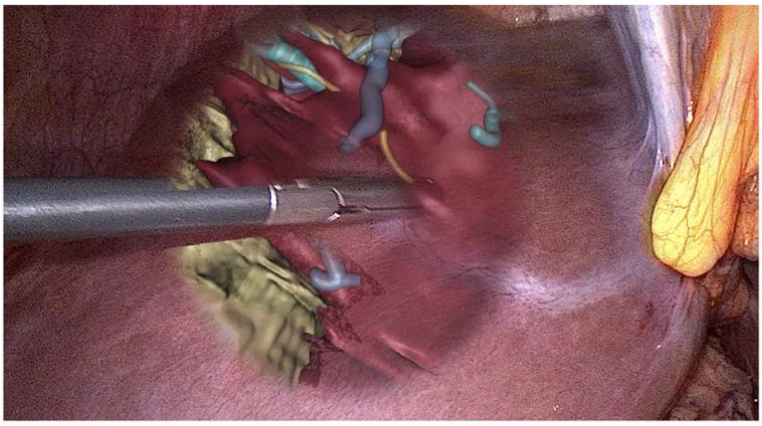

Figure 39 Resection mode visualizing the AR overlay around the surgical instrumentation [97].

Some data were collected to define the intraoperative efficacy, clinical benefits and postoperative morbidity and mortality.
For what regard the surgical room set up, the calibration takes a median of 43 s, the landmark definition between the preoperative image and the liver takes 53s of the operation time. The registration must be adequate, so different attempts were made taking 8.50 min of average.
The clinical benefit was measured through a questionnaire made by the primary surgeon. The ease of the use of the system and the potential benefit for resection of vanishing lesions was discovered very high, but the image registration for resection guidance is still tool inaccurate.
Postoperative outcomes reported complete resections in all retrieved lesions and no intra or postoperative clinical complications occur [97].

In the meanwhile, Banz et al. evaluate the image guided navigation systems in the domain of open oncologic surgery. The intraoperative setup was similar with respect to the one for laparoscopic surgery. Surgical instruments and integrated ultrasound probe were attached with geometric references to allow their spatial tracking. The surgeon has a 3D visualization of tool position and orientation relative to the available patient-specific preoperative virtual model and 2D augmentation of native US images with co-registered preoperative image data in order to correctly display anatomical features that were visible in the preoperative image data but not by intraoperative US (vanishing lesions) [98].
The setup is displayed in Figure 40.

Figure 40 (a) 3D reconstruction of the CT-scan is shown on the left monitor and the integrated US for patient-to- image registration is displayed on the right monitor. (b) integrated and navigated sonography probe. (c) set up of surgical navigation system [98].

Banz et al. conclude that image guidance is essentially aiming at reducing overall surgical invasiveness, potentially pushing forward the limits of current surgical oncological treatment strategies. Image guidance seems to provide the necessary support through accurate instrument placement and orientation to allow the treatment of complex situations.
A typical clinical situation includes resection of a larger number of small lesions (in particular the so-called vanishing lesions), a task that remains extremely challenging to carry out without instrument guidance, even for the very experienced hepatobiliary surgeon. So, in patients not qualified for formal liver resection, navigated surgery may play a fundamental role to enable parenchyma-sparing tailored treatment [98].

Since augmented reality is the view of the physical and real world with an overlay of digital elements, mixed reality (MR) and virtual reality are a further development. The former means the blend of the physical and real world with virtual elements where physical and digital elements can interact, while the latter is related to a fully immersive digital environment.
An example of mixed reality is shown in Figure 41.

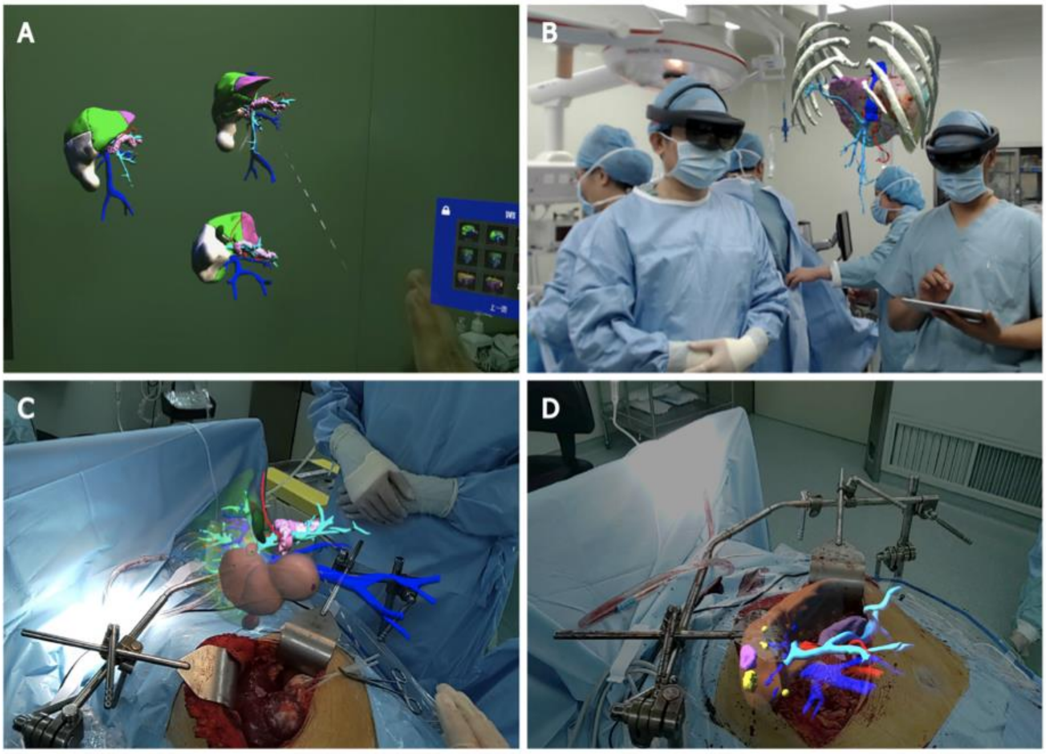

Figure 41 Mixed reality-assisted hepatectomy guided by three-dimensional holograms. A: Three-dimensional (3D) holograms were observed with the mixed reality head-mounted display in the operating room; B: The surgeon observed the tumor location and vascular anatomy with a 3D hologram and determined the surgical planning again; C: 3D hologram was placed above the surgical field; D: 3D holograms were fused with the patient's liver [76].

Previous studies have shown that MR has been gradually applied to neurosurgery, orthopedics, and urology, yielding improvements in perioperative outcomes for patients [12-14]. However, few studies have evaluated the application value of MR in hepatectomy.
One of them, evaluate the intraoperative and postoperative outcomes of 95 patients from group A and B. Patients from group A underwent MR assisted hepatectomy, while patients from group B underwent traditional hepatectomy.
This analysis underlines that group A yielded a shorter operation time (202.86 ± 46.02 min vs 229.52 ± 57.13 min, P = 0.003), less volume of bleeding (329.29 ± 97.31 mL vs 398.23 ± 159.61 mL, P = 0.028), and shorter obstructive time of the portal vein (17.71 ± 4.16 min vs 21.58 ± 5.24 min, P = 0.019). The total postoperative complications and hospitalization days in Group A were significantly less than those in Group B [14 (37.84%) vs 35 (60.34%), P = 0.032]. In conclusion this study demonstrates that mixed reality provide advantages during surgical planning and intraoperative navigation and it significantly improves the perioperative outcomes of hepatectomy [76].

Finally, Huettl et al. present the first study comparing 3D PDFs, 3D printed models (PR) and virtual reality (VR) of 3D models regarding anatomical orientation and personal preferences in a high-volume liver surgery center. Every modality has its advantages and disadvantages. While the PDF is most cost effective, the precision of tumor localization is higher when the reconstruction is presented as a PR model or in VR, while the shortest assessment times were recorded for the 3D PR. Nevertheless, the majority of participants preferred the VR application over the other modalities and they believed in a positive influence on resection planning with this modality [4].

Hence, in literature it is already increasing the number of case reports where technologies that go beyond the visualization of 3D reconstructions have been analyzed, which will catch on more and more in the medicine of future.
However, the visualization of 3D models has already many advantages over standard practice from different points of view. It represents the surgical and dynamic perception of the anatomy of a specific patient, a tool that does not replace traditional two-dimensional images, but that makes preoperative planning more immediate and ‘surgical like’.

Bibliography

[1] A. Pietrabissa *et al.*, "An overview on 3D printing for abdominal surgery," *Surg. Endosc.*, vol. 34, no. 1, pp. 1–13, 2020.

[2] T. Huber *et al.*, "Entwicklung eines interaktiven Multi-User Virtual Reality Moduls am Beispiel der Leberresektion," *74. Jahrestagung der Dtsch. Gesellschaft für Gastroenterol. Verdauungs- und Stoffwechselkrankheiten mit Sekt. Endosk. – 13. Herbsttagung der Dtsch. Gesellschaft für Allg. und Visz. Gem. mit den Arbeitsgemeinschaften*, vol. 57, no. 1, pp. 2020–2021, 2019.

[3] X. D. Wang *et al.*, "Traditional surgical planning of liver surgery is modified by 3D interactive quantitative surgical planning approach: a single-center experience with 305 patients," *Hepatobiliary Pancreat. Dis. Int.*, vol. 16, no. 3, pp. 271–278, 2017.

[4] F. Huettl *et al.*, "Virtual reality and 3D printing improve preoperative visualization of 3D liver reconstructions—results from a preclinical comparison of presentation modalities and user's preference," *Ann. Transl. Med.*, vol. 9, no. 13, pp. 1074–1074, 2021.

[5] C. Fang *et al.*, "Consensus recommendations of three-dimensional visualization for diagnosis and management of liver diseases," *Hepatol. Int.*, vol. 14, no. 4, pp. 437–453, 2020.

[6] S. Zhang *et al.*, "Three-dimensional versus two-dimensional video-assisted hepatectomy for liver disease: A meta-analysis of clinical data," *Wideochirurgia I Inne Tech. Maloinwazyjne*, vol. 16, no. 1, pp. 1–9, 2021.

[7] E. Lettieri, "Health Care Management." .

[8] EUnetHTA Joint Action, "HTA Core Model Handbook," *EUnetHTA JA*, vol. 2, pp. 1–14, 2016.

[9] F. Di Sabato, "Manuale delle procedure HTA," 1995.

[10] "Ospedale di Vimercate," *Wikipedia.org*. [Online]. Available: https://it.wikipedia.org/wiki/Ospedale_di_Vimercate.

[11] "Ospedale Vimercate," *AICOM.it*. [Online]. Available: https://www.aicom.it/it/progetti/ospedale-vimercate/.

[12] "Ospedale di Vimercate," *asst-brianza.it*. [Online]. Available: https://www.asst-brianza.it/web/index.php/presidi/ospedale/vimercate.

[13] S. Sala, "Sanità digitale, l'ospedale di Vimercate un'eccellenza: premiato a Roma," 2014. .

[14] "Fegato," *Humanitas.it*. [Online]. Available: https://www.humanitas.it/enciclopedia/anatomia/apparato-digerente/fegato/.

[15] A. Valentino, "Il fegato: ghiancola extramuarale anficrina," 2020. [Online]. Available: https://www.nurse24.it/studenti/anatomia/fegato-anatomia-fisiologia-patologie.html.

[16] "Anatomia del fegato," 2022. [Online]. Available: https://www.chirurgiadelfegato.it/il-fegato/anatomia-del-fegato/.

[17] "Fegato," *Wikipedia.org*. [Online]. Available: https://it.wikipedia.org/wiki/Fegato.

[18] "Liver," *anatomy.app*. [Online]. Available: https://anatomy.app/encyclopedia/liver.

[19] L. C. Ablation *et al.*, "Treating Liver Cancer cancer.org | 1.800.227.2345," pp. 1–34.

[20] C. I. E. Adulto, "Foglio informativo per l ' atto sanitario : EPATECTOMIA Specialità : Chirurgia," pp. 1–14, 2021.

[21] "Epatite," *Humanitas.it*. [Online]. Available: https://www.humanitas.it/malattie/epatite-virale/.

[22] "Cirrosi," *Humanitas.it*. [Online]. Available: https://www.humanitas.it/malattie/cirrosi/.

[23] D. Tholey, "Insufficienza epatica," *msdmanuals.com*. [Online]. Available: https://www.msdmanuals.com/it-it/casa/patologie-epatiche-e-della-cistifellea/manifestazioni-dell-epatopatia/insufficienza-epatica.

[24] Danielle Tholey, "Steatosi epatica," *MD, Sidney Kimmel Medical College at Thomas Jefferson University*, 2021. [Online]. Available: https://www.msdmanuals.com/it-it/casa/patologie-epatiche-e-della-cistifellea/manifestazioni-dell-epatopatia/steatosi-epatica.

[25] Danielle Tholey, "Ascite," *MD, Sidney Kimmel Medical College at Thomas Jefferson University*, 2021. [Online]. Available: https://www.msdmanuals.com/it-it/casa/patologie-epatiche-e-della-cistifellea/manifestazioni-dell-epatopatia/ascite.

[26] D. Tholey, "Encefalopatia epatica," *MD, Sidney Kimmel Medical College at Thomas Jefferson University*, 2021. [Online]. Available: https://www.msdmanuals.com/it-it/casa/patologie-epatiche-e-della-cistifellea/manifestazioni-dell-epatopatia/encefalopatia-epatica.

[27] Danielle Tholey, "Tumori benigni del fegato," *MD, Sidney Kimmel Medical*

College at Thomas Jefferson University, 2021. [Online]. Available: https://www.msdmanuals.com/it-it/professionale/malattie-del-fegato-e-delle-vie-biliari/masse-e-granulomi-epatici/tumori-benigni-del-fegato.

[28] "Carcinoma epatocellulare," *Wikipedia.org*. [Online]. Available: https://it.wikipedia.org/wiki/Carcinoma_epatocellulare.

[29] "Colangiocarcinoma," *Wikipedia.org*. [Online]. Available: https://it.wikipedia.org/wiki/Colangiocarcinoma.

[30] D. med. S. Ceruti, "Fegato in medicina intensiva," *manualidimedicina.blogspot.com*, 2015. [Online]. Available: https://manualidimedicina.blogspot.com/2015/10/fegato-in-medicina-intensiva-capitolo.html.

[31] Ospedale San Raffaele, "Intervento di resezione epatica."

[32] "Epatite Virale," *L'epidemiologia per la sanità pubblica Istituto Superiore di Sanità*. [Online]. Available: https://www.epicentro.iss.it/epatite.

[33] S. Cheemerla and M. Balakrishnan, "Global Epidemiology of Chronic Liver Disease," *Clin. Liver Dis.*, vol. 17, no. 5, pp. 365–370, 2021.

[34] "La cirrosi epatica," *epact.it*. [Online]. Available: http://www.epac.it/patologie/cirrosi.

[35] Y. Ogura, W. H. Parsons, S. S. Kamat, and B. F. Cravatt, "Epidemiology of Hepatocellular Carcinoma," *Physiol. Behav.*, vol. 176, no. 10, pp. 139–148, 2017.

[36] S. Anna Elisabetta Brunetti *et al.*, "Linee guida EPATOCARCINOMA. Assoc. Ital. Oncol. Medica (2017)," 2018.

[37] M. M. Kirstein and A. Vogel, "Epidemiology and Risk Factors of Cholangiocarcinoma," *Visc. Med.*, vol. 32, no. 6, pp. 395–400, 2016.

[38] "Il colangiocarcinoma," *Associazione pazienti italiani colangiocarcinoma*. [Online]. Available: https://www.apicinfo.it/il-colangiocarcinoma.

[39] G. B. Guido Baroni., "Methods for biomedical imaging and computer aided surgery," 2021.

[40] M. Uchida, "Recent advances in 3D computed tomography techniques for simulation and navigation in hepatobiliary pancreatic surgery," *J. Hepatobiliary. Pancreat. Sci.*, vol. 21, no. 4, pp. 239–245, 2014.

[41] D. Högemann *et al.*, "Individuelle Planung leberchirurgischer Eingriffe an einem virtuellen Modell der Leber und ihrer Leitstrukturen," *Radiologe*, vol. 40, no. 3, pp. 267–273, 2000.

[42] H. Lang *et al.*, "Impact of virtual tumor resection and computer-assisted risk analysis on operation planning and intraoperative strategy in major hepatic

resection," *Arch. Surg.*, vol. 140, no. 7, pp. 629–638, 2005.

[43] Y. Wang *et al.*, "Precise local resection for hepatocellular carcinoma based on tumor-surrounding vascular anatomy revealed by 3D analysis," *Dig. Surg.*, vol. 29, no. 2, pp. 99–106, 2012.

[44] C. H. Fang *et al.*, "Impact of three-dimensional reconstruction technique in the operation planning of centrally located hepatocellular carcinoma," *J. Am. Coll. Surg.*, vol. 220, no. 1, pp. 28–37, 2015.

[45] A. Bégin *et al.*, "Accuracy of preoperative automatic measurement of the liver volume by CT-scan combined to a 3D virtual surgical planning software (3DVSP)," *Surg. Endosc.*, vol. 28, no. 12, pp. 3408–3412, 2014.

[46] T. P. Kingham, S. Jayaraman, L. W. Clements, M. A. Scherer, J. D. Stefansic, and W. R. Jarnagin, "Evolution of Image-Guided Liver Surgery: Transition from Open to Laparoscopic Procedures," *J. Gastrointest. Surg.*, vol. 17, no. 7, pp. 1274–1282, 2013.

[47] Y. Oshiro and N. Ohkohchi, "Three-Dimensional Liver Surgery Simulation: Computer-Assisted Surgical Planning with Three-Dimensional Simulation Software and Three-Dimensional Printing," *Tissue Eng. - Part A*, vol. 23, no. 11–12, pp. 474–480, 2017.

[48] N. Zeng *et al.*, "Individualized preoperative planning using three-dimensional modeling for Bismuth and Corlette type III hilar cholangiocarcinoma," *World J. Surg. Oncol.*, vol. 14, no. 1, pp. 1–8, 2016.

[49] J. Yamanaka *et al.*, "The impact of 3-D virtual hepatectomy simulation in living-donor liver transplantation," *J. Hepatobiliary. Pancreat. Surg.*, vol. 13, no. 5, pp. 363–369, 2006.

[50] C. Cotsoglou, S. Granieri, S. Paleino, and A. Chierici, "3D preoperative assessment for locally advanced pancreatic cancer undergoing modified-Appleby procedure with reversed autologous arterial graft reconstruction: A case report," *J. Clin. Images Med. Case Reports*, vol. 2, no. 2, 2021.

[51] C. Report *et al.*, "An Extreme Downstaging as a 'Time Machine' for Experienced HPB Surgeon: A Case Report of a Patient with Unresectable Colorectal Liver Metastases," *Ann. Case Reports*, vol. 6, no. 02, 2021.

[52] "Medics 3D Tools for medicine," *medics3d.com*. [Online]. Available: https://www.medics3d.com/.

[53] "Visible Patient," *visiblepatient.com*. [Online]. Available: https://www.visiblepatient.com/en/.

[54] L. Soler, S. Nicolau, P. Pessaux, D. Mutter, and J. Marescaux, "Real-time 3D image reconstruction guidance in liver resection surgery.," *Hepatobiliary Surg.*

Nutr., vol. 3, no. 2, pp. 73–81, 2014.

[55] "Virtual Clone," *aimsacademy.org*. [Online]. Available: https://www.aimsacademy.org/en/virtual-clone/.

[56] F. Pizzutilo, "PROGETTAZIONE E PRODUZIONE DEI DISPOSITIVI MEDICI DISPOSITIVI MEDICI." 2021.

[57] E. Caiani, "m-Health, mobile applications and regulation," 2021.

[58] Medics3D, "QUALITY POLICY Medics3D," 2017.

[59] E. Caiani, "Ethical issue in E-health," 2021.

[60] V. Patient, "Website Privacy Notice," pp. 4–6.

[61] A. Ghiglia, "Provvedimento del 14 gennaio 2021 - Regione Veneto. Codice di condotta per l'utilizzo di dati sulla salute a fini didattici e di pubblicazione scientifica," 2021.

[62] S. D. Generale, S. Informativo, and S. Sanitario, "Linee guida per la predisposizione e la trasmissione dei file al NSIS," 2016.

[63] Information Comissioners Office, "Anonymisation: managing data protection risk code of practice," 2012.

[64] G. CIANCAGLINI, "Tecnologia 3D per la medicina, così oggi il chirurgo opera prima di entrare in sala," *La Stampa*, 2020.

[65] Future Market Insights, "3D Printed Medical Implants Market." [Online]. Available: https://www.futuremarketinsights.com/reports/3d-medical-implants-market.

[66] L. B. Aurelio Secinaro, "La tecnologia 3D nel contesto ospedaliero: allestimento di un 3D LAB," *QuotidianoSanità*, 2021.

[67] Slicer-Community, "3D Slicer Documentation_20210513," *3D Slicer*, pp. 2–48, 2019.

[68] C. Pinter, A. Lasso, and G. Fichtinger, "Polymorph segmentation representation for medical image computing," *Comput. Methods Programs Biomed.*, vol. 171, pp. 19–26, 2019.

[69] Y. Gong *et al.*, "Comparative safety and effectiveness of ultrasound-guided radiofrequency ablation combined with preoperative three-dimensional reconstruction versus surgical resection for solitary hepatocellular carcinoma of 3-5 cm," *J. Cancer*, vol. 10, no. 22, pp. 5568–5574, 2019.

[70] C. H. Fang, J. Liu, Y. F. Fan, J. Yang, N. Xiang, and N. Zeng, "Outcomes of hepatectomy for hepatolithiasis based on 3-dimensional reconstruction technique," *J. Am. Coll. Surg.*, vol. 217, no. 2, pp. 280–288, 2013.

[71] Y. B. He *et al.*, "Application of 3D reconstruction for surgical treatment of

hepatic alveolar echinococcosis," *World J. Gastroenterol.*, vol. 21, no. 35, pp. 10200–10207, 2015.

[72] K. Nakayama, Y. Oshiro, R. Miyamoto, K. Kohno, K. Fukunaga, and N. Ohkohchi, "The Effect of Three-Dimensional Preoperative Simulation on Liver Surgery," *World J. Surg.*, vol. 41, no. 7, pp. 1840–1847, 2017.

[73] J. Zhang, J. Dawa, D. Suolang, Y. Lei, J. Wang, and D. Basang, "The Application of Preoperative Three-Dimensional Reconstruction Visualization Digital Technology in the Surgical Treatment of Hepatic Echinococcosis in Tibet," *Front. Surg.*, vol. 8, no. August, pp. 1–6, 2021.

[74] R. Guo, H. Shi, Q. Zhao, and D. Zheng, "Secure Attribute-Based Signature Scheme with Multiple Authorities for Blockchain in Electronic Health Records Systems," *IEEE Access*, vol. 6, pp. 11676–11686, 2018.

[75] V. Velayutham, D. Fuks, T. Nomi, Y. Kawaguchi, and B. Gayet, "3D visualization reduces operating time when compared to high-definition 2D in laparoscopic liver resection: a case-matched study," *Surg. Endosc.*, vol. 30, no. 1, pp. 147–153, 2016.

[76] L.-Y. Zhu *et al.*, "Application value of mixed reality in hepatectomy for hepatocellular carcinoma," *World J. Gastrointest. Surg.*, vol. 14, no. 1, pp. 36–45, 2022.

[77] J. Hallet, B. Gayet, A. Tsung, G. Wakabayashi, and P. Pessaux, "Systematic review of the use of pre-operative simulation and navigation for hepatectomy: Current status and future perspectives," *J. Hepatobiliary. Pancreat. Sci.*, vol. 22, no. 5, pp. 353–362, 2015.

[78] X. B. Wei *et al.*, "The role of three-dimensional imaging in optimizing diagnosis, classification and surgical treatment of hepatocellular carcinoma with portal vein tumor thrombus," *Hpb*, vol. 18, no. 3, pp. 287–295, 2016.

[79] X. Zhang and S. Poslad, "Blockchain Support for Flexible Queries with Granular Access Control to Electronic Medical Records (EMR)," *IEEE Int. Conf. Commun.*, vol. 2018-May, pp. 1–6, 2018.

[80] V. Marcadelli, S., Petraia, V., Saponaro, "La dimissione del paziente anziano: uno strumento per la valutazione del rischio - l'indice di BRASS," pp. 13–17, 2008.

[81] "Barthel Index - Valutazione delle attività quotidiane," p. 2016, 2016.

[82] S. di Santo, "La scala di Braden," *Nurse24.it*, 2020. [Online]. Available: https://www.nurse24.it/studenti/scale-di-valutazione/la-scala-di-braden.html.

[83] M. Daabiss, "American society of anaesthesiologists physical status classification," *Indian J. Anaesth.*, vol. 55, no. 2, pp. 111–115, 2011.

[84] A. Tsoris and C. A. Marlar, “Use Of The Child Pugh Score In Liver Disease,” *StatPearls Publ. Treasure Isl.*, 2022.

[85] A. A. Roma, C. Magi-Galluzzi, M. A. Kral, T. T. Jin, E. A. Klein, and M. Zhou, “Peritumoral lymphatic invasion is associated with regional lymph node metastases in prostate adenocarcinoma,” *Mod. Pathol.*, vol. 19, no. 3, pp. 392–398, 2006.

[86] “Tumor grade,” *cancer.gov*, 2022. [Online]. Available: https://www.cancer.gov/about-cancer/diagnosis-staging/diagnosis/tumor-grade.

[87] P. Hermanek and Ch. Wittekind, “The Pathologist and the Residual Tumor (R) Classification,” *Pathol. - Res. Pract.*, vol. 190, no. 2, pp. 115–123, 1994.

[88] P. Aseni, M. Ballabio, A. Casati, and R. De Carlis, “Principali complicanze chirurgiche post-operatorie,” *paziente Chir. Crit.*, no. October, pp. 305–313, 2015.

[89] N. N. Rahbari *et al.*, “Posthepatectomy liver failure: A definition and grading by the International Study Group of Liver Surgery (ISGLS),” *Surgery*, vol. 149, no. 5, pp. 713–724, 2011.

[90] F. Sternini *et al.*, “Usability assessment of an intraoperative planning software,” *Heal. 2021 - 14th Int. Conf. Heal. Informatics; Part 14th Int. Jt. Conf. Biomed. Eng. Syst. Technol. BIOSTEC 2021*, vol. 5, no. Biostec, pp. 483–492, 2021.

[91] F. Porpiglia *et al.*, “Development and validation of 3D printed virtual models for robot-assisted radical prostatectomy and partial nephrectomy: urologists’ and patients’ perception,” *World J. Urol.*, vol. 36, no. 2, pp. 201–207, 2018.

[92] J. Connell *et al.*, “The importance of content and face validity in instrument development: lessons learnt from service users when developing the Recovering Quality of Life measure (ReQoL),” *Qual. Life Res.*, vol. 27, no. 7, pp. 1893–1902, 2018.

[93] J. Bernhard *et al.*, “Useful Tool for Patient Education,” vol. 34, no. 3, pp. 337–345, 2022.

[94] E. De Momi, “Clinical Technology Assessment.”

[95] G. Sparacino, “Informatica medica.”

[96] T. Igami *et al.*, “Application of a three-dimensional print of a liver in hepatectomy for small tumors invisible by intraoperative ultrasonography: Preliminary experience,” *World J. Surg.*, vol. 38, no. 12, pp. 3163–3166, 2014.

[97] G. A. Prevost *et al.*, “Efficiency, Accuracy and Clinical Applicability of a New Image-Guided Surgery System in 3D Laparoscopic Liver Surgery,” *J. Gastrointest. Surg.*, vol. 24, no. 10, pp. 2251–2258, 2020.

[98] V. M. Banz *et al.*, “Intraoperative image-guided navigation system:

development and applicability in 65 patients undergoing liver surgery," *Langenbeck's Arch. Surg.*, vol. 401, no. 4, pp. 495–502, 2016.

A Appendix A

Survey data collection, used to evaluate the difference between 2D and 3D. Both methodologies were then compared with the actual operative feedback (‘surgery’) because it is not taken for granted that what has been represented is actually equal to reality.

Surgeon j	Patient i	Parameter *p*	Evaluation	Vascular infiltration a->Nothing b->Vascular deformation c->Tangential d->Circumferential e->Not stimable
1	1	1. Right hepatic vein	2D	
			3D	
			Surgery	
		2. Medium hepatic vein	2D	
			3D	
			Surgery	
		3. Left hepatic vein	2D	
			3D	
			Surgery	
		4. Cava vein	2D	
			3D	
			Surgery	
		5. Right principle portal vein	2D	
			3D	
			Surgery	
		6. Right anterior portal vein	2D	
			3D	
			Surgery	
		7. Right posterior portal vein	2D	
			3D	
			Surgery	
		8. Left portal vein	2D	
			3D	
			Surgery	
		9. Right hepatic artery	2D	
			3D	
			Surgery	
		10. Right anterior hepatic artery	2D	
			3D	
			Surgery	
		11. Right posterior hepatic artery	2D	
			3D	
			Surgery	
		12. Left hepatic artery	2D	
			3D	
			Surgery	
		13. Right principle biliary duct	2D	

			3D	
			Surgery	
		14. Right anterior biliary duct	2D	
			3D	
			Surgery	
		15. Right posterior biliary duct	2D	
			3D	
			Surgery	
		16. Left biliary duct	2D	
			3D	
			Surgery	
		Sum of correct 2D evaluation	$\Sigma 2D_{11}$	
		Sum of correct 3D evaluation	$\Sigma 3D_{11}$	
		Difference between correct evaluation	δ_{11}	
	2	1		
		…		
		L		
		Sum of correct 2D evaluation	$\Sigma 2D_{12}$	
		Sum of correct 3D evaluation	$\Sigma 3D_{12}$	
		Difference between correct evaluation	δ_{12}	
	…			
	N			
		Sum of correct 2D evaluation	$\Sigma 2D_{1N}$	
		Sum of correct 3D evaluation	$\Sigma 3D_{1N}$	
		Difference between correct evaluation	δ_{1N}	
		Mean of difference	δ_1	
2	1			
	…			
	N			
		Mean of difference	δ_2	
3	1			
	…			
	N			
M	1			
	…			
	N			
		Mean of difference	δ_N	
		Mean of the mean of difference	Δ	

B Appendix B

Algorithm 1 was used to retrieve patient preliminary data for clinical effectiveness analysis.

Algorithm 1 Database query

```
SELECT DISTINCT d.*, ed1.E15_DESC_DIAGNOSI AS "DESCR_PROCEDURA" FROM
(SELECT DISTINCT c.*, ed.E15_DESC_DIAGNOSI AS "DESCR_DIAGNOSI" FROM
(SELECT DISTINCT b.*, ard2.A04_COD_DIAGNOSI AS "ID_PROCEDURA",
ard2.A04_DATAORA_INTERVENTO  FROM
(SELECT DISTINCT a.*, ar2.A01_DATAORA_ACCETTAZIONE, ar2.A01_DATAORA_DIMISSIONE,
ar2.A01_COD_MODALITA_DIMISSIONE, ar2.A01_DATAORA_DECESSO FROM
(SELECT DISTINCT ard.A04_ID_RICOVERO, ard.A04_COD_DIAGNOSI, ar.A08_ID_PERSONA,
ar.A08_COGNOME, ar.A08_NOME, ar.A08_SESSO , ar.A08_DATA_NASCITA,
ar.A08_COD_FISCALE
FROM ADT04_RICOVERI_DIAGNOSI ard LEFT JOIN ADT08_PERSONE_RICOVERI ar ON
ard.A04_ID_RICOVERO = ar.A08_ID_RICOVERO
WHERE ard.A04_COD_DIAGNOSI in ('1977','1569','1571','1550','N1550',
'N1571','N1569','N1977','1977N','1569N','1571N','1550N')
AND ard.A04_TIPO_DIAGNOSI = 0
AND ard.A04_POSIZIONE = 1
AND ar.A08_COD_AZIENDA IS NOT NULL) a LEFT JOIN ADT01_RICOVERI ar2 ON
a.A04_ID_RICOVERO = ar2.A01_ID_RICOVERO
WHERE A01_TIPO_RICOVERO= 0)
```

C Appendix C

Survey results: each bar diagram shows the difference in the answers of all raters between 2D and 3D for each clinical cases involved. The correct answers are highlighted in darker boxes.

PATIENT 1

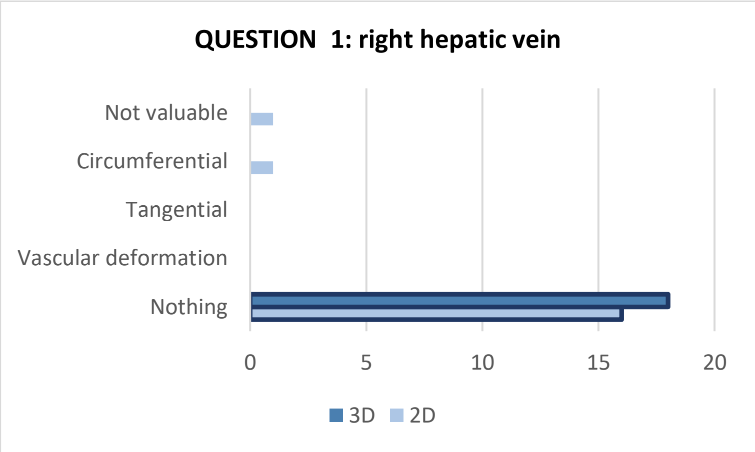

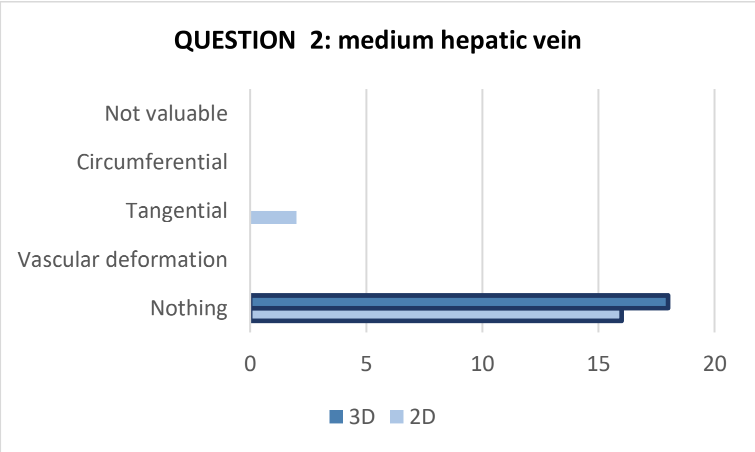

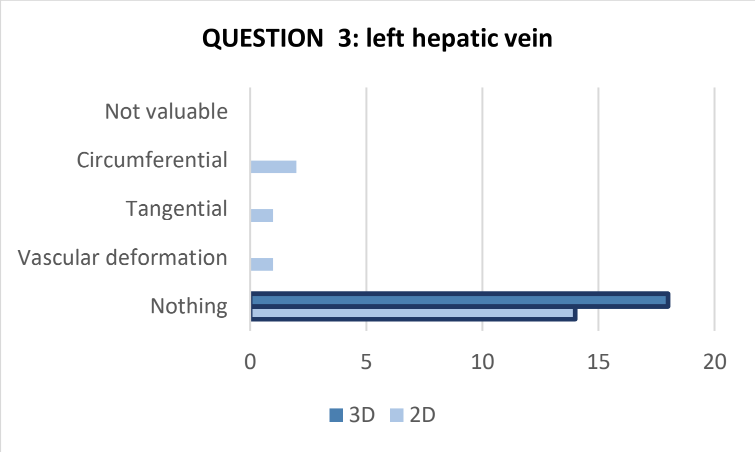
QUESTION 3: left hepatic vein
Not valuable
Circumferential
Tangential
Vascular deformation
Nothing
0
5
10
15
20
3D
2D

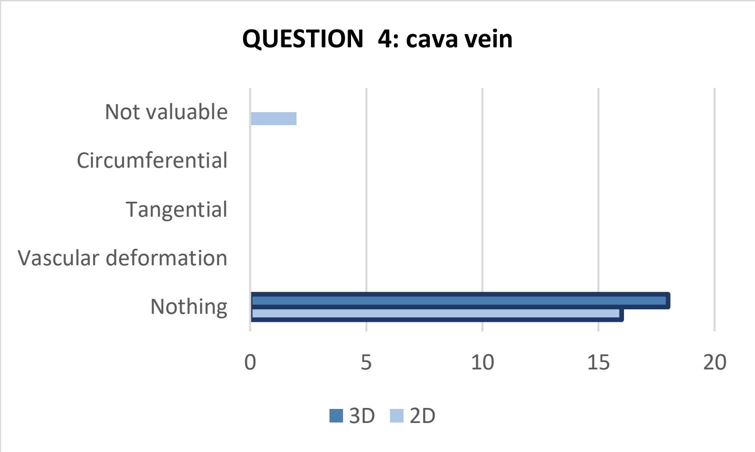
QUESTION 4: cava vein
Not valuable
Circumferential
Tangential
Vascular deformation
Nothing
0
5
10
15
20
3D
2D

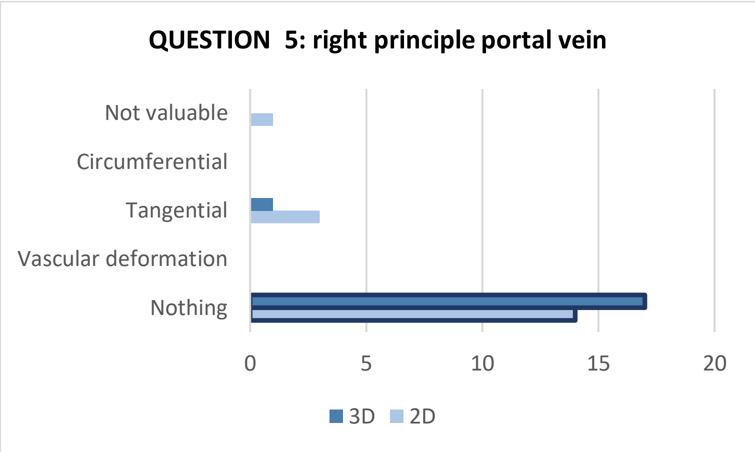
QUESTION 5: right principle portal vein
Not valuable
Circumferential
Tangential
Vascular deformation
Nothing
0
5
10
15
20
3D
2D

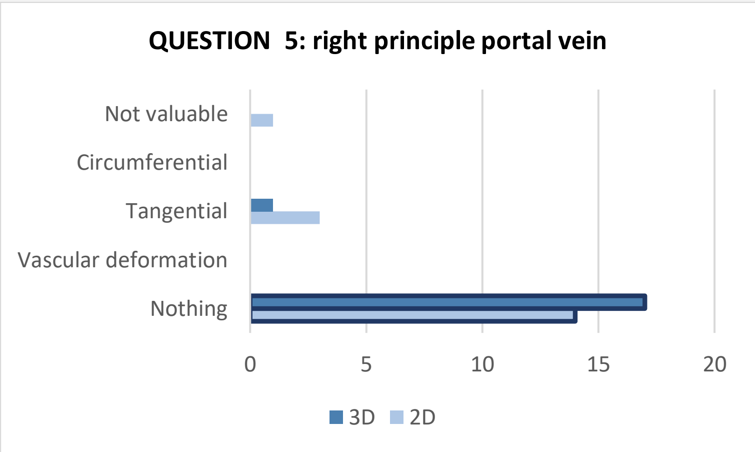
QUESTION 5: right principle portal vein
Not valuable
Circumferential
Tangential
Vascular deformation
Nothing
0
5
10
15
20
3D
2D

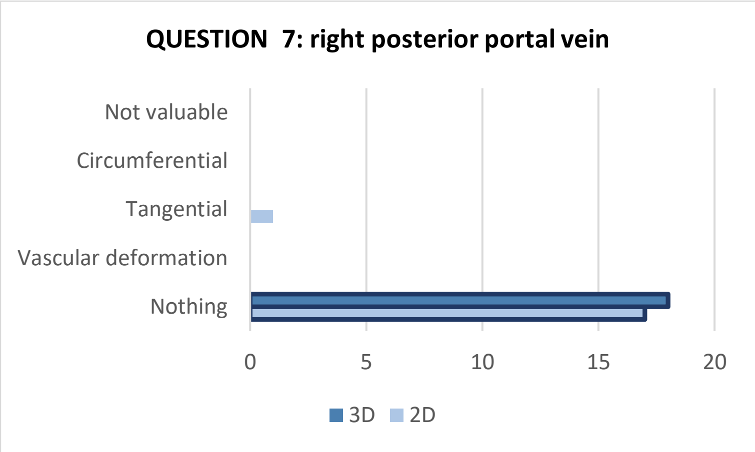
QUESTION 7: right posterior portal vein
Not valuable
Circumferential
Tangential
Vascular deformation
Nothing
0
5
10
15
20
3D
2D

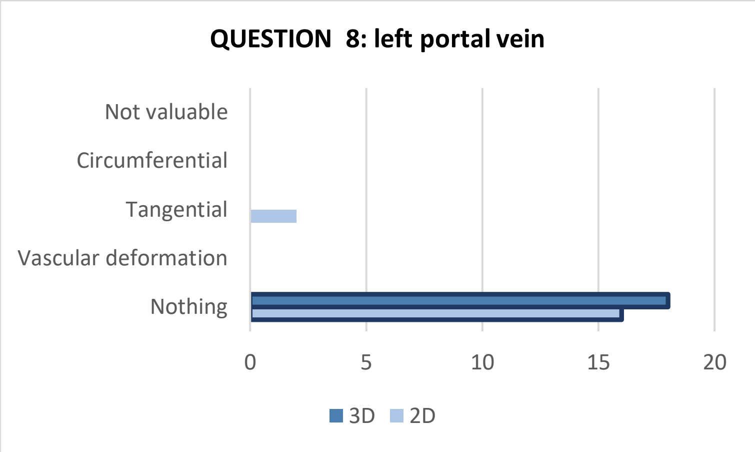
QUESTION 8: left portal vein
Not valuable
Circumferential
Tangential
Vascular deformation
Nothing
0
5
10
15
20
3D
2D

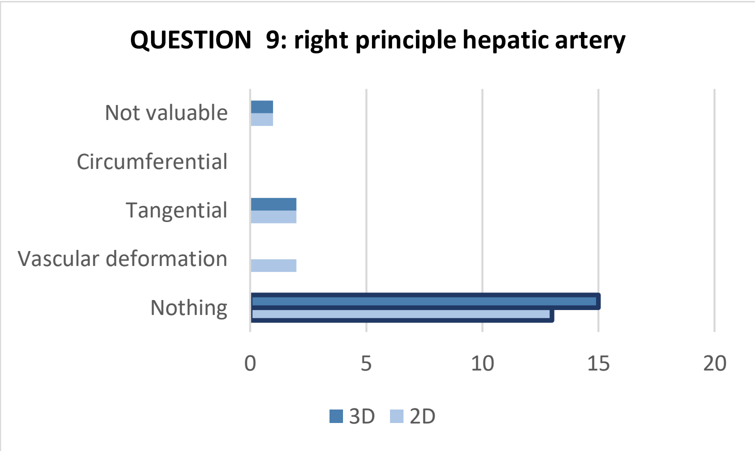
QUESTION 9: right principle hepatic artery
Not valuable
Circumferential
Tangential
Vascular deformation
Nothing
0
5
10
15
20
3D
2D

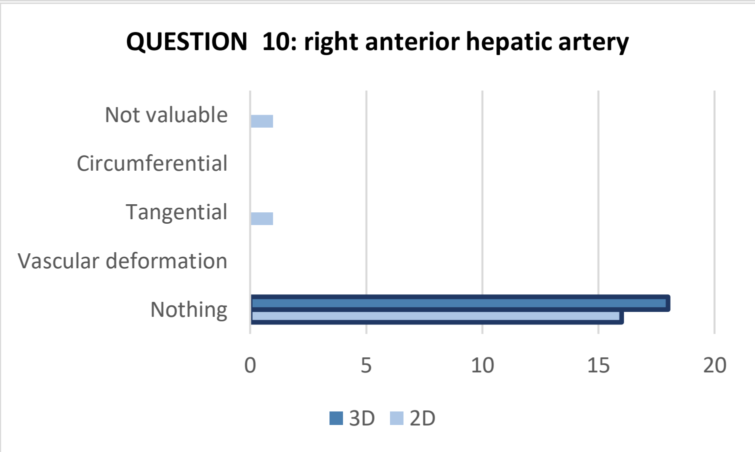
QUESTION 10: right anterior hepatic artery
Not valuable
Circumferential
Tangential
Vascular deformation
Nothing
0
5
10
15
20
3D
2D

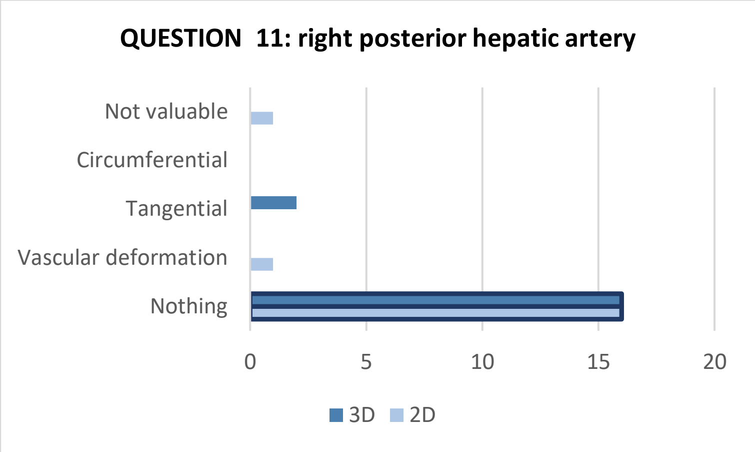
QUESTION 11: right posterior hepatic artery
Not valuable
Circumferential
Tangential
Vascular deformation
Nothing
0
5
10
15
20
3D
2D

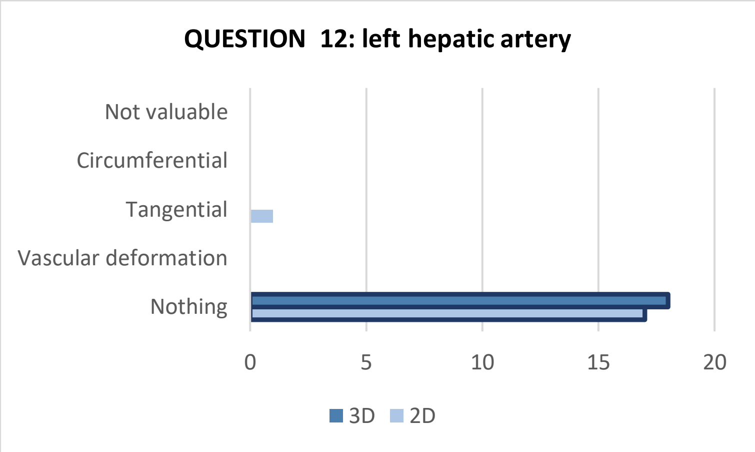
QUESTION 12: left hepatic artery
Not valuable
Circumferential
Tangential
Vascular deformation
Nothing
0
5
10
15
20
3D
2D

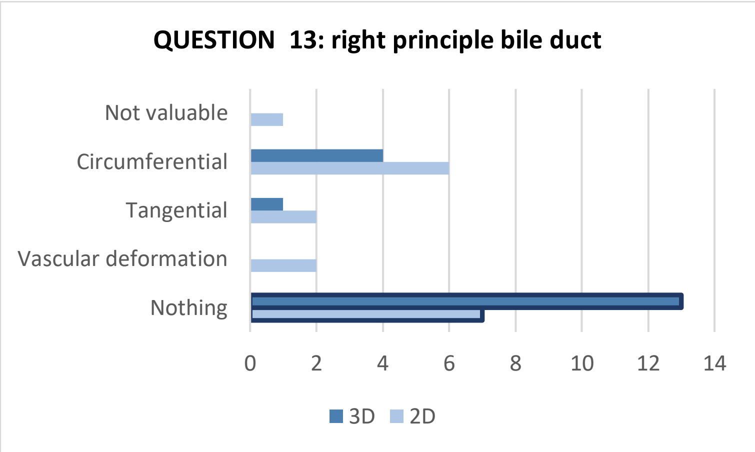
QUESTION 13: right principle bile duct
Not valuable
Circumferential
Tangential
Vascular deformation
Nothing
0
2
4
6
8
10
12
14
3D
2D

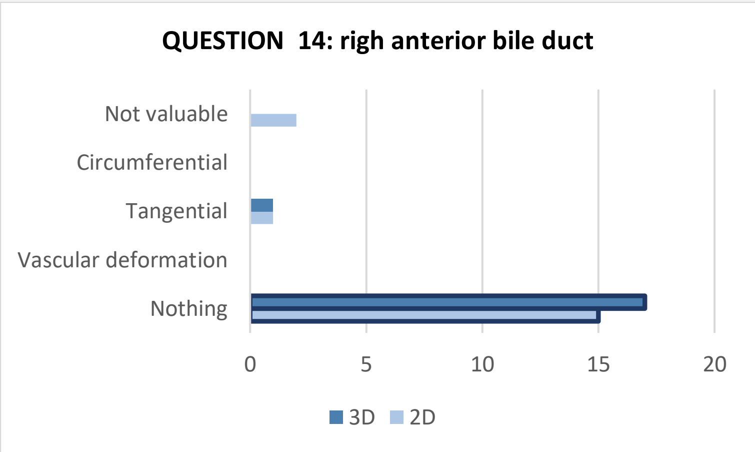
QUESTION 14: righ anterior bile duct
Not valuable
Circumferential
Tangential
Vascular deformation
Nothing
0
5
10
15
20
3D
2D

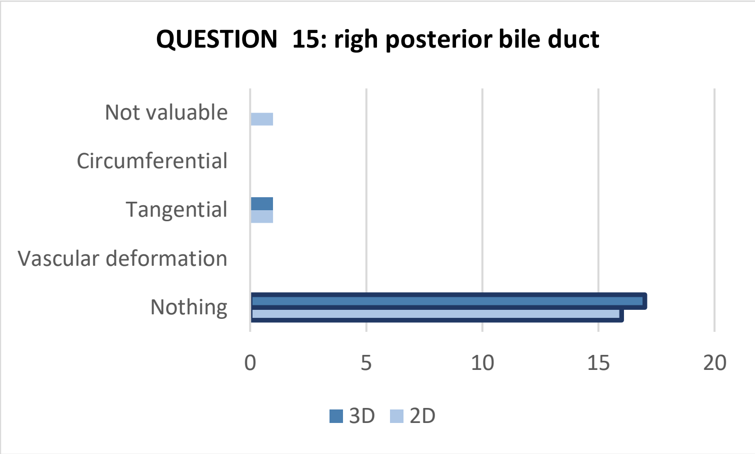
QUESTION 15: righ posterior bile duct
Not valuable
Circumferential
Tangential
Vascular deformation
Nothing
0
5
10
15
20
3D
2D

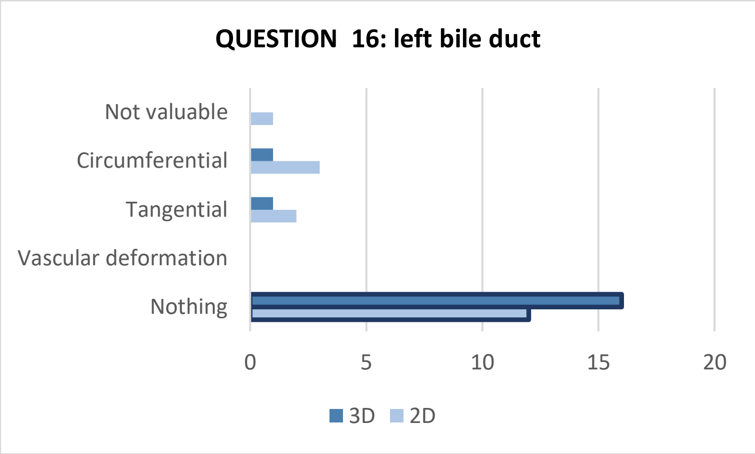
QUESTION 16: left bile duct
Not valuable
Circumferential
Tangential
Vascular deformation
Nothing
0
5
10
15
20
3D
2D

PATIENT 2

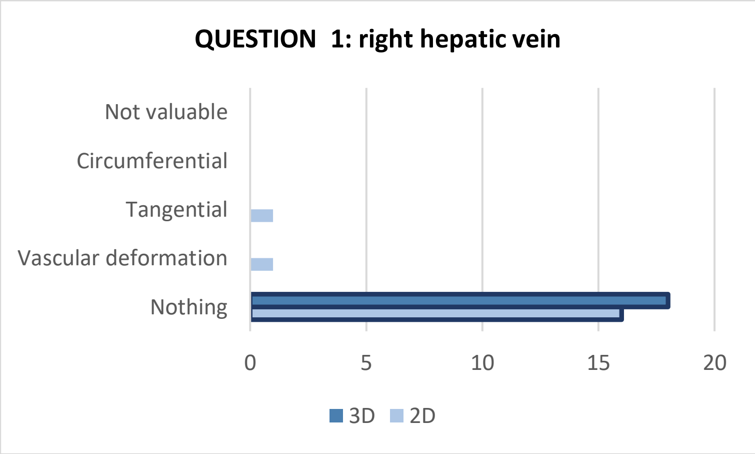
QUESTION 1: right hepatic vein
Not valuable
Circumferential
Tangential
Vascular deformation
Nothing
0
5
10
15
20
3D
2D

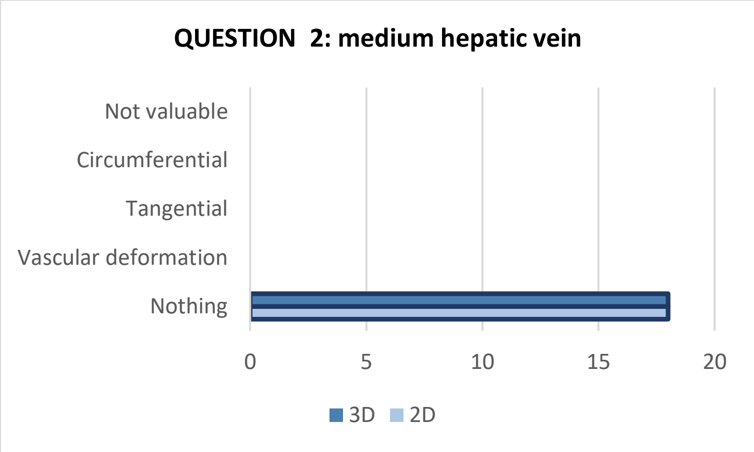
QUESTION 2: medium hepatic vein
Not valuable
Circumferential
Tangential
Vascular deformation
Nothing
0
5
10
15
20
3D
2D

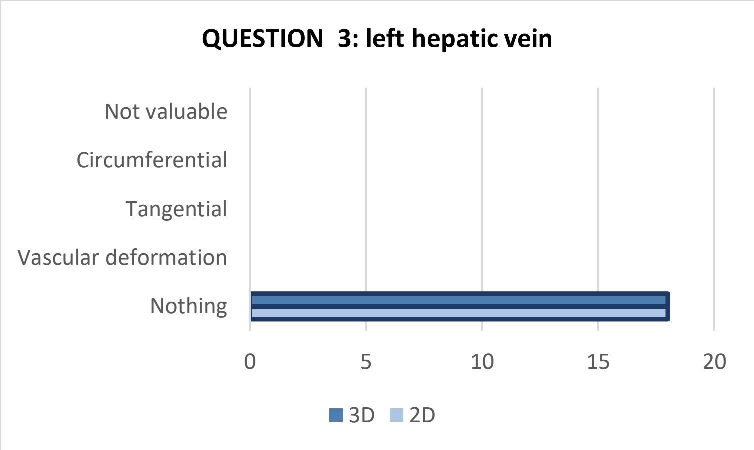
QUESTION 3: left hepatic vein
Not valuable
Circumferential
Tangential
Vascular deformation
Nothing
0
5
10
15
20
3D
2D

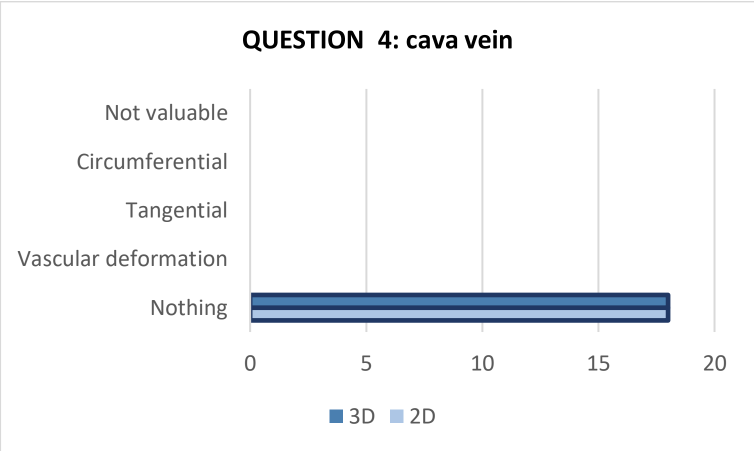
QUESTION 4: cava vein
Not valuable
Circumferential
Tangential
Vascular deformation
Nothing
0
5
10
15
20
3D
2D

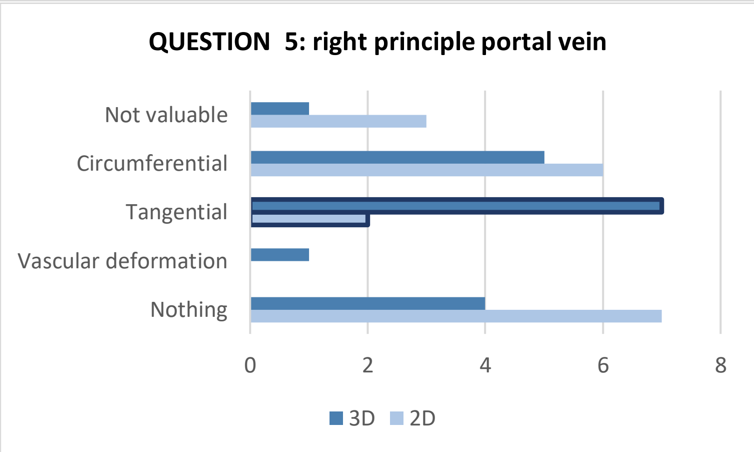
QUESTION 5: right principle portal vein
Not valuable
Circumferential
Tangential
Vascular deformation
Nothing
0
2
4
6
8
3D
2D

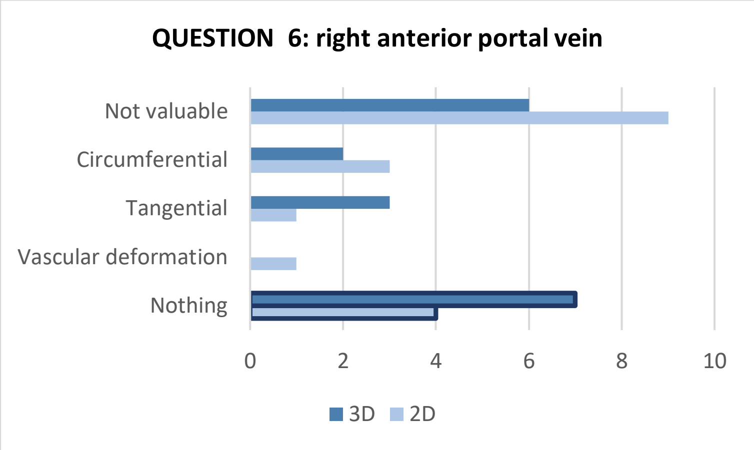
QUESTION 6: right anterior portal vein
Not valuable
Circumferential
Tangential
Vascular deformation
Nothing
0 2 4 6 8 10
3D 2D

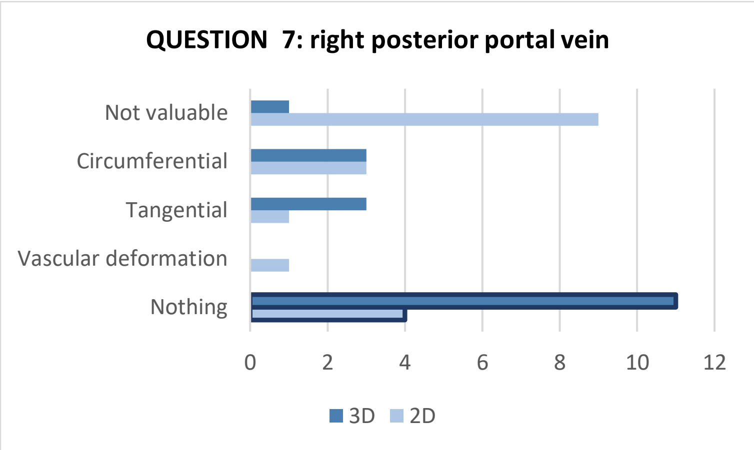
QUESTION 7: right posterior portal vein
Not valuable
Circumferential
Tangential
Vascular deformation
Nothing
0 2 4 6 8 10 12
3D 2D

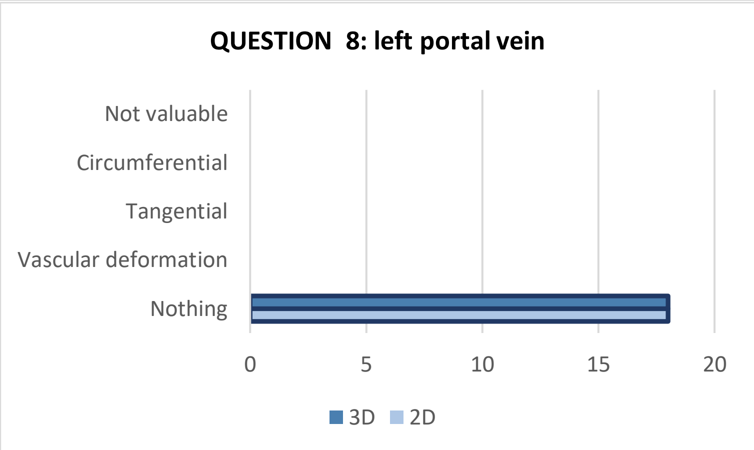
QUESTION 8: left portal vein
Not valuable
Circumferential
Tangential
Vascular deformation
Nothing
0 5 10 15 20
3D 2D

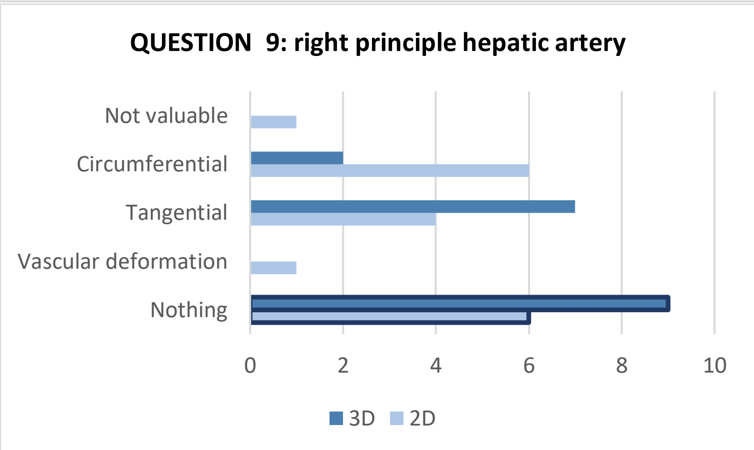
QUESTION 9: right principle hepatic artery
Not valuable
Circumferential
Tangential
Vascular deformation
Nothing
0 2 4 6 8 10
3D 2D

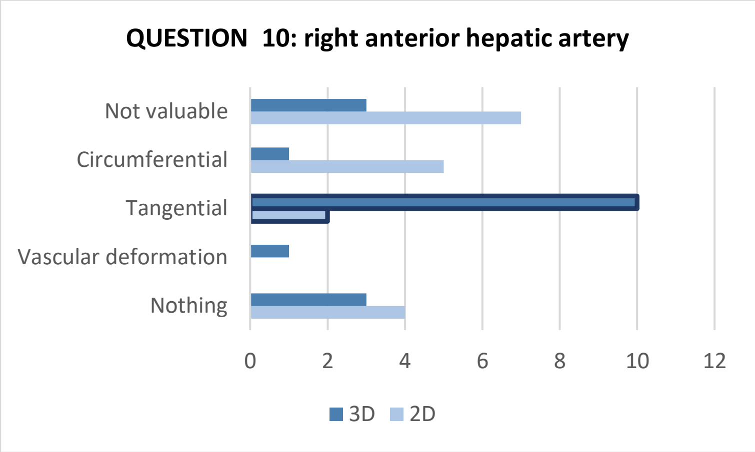
QUESTION 10: right anterior hepatic artery
Not valuable
Circumferential
Tangential
Vascular deformation
Nothing
0
2
4
6
8
10
12
3D
2D

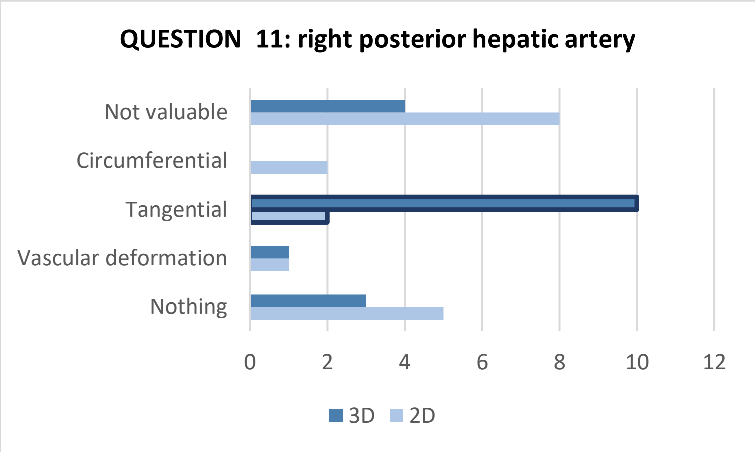
QUESTION 11: right posterior hepatic artery
Not valuable
Circumferential
Tangential
Vascular deformation
Nothing
0
2
4
6
8
10
12
3D
2D

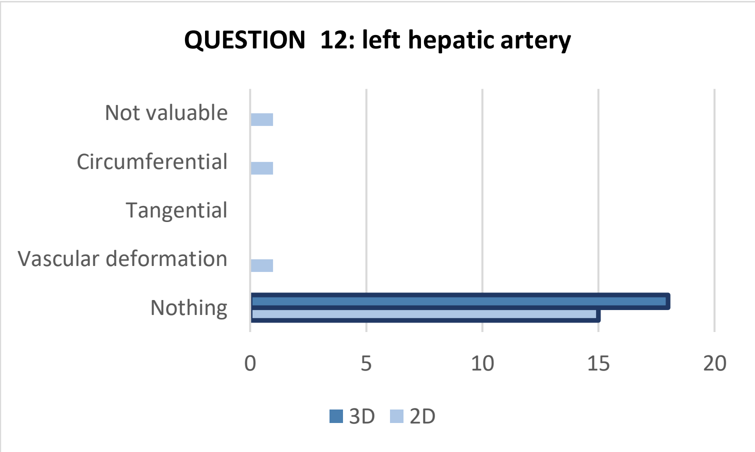
QUESTION 12: left hepatic artery
Not valuable
Circumferential
Tangential
Vascular deformation
Nothing
0
5
10
15
20
3D
2D

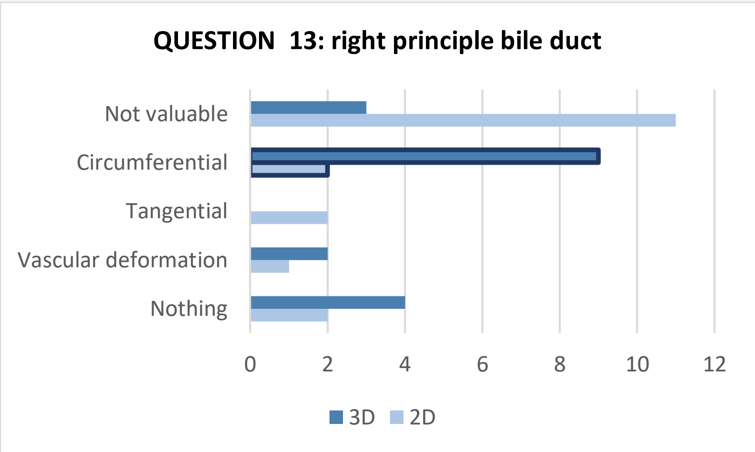
QUESTION 13: right principle bile duct
Not valuable
Circumferential
Tangential
Vascular deformation
Nothing
0
2
4
6
8
10
12
3D
2D

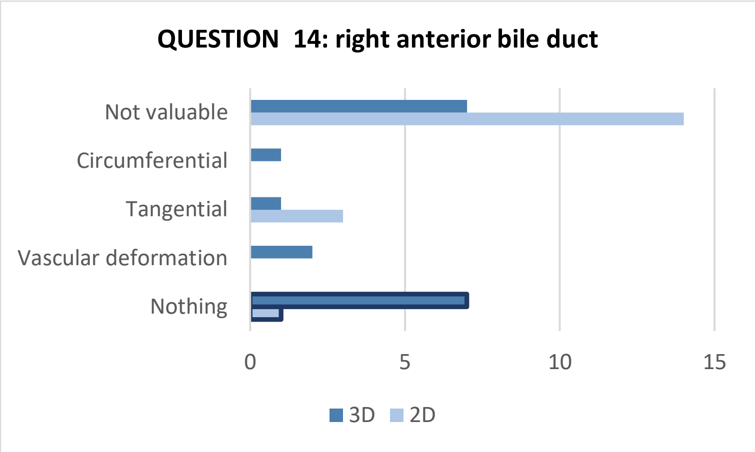
QUESTION 14: right anterior bile duct
Not valuable
Circumferential
Tangential
Vascular deformation
Nothing
0
5
10
15
3D
2D

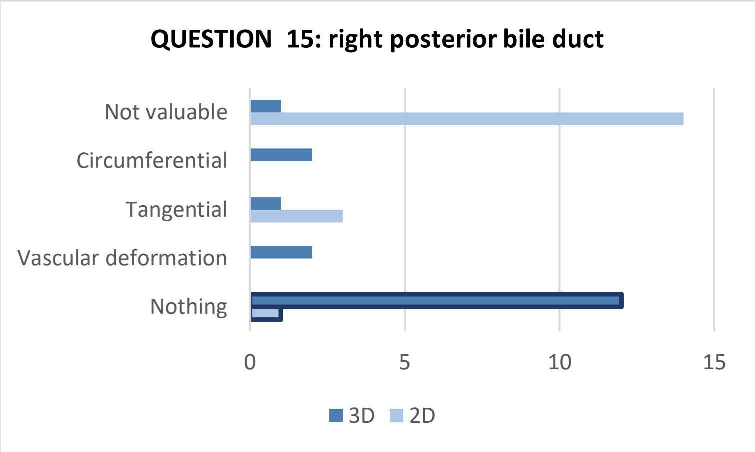
QUESTION 15: right posterior bile duct
Not valuable
Circumferential
Tangential
Vascular deformation
Nothing
0
5
10
15
3D
2D

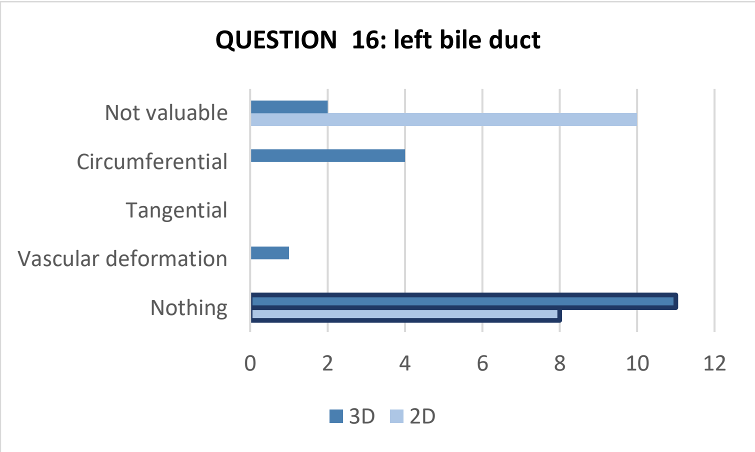
QUESTION 16: left bile duct
Not valuable
Circumferential
Tangential
Vascular deformation
Nothing
0
2
4
6
8
10
12
3D
2D

PATIENT 3

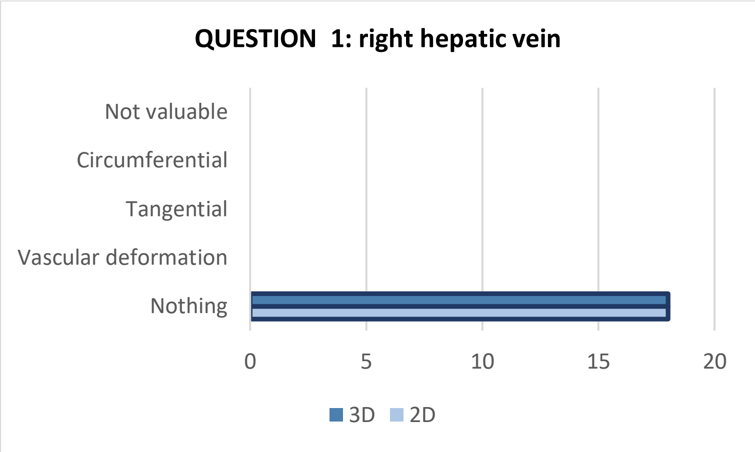
QUESTION 1: right hepatic vein
Not valuable
Circumferential
Tangential
Vascular deformation
Nothing
0
5
10
15
20
3D
2D

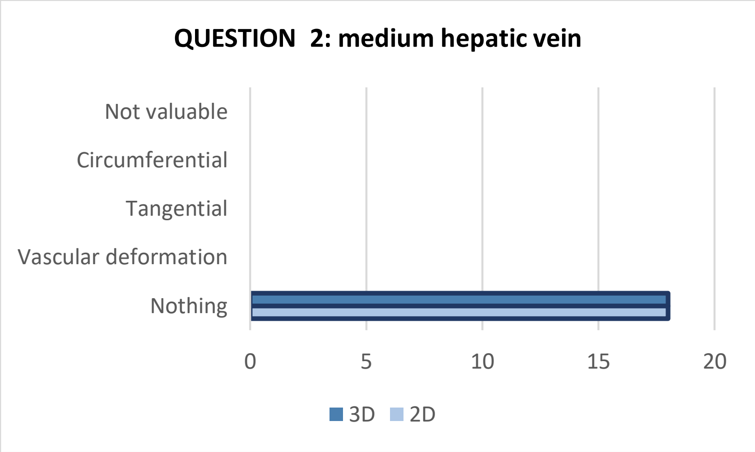
QUESTION 2: medium hepatic vein
Not valuable
Circumferential
Tangential
Vascular deformation
Nothing
0
5
10
15
20
3D
2D

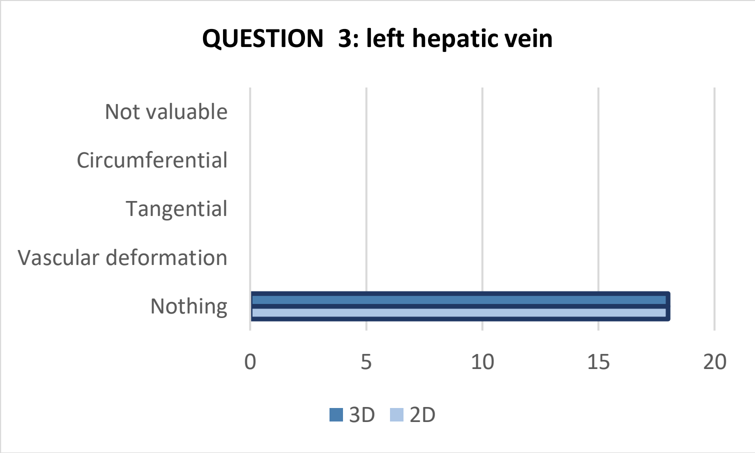
QUESTION 3: left hepatic vein
Not valuable
Circumferential
Tangential
Vascular deformation
Nothing
0
5
10
15
20
3D
2D

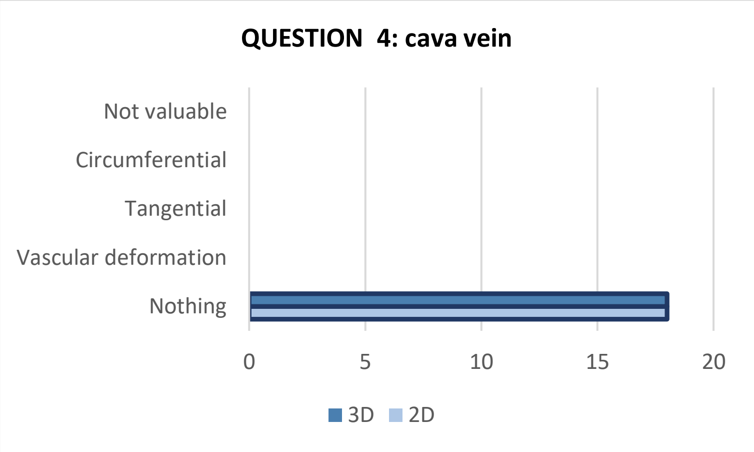
QUESTION 4: cava vein
Not valuable
Circumferential
Tangential
Vascular deformation
Nothing
0
5
10
15
20
3D
2D

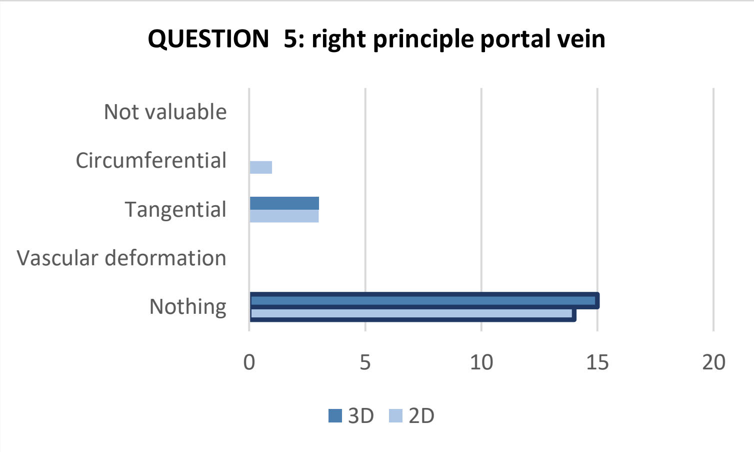
QUESTION 5: right principle portal vein
Not valuable
Circumferential
Tangential
Vascular deformation
Nothing
0
5
10
15
20
3D
2D

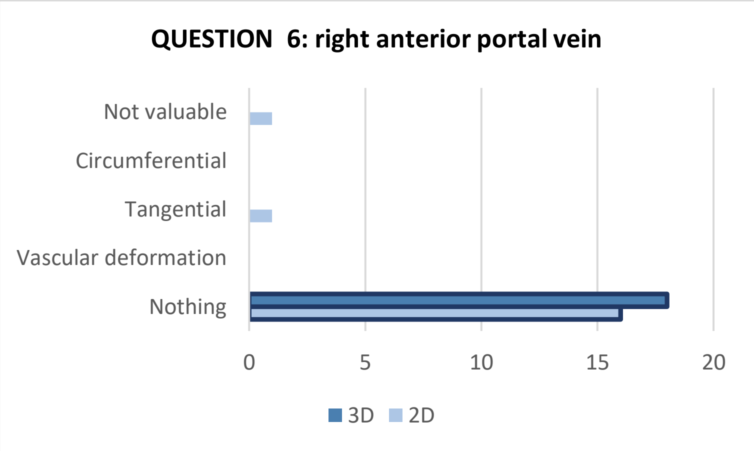
QUESTION 6: right anterior portal vein
Not valuable
Circumferential
Tangential
Vascular deformation
Nothing
0
5
10
15
20
3D
2D

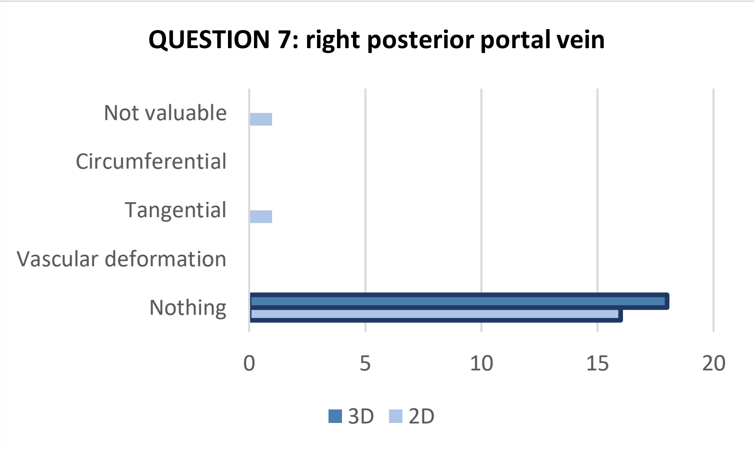
QUESTION 7: right posterior portal vein
Not valuable
Circumferential
Tangential
Vascular deformation
Nothing
0
5
10
15
20
3D
2D

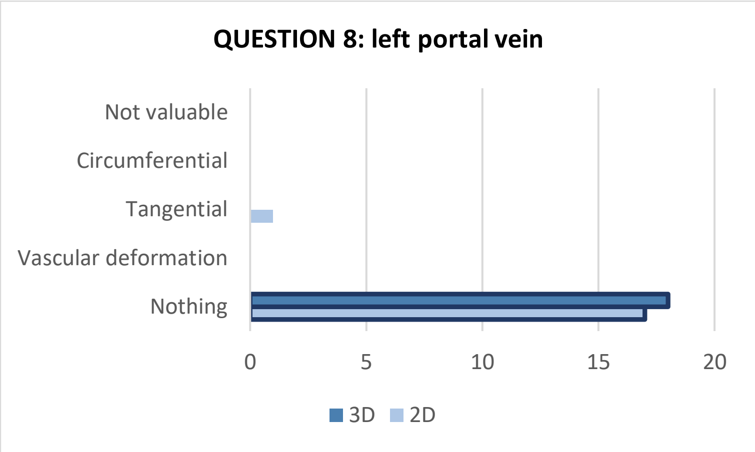
QUESTION 8: left portal vein
Not valuable
Circumferential
Tangential
Vascular deformation
Nothing
0
5
10
15
20
3D
2D

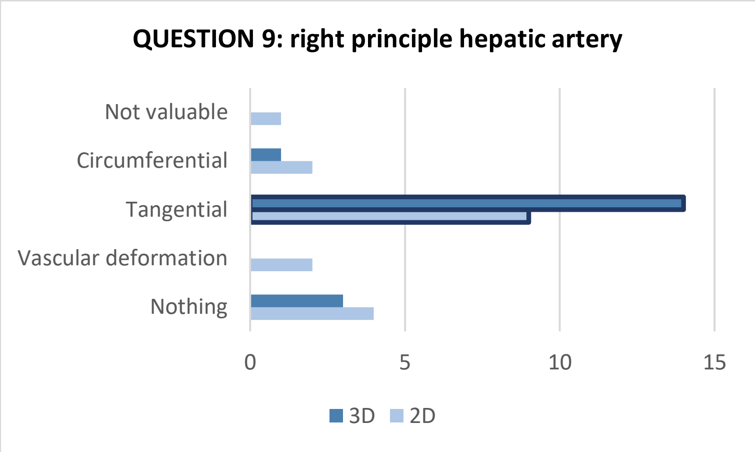
QUESTION 9: right principle hepatic artery
Not valuable
Circumferential
Tangential
Vascular deformation
Nothing
0
5
10
15
3D
2D

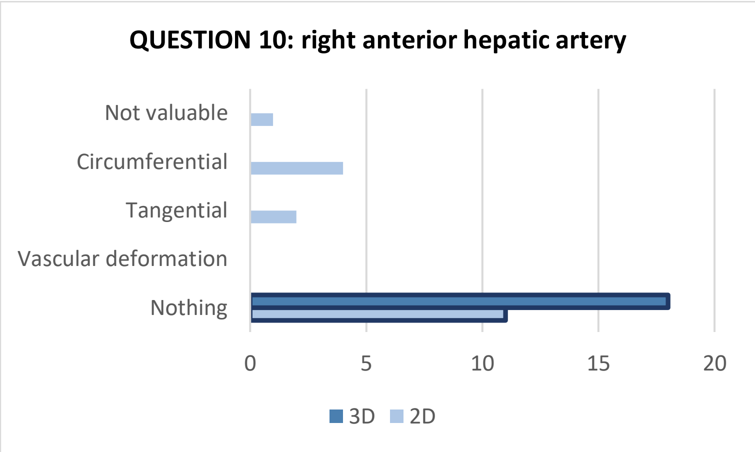
QUESTION 10: right anterior hepatic artery
Not valuable
Circumferential
Tangential
Vascular deformation
Nothing
0
5
10
15
20
3D
2D

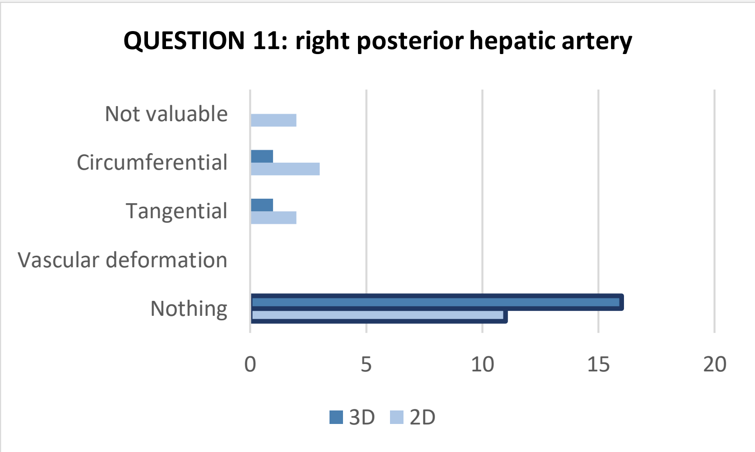
QUESTION 11: right posterior hepatic artery
Not valuable
Circumferential
Tangential
Vascular deformation
Nothing
0
5
10
15
20
3D
2D

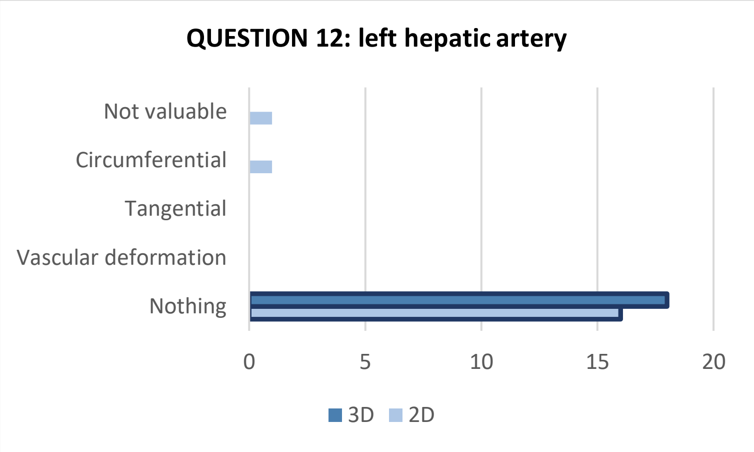
QUESTION 12: left hepatic artery
Not valuable
Circumferential
Tangential
Vascular deformation
Nothing
0
5
10
15
20
3D
2D

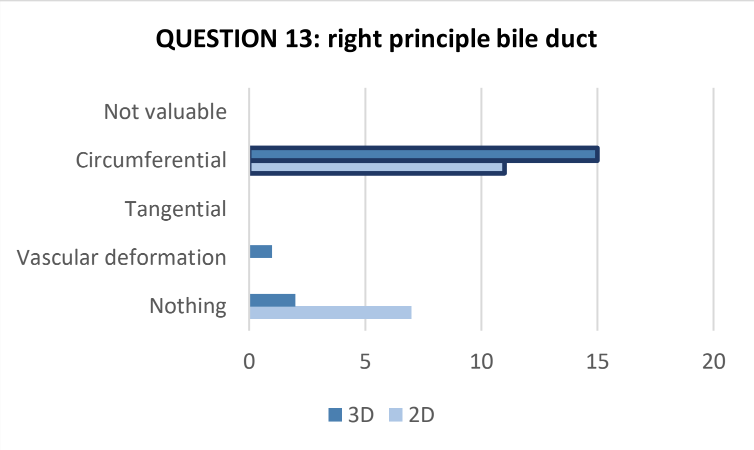
QUESTION 13: right principle bile duct
Not valuable
Circumferential
Tangential
Vascular deformation
Nothing
0
5
10
15
20
3D
2D

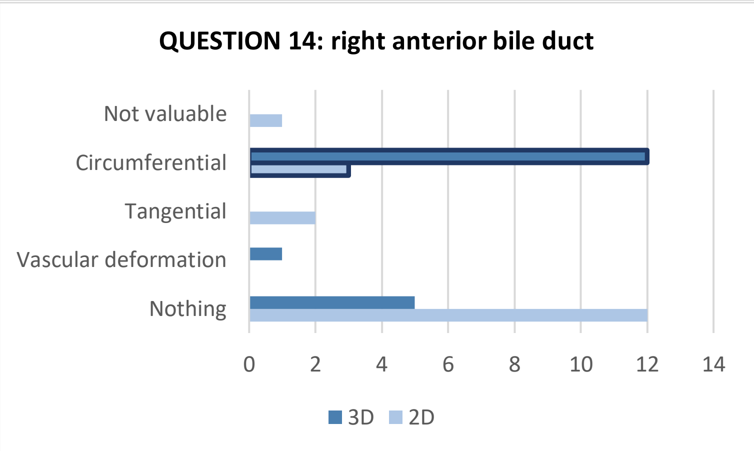
QUESTION 14: right anterior bile duct
Not valuable
Circumferential
Tangential
Vascular deformation
Nothing
0
2
4
6
8
10
12
14
3D
2D

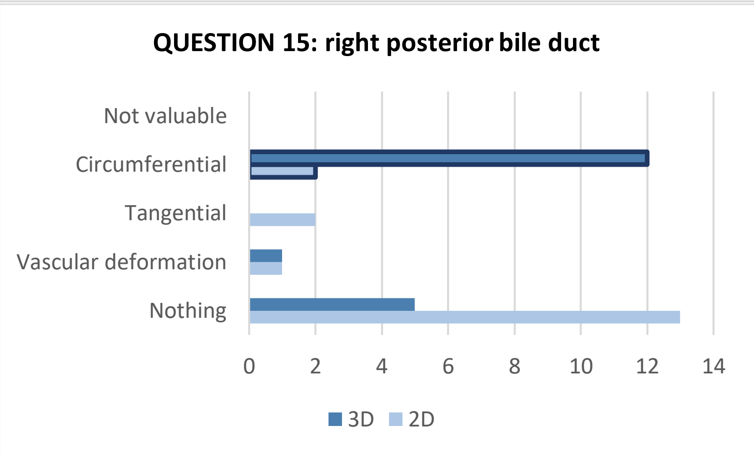
QUESTION 15: right posterior bile duct
Not valuable
Circumferential
Tangential
Vascular deformation
Nothing
0
2
4
6
8
10
12
14
3D
2D

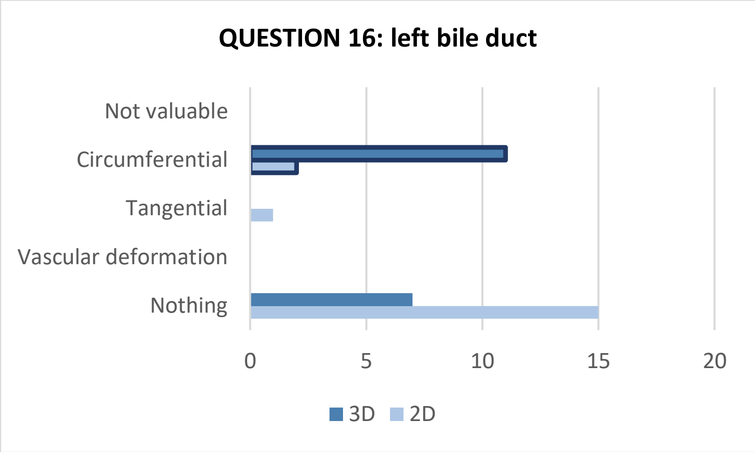
QUESTION 16: left bile duct
Not valuable
Circumferential
Tangential
Vascular deformation
Nothing
0
5
10
15
20
3D
2D

PATIENT 4

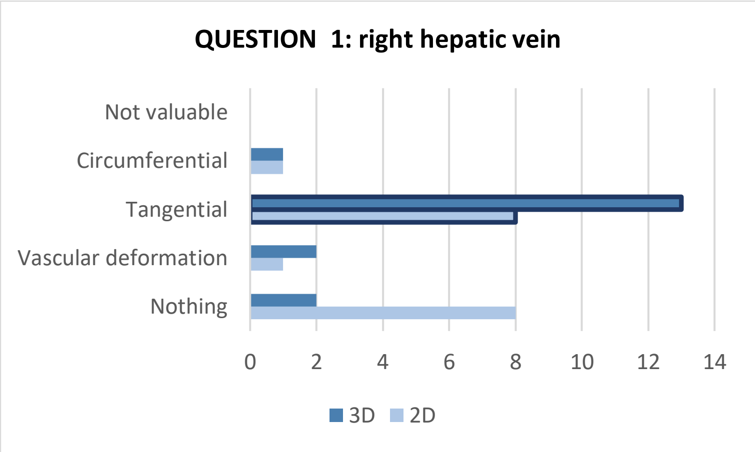
QUESTION 1: right hepatic vein
Not valuable
Circumferential
Tangential
Vascular deformation
Nothing
0
2
4
6
8
10
12
14
3D
2D

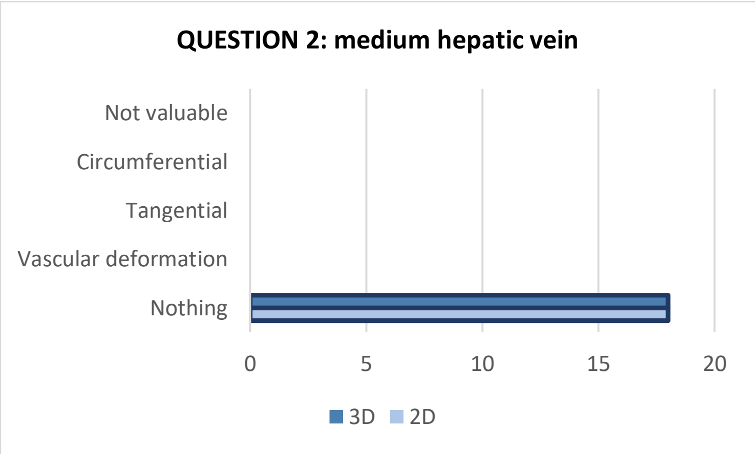
QUESTION 2: medium hepatic vein
Not valuable
Circumferential
Tangential
Vascular deformation
Nothing
0
5
10
15
20
3D
2D

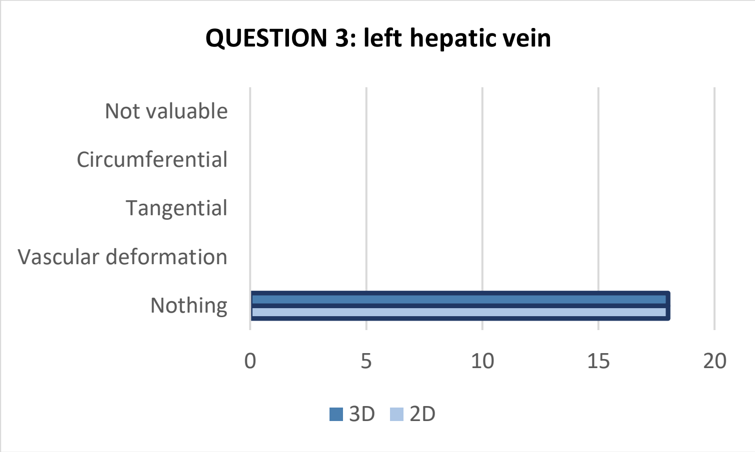
QUESTION 3: left hepatic vein
Not valuable
Circumferential
Tangential
Vascular deformation
Nothing
0 5 10 15 20
3D 2D

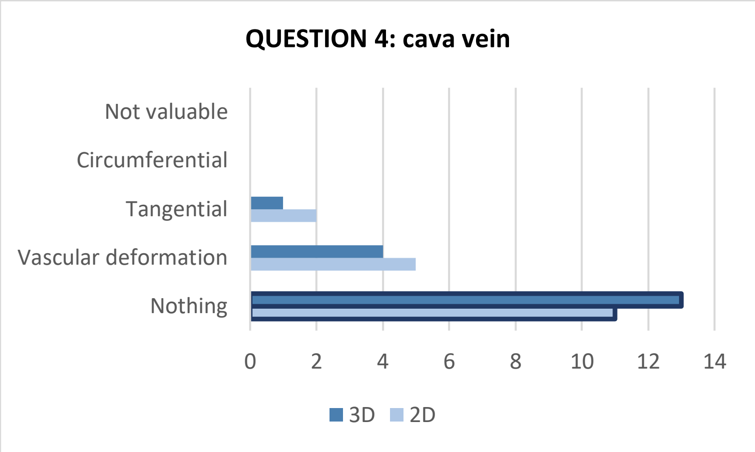
QUESTION 4: cava vein
Not valuable
Circumferential
Tangential
Vascular deformation
Nothing
0 2 4 6 8 10 12 14
3D 2D

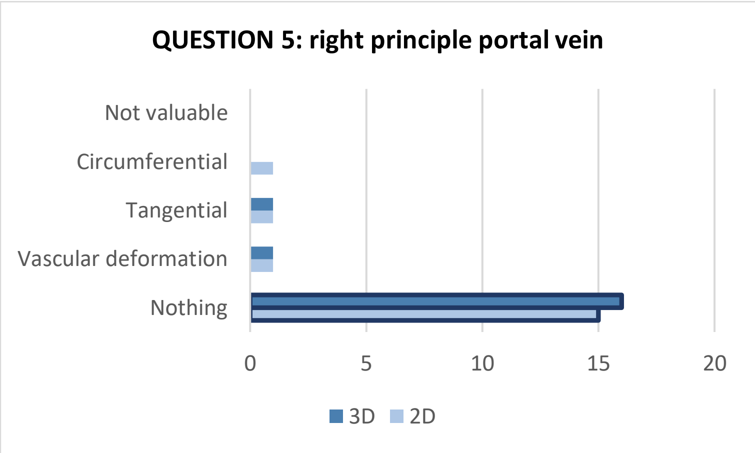
QUESTION 5: right principle portal vein
Not valuable
Circumferential
Tangential
Vascular deformation
Nothing
0 5 10 15 20
3D 2D

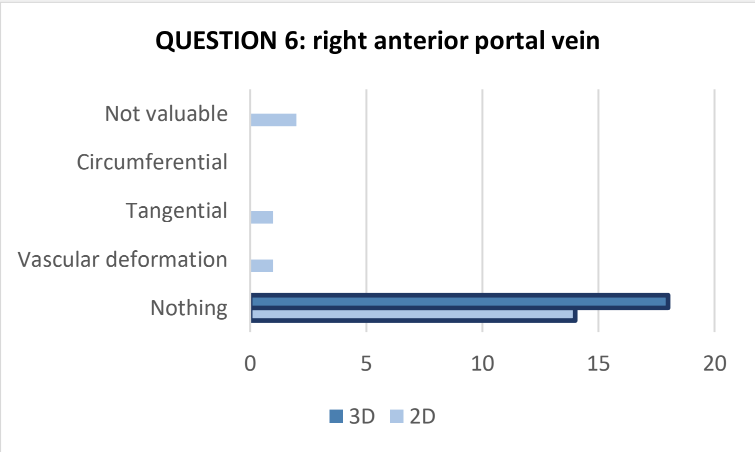
QUESTION 6: right anterior portal vein
Not valuable
Circumferential
Tangential
Vascular deformation
Nothing
0 5 10 15 20
3D 2D

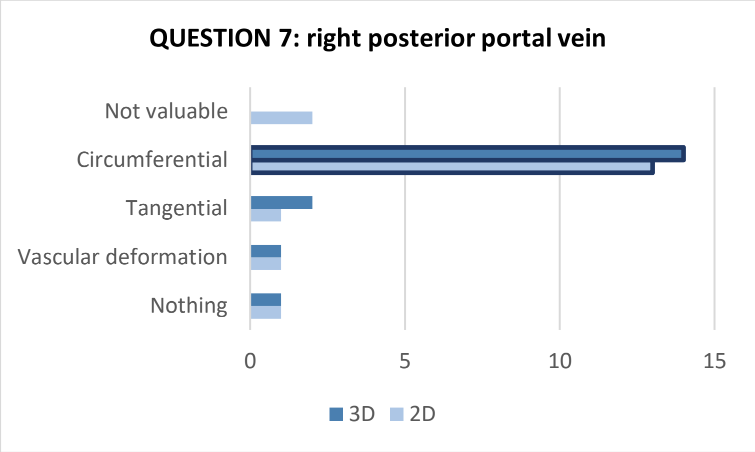
QUESTION 7: right posterior portal vein
Not valuable
Circumferential
Tangential
Vascular deformation
Nothing
0
5
10
15
3D
2D

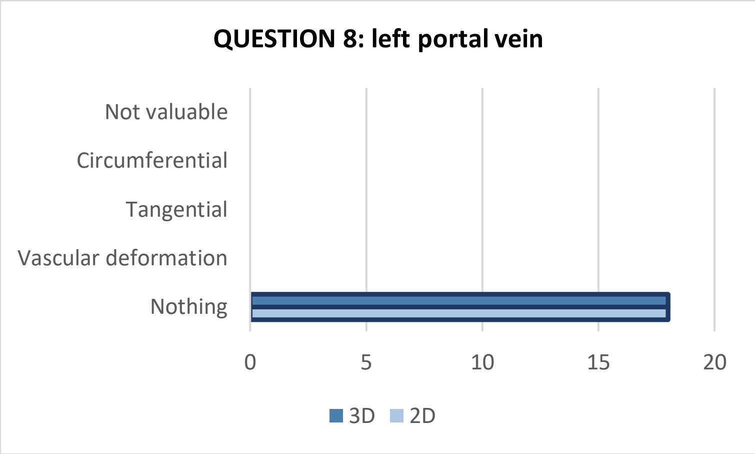
QUESTION 8: left portal vein
Not valuable
Circumferential
Tangential
Vascular deformation
Nothing
0
5
10
15
20
3D
2D

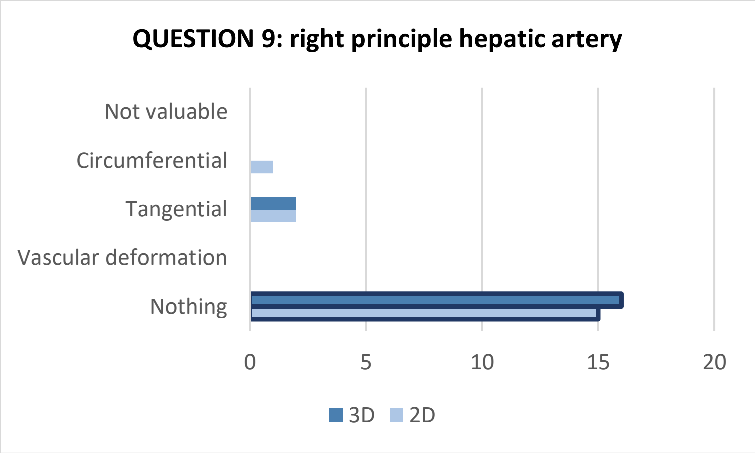
QUESTION 9: right principle hepatic artery
Not valuable
Circumferential
Tangential
Vascular deformation
Nothing
0
5
10
15
20
3D
2D

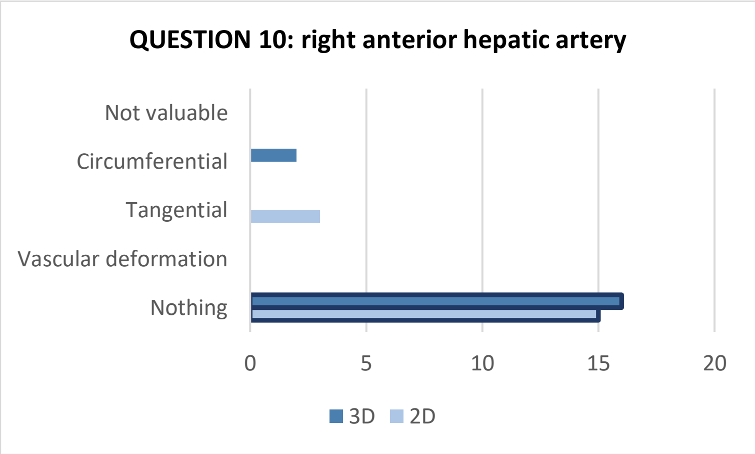
QUESTION 10: right anterior hepatic artery
Not valuable
Circumferential
Tangential
Vascular deformation
Nothing
0
5
10
15
20
3D
2D

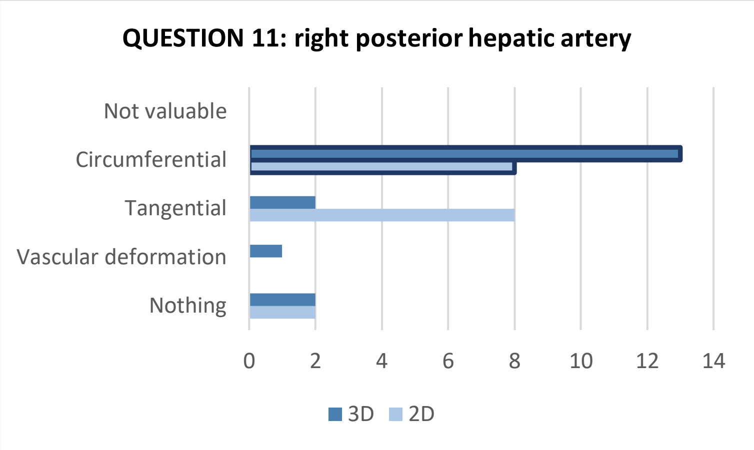
QUESTION 11: right posterior hepatic artery
Not valuable
Circumferential
Tangential
Vascular deformation
Nothing
0
2
4
6
8
10
12
14
3D
2D

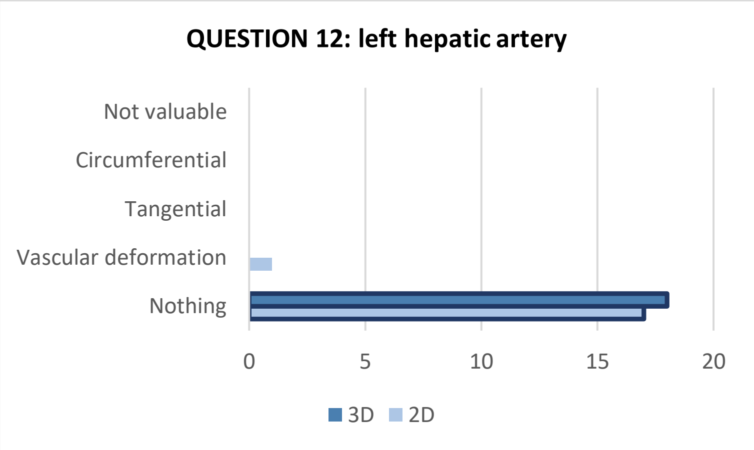
QUESTION 12: left hepatic artery
Not valuable
Circumferential
Tangential
Vascular deformation
Nothing
0
5
10
15
20
3D
2D

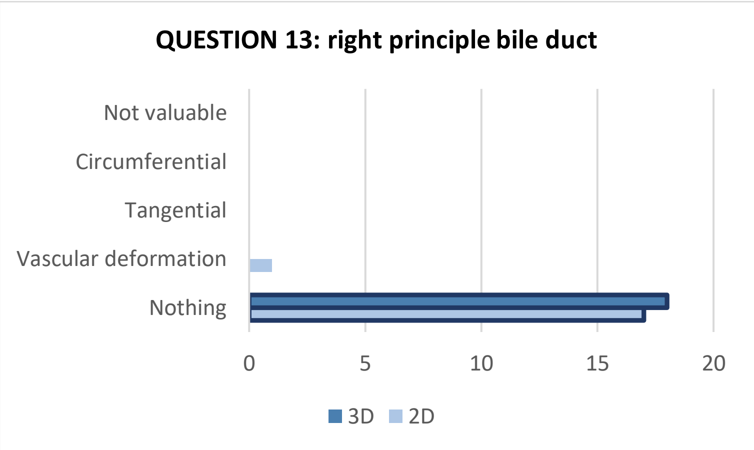
QUESTION 13: right principle bile duct
Not valuable
Circumferential
Tangential
Vascular deformation
Nothing
0
5
10
15
20
3D
2D

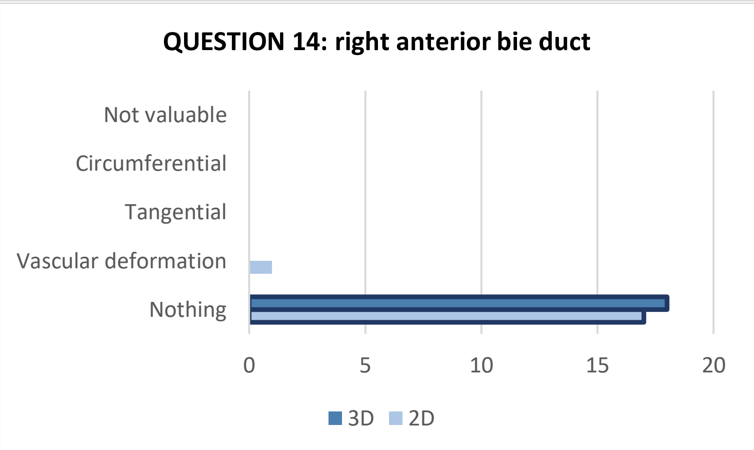
QUESTION 14: right anterior bie duct
Not valuable
Circumferential
Tangential
Vascular deformation
Nothing
0
5
10
15
20
3D
2D

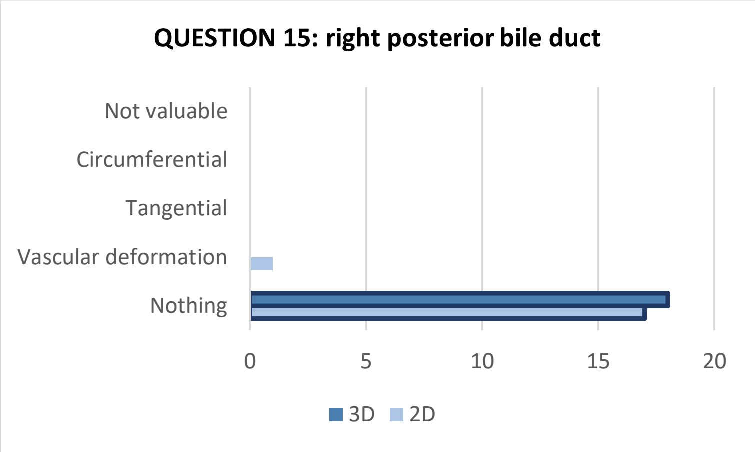
QUESTION 15: right posterior bile duct
Not valuable
Circumferential
Tangential
Vascular deformation
Nothing
0
5
10
15
20
3D
2D

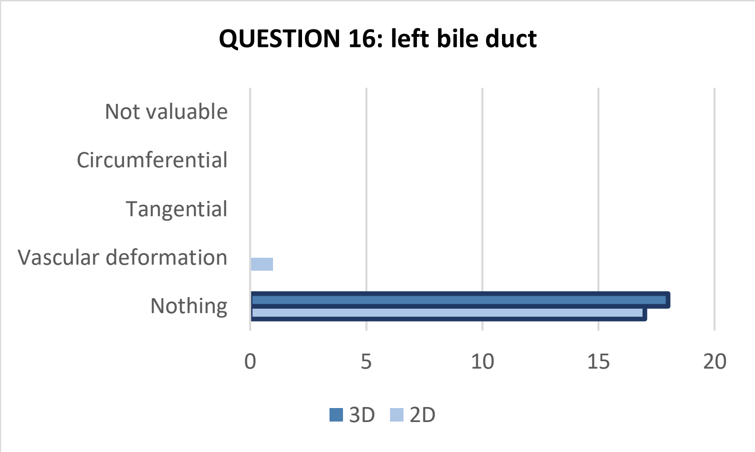
QUESTION 16: left bile duct
Not valuable
Circumferential
Tangential
Vascular deformation
Nothing
0
5
10
15
20
3D
2D

PATIENT 5

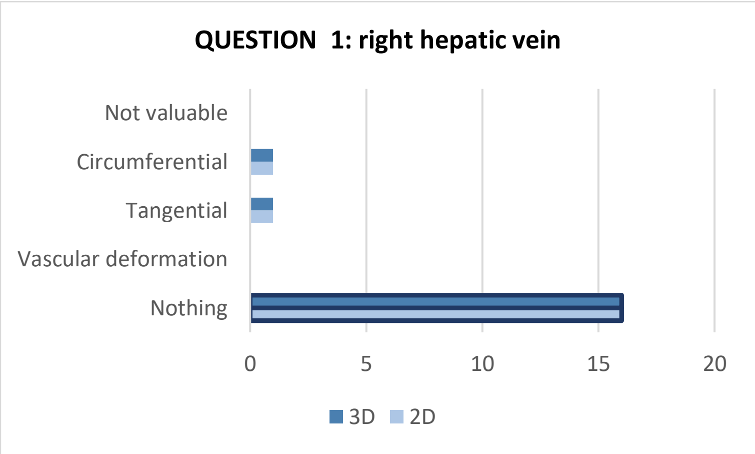
QUESTION 1: right hepatic vein
Not valuable
Circumferential
Tangential
Vascular deformation
Nothing
0
5
10
15
20
3D
2D

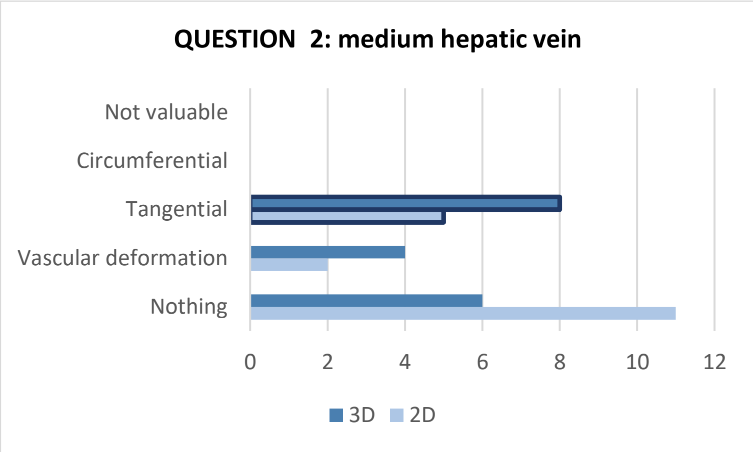
QUESTION 2: medium hepatic vein
Not valuable
Circumferential
Tangential
Vascular deformation
Nothing
0
2
4
6
8
10
12
3D
2D

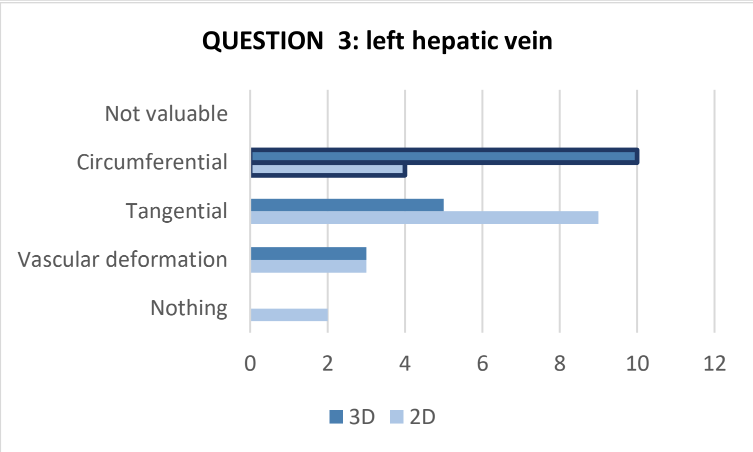
QUESTION 3: left hepatic vein
Not valuable
Circumferential
Tangential
Vascular deformation
Nothing
0
2
4
6
8
10
12
3D
2D

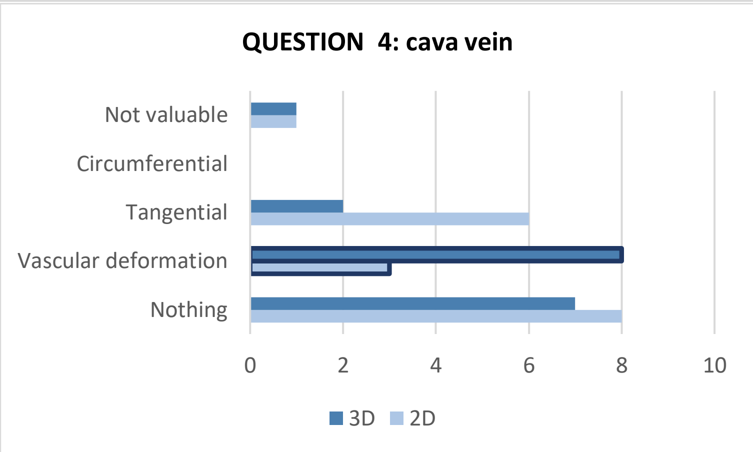
QUESTION 4: cava vein
Not valuable
Circumferential
Tangential
Vascular deformation
Nothing
0
2
4
6
8
10
3D
2D

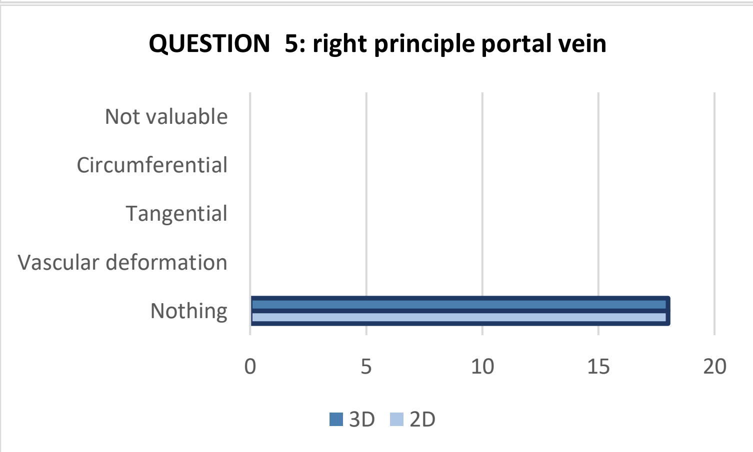
QUESTION 5: right principle portal vein
Not valuable
Circumferential
Tangential
Vascular deformation
Nothing
0
5
10
15
20
3D
2D

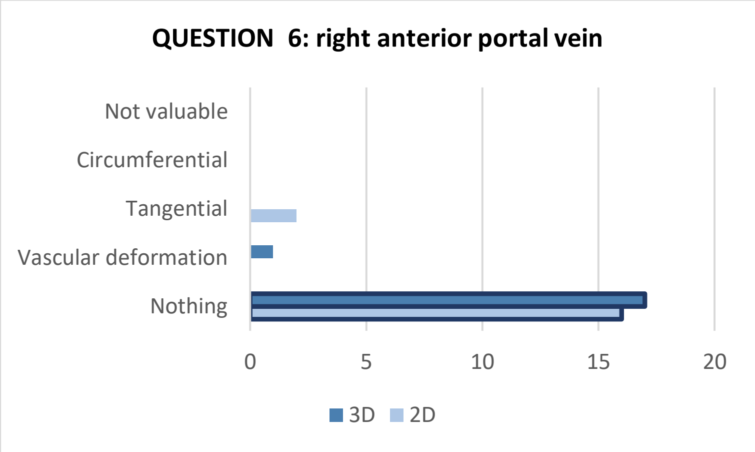
QUESTION 6: right anterior portal vein
Not valuable
Circumferential
Tangential
Vascular deformation
Nothing
0
5
10
15
20
3D
2D

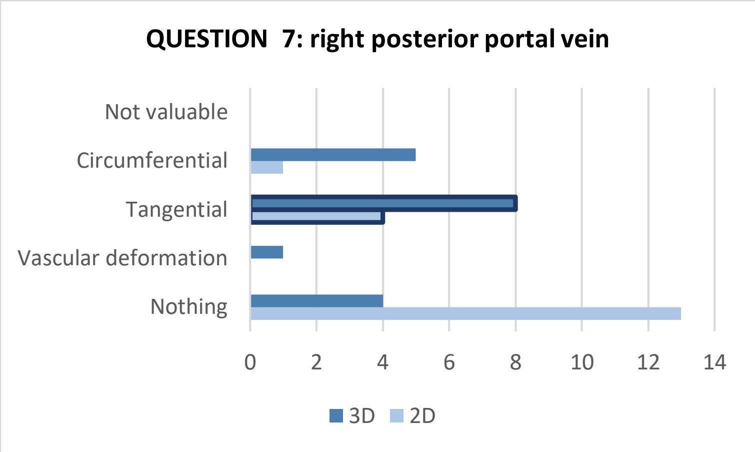
QUESTION 7: right posterior portal vein
Not valuable
Circumferential
Tangential
Vascular deformation
Nothing
0
2
4
6
8
10
12
14
3D
2D

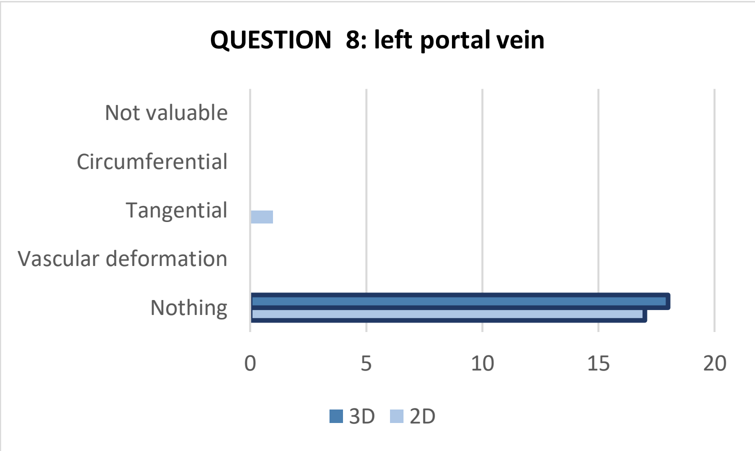
QUESTION 8: left portal vein
Not valuable
Circumferential
Tangential
Vascular deformation
Nothing
0
5
10
15
20
3D
2D

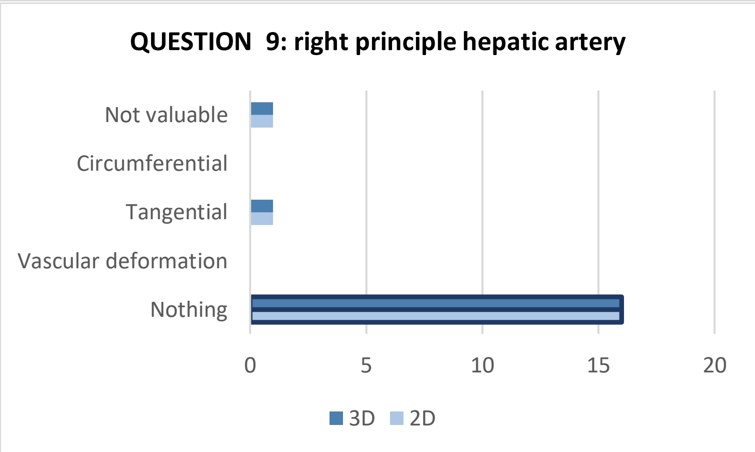
QUESTION 9: right principle hepatic artery
Not valuable
Circumferential
Tangential
Vascular deformation
Nothing
0
5
10
15
20
3D
2D

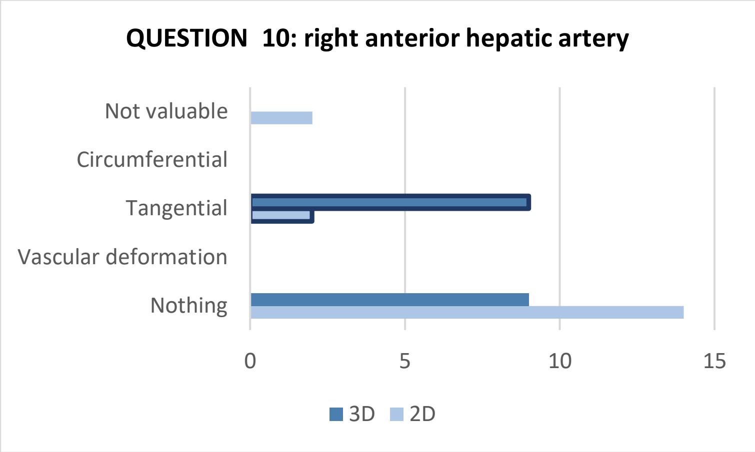
QUESTION 10: right anterior hepatic artery
Not valuable
Circumferential
Tangential
Vascular deformation
Nothing
0
5
10
15
3D
2D

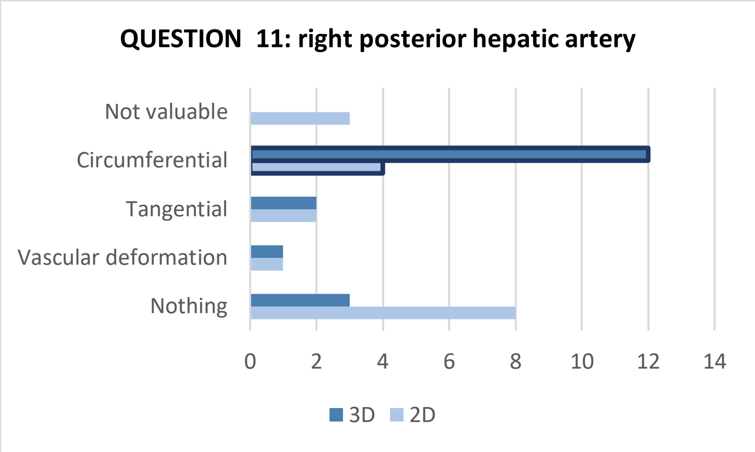
QUESTION 11: right posterior hepatic artery
Not valuable
Circumferential
Tangential
Vascular deformation
Nothing
0
2
4
6
8
10
12
14
3D
2D

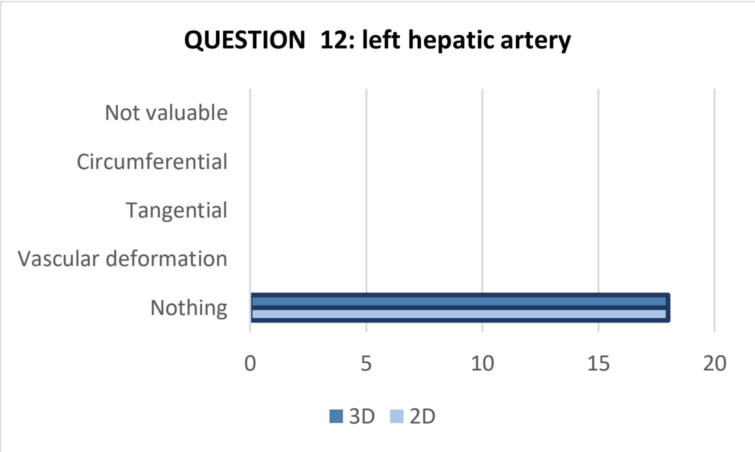
QUESTION 12: left hepatic artery
Not valuable
Circumferential
Tangential
Vascular deformation
Nothing
0
5
10
15
20
3D
2D

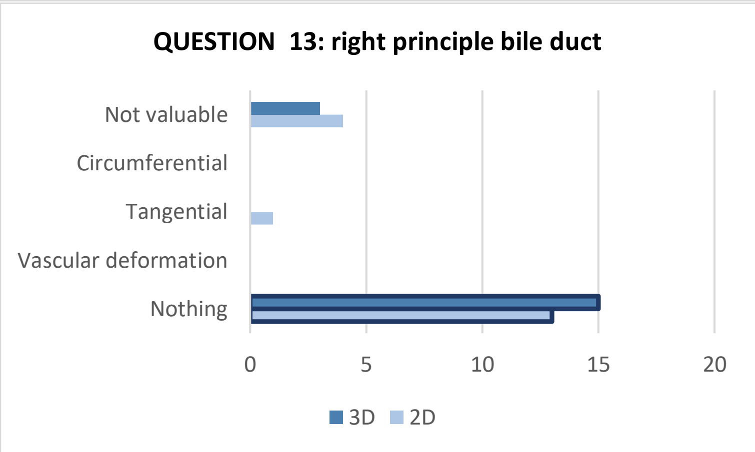
QUESTION 13: right principle bile duct
Not valuable
Circumferential
Tangential
Vascular deformation
Nothing
0
5
10
15
20
3D
2D

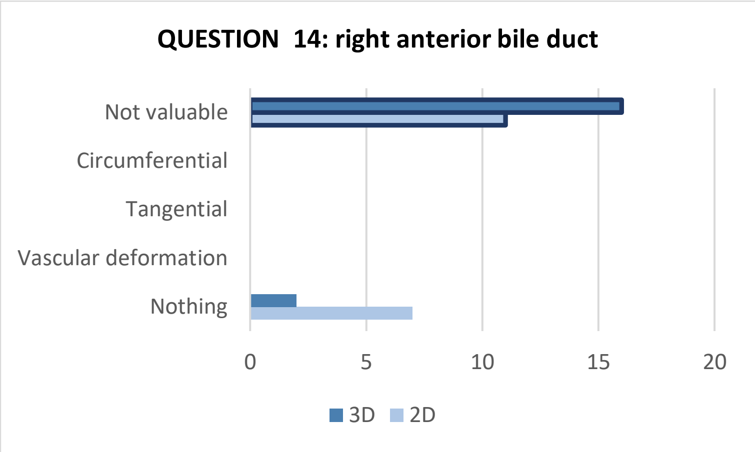
QUESTION 14: right anterior bile duct
Not valuable
Circumferential
Tangential
Vascular deformation
Nothing
0
5
10
15
20
3D
2D

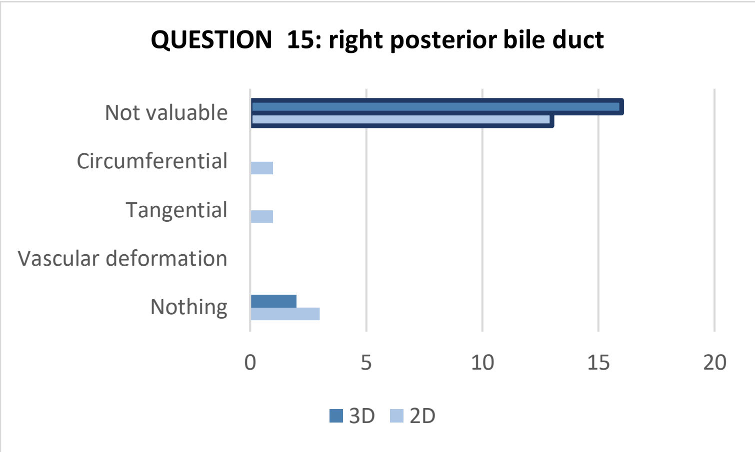
QUESTION 15: right posterior bile duct
Not valuable
Circumferential
Tangential
Vascular deformation
Nothing
0
5
10
15
20
3D
2D

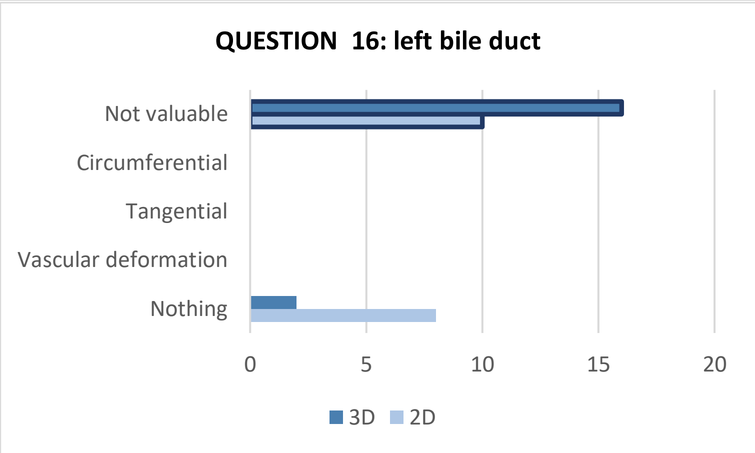
QUESTION 16: left bile duct
Not valuable
Circumferential
Tangential
Vascular deformation
Nothing
0
5
10
15
20
3D
2D

PATIENT 6

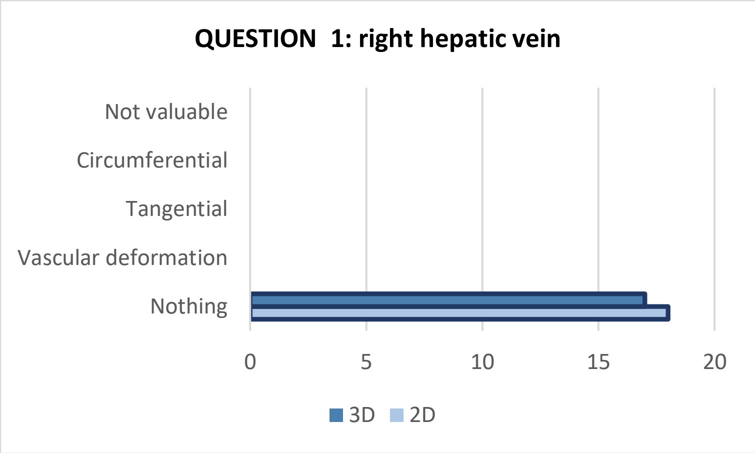
QUESTION 1: right hepatic vein
Not valuable
Circumferential
Tangential
Vascular deformation
Nothing
0
5
10
15
20
3D
2D

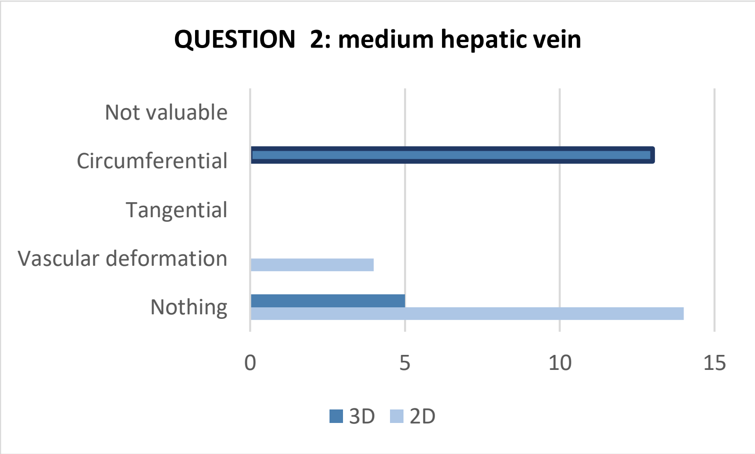
QUESTION 2: medium hepatic vein
Not valuable
Circumferential
Tangential
Vascular deformation
Nothing
0
5
10
15
3D
2D

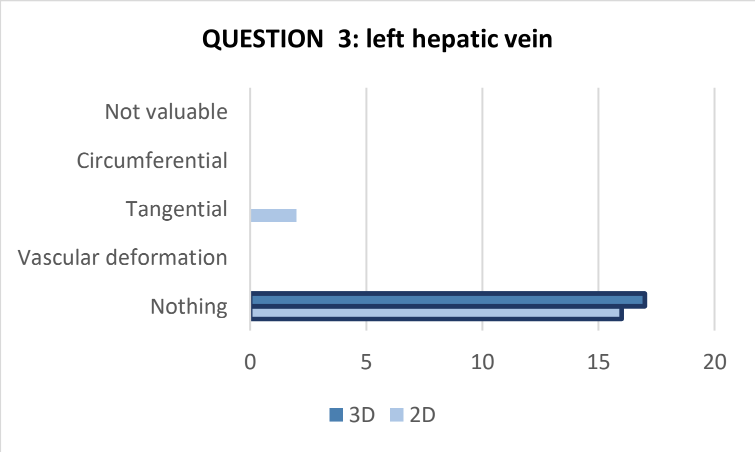
QUESTION 3: left hepatic vein
Not valuable
Circumferential
Tangential
Vascular deformation
Nothing
0
5
10
15
20
3D
2D

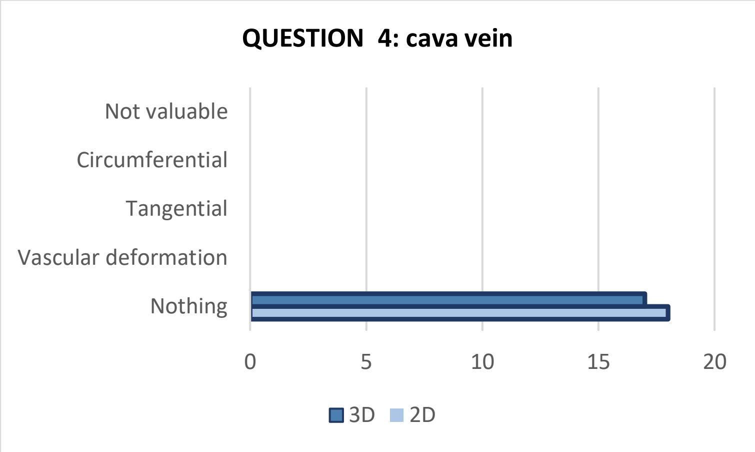
QUESTION 4: cava vein
Not valuable
Circumferential
Tangential
Vascular deformation
Nothing
0
5
10
15
20
3D
2D

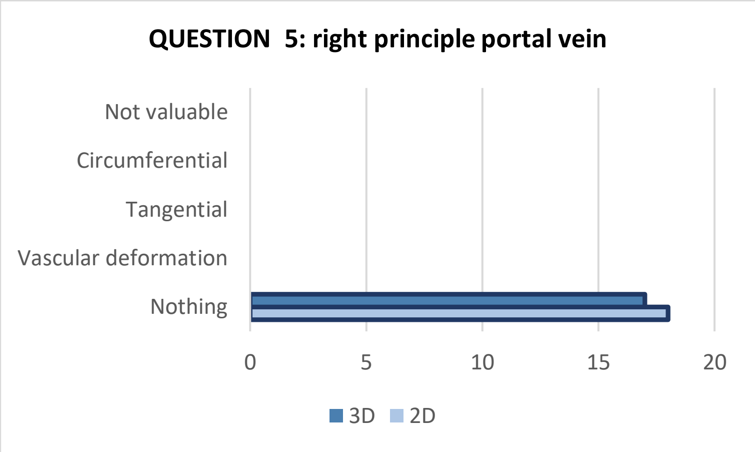
QUESTION 5: right principle portal vein
Not valuable
Circumferential
Tangential
Vascular deformation
Nothing
0
5
10
15
20
3D
2D

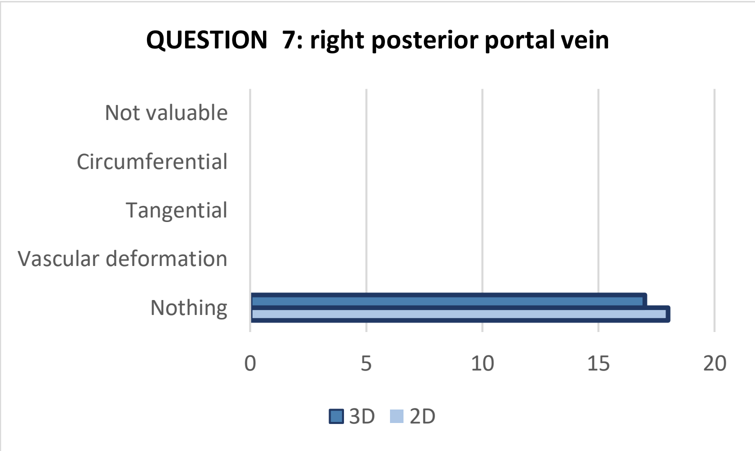
QUESTION 7: right posterior portal vein
Not valuable
Circumferential
Tangential
Vascular deformation
Nothing
0
5
10
15
20
3D
2D

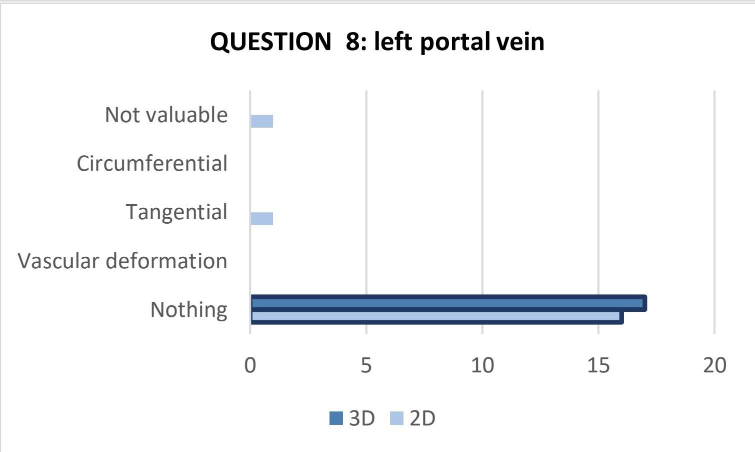
QUESTION 8: left portal vein
Not valuable
Circumferential
Tangential
Vascular deformation
Nothing
0
5
10
15
20
3D
2D

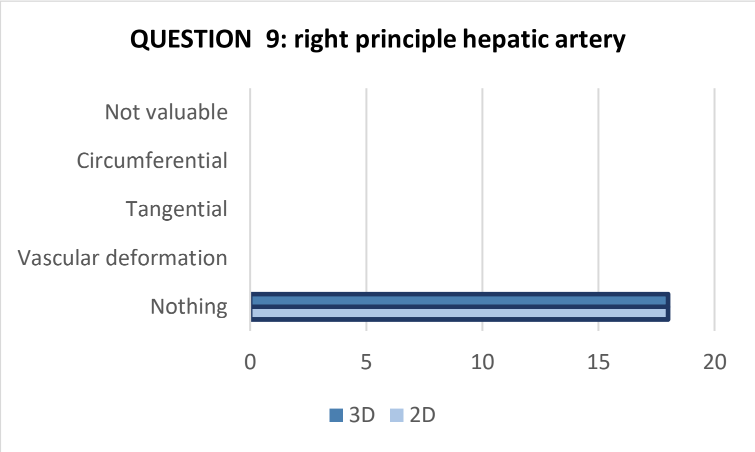
QUESTION 9: right principle hepatic artery
Not valuable
Circumferential
Tangential
Vascular deformation
Nothing
0
5
10
15
20
3D
2D

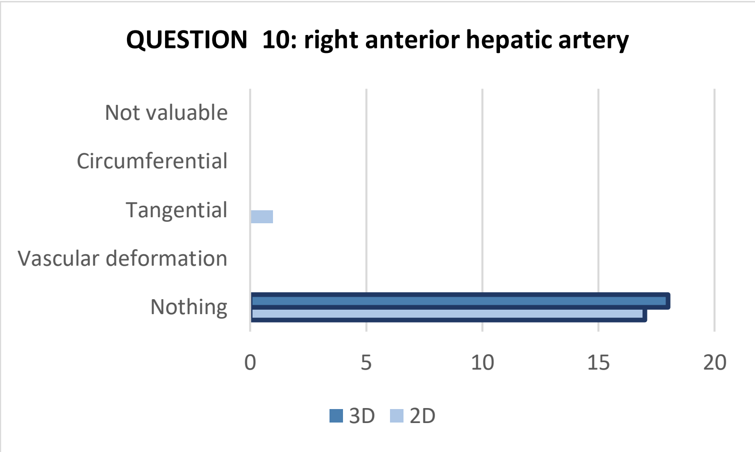
QUESTION 10: right anterior hepatic artery
Not valuable
Circumferential
Tangential
Vascular deformation
Nothing
0
5
10
15
20
3D
2D

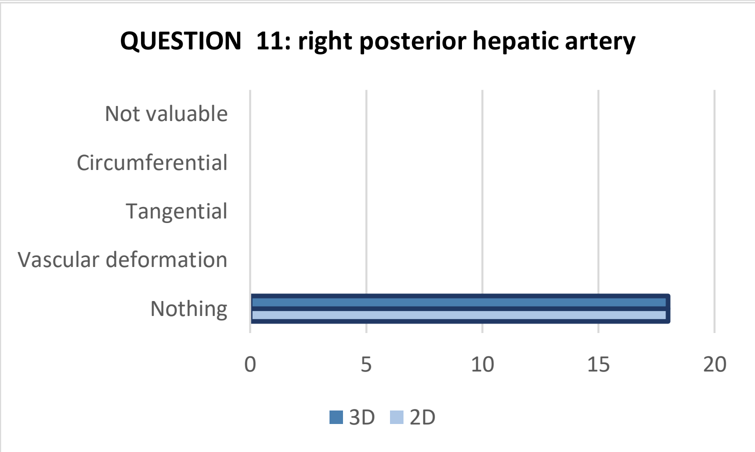
QUESTION 11: right posterior hepatic artery
Not valuable
Circumferential
Tangential
Vascular deformation
Nothing
0
5
10
15
20
3D
2D

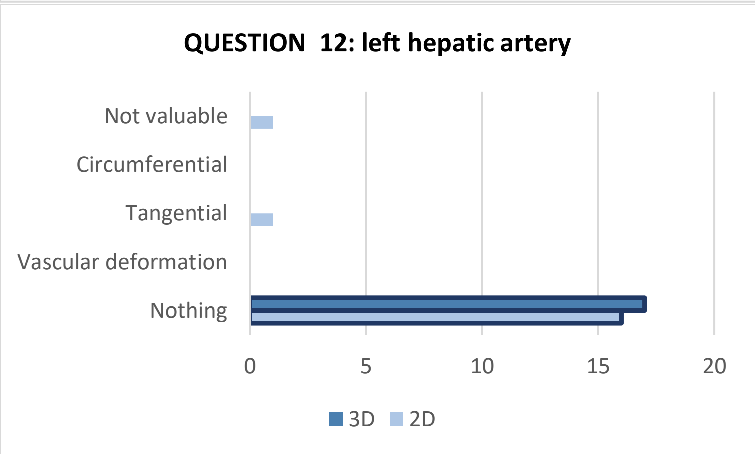
QUESTION 12: left hepatic artery
Not valuable
Circumferential
Tangential
Vascular deformation
Nothing
0
5
10
15
20
3D
2D

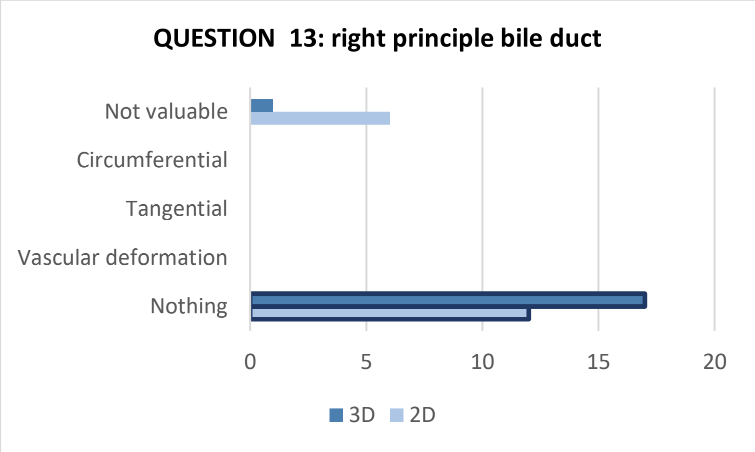
QUESTION 13: right principle bile duct
Not valuable
Circumferential
Tangential
Vascular deformation
Nothing
0
5
10
15
20
3D
2D

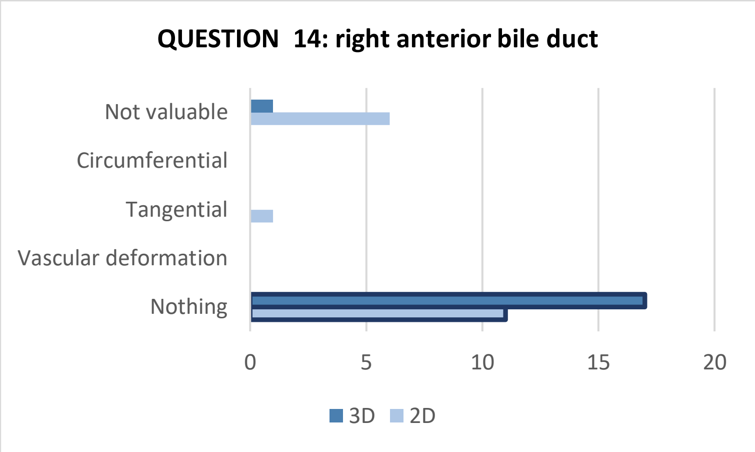
QUESTION 14: right anterior bile duct
Not valuable
Circumferential
Tangential
Vascular deformation
Nothing
0
5
10
15
20
3D
2D

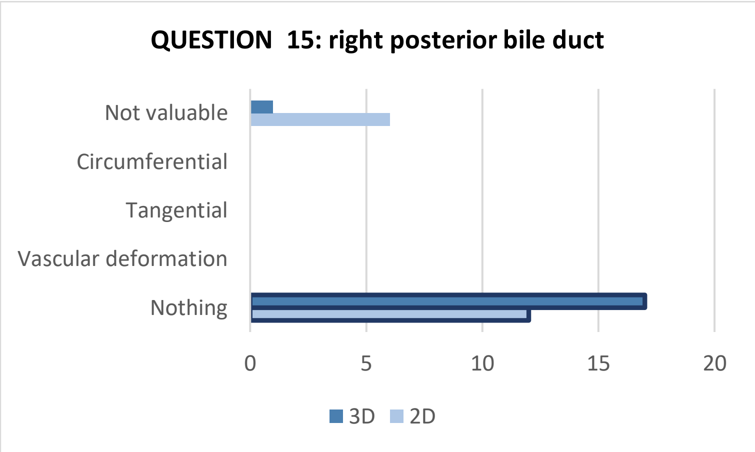
QUESTION 15: right posterior bile duct
Not valuable
Circumferential
Tangential
Vascular deformation
Nothing
0
5
10
15
20
3D
2D

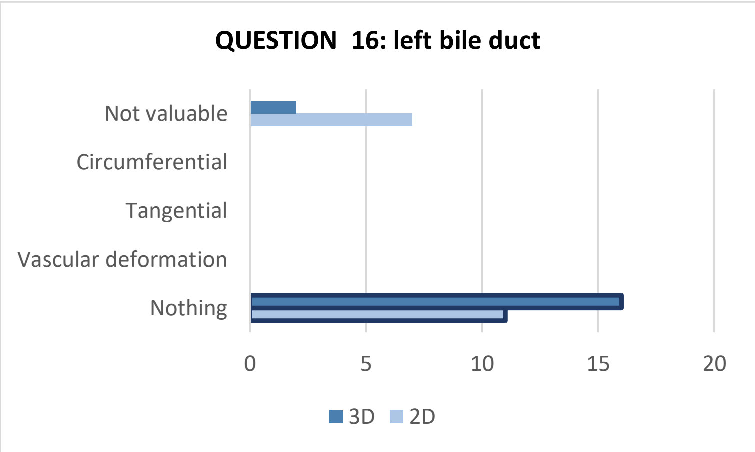
QUESTION 16: left bile duct
Not valuable
Circumferential
Tangential
Vascular deformation
Nothing
0
5
10
15
20
3D
2D

PATIENT 7

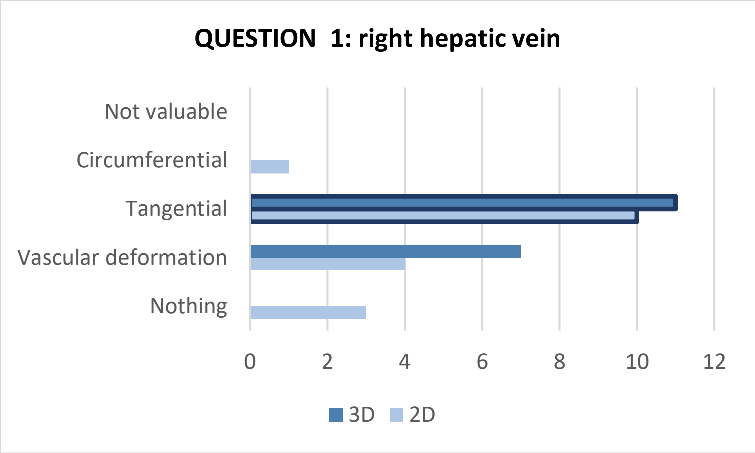
QUESTION 1: right hepatic vein
Not valuable
Circumferential
Tangential
Vascular deformation
Nothing
0 2 4 6 8 10 12
3D 2D

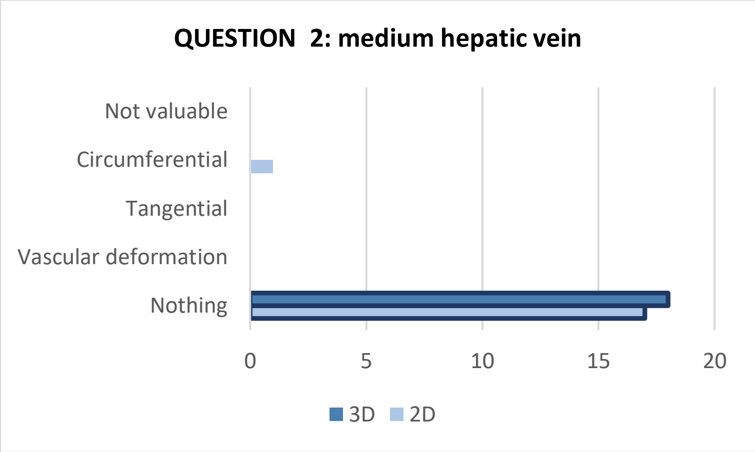
QUESTION 2: medium hepatic vein
Not valuable
Circumferential
Tangential
Vascular deformation
Nothing
0 5 10 15 20
3D 2D

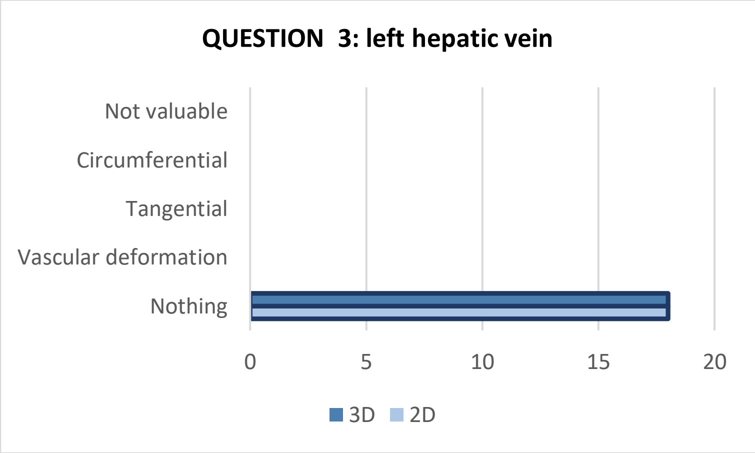
QUESTION 3: left hepatic vein
Not valuable
Circumferential
Tangential
Vascular deformation
Nothing
0 5 10 15 20
3D 2D

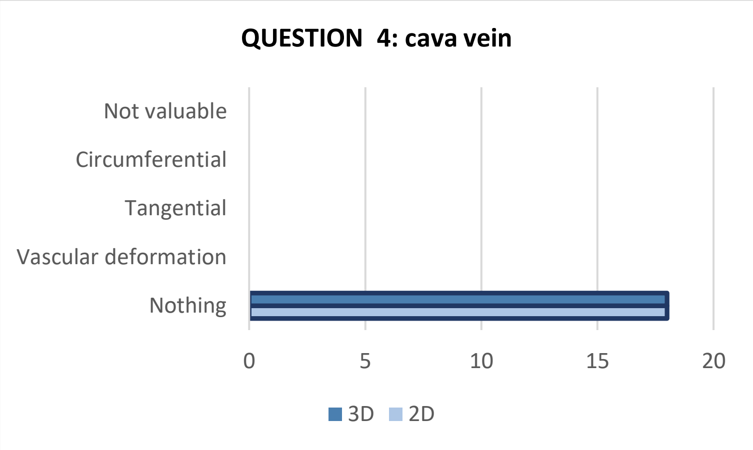
QUESTION 4: cava vein
Not valuable
Circumferential
Tangential
Vascular deformation
Nothing
0
5
10
15
20
3D
2D

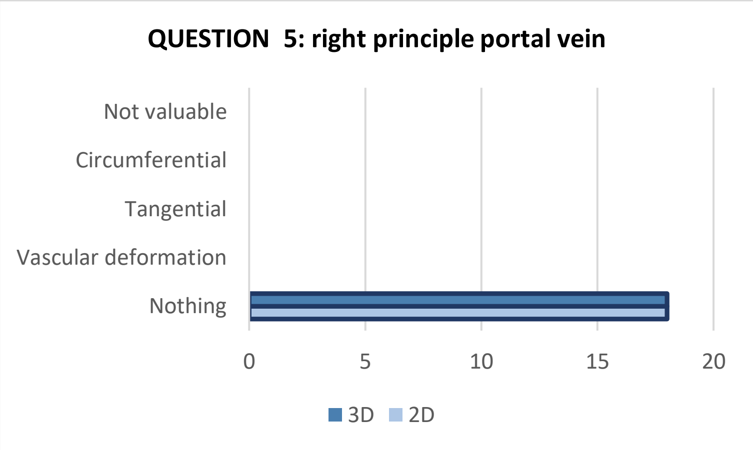
QUESTION 5: right principle portal vein
Not valuable
Circumferential
Tangential
Vascular deformation
Nothing
0
5
10
15
20
3D
2D

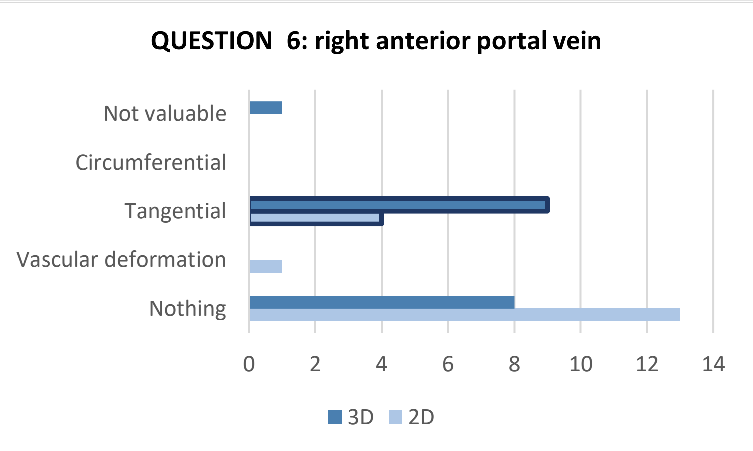
QUESTION 6: right anterior portal vein
Not valuable
Circumferential
Tangential
Vascular deformation
Nothing
0
2
4
6
8
10
12
14
3D
2D

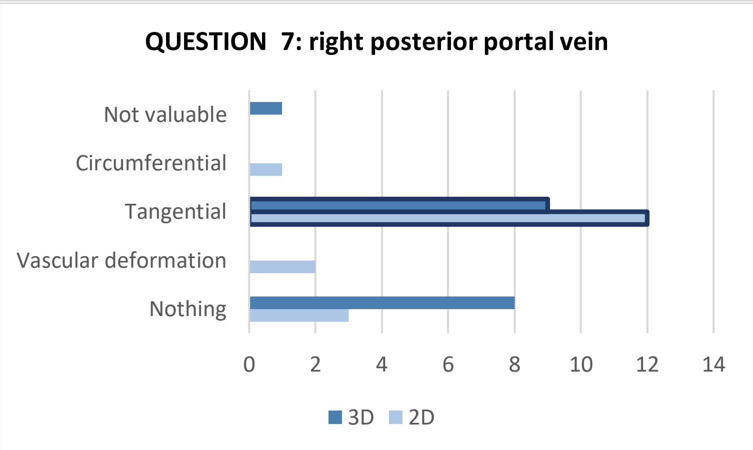
QUESTION 7: right posterior portal vein
Not valuable
Circumferential
Tangential
Vascular deformation
Nothing
0
2
4
6
8
10
12
14
3D
2D

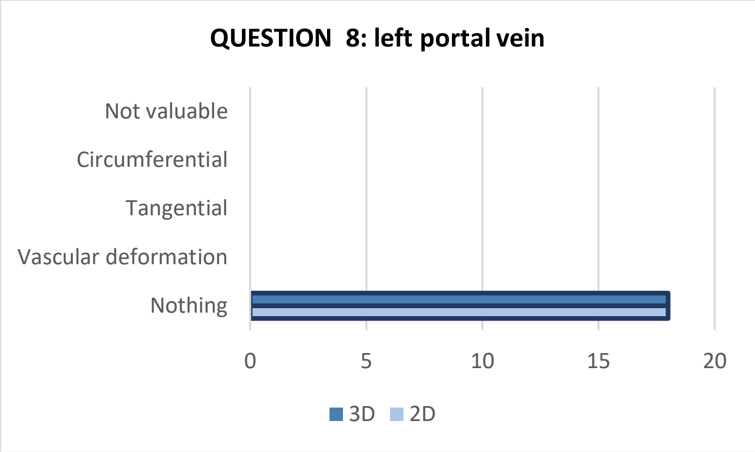
QUESTION 8: left portal vein
Not valuable
Circumferential
Tangential
Vascular deformation
Nothing
0
5
10
15
20
3D
2D

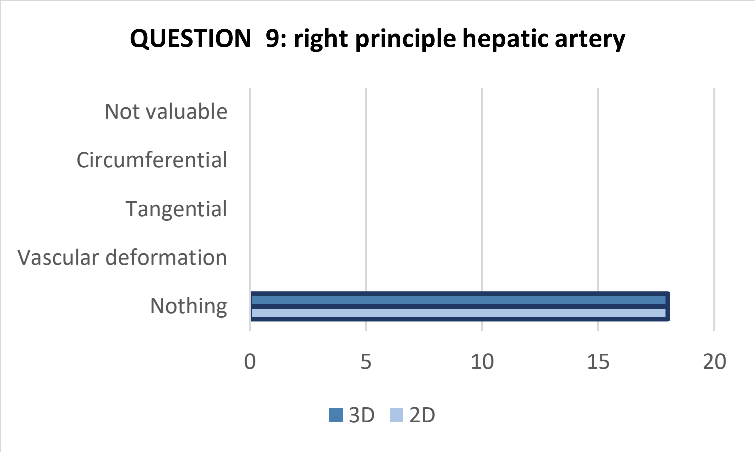
QUESTION 9: right principle hepatic artery
Not valuable
Circumferential
Tangential
Vascular deformation
Nothing
0
5
10
15
20
3D
2D

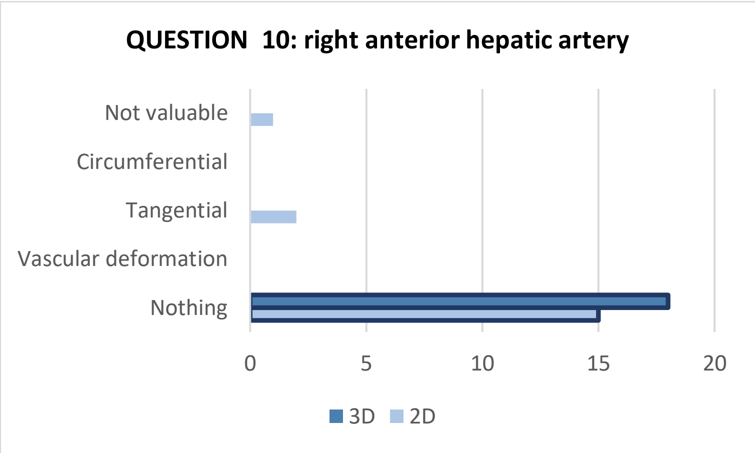
QUESTION 10: right anterior hepatic artery
Not valuable
Circumferential
Tangential
Vascular deformation
Nothing
0
5
10
15
20
3D
2D

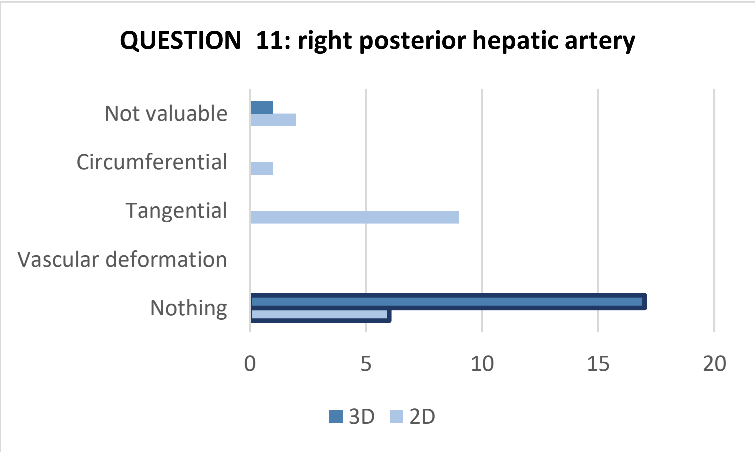
QUESTION 11: right posterior hepatic artery
Not valuable
Circumferential
Tangential
Vascular deformation
Nothing
0
5
10
15
20
3D
2D

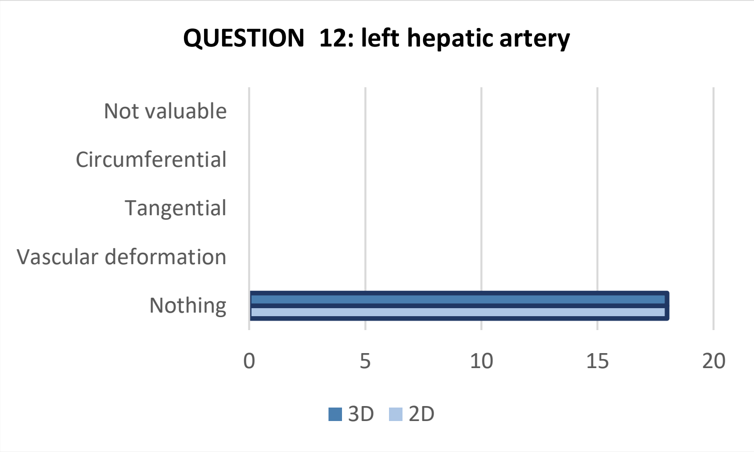
QUESTION 12: left hepatic artery
Not valuable
Circumferential
Tangential
Vascular deformation
Nothing
0
5
10
15
20
3D
2D

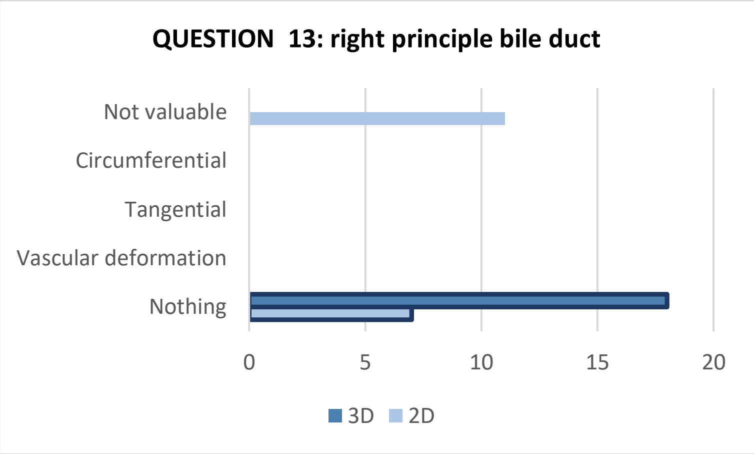
QUESTION 13: right principle bile duct
Not valuable
Circumferential
Tangential
Vascular deformation
Nothing
0
5
10
15
20
3D
2D

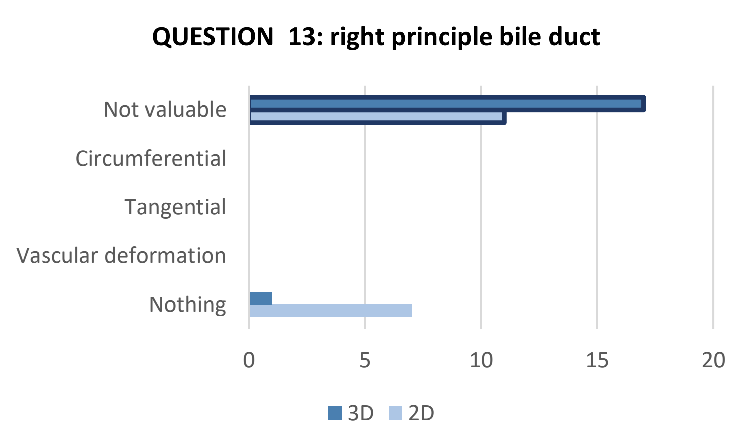
QUESTION 13: right principle bile duct
Not valuable
Circumferential
Tangential
Vascular deformation
Nothing
0
5
10
15
20
3D
2D

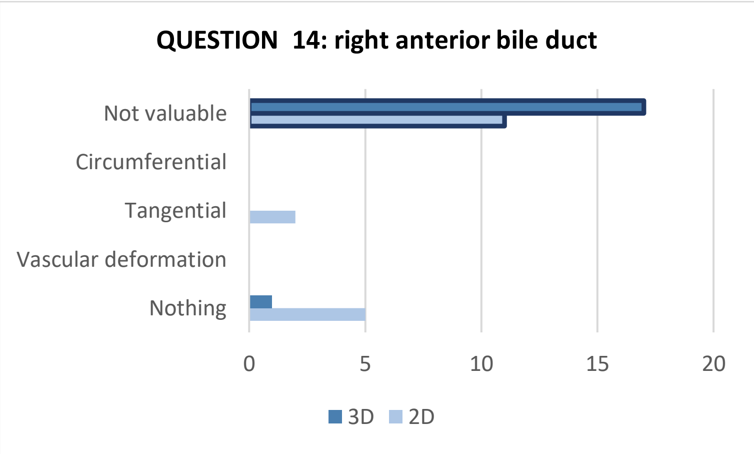
QUESTION 14: right anterior bile duct
Not valuable
Circumferential
Tangential
Vascular deformation
Nothing
0
5
10
15
20
3D
2D

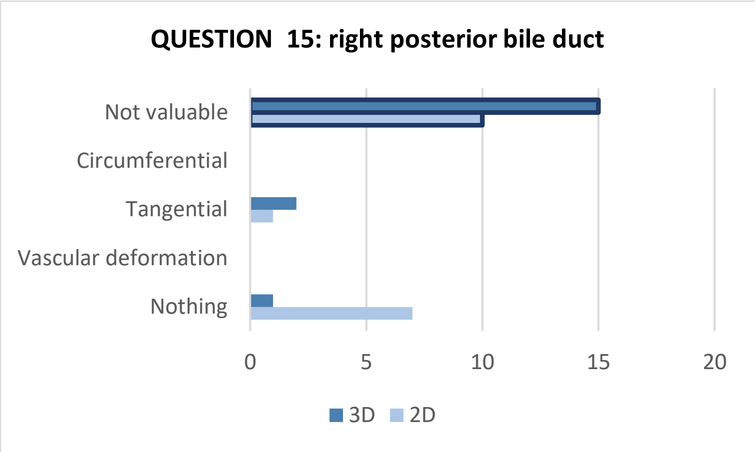
QUESTION 15: right posterior bile duct
Not valuable
Circumferential
Tangential
Vascular deformation
Nothing
0
5
10
15
20
3D
2D

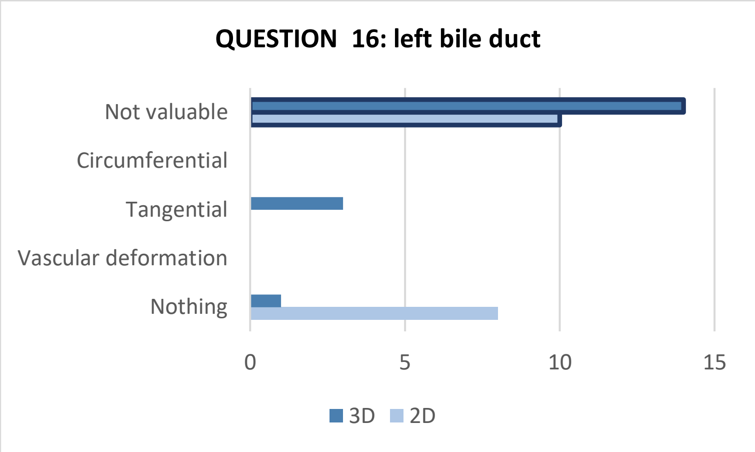
QUESTION 16: left bile duct
Not valuable
Circumferential
Tangential
Vascular deformation
Nothing
0
5
10
15
3D
2D

PATIENT 8

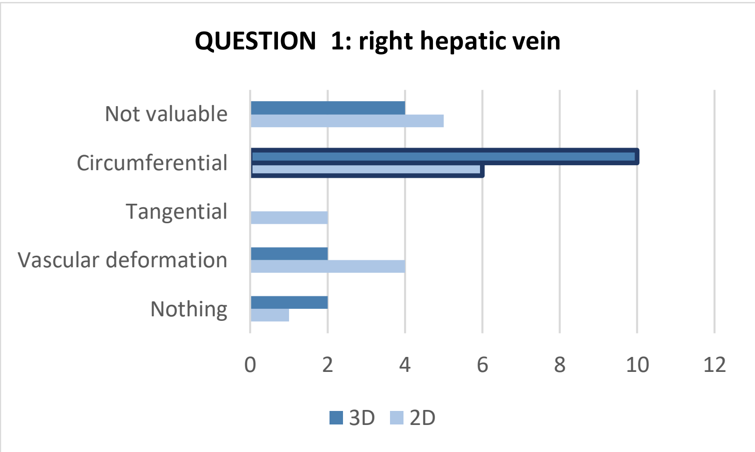
QUESTION 1: right hepatic vein
Not valuable
Circumferential
Tangential
Vascular deformation
Nothing
0
2
4
6
8
10
12
3D
2D

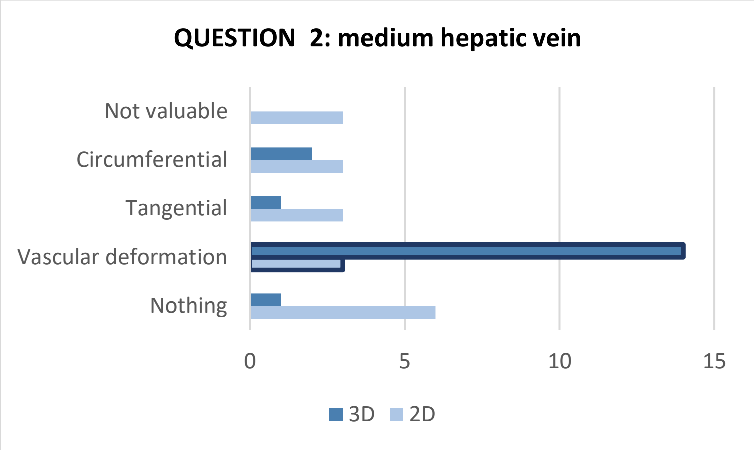
QUESTION 2: medium hepatic vein
Not valuable
Circumferential
Tangential
Vascular deformation
Nothing
0
5
10
15
3D
2D

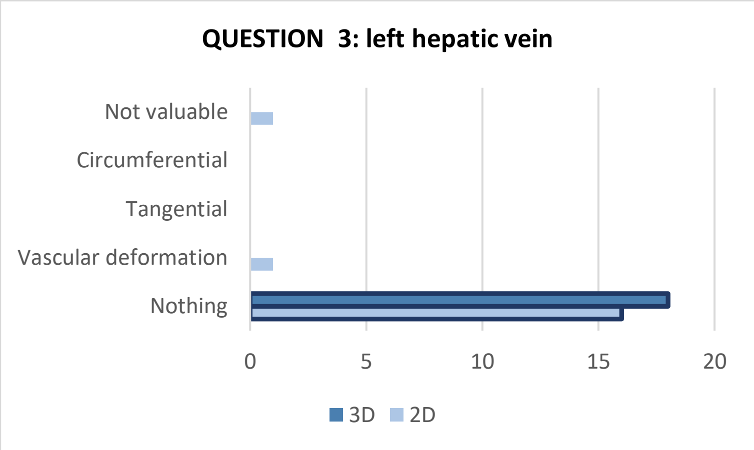
QUESTION 3: left hepatic vein
Not valuable
Circumferential
Tangential
Vascular deformation
Nothing
0
5
10
15
20
3D
2D

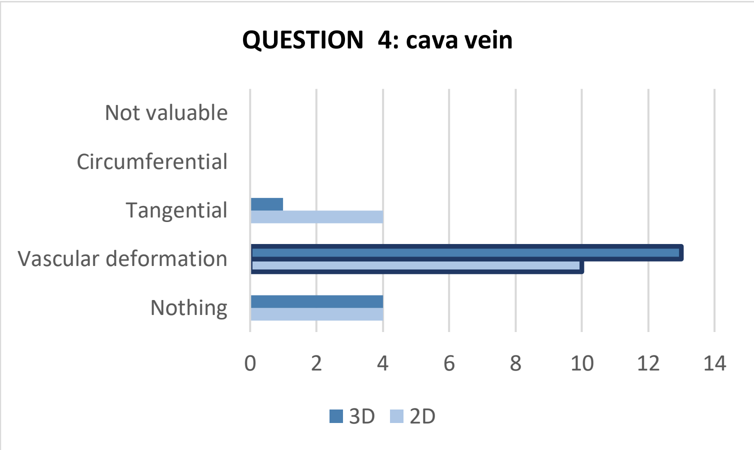
QUESTION 4: cava vein
Not valuable
Circumferential
Tangential
Vascular deformation
Nothing
0
2
4
6
8
10
12
14
3D
2D

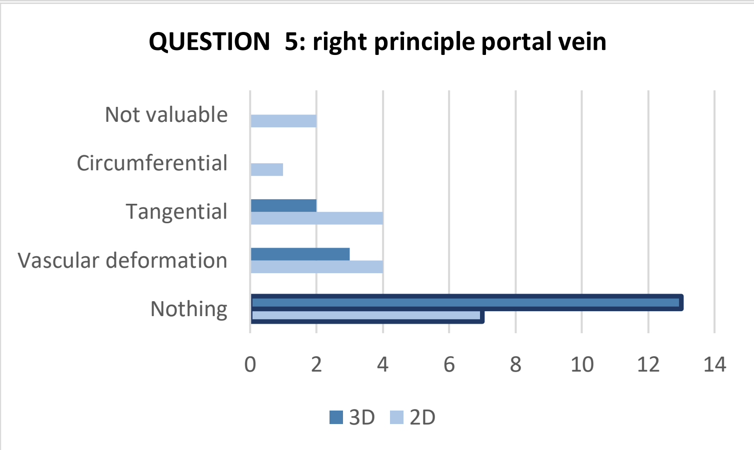
QUESTION 5: right principle portal vein
Not valuable
Circumferential
Tangential
Vascular deformation
Nothing
0
2
4
6
8
10
12
14
3D
2D

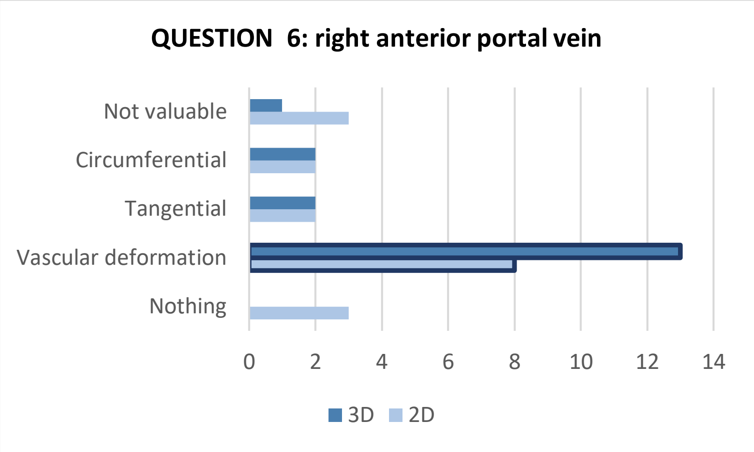
QUESTION 6: right anterior portal vein
Not valuable
Circumferential
Tangential
Vascular deformation
Nothing
0 2 4 6 8 10 12 14
3D 2D

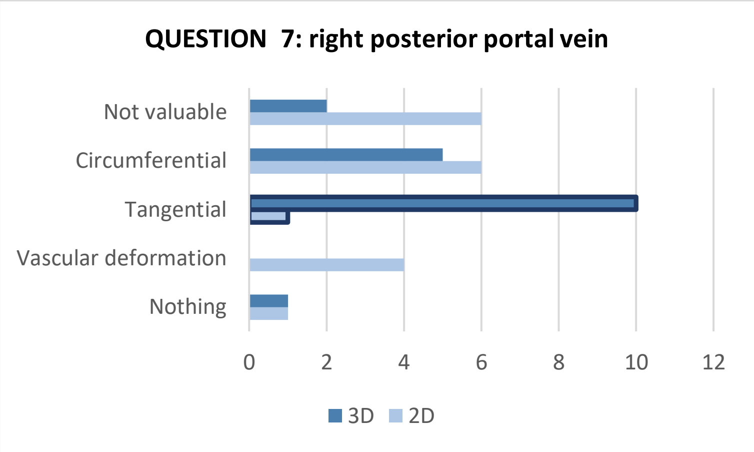
QUESTION 7: right posterior portal vein
Not valuable
Circumferential
Tangential
Vascular deformation
Nothing
0 2 4 6 8 10 12
3D 2D

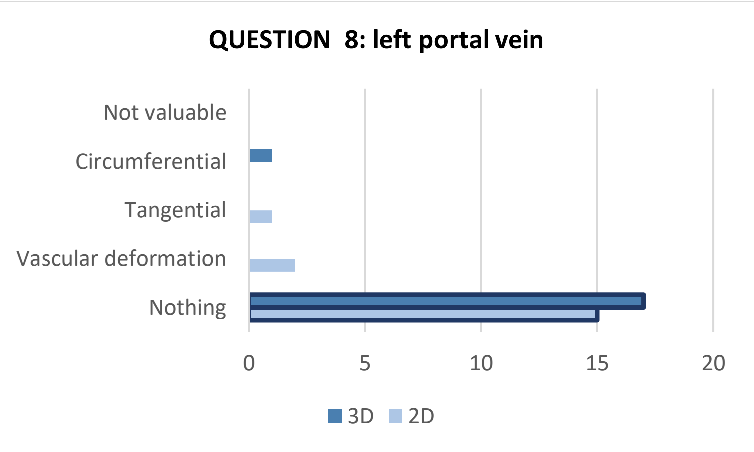
QUESTION 8: left portal vein
Not valuable
Circumferential
Tangential
Vascular deformation
Nothing
0 5 10 15 20
3D 2D

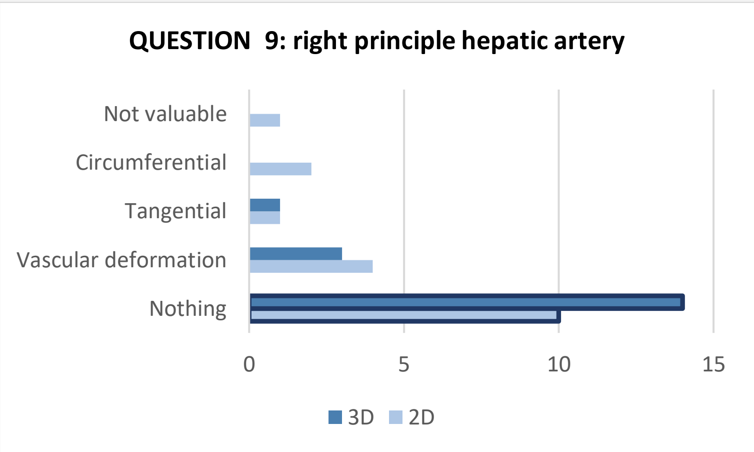
QUESTION 9: right principle hepatic artery
Not valuable
Circumferential
Tangential
Vascular deformation
Nothing
0 5 10 15
3D 2D

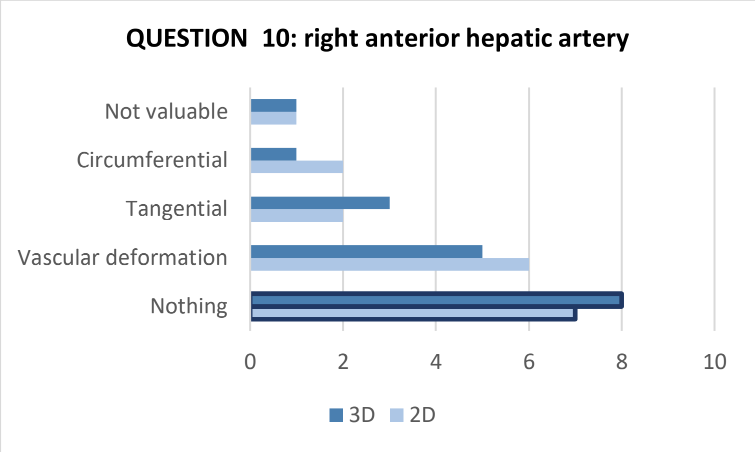
QUESTION 10: right anterior hepatic artery
Not valuable
Circumferential
Tangential
Vascular deformation
Nothing
0
2
4
6
8
10
3D
2D

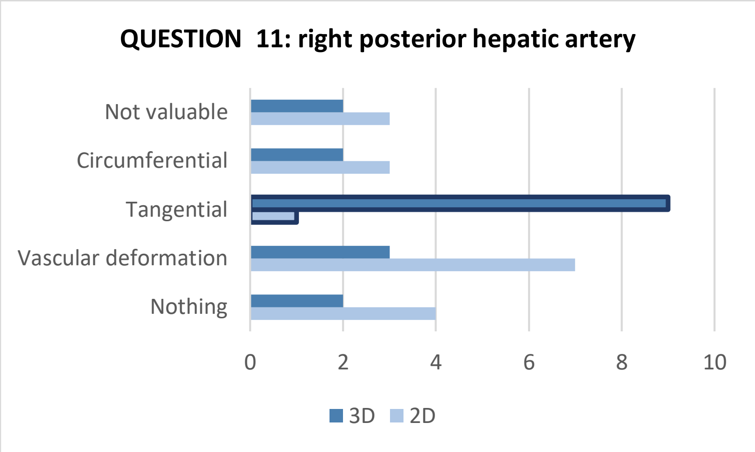
QUESTION 11: right posterior hepatic artery
Not valuable
Circumferential
Tangential
Vascular deformation
Nothing
0
2
4
6
8
10
3D
2D

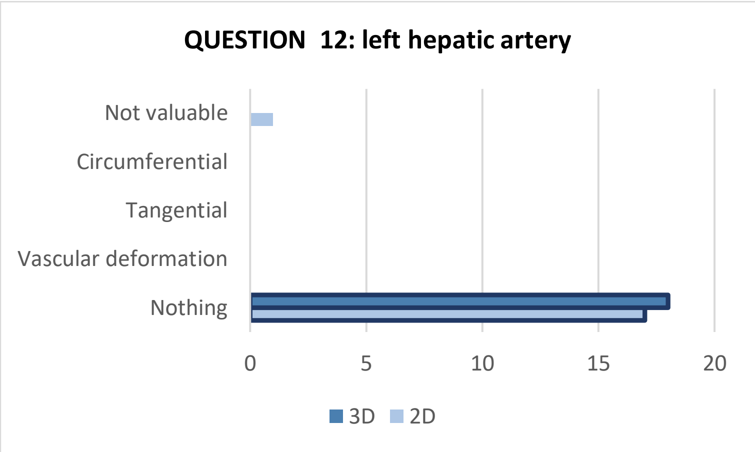
QUESTION 12: left hepatic artery
Not valuable
Circumferential
Tangential
Vascular deformation
Nothing
0
5
10
15
20
3D
2D

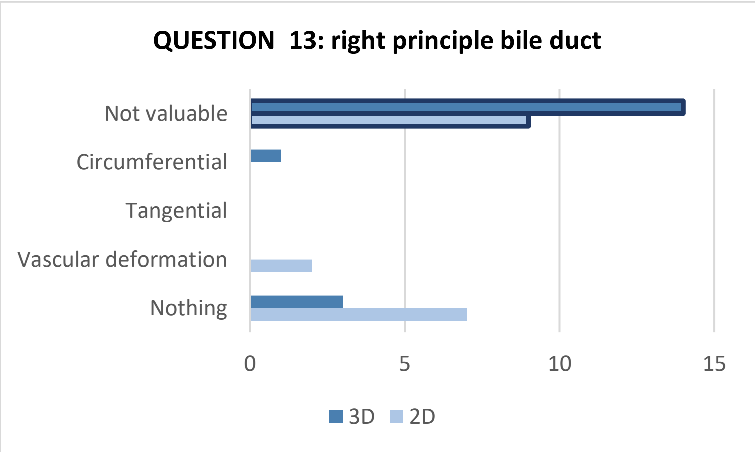
QUESTION 13: right principle bile duct
Not valuable
Circumferential
Tangential
Vascular deformation
Nothing
0
5
10
15
3D
2D

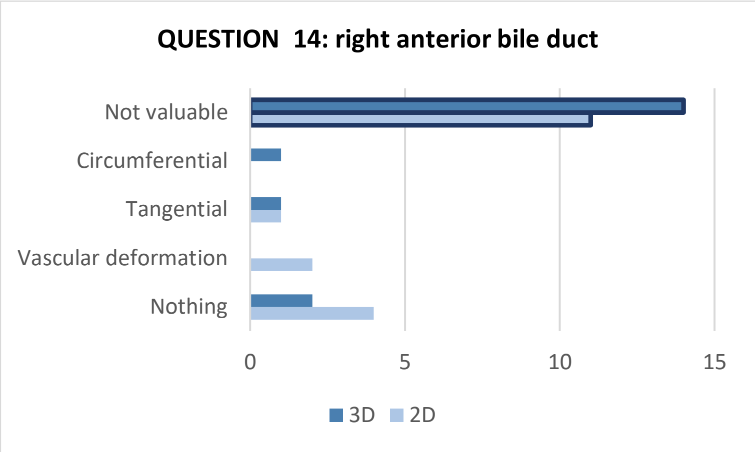
QUESTION 14: right anterior bile duct
Not valuable
Circumferential
Tangential
Vascular deformation
Nothing
0
5
10
15
3D
2D

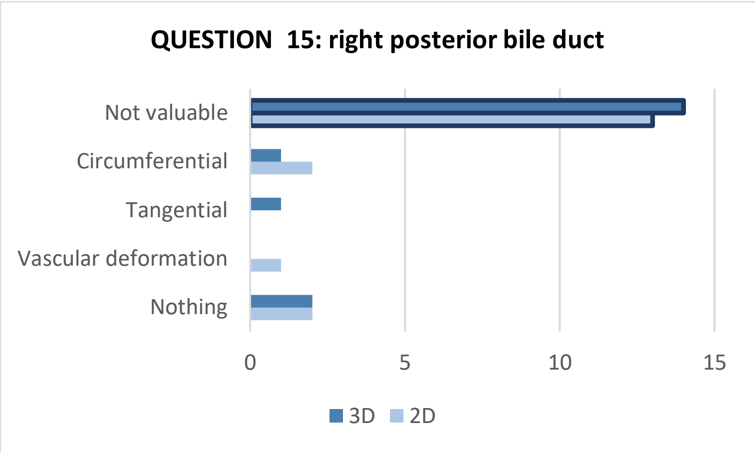
QUESTION 15: right posterior bile duct
Not valuable
Circumferential
Tangential
Vascular deformation
Nothing
0
5
10
15
3D
2D

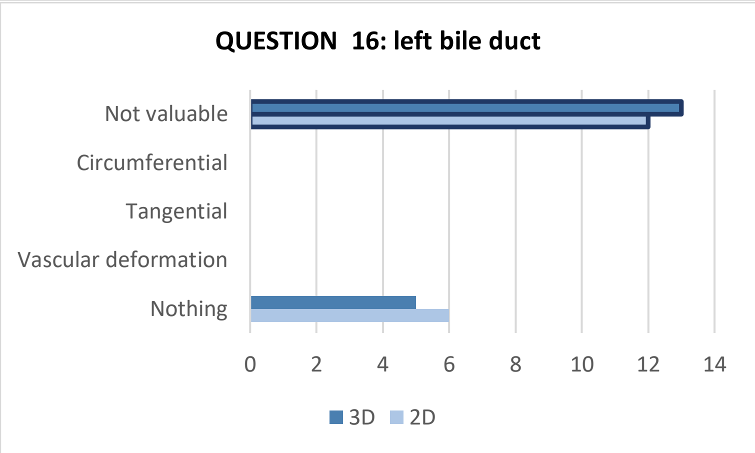
QUESTION 16: left bile duct
Not valuable
Circumferential
Tangential
Vascular deformation
Nothing
0
2
4
6
8
10
12
14
3D
2D

PATIENT 9

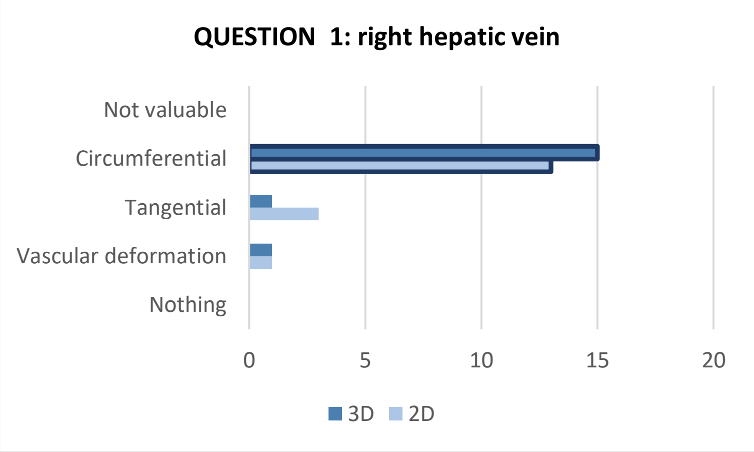
QUESTION 1: right hepatic vein
Not valuable
Circumferential
Tangential
Vascular deformation
Nothing
0
5
10
15
20
3D
2D

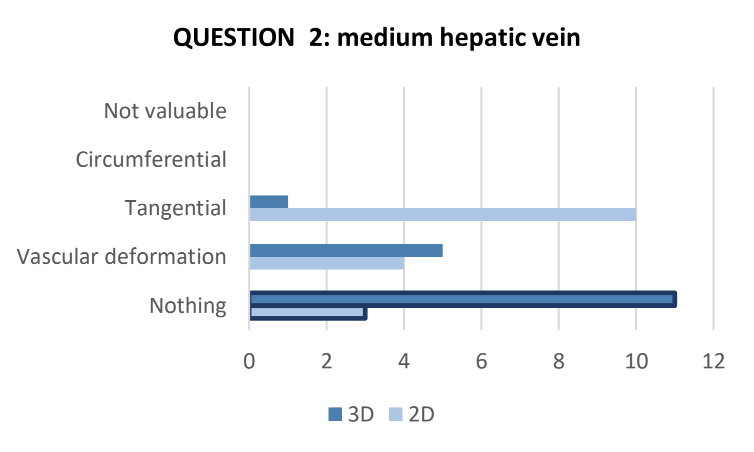
QUESTION 2: medium hepatic vein
Not valuable
Circumferential
Tangential
Vascular deformation
Nothing
0
2
4
6
8
10
12
3D
2D

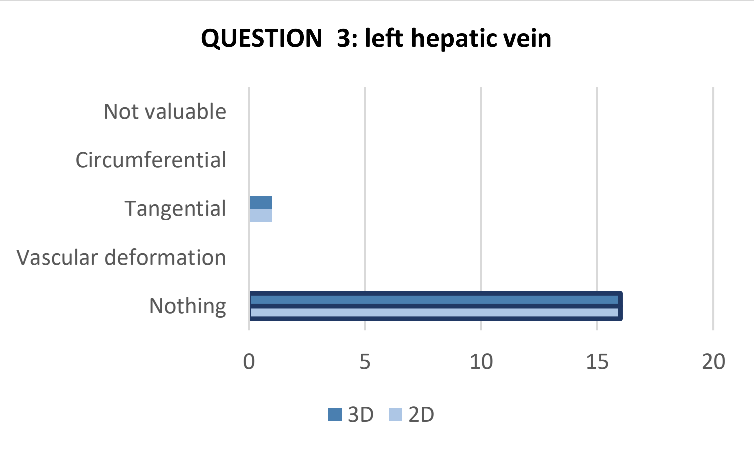
QUESTION 3: left hepatic vein
Not valuable
Circumferential
Tangential
Vascular deformation
Nothing
0
5
10
15
20
3D
2D

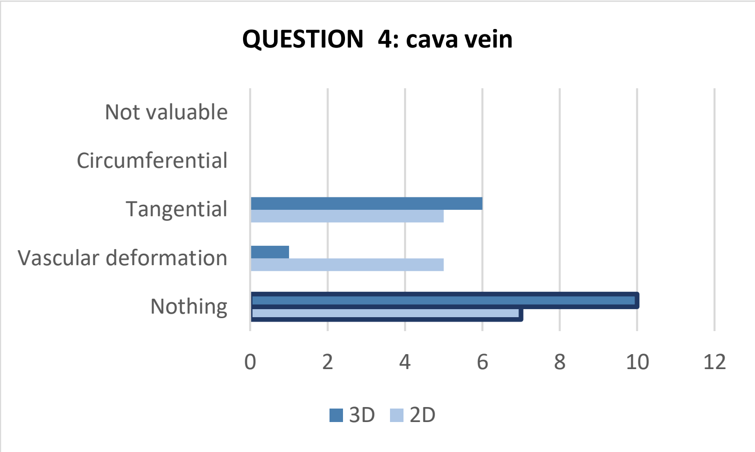
QUESTION 4: cava vein
Not valuable
Circumferential
Tangential
Vascular deformation
Nothing
0
2
4
6
8
10
12
3D
2D

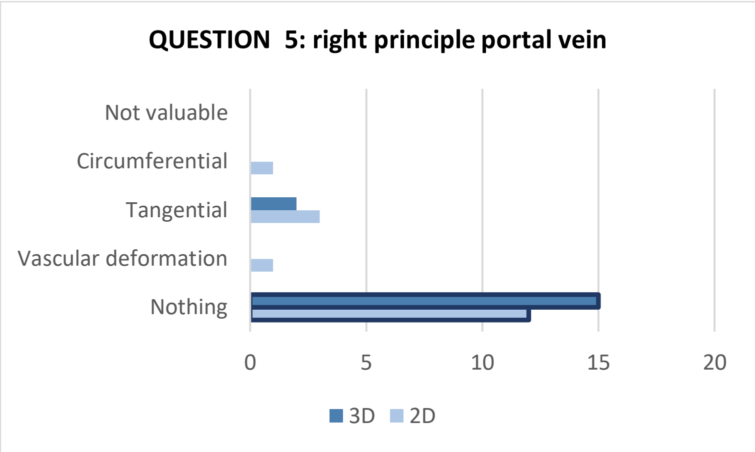
QUESTION 5: right principle portal vein
Not valuable
Circumferential
Tangential
Vascular deformation
Nothing
0
5
10
15
20
3D
2D

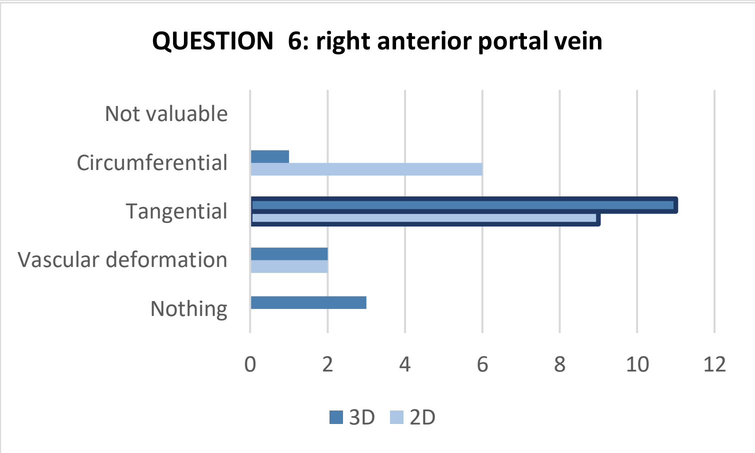
QUESTION 6: right anterior portal vein
Not valuable
Circumferential
Tangential
Vascular deformation
Nothing
0
2
4
6
8
10
12
3D
2D

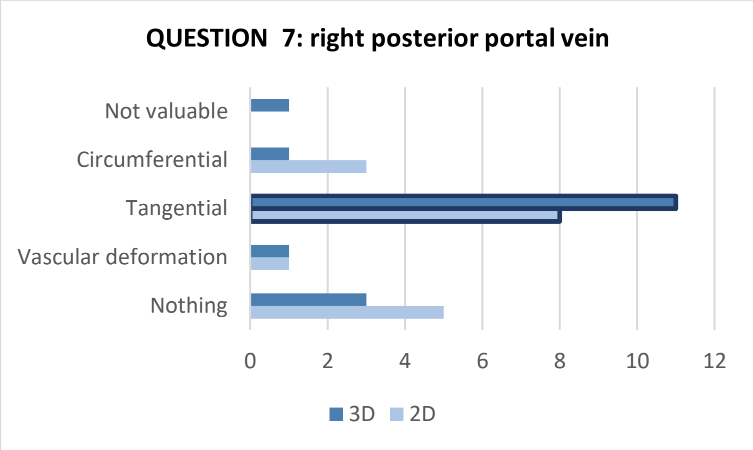
QUESTION 7: right posterior portal vein
Not valuable
Circumferential
Tangential
Vascular deformation
Nothing
0
2
4
6
8
10
12
3D
2D

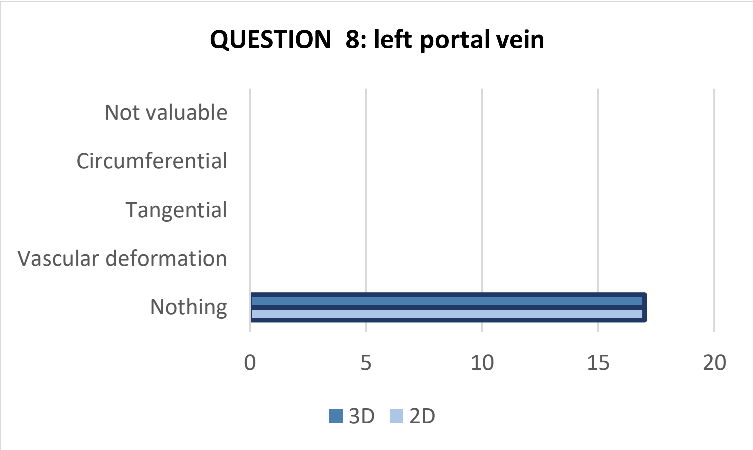
QUESTION 8: left portal vein
Not valuable
Circumferential
Tangential
Vascular deformation
Nothing
0
5
10
15
20
3D
2D

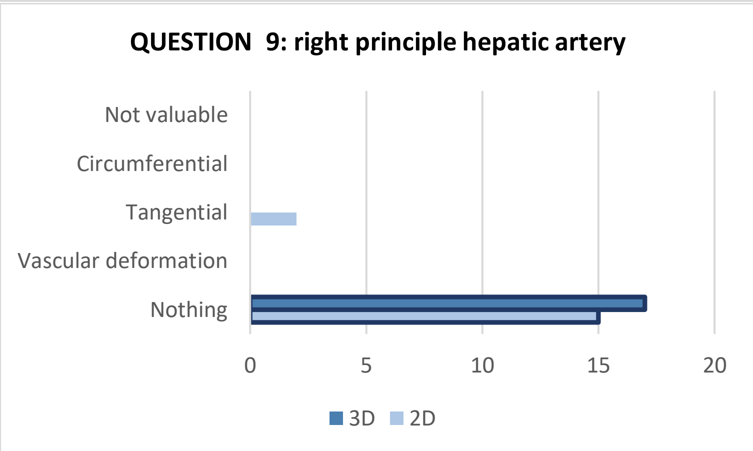
QUESTION 9: right principle hepatic artery
Not valuable
Circumferential
Tangential
Vascular deformation
Nothing
0
5
10
15
20
3D
2D

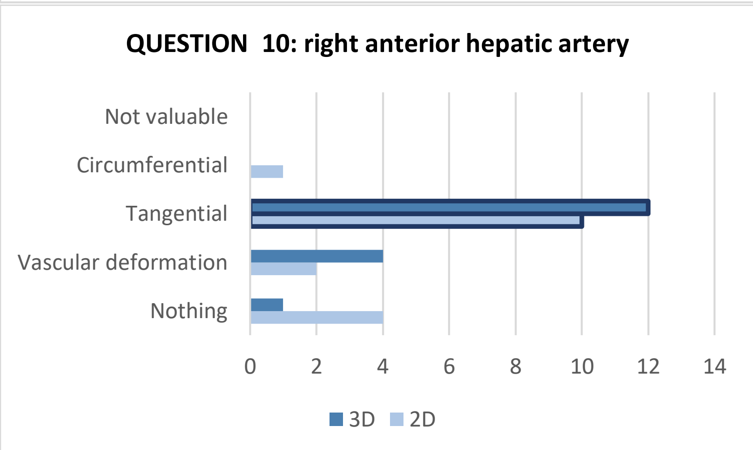
QUESTION 10: right anterior hepatic artery
Not valuable
Circumferential
Tangential
Vascular deformation
Nothing
0
2
4
6
8
10
12
14
3D
2D

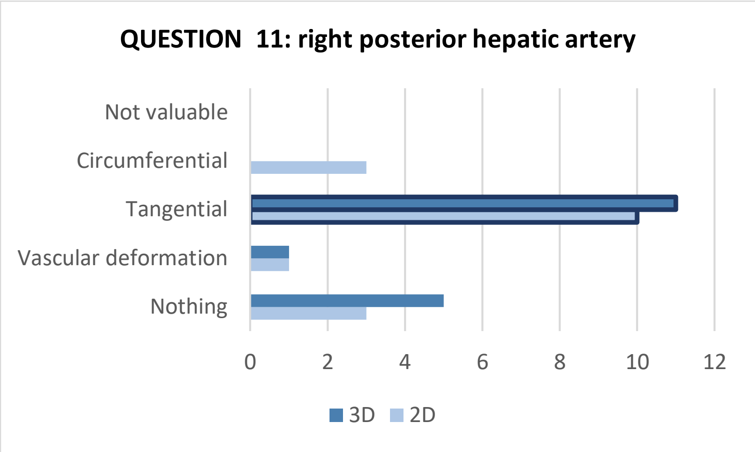
QUESTION 11: right posterior hepatic artery
Not valuable
Circumferential
Tangential
Vascular deformation
Nothing
0
2
4
6
8
10
12
3D
2D

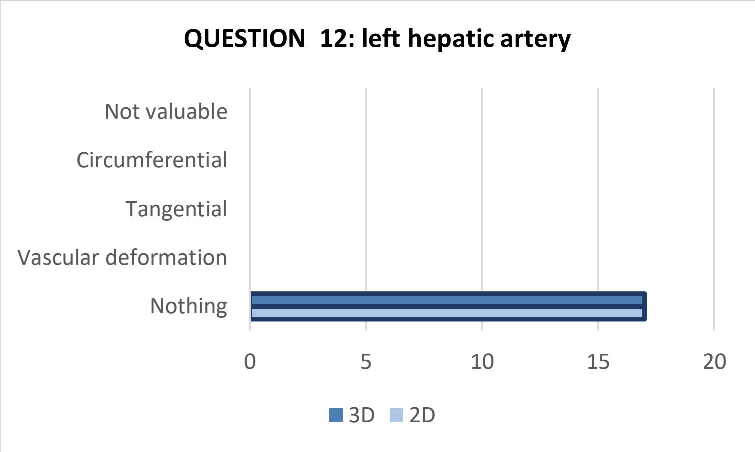
QUESTION 12: left hepatic artery
Not valuable
Circumferential
Tangential
Vascular deformation
Nothing
0
5
10
15
20
3D
2D

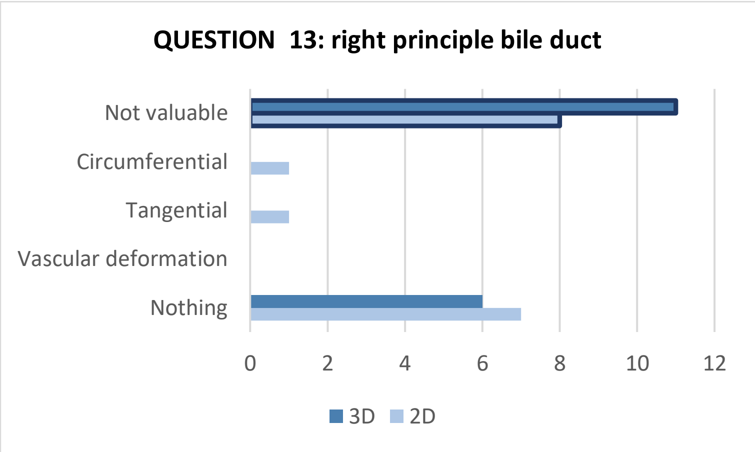
QUESTION 13: right principle bile duct
Not valuable
Circumferential
Tangential
Vascular deformation
Nothing
0
2
4
6
8
10
12
3D
2D

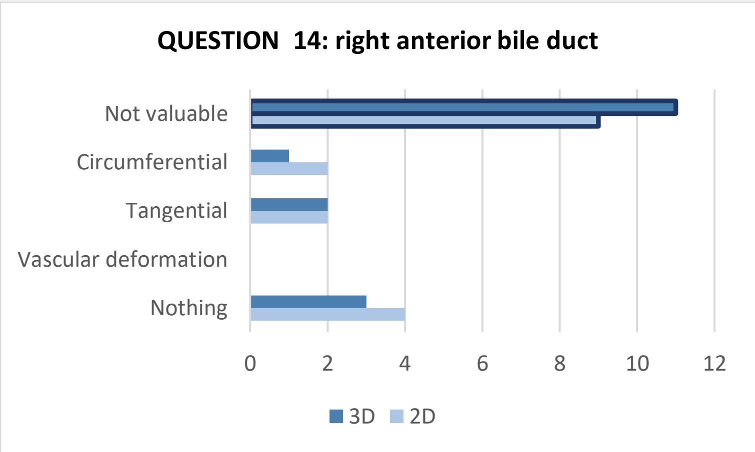
QUESTION 14: right anterior bile duct
Not valuable
Circumferential
Tangential
Vascular deformation
Nothing
0
2
4
6
8
10
12
3D
2D

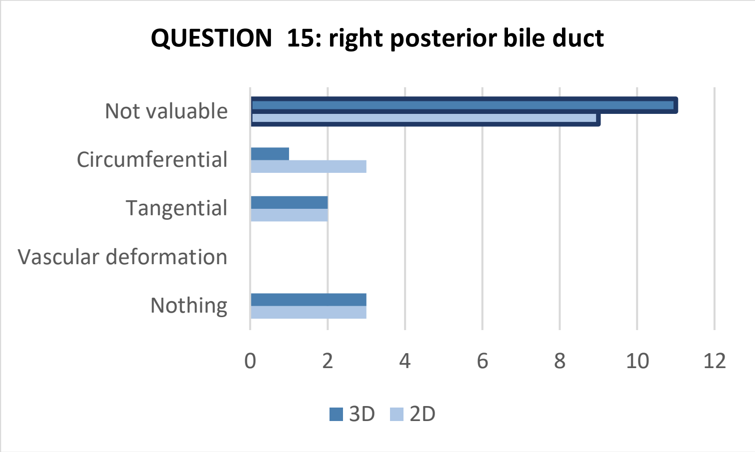
QUESTION 15: right posterior bile duct
Not valuable
Circumferential
Tangential
Vascular deformation
Nothing
0
2
4
6
8
10
12
3D
2D

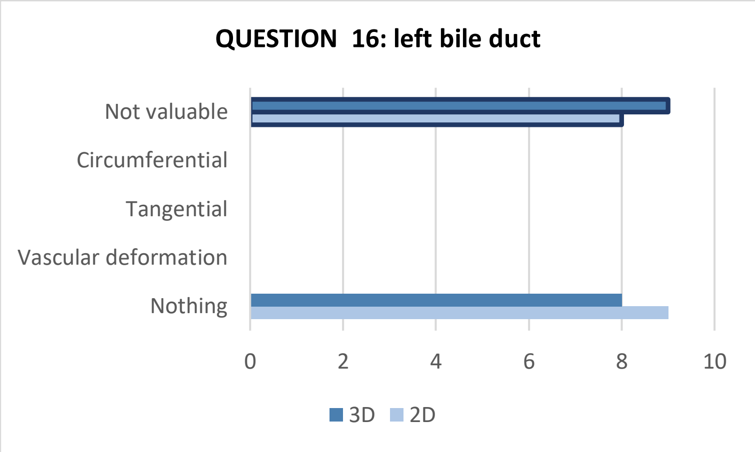
QUESTION 16: left bile duct
Not valuable
Circumferential
Tangential
Vascular deformation
Nothing
0
2
4
6
8
10
3D
2D

PATIENT 10

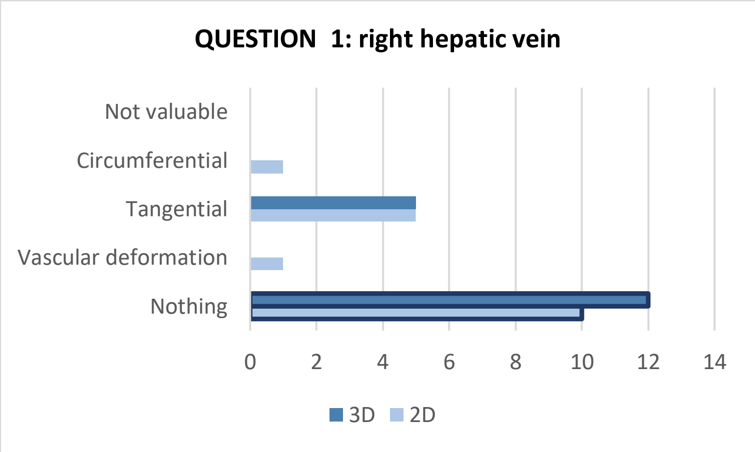
QUESTION 1: right hepatic vein
Not valuable
Circumferential
Tangential
Vascular deformation
Nothing
0
2
4
6
8
10
12
14
3D
2D

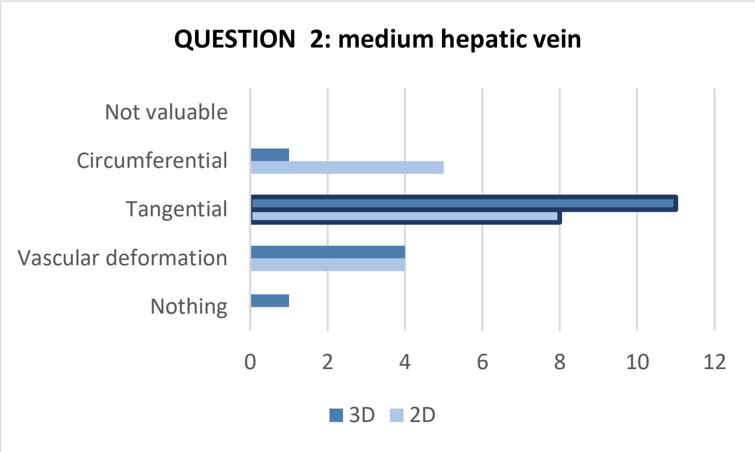
QUESTION 2: medium hepatic vein
Not valuable
Circumferential
Tangential
Vascular deformation
Nothing
0 2 4 6 8 10 12
3D 2D

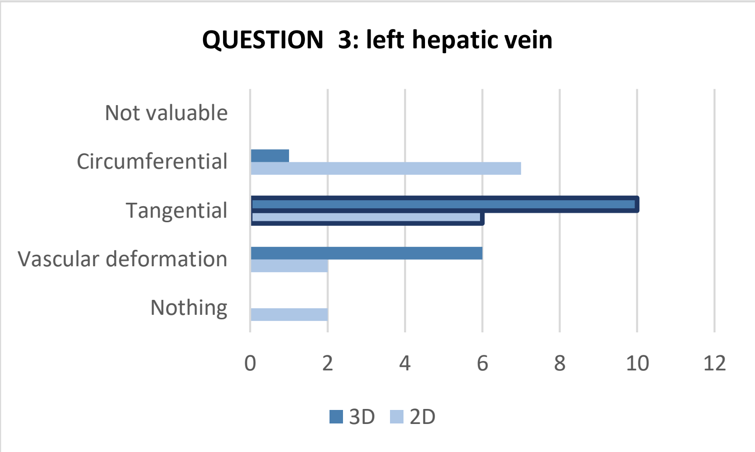
QUESTION 3: left hepatic vein
Not valuable
Circumferential
Tangential
Vascular deformation
Nothing
0 2 4 6 8 10 12
3D 2D

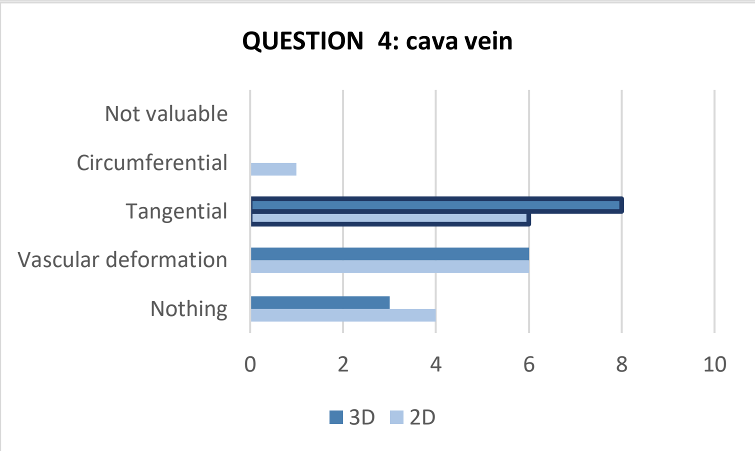
QUESTION 4: cava vein
Not valuable
Circumferential
Tangential
Vascular deformation
Nothing
0 2 4 6 8 10
3D 2D

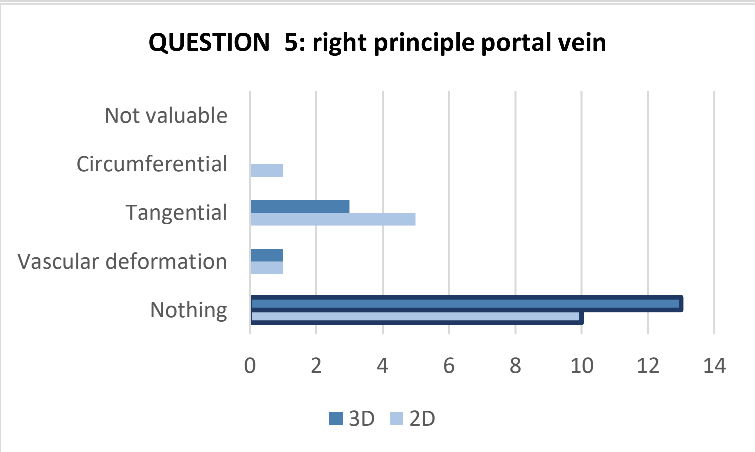
QUESTION 5: right principle portal vein
Not valuable
Circumferential
Tangential
Vascular deformation
Nothing
0 2 4 6 8 10 12 14
3D 2D

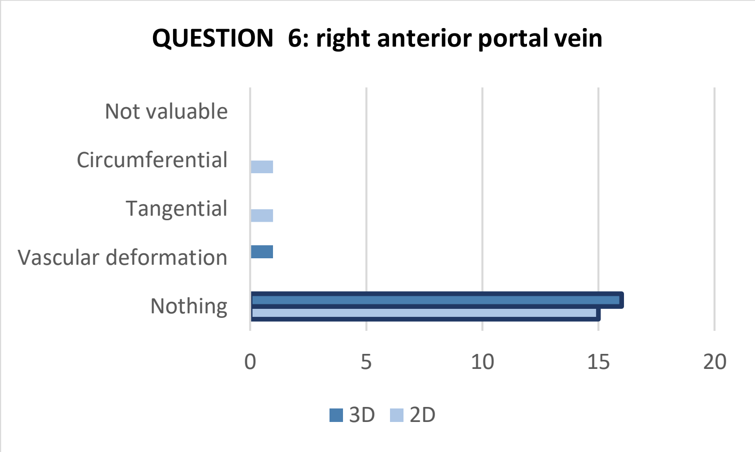
QUESTION 6: right anterior portal vein
Not valuable
Circumferential
Tangential
Vascular deformation
Nothing
0
5
10
15
20
3D
2D

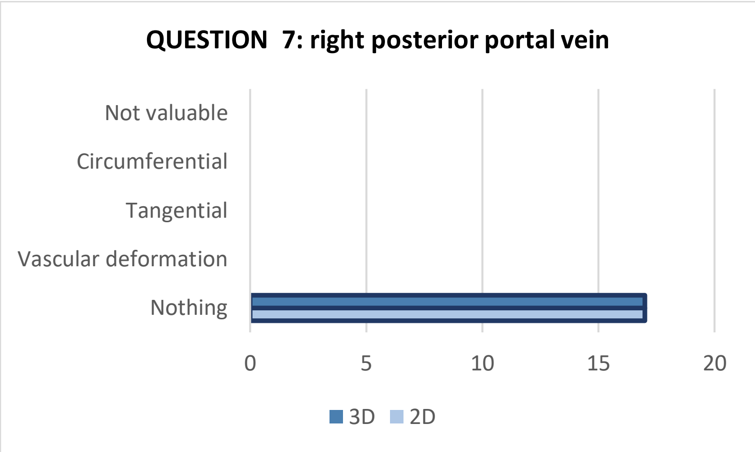
QUESTION 7: right posterior portal vein
Not valuable
Circumferential
Tangential
Vascular deformation
Nothing
0
5
10
15
20
3D
2D

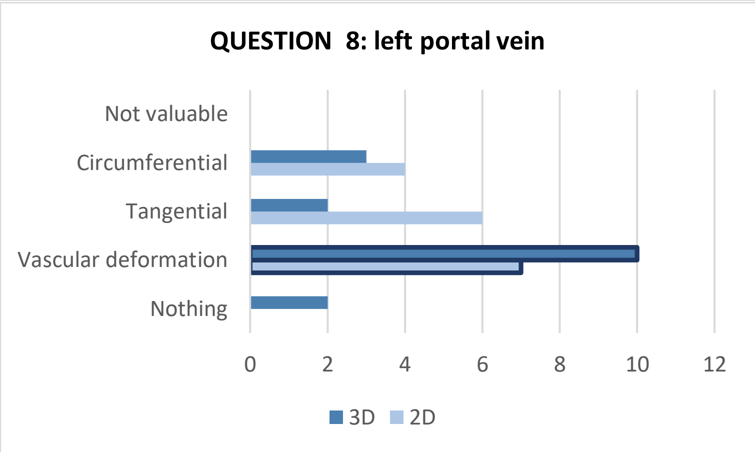
QUESTION 8: left portal vein
Not valuable
Circumferential
Tangential
Vascular deformation
Nothing
0
2
4
6
8
10
12
3D
2D

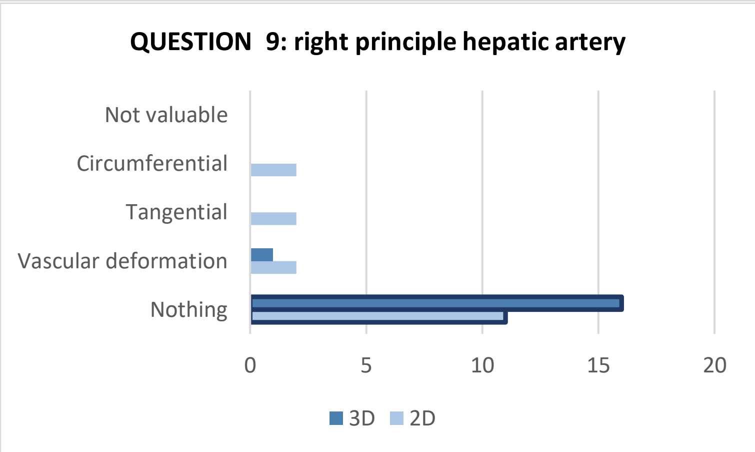
QUESTION 9: right principle hepatic artery
Not valuable
Circumferential
Tangential
Vascular deformation
Nothing
0
5
10
15
20
3D
2D

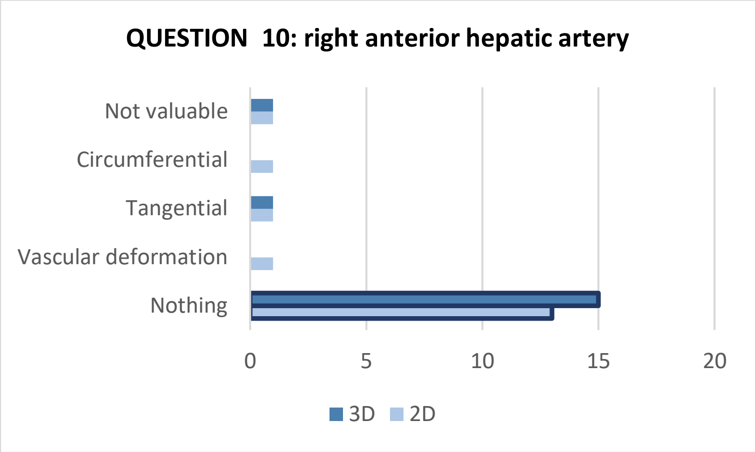
QUESTION 10: right anterior hepatic artery
Not valuable
Circumferential
Tangential
Vascular deformation
Nothing
0
5
10
15
20
3D
2D

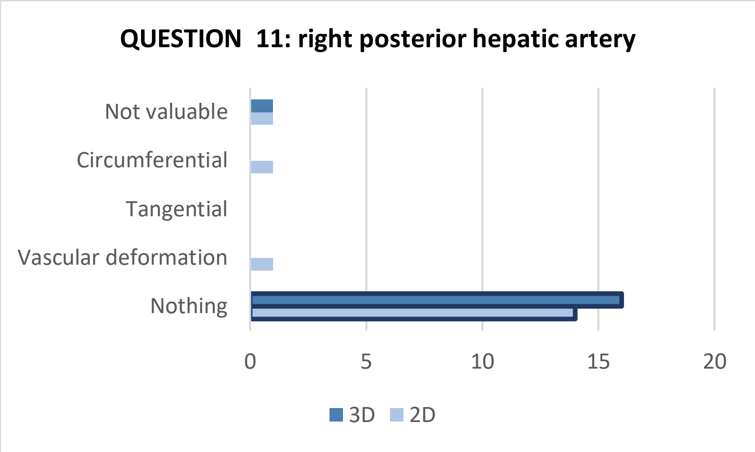
QUESTION 11: right posterior hepatic artery
Not valuable
Circumferential
Tangential
Vascular deformation
Nothing
0
5
10
15
20
3D
2D

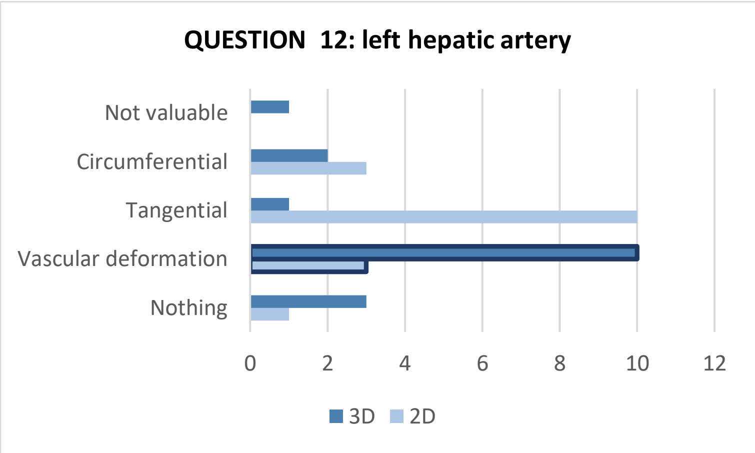
QUESTION 12: left hepatic artery
Not valuable
Circumferential
Tangential
Vascular deformation
Nothing
0
2
4
6
8
10
12
3D
2D

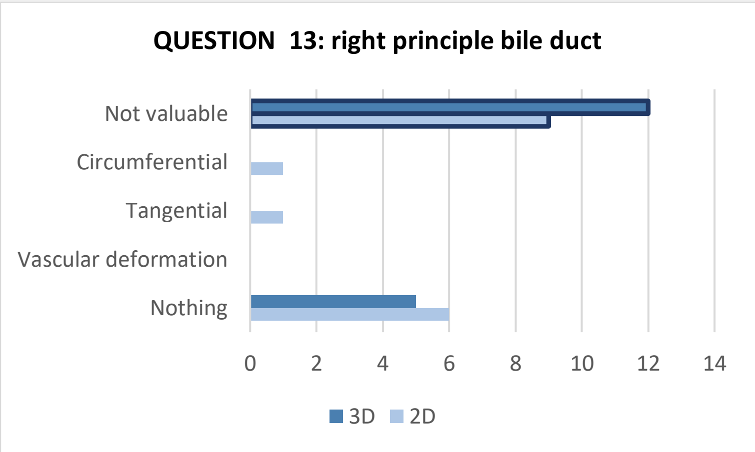
QUESTION 13: right principle bile duct
Not valuable
Circumferential
Tangential
Vascular deformation
Nothing
0
2
4
6
8
10
12
14
3D
2D

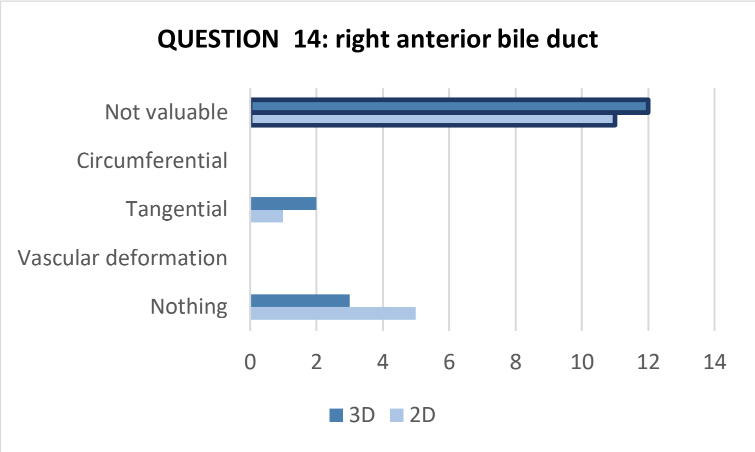
QUESTION 14: right anterior bile duct
Not valuable
Circumferential
Tangential
Vascular deformation
Nothing
0 2 4 6 8 10 12 14
3D 2D

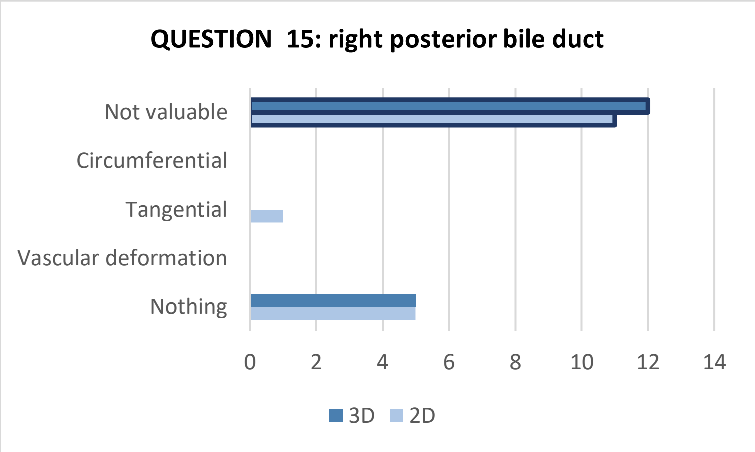
QUESTION 15: right posterior bile duct
Not valuable
Circumferential
Tangential
Vascular deformation
Nothing
0 2 4 6 8 10 12 14
3D 2D

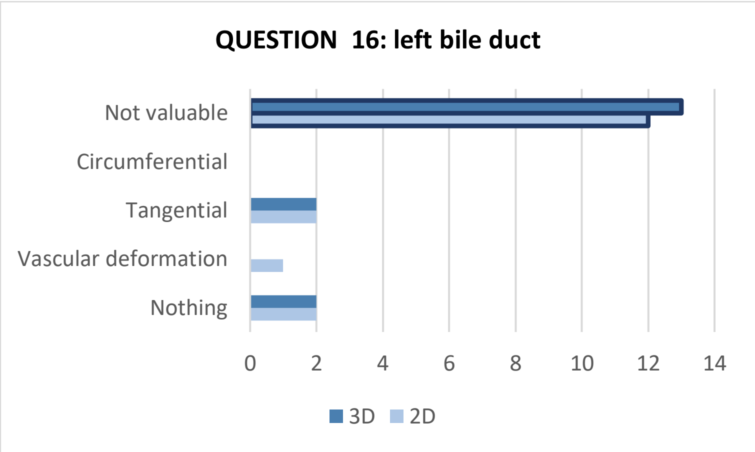
QUESTION 16: left bile duct
Not valuable
Circumferential
Tangential
Vascular deformation
Nothing
0 2 4 6 8 10 12 14
3D 2D

PATIENT 11

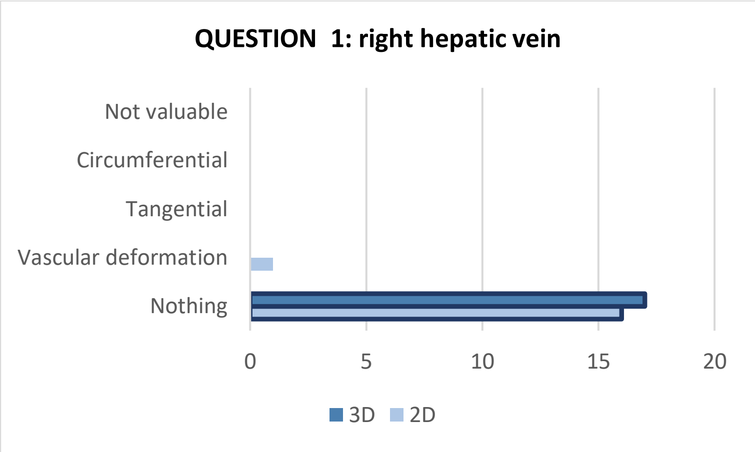
QUESTION 1: right hepatic vein
Not valuable
Circumferential
Tangential
Vascular deformation
Nothing
0
5
10
15
20
3D
2D

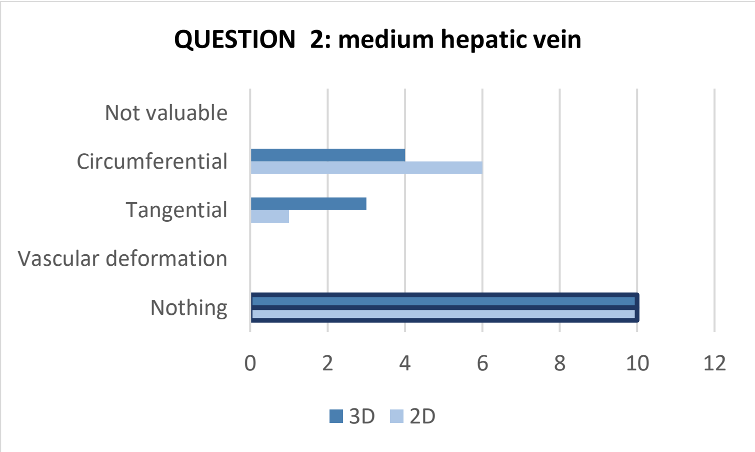
QUESTION 2: medium hepatic vein
Not valuable
Circumferential
Tangential
Vascular deformation
Nothing
0
2
4
6
8
10
12
3D
2D

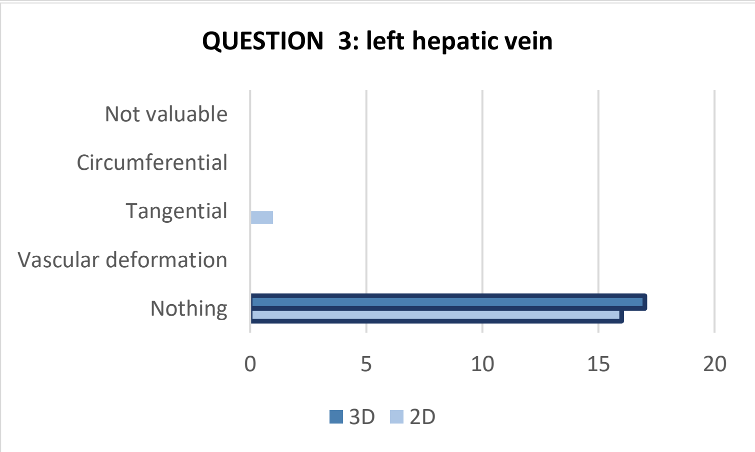
QUESTION 3: left hepatic vein
Not valuable
Circumferential
Tangential
Vascular deformation
Nothing
0
5
10
15
20
3D
2D

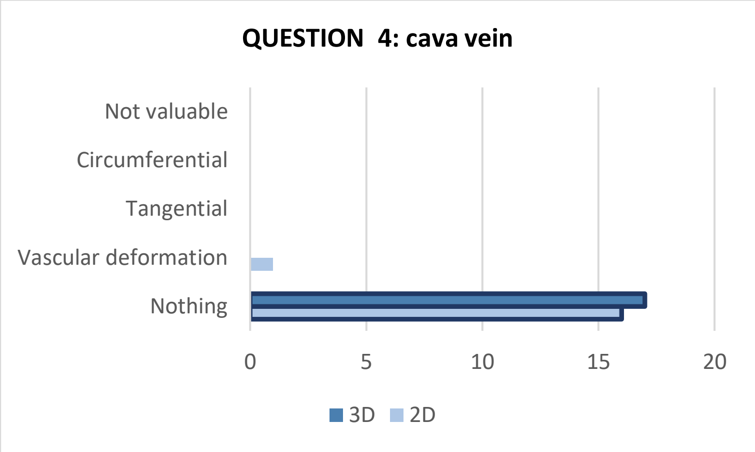
QUESTION 4: cava vein
Not valuable
Circumferential
Tangential
Vascular deformation
Nothing
0
5
10
15
20
3D
2D

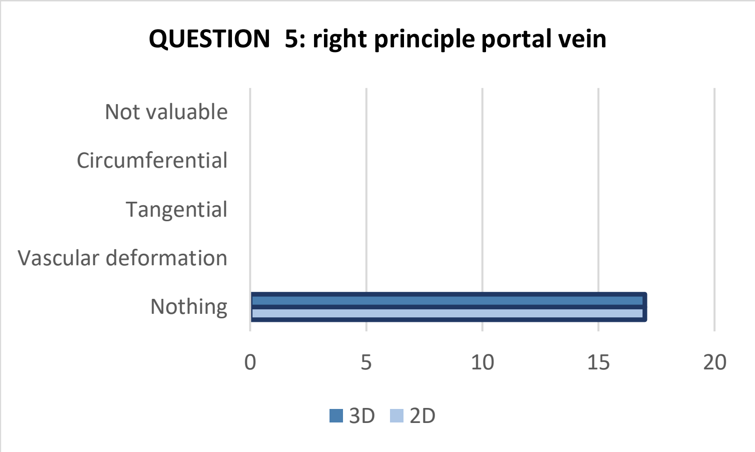
QUESTION 5: right principle portal vein
Not valuable
Circumferential
Tangential
Vascular deformation
Nothing
0
5
10
15
20
3D
2D

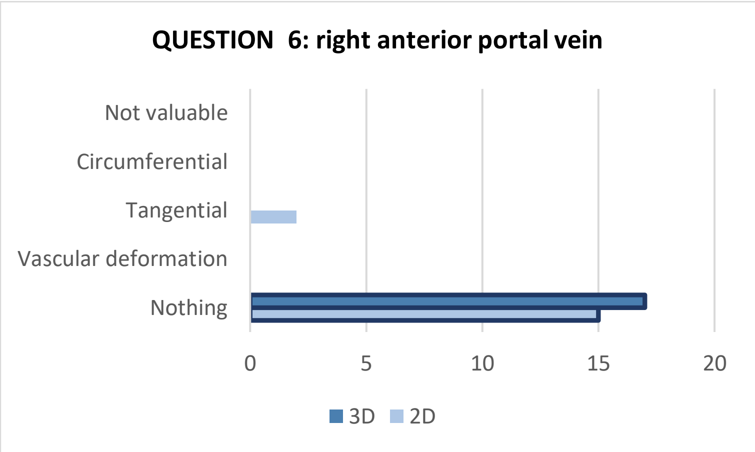
QUESTION 6: right anterior portal vein
Not valuable
Circumferential
Tangential
Vascular deformation
Nothing
0
5
10
15
20
3D
2D

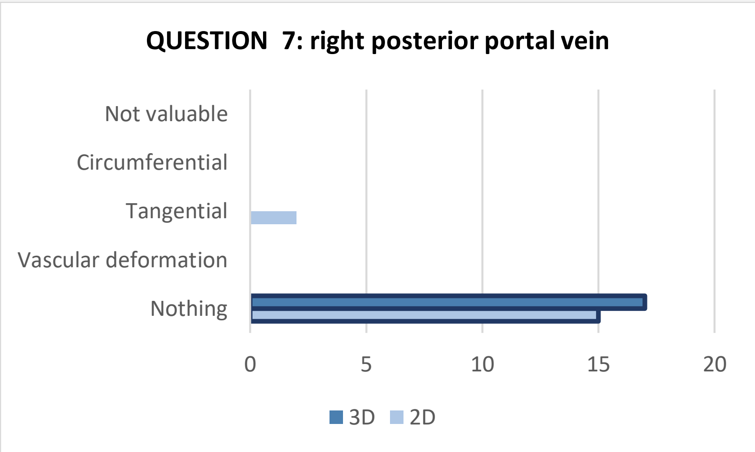
QUESTION 7: right posterior portal vein
Not valuable
Circumferential
Tangential
Vascular deformation
Nothing
0
5
10
15
20
3D
2D

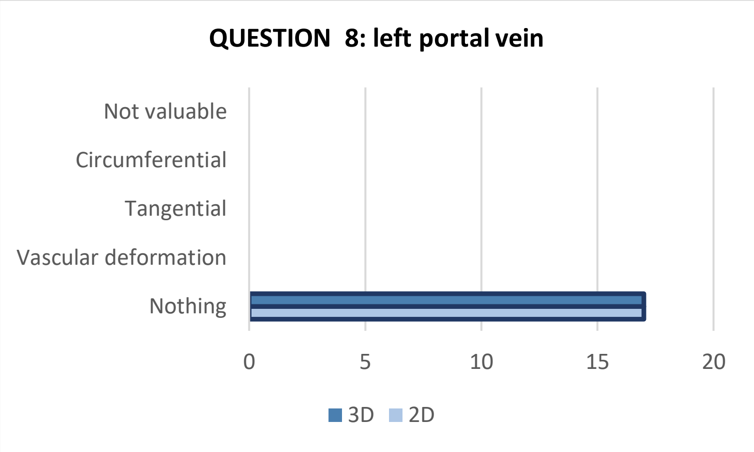
QUESTION 8: left portal vein
Not valuable
Circumferential
Tangential
Vascular deformation
Nothing
0
5
10
15
20
3D
2D

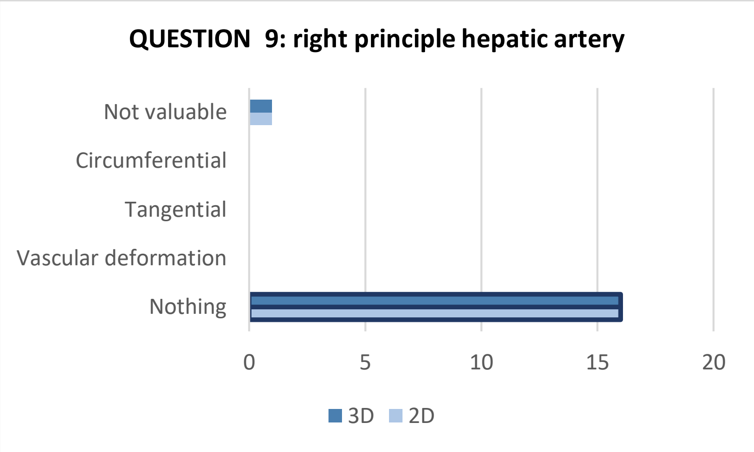
QUESTION 9: right principle hepatic artery
Not valuable
Circumferential
Tangential
Vascular deformation
Nothing
0
5
10
15
20
3D
2D

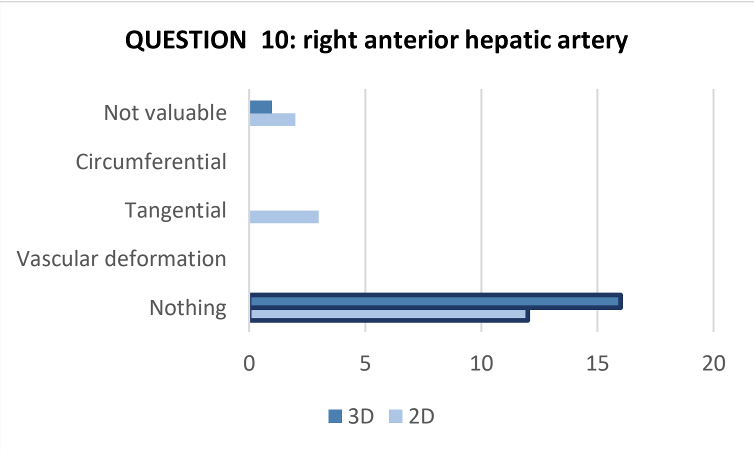
QUESTION 10: right anterior hepatic artery
Not valuable
Circumferential
Tangential
Vascular deformation
Nothing
0
5
10
15
20
3D
2D

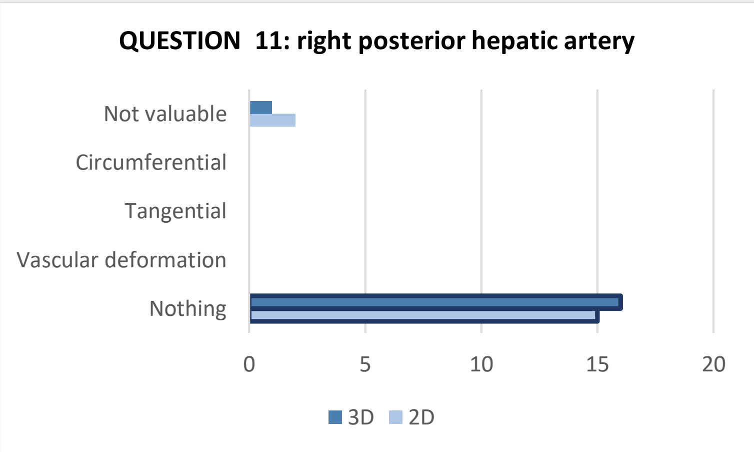
QUESTION 11: right posterior hepatic artery
Not valuable
Circumferential
Tangential
Vascular deformation
Nothing
0
5
10
15
20
3D
2D

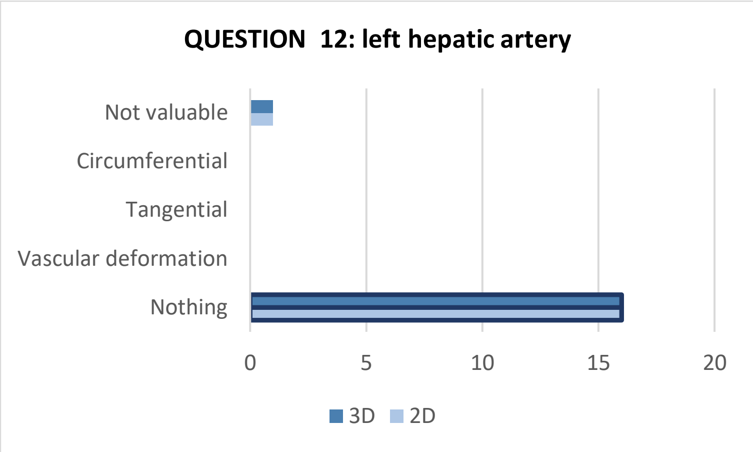
QUESTION 12: left hepatic artery
Not valuable
Circumferential
Tangential
Vascular deformation
Nothing
0
5
10
15
20
3D
2D

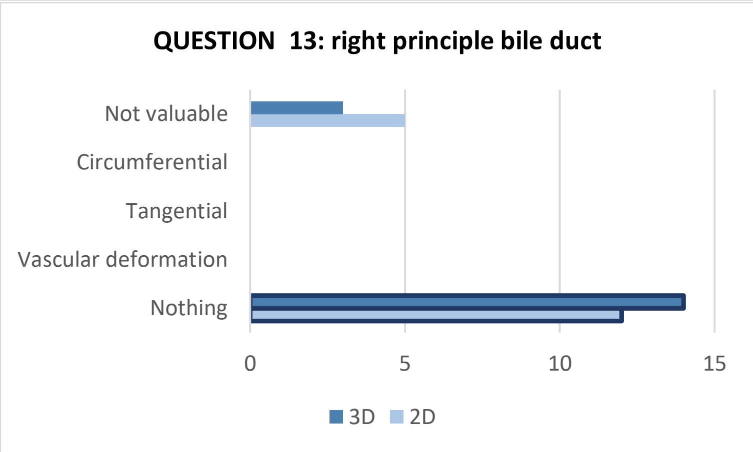
QUESTION 13: right principle bile duct
Not valuable
Circumferential
Tangential
Vascular deformation
Nothing
0
5
10
15
3D
2D

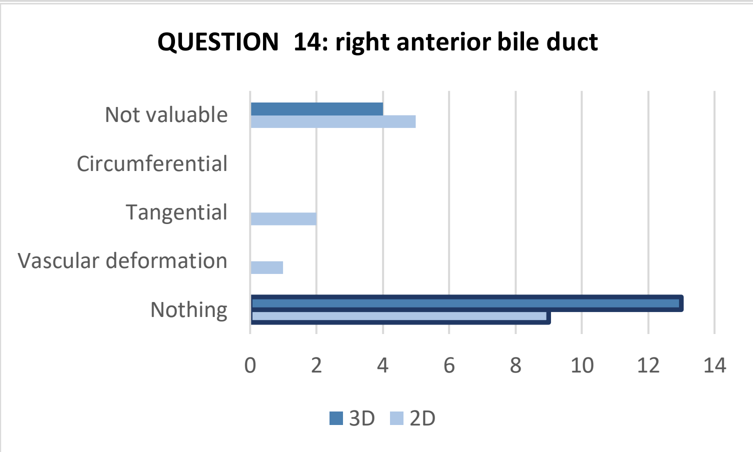
QUESTION 14: right anterior bile duct
Not valuable
Circumferential
Tangential
Vascular deformation
Nothing
0
2
4
6
8
10
12
14
3D
2D

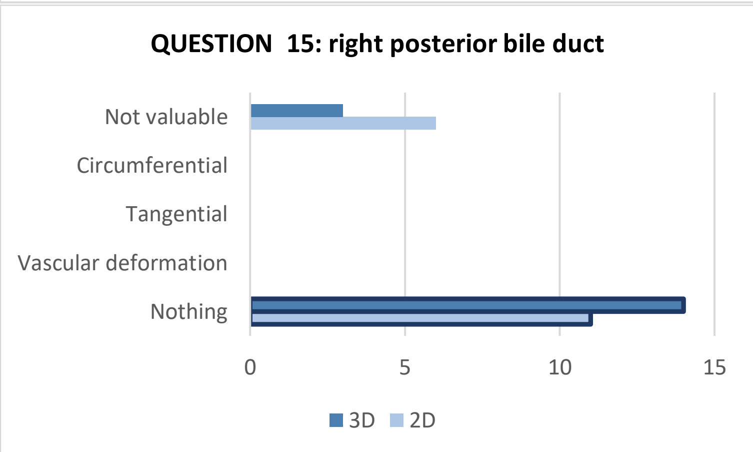
QUESTION 15: right posterior bile duct
Not valuable
Circumferential
Tangential
Vascular deformation
Nothing
0
5
10
15
3D
2D

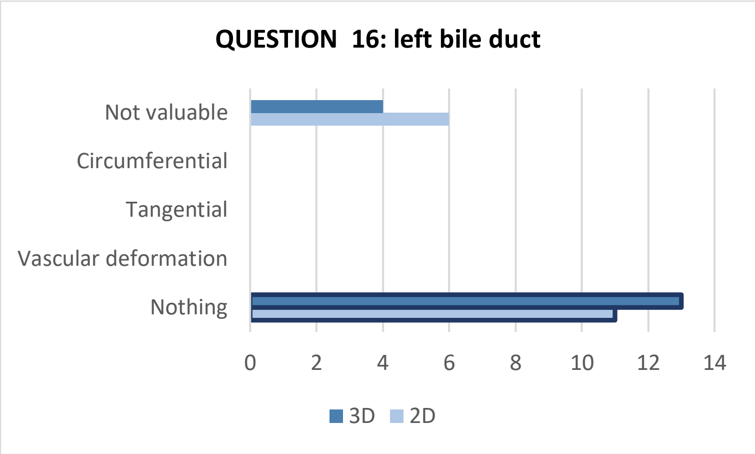
QUESTION 16: left bile duct
Not valuable
Circumferential
Tangential
Vascular deformation
Nothing
0
2
4
6
8
10
12
14
3D
2D

List of Figures

List of Tables

List of symbols

CT: computed tomography
MRI: magnetic resonance imaging
HBP: hepato-bilio-pancreatic
HTA: health technology assessment
EUnetHTA: European Network for HTA
AGENAS: *Agenzia Nazionale per i Servizi Regionali*
NAFLD: non-alcoholic fatty liver disease
HCC: hepato-cellular carcinoma
AJCC: American Joint Committee on Cancer
UICC: International Union Against Cancer
CCA: cholangiocarcinoma
IH-CCA: intrahepatic cholangiocarcinoma
EH-CCA: extrahepatic cholangiocarcinoma
CVC: central venous catheter
NGT: nose-gastric tube
PTBD: percutaneous transhepatic biliary drainage
WHO: world health organization
HAV: human hepatitis a virus
HBV: human hepatitis b virus
HCV: human hepatitis c virus
SEIEVA*: Sistema Epidemiologico Integrato dell'Epatite Virale Acuta*
ALD: alcoholic liver disease
AIRTUM: *Associazione Italiana Registri Tumori*
CAS: computer aided surgery
IRCAD: *Institut de Recherche Contre le Cancers de l'Appareil Digestif*
AIMS: Minimally Invasive Surgery Association
GDPR: General Data Protection Regulation
CAGR: compound annual growth rate
FLRV: future liver remnant volume
BMI: body mass index
EHR: electronic health record
ASA: American society of Anesthesiologists
DB: diabetes mellitus
HTN: hypertension
COPD: chronic obstructive disease
ESRD: end stage renal disease
MI: myocardial infraction
CVA: cerebrovascular infraction
TIA: transient ischemic attack
CAD: coronary artery disease.

HGB: hemoglobulin
INR: international normalized ratio
AST: aspartate transferase
ALT: alanine transferase
CA: antigen carbohydrate
CEA: carcinoembryonic antigen
AFP: alpha fetoprotein
ICO: Information Commissioner's Officer
3DVQS: 3D visualization quality score
IQR: interquartile range
QoL: quality of life
QALYs: quality adjusted life years
CMA: cost minimization analysis
CEA: cost-effectiveness analysis
CUA: cost-utility analysis
CBA: cost-benefit analysis
BIA: budget-impacts analysis
DRG: diagnosis related group
AR: augmented reality
MR: mixed reality
VR: virtual reality

Ringraziamenti

Il primo ringraziamento va alla prof. ssa Veronica Cimolin e all'ing. Daniela Motta per avermi guidato con preziosi consigli e supervisionato nella stesura della tesi. Grazie per aver risposto ad ogni mia richiesta con grande disponibilità e tempestività, lasciandomi la giusta autonomia e libertà d'espressione.

Un sentito grazie al dott. Christian Cotsoglou per il supporto costante e la sua complicità nella realizzazione dei capitoli principali della tesi. Grazie per avermi trasmesso lezioni di vita, passione per il proprio lavoro e l'irrefrenabile ambizione al progresso.

Ringrazio l'ASST Brianza per avermi dato la possibilità di svolgere il mio lavoro di tesi in un luogo interessante e dinamico, che mi ha permesso di mettermi in gioco e fare un'esperienza che sarà preziosa per il mio futuro.

A mamma e papà, al loro sostegno e capacità di lasciarmi intraprendere i miei sogni anche se questi mi portavano lontano. Grazie per avermi dato quella mentalità razionale e critica e la tenacia di chi non ha paura di lavorare sodo.
Senza di voi, tutto questo non sarebbe stato possibile.

A mio fratello, che senza grandi dimostrazioni d'affetto, crede in me ed è orgoglioso di questo mio percorso e traguardo raggiunto.

Il più sentito dei grazie ad Andrea, che mi ha accompagnata per mano verso la fine di questo percorso, facendo il tifo per me come mio più grande sostenitore, lasciandomi il giusto spazio per permettermi di portare a termine i miei impegni, festeggiando con me ogni piccola vittoria ed aiutandomi in ogni momento più difficile. Sei stato il perfetto compagno in un anno così importante e non posso che sentirmi felice e fortunata.

Alle amiche d'infanzia, siete il mio porto sicuro con cui sono cresciuta. Grazie per essere una certezza e per essermi state vicine anche quando siamo fisicamente lontane.

Ai miei compagni del liceo e dell'università, i libri non mi hanno portato solo a questo traguardo ma mi hanno anche fatto incontrare delle persone ora indispensabili nella mia vita. Grazie per ogni momento spensierato, per essere stati per me fonte d'ispirazione e complici fedeli in un percorso intenso, nei giorni più felici ed in quelli più difficili.

Grazie a tutte le persone che ho incontrato durante questo percorso che mi hanno trasmesso affetto ed orgoglio.

Tutti voi avete aggiunto un tassello fondamentale per realizzare questo grande traguardo, pronti ad essermi accanto ancora di più nella realizzazione dei miei sogni futuri.